

Development of a latent IL-17 antagonist for targeted therapy of rheumatoid arthritis

Gayatri Arvind Mittal

Thesis submitted to the University of London for the
degree of Doctor of Philosophy

November 2012

Bone and Joint Research Unit
William Harvey Research Institute
Barts and The London School of Medicine and Dentistry
Queen Mary University of London

Declaration

This is to certify that the thesis comprises only my original work towards the PhD and due acknowledgement has been made in the text to all other materials used.

Gayatri Mittal

Acknowledgements

I am grateful to the **Barts and The London Charity** and **Arthritis Research UK** for funding the research project towards my PhD degree.

I would like to thank my supervisors **Professors Yuti Chernajovsky** and **Rizgar Mageed** for the excellent guidance and invaluable support they have provided throughout this work.

I am appreciative of **Professor Bruce Kidd** who introduced me to my supervisors and the Bone and Joint research Unit.

I am especially thankful to **Ms Gill Adams** for teaching me the basic techniques of molecular biology.

I am very appreciative of the fact that almost every member of the team has contributed to project some way or the other by either offering their skills, time or support. I am therefore grateful to **my colleagues in Bone and Joint Research Unit and Centre for Microvascular Research**. I would particularly like to extend my thanks to **Drs Sandrine Vessillier** and **Lisa Mullen** for sharing their knowledge and their willingness to help.

TABLE OF CONTENTS

LIST OF FIGURES.....	13
LIST OF TABLES.....	16
ABBREVIATIONS.....	17
ABSTRACT.....	21

CHAPTER I: INTRODUCTION

1.1 RA.....	23
1.1.1 <i>Pathogenesis of RA</i>	25
1.1.1a Cellular mediators of inflammation and joint damage.....	26
1.1.1b Soluble mediators of inflammation and joint damage.....	29
1.1.2 <i>Current therapies for RA</i>	32
1.1.2a Non-biologic DMARDs.....	32
1.1.2b Biologic DMARDs.....	36
1.1.2c Targeting intracellular pathways in RA.....	39
1.2 IL-17 family of cytokines.....	40
1.2.1 <i>IL17A</i>	40
1.2.2 <i>IL-17F</i>	43
1.2.3 <i>IL-17A/F heterodimer</i>	44
1.2.4 <i>Other IL-17 cytokine family members</i>	45

1.2.5	<i>IL-17F (H161R) mutant</i>	46
1.2.6	<i>IL-17 receptor family</i>	48
1.2.6a	IL-17 receptor A.....	48
1.2.6b	IL-17 receptor C.....	51
1.2.6c	Other IL-17 receptors.....	52
1.2.7	<i>IL-17 induced signaling pathways</i>	52
1.3	Th17 Cells	55
1.3.1	<i>Differentiation of Th17 cells</i>	55
1.3.2	<i>Th17 transcriptional regulatory networks</i>	58
1.3.3	<i>Plasticity, instability and heterogeneity of Th17 cells</i>	62
1.3.3a	Th17/Treg cells.....	62
1.3.3b	Th17/Th1 cells.....	62
1.3.3c	Th17/Th2 cells.....	63
1.4	Targeting IL-17 For the treatment of RA	64
1.5	Targeted therapies	67
1.5.1	<i>Immunocytokines</i>	67
1.5.2	<i>Latent cytokines</i>	68
1.6	Preclinical <i>in vivo</i> testing of new therapies for RA	70
1.6.1	<i>Gene therapy as a modality for <i>in vivo</i> testing of new therapies</i>	70
1.6.1a	Viral vectors.....	71
1.6.1b	Non viral vectors.....	72
1.6.2	<i>Mouse models of experimental arthritis</i>	75

1.6.2a	Collagen induced arthritis mice.....	75
1.6.2b	Anti-collagen II antibody induced arthritis mice.....	76
1.6.2c	Human T cell-leukemia virus type I transgenic mice.....	76
1.6.2d	IL-1 receptor antagonist deficient mice.....	76
1.6.2e	SKG mice.....	77
1.6.2f	TNF transgenic mice.....	77
1.6.2g	K/BxN mice.....	77
1.6.2h	RA/severe combined immunodeficient mice.....	78
1.7	Summary and objectives.....	79

CHAPTER II: MATERIALS AND METHODS

2.1	Cloning and expression of IL-17.....	81
2.1.1	<i>Harvesting cDNA from mouse splenocytes.....</i>	81
2.1.1a	Harvesting T cells from mouse spleen.....	81
2.1.1b	RNA extraction	81
2.1.1c	Reverse transcription with oligo dT primers.....	82
2.1.2	<i>Cloning of human and mouse full-length-IL-17</i>	82
2.1.2a	Cloning of human and mouse wild-type full-length IL-17.....	82
2.1.2b	Cloning of human full-length IL-17F mutant.....	84
2.1.2c	Cloning of mouse analogues of human IL-17F mutant.....	85
2.1.3	<i>Cloning of human and mouse wild-type and mutated LAP-IL-17.....</i>	87
2.1.4	<i>Polymerase chain reaction DNA amplification.....</i>	88

2.1.4a	Hot start PCR.....	88
2.1.4b	Phenol: chloroform extraction and sodium acetate precipitation.....	88
2.1.5	<i>DNA restriction enzyme digestion</i>	89
2.1.5a	DNA gel purification	89
2.1.6	<i>DNA ligation</i>	90
2.1.7	<i>Transformation of E. coli</i>	90
2.1.7a	Preparation of competent E. coli.....	90
2.1.7b	Transformation of competent E. coli DH 5 α	90
2.1.8	<i>Extraction of plasmid DNA from E. coli</i>	91
2.1.8a	Small scale plasmid DNA extraction	91
2.1.8b	Large scale isolation of plasmid DNA.....	91
2.1.9	<i>Expression of IL-17 in mammalian cells</i>	92
2.1.9a	Transient transfection of mammalian cells.....	93
2.1.9b	Expression of non-secreted proteins.....	94
2.1.10	<i>Expression and affinity purification of human IL-17F mutant</i>	95
2.1.10a	Expression of human IL-17F mutant in CHO-S cells.....	95
2.1.10b	Binding of anti-human IL-17F antibody to Glycolink column	95
2.1.10c	Fast Protein Liquid Chromatography	96
2.2	Characterisation of immunological properties of expressed IL-17 proteins	98

2.2.1	<i>Western blotting</i>	98
2.2.2	<i>Determining quantity of the expressed IL-17 proteins</i>	99
2.3	Characterisation of <i>in vitro</i> biological properties of expressed IL-17 proteins	102
2.3.1	<i>Characterisation of in vitro biological properties of human IL-17 proteins</i> ..	103
2.3.1a	Determining receptor binding ability of FL-IL-17F mutant.....	103
2.3.1b	Fibroblast cells IL-6 induction IL-17 bioassay.....	104
2.3.1c	Epithelial cells IL-6 induction IL-17 bioassay.....	105
2.3.1d	Analysing ERK1/2 phosphorylation in HeLa cells.....	106
2.3.1e	Development of a novel luciferase reporter system to analyse bioactivity of human IL-17.....	107
2.3.2	<i>Characterisation of in vitro biological properties of mouse IL-17 proteins</i> ...	112
2.3.2a	Determining ability of mouse FL-IL- 17F mutants to bind to mouse IL-17RC.....	112
2.3.2b	Fibroblast cells IL-6 induction mouse IL-17 bioassay.....	112
2.3.2c	Developing a novel luciferase reporter assay to analyse bioactivity of mouse IL-17.....	115
2.4	Gene therapy in mouse models of inflammation	117
2.4.1	<i>Evaluation of human IL-17A systemic gene therapy in naïve SCID mice</i>	120
2.4.2	<i>Evaluation of human IL-17F mutant systemic gene therapy in mouse airpouch inflammation</i>	121

CHAPTER III: CLONING OF HUMAN AND MOUSE IL-17

3.1	Introduction.....	124
3.1.1	<i>Aims.....</i>	127
3.2	Results.....	128
3.2.1	<i>Confirming integrity of mouse splenic T cells mRNA.....</i>	128
3.2.2	<i>Cloning of human IL-17.....</i>	128
3.2.3	<i>Cloning of mouse IL-17.....</i>	130
3.3	Discussion.....	132

CHAPTER IV: CHARACTERISATION OF IMMUNOLOGICAL PROPERTIES OF THE EXPRESSED IL-17 PROTEINS

4.1	Introduction.....	135
4.1.1	<i>Fast protein liquid chromatography.....</i>	136
4.1.2	<i>Immunoaffinity chromatography.....</i>	136
4.1.3	<i>Aims.....</i>	137
4.2	Results.....	138
4.2.1	<i>Confirming the correct expression of 293T cells expressed IL-17 proteins...</i>	138
4.2.1a	Determining optimum concentration of MMP-1 required for the complete cleavage of LAP-IL-17 proteins.....	138
4.2.1b	Expression of IL-17 homodimers.....	139
4.2.1c	LAP-IL-17 proteins are secreted as homodimers.....	142

4.2.1d	Expression of IL-17 heterodimers.....	142
4.2.1e	Transfection efficiency of PEI is superior to calcium phosphate.....	146
4.2.1f	Expression of human IL-17F mutant in CHO-S cells.....	147
4.2.2	<i>Confirming correct expression and purity of human IL-17F mutant.....</i>	148
4.2.3	<i>Quantitation of the expressed IL-17 proteins.....</i>	149
4.3	Discussion.....	151

CHAPTER V: EVALUATION OF *IN VITRO* BIOLOGICAL ACTIVITY OF IL-17F MUTANT

5.1	Introduction.....	154
5.1.1	<i>Aims.....</i>	155
5.2	Results.....	156
5.2.1	<i>Human IL-17F mutant lacks the ability to induce secretion of IL-6 in human and mouse fibroblast cells.....</i>	156
5.2.2	<i>Human IL-17F mutant inhibits IL-17A induced secretion of IL-6 in human and mouse fibroblast cells</i>	156
5.2.3	<i>Biological effects of IL-17F mutant are specific to its biological activity ...</i>	159
5.2.3a	IL-17F mutant binds to IL-17RC.....	159
5.2.3b	Affinity purified IL-17F mutant is unable to stimulate IL-6 secretion and ERK1/2 activation in HeLa cells.....	160
5.2.3c	Inhibition of IL-17A by immunoaffinity purified IL-17F mutant is reversed by a neutralising anti-IL-17F antibody	163

5.2.4	<i>Treatment with MMP-1 releases IL-17 activity from latent LAP-IL-17 molecules.....</i>	164
5.2.5	<i>IL-17 was unable to activate luciferase in 57HeLa cells.....</i>	165
5.2.6	<i>IL-17 was unable to activate IL-6 promoter responsive luciferase in epithelial cells.....</i>	166
5.2.7	<i>Mouse IL-17F mutant 1 but not IL-17F mutant 3 binds to IL-17RC.....</i>	166
5.2.8	<i>Mouse IL-17F mutant 1 is an agonist of IL-17.....</i>	168
5.2.9	<i>Biological activity of mouse LAP-IL-17 proteins is released by MMP.....</i>	169
5.2.10	<i>A novel IL-6 promoter responsive luciferase reporter system to assess bioactivity of mouse IL-17 is developed and standardised.....</i>	170
5.3	Discussion.....	172

CHAPTER VI: INVESTIGATION OF *IN VIVO* EXPRESSION OF HUMAN IL-17 TRANSGENE IN MOUSE MODELS OF INFLAMMATION

6.1	Introduction.....	177
6.1.1	<i>Aims.....</i>	179
6.2	Results.....	180
6.2.1	<i>Expression of human IL-17 transgene in naïve SCID mice.....</i>	180
6.2.2	<i>Expression of human IL-17 transgene in C57BL/6 mice.....</i>	182
6.3	Discussion.....	184
	CHAPTER VII: GENERAL DISCUSSION.....	187

CHAPTER VIII: FUTURE STUDIES.....	193
APPENDIX.....	196
SCIENTIFIC COMMUNICATIONS.....	225
REFERENCES.....	226

LIST OF FIGURES

CHAPTER I: INTRODUCTION

Figure 1.1	Clinical manifestations of RA.....	23
Figure 1.2	Cellular mediators of inflammation and joint damage.....	27
Figure 1.3	Biological functions of IL-17A.....	41
Figure 1.4	IL-17-induced signaling pathways.....	54
Figure 1.5	Differentiation of pathogenic versus non-pathogenic Th 17 cells	57
Figure 1.6	Th17 transcriptional regulatory network.....	58
Figure 1.7	Structure of a latent cytokine	69
Figure 1.8	Gene therapy as a modality for preclinical testing of new therapies	74

CHAPTER II: MATERIAL AND METHODS

Figure 2.1	Cloning of full-length IL-17 in pcDNA3.....	84
Figure 2.2	Creating human full-length (H161R) IL-17F mutant.....	85
Figure 2.3	C-terminal sequences of human and mouse IL-17F.....	86
Figure 2.4	Cloning of mature IL-17 in pcDNA3-LAP.....	87
Figure 2.5	Testing immunoactivity of purified mouse anti-IL-6 antibodies.....	114
Figure 2.6	Evaluation of human IL-17A systemic gene therapy in naïve SCID mice ...	120
Figure 2.7	Evaluation of human IL-17F mutant systemic gene therapy in mouse airpouch inflammation.....	122

CHAPTER III: CLONING OF HUMAN AND MOUSE IL-17

Figure 3.1	Plasmid expression vector pcDNA3.....	125
Figure 3.2	Confirming integrity of mouse splenic T cells mRNA.....	128
Figure 3.3	Restriction enzyme analysis of human FL-IL-17.....	129
Figure 3.4	Restriction enzyme analysis of human LAP-IL-17.....	129
Figure 3.5	Restriction enzyme analysis of mouse FL-IL-17.....	130
Figure 3.6	Restriction enzyme analysis of mouse LAP-IL-17.....	131

CHAPTER IV: CHARACTERISATION OF IMMUNOLOGICAL PROPERTIES OF IL-17 PROTEINS

Figure 4.1	Western blot analysis demonstrating optimum dilution of MMP-1 that is required for complete cleavage of LAP-IL-17.....	139
Figure 4.2	Western blot analysis of human IL-17 homodimers.....	140
Figure 4.3	Western blot analysis of mouse IL-17 homodimers.....	141
Figure 4.4	LAP-IL-17 proteins are secreted as homodimers.....	142
Figure 4.5	Western blot analysis of human IL-17 heterodimers.....	144
Figure 4.6	Western blot analysis of mouse IL-17 heterodimers.....	145
Figure 4.7	Transfection efficiency of PEI is superior to calcium phosphate co-precipitation.....	146

Figure 4.8	Western blot analysis of CHO-S expressed human IL-17F mutant.....	147
Figure 4.9	Immunoaffinity purified human IL-17F mutant is more than 90% pure.....	148
Figure 4.10	Semi-quantitation of expressed human full-length IL-17 proteins.....	150

CHAPTER V: EVALUATION OF *IN VITRO* BIOLOGICAL ACTIVITY OF IL-17F MUTANT

Figure 5.1	Human IL-17F mutant is unable to induce secretion of IL-6 in HFFF2 and 3T3 cells	157
Figure 5.2	Human IL-17F mutant inhibits IL-17A induced secretion of IL-6 in HFFF2 and 3T3 cells.....	158
Figure 5.3	Human IL-17F mutant binds to IL-17RC.....	160
Figure 5.4	Immunoaffinity purified IL-17F mutant is unable to induce IL-6 secretion and ERK1/2 activation in HeLa cells.....	162
Figure 5.5	Inhibition of IL-17A by IL-17F mutant is reversed by a neutralising anti-IL-17F antibody.....	163
Figure 5.6	Biological latency of human LAP-IL-17 proteins is released by MMP.....	164
Figure 5.7	IL-17A is unable to activate luciferase in 57A HeLa cells.....	165
Figure 5.8	Mouse IL-17F mutant 1 but not IL-17F mutant 3 binds to IL-17RC	167
Figure 5.9	Mouse IL-17F mutant 1 is an agonist of IL-17.....	168
Figure 5.10	Biological activity of mouse LAP-IL-17 proteins is released by MMP.....	169
Figure 5.11	DTF cells stably transfected with IL-6 promoter driven luciferase are responsive to mouse IL-17A.....	171

**CHAPTER VI: INVESTIGATION OF *IN VIVO* EXPRESSION OF HUMAN IL-17 TRANSGENE IN
MOUSE MODELS OF INFLAMMATION**

Figure 6.1	Expression of human IL-17 transgene in naïve SCID mice.....	181
Figure 6.2	Expression of human IL-17 transgene in C57BL/6 mice.....	183

LIST OF TABLES

CHAPTER I: INTRODUCTION

Table 1.1	The 2010 ACR/EULAR criteria for the diagnosis of RA.....	25
Table 1.2	Soluble mediators of inflammation and joint damage.....	31
Table 1.3	Non-biologic DMARDs.....	35
Table 1.4	Biologic DMARDS.....	38
Table 1.5	IL-17 family of cytokines.....	42
Table 1.6	Association of H161R IL-17F mutant polymorphism with risk of susceptibility to various diseases.....	47
Table 1.7	IL-17 receptor family.....	50

CHAPTER II: MATERIAL AND METHODS

Table 2.1	List of primers used for cloning of human and mouse full-length and LAP- IL-17 constructs.....	83
------------------	---	-----------

CHAPTER IV: CHARACTERISATION OF IMMUNOLOGICAL PROPERTIES OF IL-17 PROTEINS

Table 4.1	ELISA quantitation of 293T cells expressed mouse IL-17 proteins.....	149
Table 4.2	Western blot quantitation of human IL-17 proteins in concentrated 293T cells supernatants.....	150

LIST OF ABBREVIATIONS

Ab	Antibody
ACR	American College of Rheumatology
APC	Antigen Presenting Cell
BJRU	Bone and Joint Research Unit
BSA	Bovine Serum Albumin
CII	Collagen Type II
CD	Cluster of Differentiation
CHO	Chinese Hamster Ovary
CIA	Collagen Induced Arthritis
ConA	Concanavalin A
COX	Cyclooxygenase
DCs	Dendritic Cells
DMARDs	Disease Modifying Anti-Rheumatic Drugs
DMEM	Dulbeco's Modified Eagle's Medium
DNA	Deoxyribonucleic Acid
DTT	Dithiothreitol
ECL	Enhanced Chemiluminescence
EDTA	Ethylene Diamine Tetra Acetic Acid
ELISA	Enzyme-Linked Immunosorbent Assay
ERK	Extracellular Signal Regulated Kinase
Fc	Fragment, Crystallizable Region
FBS	Foetal Bovine Serum
FNIII	Fibronectin type III

GM-CSF	Granulocyte Macrophage Colony Stimulating Factor
HLA	Human Leukocyte Antigen
HRP	Horseradish Peroxidase
IFN	Interferon
ICAM-1	Intracellular Adhesion Molecule-1
Ig	Immunoglobulin
IL	Interleukin
IL-1Ra	Interleukin-1 Receptor Antagonist
iNOS	Inducible Nitric Oxide Synthase
i.v.	Intravenous
Kb	Kilobase
kDa	Kilodalton
LAP	Latency Associated Peptide
LB	Luria Bertani
LFA	Lymphocyte Function Associated Antigen
LT	Lymphotoxin
LPS	Lipopolysaccharide
LTR	Long Terminal Repeat
mAb	monoclonal Antibody
MHC	Major Histocompatibility Complex
MMP	Matrix Metalloproteinase
MOPS	Morpholino-Propane Sulfonic Acid
mRNA	messenger Ribonucleic Acid
MW	Molecular Weight
MWCO	Molecular Weight Cut Off

Nab	Neutralising Antibody
NF- κ B	Nuclear Factor-kappa B
NICE	National Institute of Clinical Excellence
NK	Natural Killer Cell
NSAID	Non-steroidal Anti-inflammatory Drugs
OD	Optical Density
PBS	Phosphate Buffered Saline
PGE ₂	Prostaglandin E ₂
PAGE	Polyacrylamide Gel Electrophoresis
PCR	Polymerase Chain Reaction
PBMC	Peripheral Blood Mononuclear Cells
PKC	Protein Kinase C
PMA	Phorbol 12-Myristate-13-acetate
PVDF	Polyvinylidene Difluoride
RA	Rheumatoid Arthritis
RANTES	Regulated upon Activation, Normal T cell Expressed, and Secreted
RASF	Rheumatoid Arthritis Synovial Fibroblasts
RPMI	Roswell Park Memorial Institute Medium
SCID	Severe Combined Immunodeficiency
SDS	Sodium Dodecyl Sulphate
SEM	Standard Error of Mean
SNP	Single Nucleotide Polymorphism
STAT	Signal Transducer and Activator of Transcription
sTNFR	Soluble TNF- α Receptor
TCR	T-cell Antigen Specific Receptor

TNF	Tumour Necrosis Factor
Th	T Helper Cell
TGF	Transforming Growth Factor
TLR	Toll-like Receptor
Treg	Regulatory T cells
VCAM	Vascular Cell Adhesion Molecule

Abstract

Cytokine based therapies can be targeted to the sites of active inflammation by modifying a given cytokine as a LAP-cytokine. IL-17A has been shown to directly contribute to pathogenesis of rheumatoid arthritis (RA). IL-17F, another member of the IL-17 cytokines family shares structural homology, receptor binding and biological properties with IL-17A but is 30-100 times less potent than IL-17A. (H161R) IL-17F mutant, a natural variant of IL-17F was shown to be protective against asthma in Japanese population. *In vitro*, IL-17F mutant competitively inhibited wild-type IL-17F and lacked the ability to activate downstream signaling pathways. I hypothesized that (H161R) IL-17F mutant is an additional inhibitor of IL-17A and if modified as LAP-IL-17F mutant, would be an effective targeted therapy for RA.

(H161R) IL-17F mutant was created by substituting nucleotide A at position 485 in the wild type IL-17F by G. *In vitro* assays showed that the IL-17F mutant could bind to IL-17RC but lacked the ability to stimulate IL-6 secretion in HFFF2, 3T3 and HeLa cells and phosphorylate ERK1/2 in HeLa cells. IL-17F mutant also inhibited IL-17A induced secretion of IL-6 in all these cell lines.

In order to assess *in vivo* therapeutic efficacy of LAP-IL-17F mutant in collagen induced arthritis mice, three mouse analogues of human IL-17F mutant were developed. Of these, (Q158R) IL-17F mutant displayed IL-17 agonistic properties, (H157R) IL-17F mutant could not be expressed *in vitro* and the truncated IL-17F mutant could not bind to mouse IL-17RC.

Investigation of *in vivo* expression and pharmacokinetics of intravenous hydrodynamically delivered human full-length and LAP-IL-17 plasmid DNAs in naïve SCID and C57BL/6 mice showed that human IL-17 transgene expression was detectable in mouse serum at 48 hours post-delivery. The transgene expression however declined rapidly over the next two weeks. The local expression of transgene in C57BL/6 airpouch lavage fluid was less than 5% of its systemic levels.

Taken together, the findings of the study warrant an investigation of *in vivo* therapeutic efficacy of human (H161F) IL-17F mutant in a suitable preclinical RA model, such as RA synovium/SCID mice.

CHAPTER I

INTRODUCTION

1.1 Rheumatoid arthritis

RA is a systemic autoimmune disease characterised by chronic synovial inflammation, cartilage damage and bone destruction. It is the most common inflammatory arthritis that affects adults with a remarkably consistent worldwide prevalence of approximately 1%. RA usually affects people in their fourth and fifth decades and women are three times more commonly affected than men. RA classically presents as symmetrical polyarthritis affecting both the small and large joints of upper and lower extremities. The arthritis although principally affects synovial joints, is truly a systemic disease and may affect many other organ systems (Fig. 1.1). Some of the extra-articular manifestations of RA include fever, anorexia, weight loss, fatigue, subcutaneous nodules, dry eyes, lung fibrosis, pleuritis, pericarditis and vasculitis. RA is associated with an increased prevalence of co-morbid conditions such as cardiovascular disease, infections and lymphoproliferative disorders (1). RA patients are at risk of premature mortality and the life expectancy of the patients is shortened by 3-10 years (2).

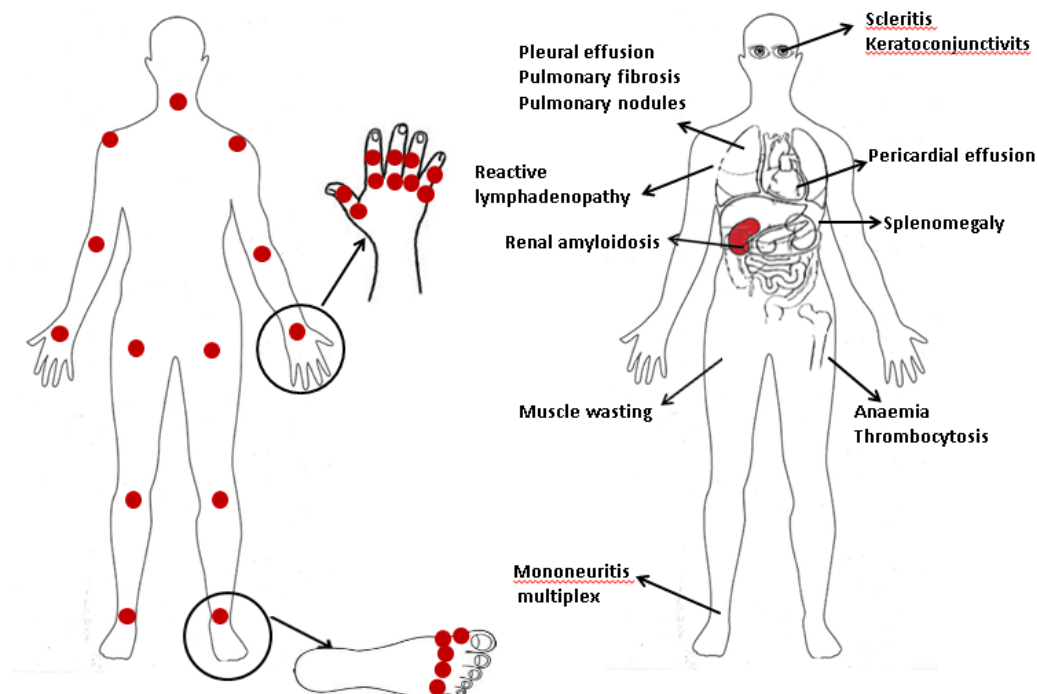


Figure 1.1 Clinical manifestations of RA. RA characteristically affects small and large joints in a symmetrical distribution. Although predominantly affecting joints, RA is truly a systemic disease and can involve many other organ systems. The extra-articular manifestations of RA include fatigue, weight loss, anaemia, dryness of eyes or mouth, pleural and pericardial effusions, pulmonary nodules, fibrosis, lymphadenopathy, splenomegaly and small vessel vasculitis.

RA is diagnosed clinically on the basis of clinical features of inflammatory arthritis that affects three or more joint and is of more than 6 weeks duration in association with radiology and blood findings. Using the most recent American College of Rheumatology and the European League Against Rheumatism (ACR/EULAR) classification criteria, last revised in 2010 (Table 1.1), a definite diagnosis of RA is established if the combined score in four individual domains (the number and site of joints involved, positivity of rheumatoid factor (RF) or anti-citrullinated peptide antibody (ACPA), raised erythrocyte sedimentation rate or C-reactive protein and symptom duration of at least six weeks) in the absence of an alternative diagnosis is ≥ 6 (from the maximum possible of 10).

Although the course of RA is variable, most patients suffer a progressive disease. The overall outcome of RA is dependent upon the degree of disease activity, joint damage, the physical function and psychological health of the patient and the presence of comorbid illness. Much of the joint damage that ultimately results in disability begins early in the course of the disease. Two thirds of patients with RA of less than two years duration have joint erosions on plain radiographs of the hands. The key to prevent serious disease outcomes is instituting disease modifying anti-rheumatic drug (DMARD) therapy as soon as possible. With such a shift in the strategy, the goal of treatment now is to achieve remission or at least the lowest possible level of disease activity.

Table 1.1 2010 ACR/EULAR classification criteria for RA

Domain	Score
A Joint involvement*	
Large joints	
1	0
2-10	1
Small joints	
1-3	2
3-10	3
>10 joints (at least 1 small joint)	5
B Serology **	
RF/ACPA negative	0
RF/ACPA low positive	2
RF/ACPA high positive	3
C Acute phase reactants	
CRP/ESR normal	0
CRP/ESR abnormal	1
D Duration of symptoms	
< 6 weeks	0
≥ 6 weeks	1

The criteria are aimed at classification of newly presenting patients. The scores in categories A-D are added; the patient is classified to have definite RA if the total score is ≥ 6 . * Joint involvement refers to any swollen or tender joint on examination, which may be confirmed by radiology evidence of synovitis; **At least one test result is needed. ACR, American College of Rheumatology; EULAR, European League Against Rheumatism; RF, rheumatoid factor; ACPA, anti-citrullinated protein antibody; CRP, C-reactive protein; ESR, erythrocyte sedimentation rate.

1.1.1 Pathogenesis of RA

RA is not just a single disease, instead a common end result of activation of different pathways, depending on the genetic makeup of the patient, leading to autoreactivity and chronic synovial inflammation. Exogenous or endogenous environmental triggers cause repeated activation of innate immunity, which leads to gradually increasing. The exact trigger or the cause of RA is not known.

Amongst the genetic factors, RA is strongly linked to the major histocompatibility class II antigens HLA-DRB1*0404 and HLADRB1*0401(3, 4); HLA alleles that contain the shared epitope (QKRAA) particularly confer susceptibility to RA (4). Likewise *PTPN22*, *STAT4*, *CTLA4*, *TRAF1-C5*, *c-REL*, which aggregate around immune regulatory functions are the other identified risk alleles (5-9). These single nucleotide polymorphisms increase the risk for RF or ACPA positive disease whereas *HLA-DRB1*03*,

interferon regulatory factor 5 and C-type lectin domain family 4 member A, some of the less established genetic risk factors are associated with ACPA negative RA (10-12).

Of the environmental stimuli, the best defined is smoking, which in association with susceptible *HLA-DRB1* alleles, synergistically increases the risk of having ACPA and RA (13, 14). Although no causative infectious agent has ever been isolated from RA patients, infections such as Parvovirus, Rubella, Epstein Barr virus, Cytomegalovirus, Proteus species, Escherichia coli and Borrelia Burgdorferi have been associated with arthritis (15). Porphyromonas gingivalis, the predominant pathogenic organism in chronic periodontitis expresses the enzyme, peptidyl arginine deiminase, type IV (PADI 4), which is capable of promoting citrullination of mammalian proteins (16). Endogenous antigens such as human cartilage glycoprotein 39 and heavy-chain-binding protein have also been ascribed as possible triggers RA (17). Although RF and ACPA are often positive even before the onset of RA, a pathogenic role for these has not been established.

Whatever the trigger, very early during the course of RA, the synovium undergoes hyperplasia, neoangiogenesis and cellular infiltration. Once initiated, the chronic synovial inflammation is self-perpetuated and propagated via activated resident (macrophages, fibroblasts, endothelial cells) and infiltrated cells (T lymphocytes, B lymphocytes, monocytes, plasma cells, mast cells and dendritic cells), which in turn secrete cytokines, chemokines, growth factors, matrix degrading enzymes, PGE2 and NO. The hyperplastic synovium ultimately expands and forms finger-like projections termed pannus, which invades and destroys the adjacent cartilage and bone resulting in the characteristic joint damage of RA (18). Once initiated, the chronic synovial inflammation in RA is self-perpetuated. Distinct mechanisms regulate inflammation and destruction of matrix, cartilage and bone.

1.1.1a Cellular mediators of inflammation and joint damage (Fig. 1.2)

Macrophages are central effectors of synovitis. The rheumatoid synovium is predominantly infiltrated by monocytes and macrophages. Clinically effective biologic agents consistently reduce macrophage infiltration in the synovium (19). Macrophages are responsible for antigen presentation,

phagocytosis, production of various cytokines (TNF- α , and IL-1, 6, 12, 15, 18, and 23), prostanoids and matrix-degrading enzymes, release of reactive oxygen and nitrogen intermediates, stimulation of angiogenesis and maturation of osteoclasts (20, 21).

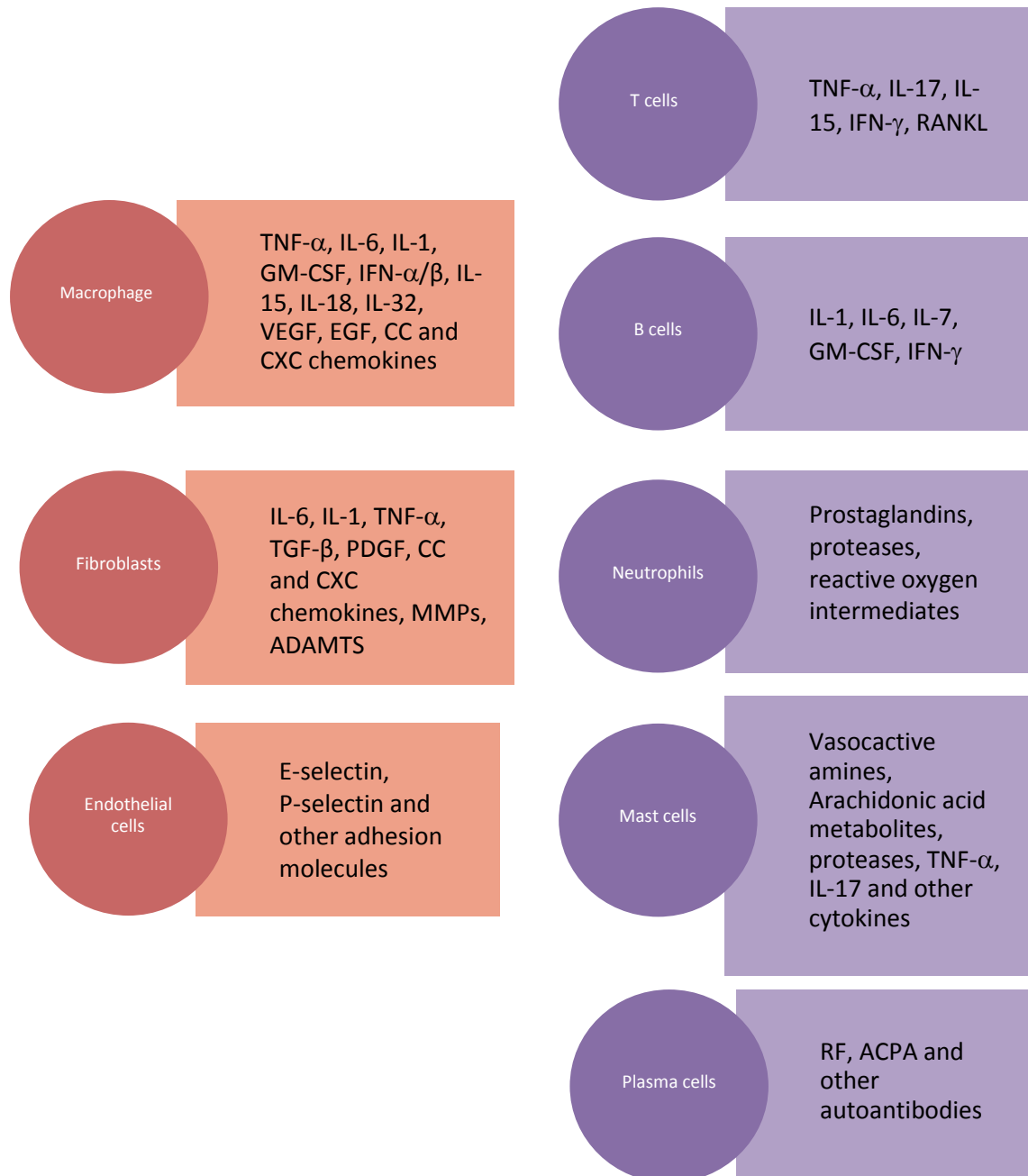


Figure 1.2 Cellular mediators of inflammation and joint damage in RA. RA synovitis is characterised by activated resident and infiltrated cells which secrete cytokines, chemokines, growth factors, matrix degrading enzymes, prostaglandins, nitric oxide, thus playing a crucial role in the propagation and maintenance of self-perpetuating chronic synovitis accompanied by matrix, cartilage and bone damage.

Fibroblasts are the other principal cells in RA synovium and mainly involved in effecting the destructive response. Fibroblasts in RA synovium demonstrate properties of anchorage independence, loss of contact inhibition, inability to undergo apoptosis, invade cartilage and stimulate differentiation and activation of osteoclasts (22-26). Additionally, RA synovial fibroblasts promote expression of proinflammatory cytokines, chemokines, adhesion molecules and MMPs and directly contribute to the chronic synovial inflammation (27).

T cells constitute approximately 50% or more of RA synovial cells, the majority of which are memory type Th1 and Th17 CD4+ cells. T cell activated by the inciting and other autoantigens in association with costimulatory molecules initiate a pathogenic chronic synovial immune response. Antigen-activated CD4+ T cells stimulate monocytes, macrophages and synovial fibroblasts cells to produce cytokines and matrix-degrading enzymes, activate B cells to produce autoantibodies, and express ligands that stimulate osteoclastogenesis. T cell activation in RA can also take place without specific antigen and results in self-perpetuating cycles of T cell proliferation sufficient to sustain autoimmunity (28). Although T cells modulate synovial inflammatory responses, a direct role of T cells has not been confirmed in RA (29-31). Abatacept or CTLA4-Ig, which restricts T cell activation via inhibition of T cell costimulation has proven to be effective in the treatment of RA.

B cells have a multifaceted role in the pathogenesis of RA having the ability to maintain synovial ectopic germinal centres, to mediate pathological immune responses and to drive the humoral autoimmune process. B cells in RA produce RF, APCA, anti-nuclear antibody and also specific autoantibodies against collagen II, human cartilage gp39, matrix components in cartilage and cartilage link protein. These cells exhibit an increased expression of IL-1 β , IL-6, IL-7, IFN- γ and G-CSF, and have been recently identified to have novel functions such as participation in angiogenesis (32). Rheumatoid B cells show evidence of inappropriate proliferation, oligoclonality, autoreactivity and self-perpetuation. Although the naïve B cells can be activated in a T cell-dependent or independent manner, they themselves are crucial in T cell activation (33).

Neutrophils contribute to synovitis by synthesizing prostaglandins, proteases, and reactive oxygen intermediates (34). Mast cells are activated at the very onset of RA and secrete cytokines such as TNF- α , IL-1 β and IL-17, chemokines and produce high levels of vasoactive amines and proteases (35, 36). The activated macrophages, lymphocytes and fibroblasts, and their products stimulate angiogenesis. Endothelial cells in the synovium are activated and express adhesion molecules such as E-selectin, P-selectin, LFA-1, ICAM-1, VLA-4, and α 4 β 7. The adhesion molecules, in association with IL-8 promote the recruitment of inflammatory cells into the joint. Anti-ICAM-1, an anti-adhesion molecule therapy, prevented synovial inflammation and disease development in animal models and humans (37).

1.1.1b Soluble mediators of inflammation and joint damage

The cells in RA synovium secrete numerous cytokines, chemokines, growth factors and other mediators of inflammation (20, 38). Of these, cytokines particularly TNF, IL-1, IL-6 and IL-17 are fundamental to both chronic inflammatory and the destructive phases of RA; their role in RA pathogenesis is summarised in Table 1.2.

IL-6 drives local leukocyte activation and autoantibody production, mediates systemic effects that promote acute phase responses, inhibits bone formation and stimulates bone resorption (39, 40). Its critical role in RA is demonstrated by the positive outcomes in the patients after treatment with IL-6 receptor inhibiting antibody (41).

TNF- α plays the most important role in mediating and sustaining the chronic inflammatory response in RA. It activates expression of other cytokines, chemokines and endothelial cell adhesion molecules and promotes protection of synovial fibroblasts, angiogenesis and suppression of regulatory T cells (42, 43). The significance of TNF- α in the pathogenesis of RA is evidenced by the fact that the TNF inhibitors are the most widely used biologics in the treatment of RA.

IL-1 promotes activation of leukocytes, endothelial cells, chondrocytes, and osteoclasts (44, 45). However, benefits of IL-1 inhibition in the treatment of RA have only been modest (46).

Despite substantial lymphocytic infiltration, activated T cells secreted cytokines such as IFN- γ , IL-2 and IL-4 except IL-17 are sparsely expressed in RA (47).

Proinflammatory cytokines such as IL-7, IL-15, IL-18, IL-21, IL-23, IL-33 (48-55) are also upregulated in RA and play a role in the pathogenesis. Other proinflammatory cytokines such as IL-20, IL-22, IL-32, TNF-like weak inducer of apoptosis (TWEAK) and macrophage chemoattractant protein (MCP)-1 (56-61) also contribute to the pathogenesis of RA.

Inflammatory enzymes such as inducible nitric oxide synthase (iNOS) and cyclooxygenase-2 (Cox-2) are upregulated in RA and their inhibition reduces pain and inflammation in arthritic joints (62-66).

Enzymatic factors such as matrix metalloproteases (MMPs), cathepsins, aggrecanases-1 and 2 (also called ADAMTS-4 and -5 respectively) (67-70) are overexpressed in RA and are predominantly responsible for inducing cartilage damage. Endogenous enzyme inhibitors such as TIMPs fail to reverse this destructive cascade due to their lower expression levels.

Synovial cytokines, particularly macrophage colony stimulating factor (M-CSF) and receptor activator of NF- κ B ligand (RANKL) promote osteoclast differentiation and invasion of the periosteal surface adjacent to articular cartilage (71). Cytokine-induced mediators such as dickkopf-1 and frizzled-related protein 1 potentially inhibit the differentiation of mesenchymal precursors into chondroblasts and osteoblasts (72).

Although multiple anti-inflammatory molecules such as IL-10 (73), TGF- β (74), soluble p55 and p75 TNFR (75-77) and IL-1 receptor antagonist (IL-1ra) are also upregulated in RA, their levels are insufficient to counterregulate the on-going chronic synovial inflammation. In RA, the cytokine homeostasis is imbalanced in favour of more pro-inflammatory than anti-inflammatory cytokines (42).

Table 1.2 Soluble protein mediators of inflammation and joint damage in RA

Mediator	Role played in the pathogenesis of RA
Cytokines	
IL-6	Activates leukocytes and osteoclasts, promotes B-lymphocyte differentiation, mediates acute-phase response
TNF- α	Activates leukocytes, endothelial cells, and synovial fibroblasts; induces production of cytokines, chemokines, adhesion molecules, and matrix enzymes; suppresses regulatory T-cell function; activates osteoclasts; and promotes resorption of cartilage and bone
IL-1 β	Activates leukocytes, endothelial cells, and synovial fibroblasts; induces matrix enzyme production by chondrocytes; activate osteoclasts
IL-17	Activates synovial fibroblasts, chondrocytes, and osteoclasts; stimulates secretion of cytokines, chemokines, growth factors, and matrix enzymes; suppresses regulatory T-cell function; and promotes resorption of cartilage and bone
IL-21	Activates Th17 and B cell subsets
IL-23	Expands Th17 cells
IL-7 and IL-15	Activate T and NK cells; promote and maintain memory T cells, and survival and activation of neutrophils and B cells; promote TNF production; drive activation of Th17 cells
IL-18	Activates Th1, NK cells and neutrophils
IL-32	Stimulates cytokine production by various leukocytes, promotes differentiation of osteoclasts
IL-33	Activates mast cells and neutrophils
Growth and differentiation factors	
GM- and M-CSF	Enhance differentiation of granulocyte and myeloid-lineage cells in the bone marrow and synovium
RANKL	Promotes maturation and activation of osteoclasts
BLYS and APRIL	Activate B cells, promote maturation of B cells and production of autoantibodies
Enzymatic factors	
MMPs	Promote disassembly of the type II collagen network, degrade collagenous cartilage matrix
Aggrecanases	Degrade aggrecan
Cathepsins	Promote proteolysis of collagen in non-triple helical region, degradation of matrix, activation of other enzymes and amplification of destructive process

GM-CSF granulocyte-macrophage colony-stimulating factor; M-CSF, macrophage colony-stimulating factor; BLYS, B-lymphocyte stimulator; APRIL, a proliferation-inducing ligand; RANKL, receptor activator of NF- κ B ligand; MMPs, matrix metalloproteases; Th1, type 1 helper T cells; NK cells, natural killer cells.

1.1.2 Current therapies for RA

Patients are best managed using a multidisciplinary team approach and an early institution of DMARD therapy. The National Institute of Clinical Excellence (NICE) recommends use of combination DMARDs plus short-term glucocorticoids as soon as possible after the onset of RA. The treatment is escalated rapidly until an adequate disease control is achieved; biologics introduced if necessary. Patients receive additional analgesics, NSAIDs/COX2 inhibitors and intra-articular steroid injections as needed. RA disease activity is monitored using CRP and DAS 28, a composite disease activity score. The goal of therapy is to achieve total remission if possible or an acceptable 'low-disease-activity' status.

A number of therapies, both biologic and non-biologic as outlined below are effective in the treatment of RA yet at least one third of patients remain unresponsive to the currently available therapies. Introduction of anti-TNFs, the first biologics in the treatment of RA two decades ago, almost revolutionised the management of RA but systemic side-effects such as increased risk of infections still remain major concerns. Since the advent of anti-TNFs, similar biologics targeting other cytokines or cell molecules such as IL-6, CD20 and CTLA-IgG have been developed and successfully used to treat RA. All these therapies are however based on the principle of inhibiting a proinflammatory cytokine or downregulating B or T cells, either via use of monoclonal antibodies or receptor blockers. This approach results in non-selective inhibition of targeted cytokine or immune cell, which is also required for normal immune regulatory functions such as host defence against microbial infection. There is therefore still an unmet need for better and safer therapies in RA.

Generalised immune suppression, the major limitation of currently available highly efficacious biologic therapies can be avoided if such a therapy is targeted to the actively inflamed RA joints, the actual site of pathology. Latent cytokines by allowing targeting of therapeutic biological activity of a given cytokine to disease sites where MMPs are overexpressed, such as actively inflamed joints in RA offer such an opportunity. A cytokine if covalently fused to latency-associated peptide (LAP) of TGF- β via a MMP-sensitive linker is unable to interact with its receptor and therefore becomes biologically

latent. The biological activity of a latent cytokine however can be released by the action of MMP, which is able to cleave the linker between LAP and a given cytokine, thus freeing the cytokine to exert its therapeutic actions. The latent cytokine approach was first pioneered in our laboratory using IFN- β and since then has been validated for a number of other cytokines and small molecules. LAP-IFN- β was superior to naïve IFN- β in ameliorating CIA in mice and had a significantly prolonged half life *in vivo*. LAP-MSH- α was more efficacious than naïve MSH- α in a mouse peritonitis model. IL-17A (or IL-17), the prototype effector cytokine of Th17 cells, the recently discovered independent T helper cell lineage plays an important role in the pathogenesis of RA. Phase 1/2 clinical trials of inhibition of IL-17 in RA have demonstrated therapeutic efficacy without notable side-effects, thus confirming its previously reported beneficial effects in experimental arthritis. Exogenous administration of IL-17 exacerbated arthritis whereas its neutralisation suppressed experimental arthritis. *In vitro* and *in vivo* preclinical studies have demonstrated that IL-17 works both in synergy as well as independently of TNF- α and IL-1 β in mediating joint inflammation and joint damage in inflammatory arthritis. A combined blockage of IL-17 and TNF- α and IL-1 β is therapeutically more efficacious in experimental arthritis than TNF- α or IL-1 β alone. Inhibition of IL-17 for the treatment of RA therefore is likely to be effective as an independent therapy as well as an adjunct to TNF- α and IL-1 β . Moreover, a given IL-17 antagonist if by using LAP cytokine approach is modified as latent IL-17 antagonist would offer a highly efficacious therapy for RA, which would be targeted to the active arthritic joints and devoid of the side-effects of generalised immune suppression and increased risk of infections.

The therapies both non-biologics and biologics that are in the current use to treat RA are in brief described below.

1.1.2a Non-biologic DMARDs

Methotrexate

MTX is the preferred first-line DMARD and often the 'anchor drug' for the most RA patients (78-80). MTX is the most effective and the best tolerated DMARD in the long-term and results in the

enhancement of therapeutic efficacy of other DMARDs (both non-biologic and biologic) when combined together (81-83).

Sulfasalazine

Sulfasalazine alone or in combination with Hydroxychloroquine is generally used in patients who are poor candidates for MTX or who lack poor prognostic factors (RF or ACPA positivity, extra-articular manifestations, radiographic erosions and functional limitations).

Hydroxychloroquine

Hydroxychloroquine may be appropriate for some patients with RA, particularly those who lack poor prognostic features and are at the milder end of the spectrum of disease activity.

Leflunomide

Leflunomide is effective for the treatment of early, moderate to severely active RA, regardless of the presence or absence of poor prognostic factors (84). Leflunomide is most commonly used in combination with MTX in patients who have an inadequate response to MTX but are not candidates for triple therapy with MTX, Hydroxychloroquine and Sulfasalazine.

Glucocorticoids

Short-term treatment with glucocorticoids is indicated as part of initial DMARD combination therapy and treatment of flares. Long-term treatment with glucocorticoids is used only when all other treatments have been offered and have failed. Both intra-articular and oral glucocorticoids are used depending on the clinical indication (85, 86).

Table 1.3 Non-biologic DMARDs

Agent	Usual dose	Mechanism of action	Side-effects
Methotrexate	7.5 – 20mg per week	Blockage of tetrahydrofolate dependent cell metabolism via Inhibition of dihydrofolate reductase; accumulation of adenosine; induction of apoptosis and inhibition of immune/inflammatory cell proliferation; inhibition of IL-1, IL-6 and TNF- α production	Oral ulcers, bone marrow suppression, GI intolerance, hepatotoxicity, hypersensitivity pneumonitis, pulmonary fibrosis, alopecia, rash, dermatitis, lymphoproliferative disorders
Sulfasalazine	1gm BD	Inhibition of IL-8, MCP-1, TNF- α , NF- κ B; increased production of adenosine; inhibition of osteoclast formation; apoptosis of macrophages; suppression of B cell function	GI intolerance, headache, anorexia, hepatic toxicity, hematologic toxicity, haemolytic anaemia, DRESS syndrome**
Hydroxychloroquine*	200mg BD	Blockage of TLR9 and B cell antigen receptor costimulation; inhibition of TLR signaling; decreased inflammatory mediators and lymphocyte proliferation secondary to lysosomotropic actions; inhibition of TNF- α , phospholipase, metalloproteinase; blockage of superoxide release; antagonism of PG	GI intolerance, skin rash, headache, light headedness, tinnitus, toxic neuropathy, skeletal myopathy, cardiomyopathy, corneal deposits, retinopathy.
Leflunomide	20mg OD	Reduced synthesis of rUMP via inhibition of dihydro-orotate dehydrogenase; inhibition of memory T cells, dendritic cells; inhibition of leukocyte adhesion to endothelial cells and synovial infiltration of lymphocytes and macrophages; blocking of NF- κ B and JAK1 and JAK3 signaling	Diarrhoea, hypertension, hyperkalemia, hepatotoxicity, leukopenia, interstitial lung disease, peripheral neuropathy

* Hydroxychloroquine is one of the safest DMARDs. Serious side-effects are rare. ** DRESS syndrome, drug rash with eosinophilia and systemic symptoms.

1.1.2b Biologic DMARDs

Biological agents represent a major advance for the treatment of patients who have inadequate response to non-biologic DMARDs.

Biologic DMARDs are produced using recombinant DNA technology, and target cytokines or their receptors or are directed against other cell surface molecules. The current NICE approved biologics for the treatment of RA are listed in the Table 1.4 and include TNF inhibitors (Etanercept, Infliximab, Adalimumab, Certolizumab and Golimumab), T cell co-stimulation inhibitor (Abatacept), IL-6 inhibitor (Tocilizumab) and B cell depleting agent (Rituximab).

TNF inhibitors

TNF antagonists have held to their place as the biologics of choice since being introduced two decades ago as the first biological therapy for RA. Targeting TNF by means of either monoclonal antibodies or TNF receptor-IgG fusion protein proved to be extremely effective in control of RA (87). The unprecedented success of TNF inhibiting biologics has translated into the development and availability of similar therapies targeting other mediators of inflammation.

It has been well established that combination of an anti-TNF agent and MTX reduces disease activity to a greater extent and slows radiographic progression further than achieved by monotherapy with either of the agents (83).

Etanercept is a soluble p75 TNF receptor fusion protein that consists of two p75 TNF receptor extracellular domains bound to the Fc portion of immunoglobulin G1 (IgG1). It is capable of also binding lymphotoxin.

Infliximab is a mouse chimeric monoclonal antibody directed against TNF. Within infliximab, the VL and VH domains of the antigen-binding portion of the molecule are murine, and the constant Fc domain is human IgG1.

Adalimumab is a recombinant fully human monoclonal antibody and therefore associated with a lower risk of anti-drug antibody formation compared with chimeric or humanised anti-TNF preparations.

Certolizumab pegol is a Fab' fragment of a humanised IgG1 monoclonal anti-TNF antibody that is chemically linked to polyethylene glycol. It neutralizes membrane-associated and soluble TNF- α . In contrast to other anti-TNFs, Certolizumab does not contain an Fc portion and therefore does not induce complement activation, antibody-dependent cellular cytotoxicity or apoptosis.

Golimumab is a human monoclonal antibody that binds to both the soluble and transmembrane bioactive forms of human TNF- α .

IL-1 inhibitors

By comparison to the TNF inhibitors, inhibition of IL-1 had a smaller impact on RA. Anakinra, a recombinant human IL-1Ra differs from the native human protein in that it is not glycosylated and has an additional N-terminal methionine. The effects of Anakinra were only modest in most RA patients (46) whereas effectiveness of other IL-1 inhibitors such as Rilonacept, an IL-1R fusion protein and Canakinumab, an IL-1 β monoclonal antibody in RA has not been established.

IL-6 inhibitor

Tocilizumab is a humanized anti-human IL-6 receptor antibody having complementarity determining regions of a mouse anti-human IL-6 receptor monoclonal antibody grafted onto human IgG1. Tocilizumab competes for both the membrane-bound and soluble forms of human IL-6 receptor, thereby inhibiting the binding of the native IL-6 to its receptor and interfering with its effects.

Abatacept

Abatacept (also called CTLA4-Ig) is a soluble fusion protein comprising CTLA-4 and the Fc portion of IgG1. It prevents activation of T cells by competing with CD28 to bind to its counter-receptor, CD80/CD86, due to its higher affinity for CD80/CD86. Abatacept was initially available only for intravenous use but can also be administered subcutaneously (88).

Rituximab

Rituximab is a B cell mouse chimeric monoclonal anti-CD20 antibody. Rituximab causes B cell depletion through antibody dependent mechanisms (89), which include Fc receptor gamma-

mediated antibody-dependent cytotoxicity, antibody-dependent complement mediated cell lysis, growth arrest and B cell apoptosis. Rituximab is given in combination with MTX (90).

Table 1.4 Biologic DMARDs

Agent	Target	Structure	Usual dose	Half-life
Infliximab	TNF- α	Chimeric monoclonal antibody	IV – 3mg/kg in combination with MTX at 0, 2, 4 weeks, thereafter every 8 weeks	9 days
Etanercept	TNF- α	TNFRII-IgG fusion protein	SC – 50mg/week with or without MTX	4 days
Adalimumab	TNF- α	Human monoclonal antibody	SC – 40mg/every fortnight with or without MTX	14 days
Certolizumab	TNF- α	Pegylated humanised Fab' fragment of monoclonal antibody	SC – 400mg at 0, 2, 4 weeks, thereafter 200mg every fortnight	14 days
Golimumab	TNF- α	Human monoclonal antibody	SC – 50mg every 4 weeks in combination with MTX	14 days
Anakinra	IL-1	IL-1 receptor antagonist	SC – 100mg/day	4-6 hours
Abatacept	T cell	CTLA4-IgG fusion protein	IV – 500mg, 750mg or 1gm for body weight 60, 60-100 and >100kg at 0, 2, 4 weeks, thereafter every 4 weeks SC – weight-based iv loading dose, thereafter 125mg SC/week	14 days
Tocilizumab	IL-6	Humanised IL-6 receptor antibody	IV – 8mg/kg every 4 weeks	14 days
Rituximab	B cell	Chimeric anti-CD20 antibody	IV – 1gm infusion separated by 2 weeks, not to be repeated sooner than 16 weeks	7 days

TNF- α , tumour necrosis factor- α ; MTX, methotrexate; SC, subcutaneous; IV, intravenous.

1.1.2c Targeting intracellular signaling pathways in RA

Recent evidence suggests hierarchical importance of JAK pathways amongst the intracellular signalling pathways in the pathogenesis of RA. Tofacitinib, a JAK 3 and 1 inhibitor in phase 2 clinical trials demonstrated an acceptable safety and therapeutic efficacy, which was equivalent to the current biologics (91, 92). Inhibition of spleen tyrosine kinase by Fostamatinib, is effective in some subgroups of RA patients (93, 94). In contrast, despite a strong preclinical rationale, the targeting of p38 mitogen-activated protein kinase has been disappointing in clinical settings.

1.2 IL-17 family of cytokines

IL-17 which was identified in 1995 lacked sequence similarity with any other known family of cytokines and was therefore classified as a new family of cytokines. The IL-17 family now includes 6 members, IL-17A to IL-17F (Table 1.5). Amongst these IL-17A and IL-17F are best characterised and shown to play a role in host defence and autoimmunity.

1.2.1 IL-17A

IL-17A, also termed IL-17 is the prototype IL-17 cytokine. IL-17A is produced mainly by activated peripheral CD4⁺ T lymphocytes (95, 96) but also other cells such as CD8⁺ T lymphocytes (97), $\gamma\delta$ T cells (98), natural killer T (NKT) cells, natural killer (NK) cells (99), dendritic cells (100), mast cells (36) lymphoid-tissue inducer (LTi)-like cells, paneth cells and neutrophils (101). Human IL-17 mRNA is detected in neutrophils, eosinophils and monocytes (102, 103).

IL-17 mediates predominantly proinflammatory and hematopoietic responses. IL-17A stimulates secretion of TNF- α , IL-1 β , IL-6, IL-8, G-CSF, ICAM-1 and PGE2 from fibroblast, endothelial, epithelial and macrophage cells (96, 104-107). IL-17 mediates activation of neutrophils through promotion of granulopoiesis (108, 109) and expression of ELR-positive CXC chemokines CXCL1/KC/GRO α and CXCL5/LIX in mice (110-113) and IL-8 in humans (96). The action of IL-17 is synergistic to both IL-1 β and TNF- α (114-116).

IL-17 plays a critical role in host defence against extracellular pathogens in epithelial and mucosal tissues such as the skin, lung and intestine. IL-17R signalling is required for host defence against extracellular bacterial and fungal infection in the skin and lung (117). Th17 cell differentiation is promoted in response to muramyl dipeptides from bacterial cell walls and β -glucans in zymosans and fungi (118). IL-17 promotes expression of various anti-microbial genes including acute phase reactant protein lipocalin 2/24p3 (119) and molecules with direct antimicrobial activity, such as β -defensins, mucins and calgranulins (120-122).

IL-17A plays an important role in the initiation and/or maintenance of an inflammatory response in autoimmune conditions such as RA, multiple sclerosis, psoriasis and inflammatory bowel disease (123-126).

Regulatory effects of IL-17A

Although identified as a predominantly proinflammatory cytokine, IL-17A has also been shown to exert protective effects. In asthma, IL-17A although is required for antigen-sensitization, it plays a protective role in the effector phase of the disease (127).

In GVHD, the weight loss and diarrhoea is accentuated in the absence of IL-17A, mainly due to increase in IFN- γ (128). In the dextran sodium sulfate-induced colitis model, IL-17A plays a protective role against epithelial ulceration, mainly due to decreased IFN- γ and osteopontin (129) in contrast to pathogenic IL-17F, which contributes to excessive tissue damage and wasting disease (130).

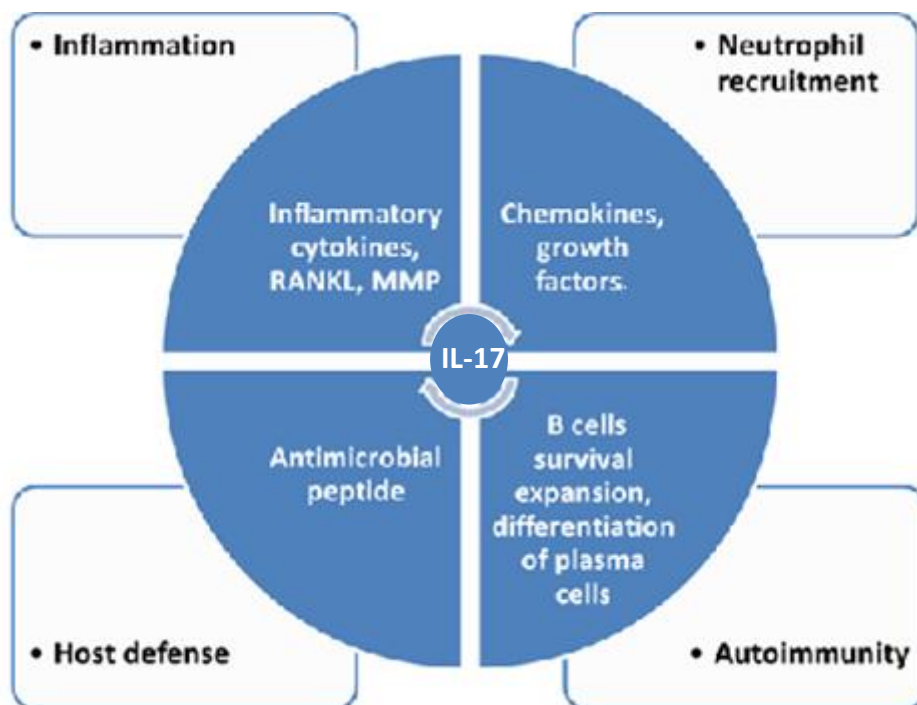


Figure 1.3 Biological functions of IL-17. IL-17 mediates tissue inflammation and damage, leads to autoimmunity and protects the host against infections by inducing secretion of inflammatory cytokines, MMPs, RANKL, chemokines and growth factors in cell of target tissues, promoting the survival and expansion of B-cells and the differentiation of B-cells into antibody-producing plasma cells and acting directly on epithelial cells of peripheral tissues to promote release of peptides with antibacterial properties such as defensins, regenerating proteins and S100 proteins.

Table 1.5 IL-17 cytokine family

Family member	Size (aa)	% Homology (to IL-17A)	% Homology (mouse/human)	Produced by	Receptor complex	Receptor	Main functions
IL-17A	155	100	62	Th17 cells, CD8+T cells, $\gamma\delta$ T cells, NK cells, NKT cells, LTi cells	IL-17RA/RC	Prefer IL-17RA to IL-17RC	Promote autoimmune diseases and protect against extracellular bacterial and fungal infection
IL-17F	163	55	77	T cells, innate immune cells, epithelial cells	IL-17RA/RC	Prefer IL-17RC to IL-17RA	Drive inflammation and autoimmunity, neutrophil recruitment
IL-17B	180	29	88	Cells of gastrointestinal tract, pancreas and neurons	–	IL-17RB	Activate TNF- α and IL-1 β release in THP-1 cells
IL-17C	197	23	83	Cells of prostate, foetal kidney	–	IL-17RE	Activate TNF- α and IL-1 β release in THP-1 cells
IL-17D	202	25	78	Cells of muscles, brain, heart, lung, pancreas, adipose tissue	–	Unknown	Promote proinflammatory gene profile in endothelial cells
IL-17E	161	17	81	Th2 cells, mast cells, alveolar macrophages, eosinophils, epithelial cells, brain capillary endothelial cells	IL-17RB/RA	Prefer IL-17RB to IL-17RA	Promote type 2 immune response and inhibit autoimmune diseases

aa, amino acid; Adapted from Alcorn JF *et al.* Annu Rev Physiol 2010; 72:495-516 and Zhang X *et al.* Protein Cell 2011; 2: 26–40

1.2.2 IL-17F

Amongst all IL-17 family members, IL-17F is most closely related to IL-17A sharing 55% structural homology, receptor binding and biological functions. The *IL-17f* and *IL-17a* genes are co-localised at 6p12 into a tail-to-tail orientation, only 50kb apart (GenBank accession no. AL391221), which points towards a potential gene duplication event.

Two different but functionally similar isoforms of human IL-17F have been identified (the longer and the shorter isoform) (131). The full-length IL-17F contains 163 amino acid residues and like IL-17A is secreted as a disulfide-linked homodimeric glycoprotein. The crystallographic structure of IL-17F revealed a cystine knot fold, which is similar to neurotrophin growth factors (132).

IL-17F has a much wider expression than IL-17A suggesting that IL-17F has more biological functions. Rapid scan gene expression panel showed a strong expression of IL-17F in liver, lung, spleen, placenta, adrenal gland, ovary, and foetal liver. In addition, IL-17F expression was upregulated in activated PBMCs, activated Th0, Th1, and Th2 cells, activated basophils, activated mast cells, and activated peripheral blood CD4⁺ T but not CD8⁺ T cells and monocytes. In contrast, *IL-17a* gene expression is increased only in activated peripheral blood CD4⁺ T cells, Th0 clones and PBMCs.

IL-17F is generally co-expressed with IL-17A in naive T cells under Th17 polarising conditions. The possibility of differential ratios of these two cytokines in different T cell states or in different tissues has been suggested (130).

Like IL-17A, IL-17F induces many proinflammatory cytokines and chemokines. It induces TGF- β , IL-2 in endothelial cells (133); ICAM-1, GM-CSF in airway bronchial epithelial cells (131, 134); and IL-6 and CXCL-1 in fibroblasts and epithelial cells (130). In lung fibroblasts, IL-17F induces CCL2, CCL7, TSLP and MMP-13 (130). IL-17F by stabilising mRNA transcript synergises with other cytokines (135). In combination with TNF- α , IL-17F induces G-CSF expression in human bronchial epithelial cells (136) and, together with IL-22, IL-17F induces antimicrobial-peptides, hBD-2, S100A7, S100A8 and S100A9 (121).

IL-17F along with IL-17A is required for host defence to extracellular bacteria and fungi in skin and mucosal epithelial tissues (137, 138). IL-17F, however, plays a less important role than IL-17A in systemic infection of *C. albicans*. It was shown that only Il17a^{-/-} mice but not Il17f^{-/-} mice, showed increased susceptibility to candidial infection (139).

Studies in Il17a^{-/-} mice and Il17f^{-/-} mice indicated that in comparison to IL-17A, IL-17F plays a minor role in driving autoimmunity (130, 138). In experimental autoimmune encephalitis (EAE) while both the IL-17A and IL-17F contributed to the chronic inflammatory phase, IL-17A was more important initiating factor than IL-17F.

IL-17F also may function differently than IL-17A in mediating allergy and autoimmunity. IL-17F is more important than IL-17A in allergen-mediated immune response (130). Mice deficient in IL-17F, but not IL-17A show defective airway neutrophilia in response to allergen challenge. A sustained expression of IL-17F mediates tissue infiltration by lymphocytes and macrophages, and mucus hyperplasia in asthma suggestive of a regulatory rather than a pathogenic role for IL-17F in this condition (127, 130, 140). In the dextran sulfate sodium (DSS)-induced colitis model, IL-17F played a pathogenic role as opposed to IL-17A, which plays a protective role (129, 130).

Hymowitz *et al.* demonstrated that, *in vitro*, IL-17F induced cartilage matrix release and inhibited new cartilage matrix synthesis with an efficiency that was comparable to IL-17A (132). *In vivo* studies in IL-17F-deficient mice however, showed that the development of arthritis in Il17f^{-/-}/Il17ra^{-/-} mice was partially suppressed whereas CIA developed normally in the Il17f^{-/-} mice (138). These findings suggest that IL-17F, although contributing to the development of arthritis in IL-1 receptor antagonist-deficient mice, is not required for CIA.

1.2.3 IL-17A/F heterodimer

As activated T cells from both mouse and humans co-express IL-17F and IL-17A (107, 133, 141), existence of IL-17A/IL-17F heterodimer appeared to be a strong possibility, which has now been confirmed (142, 143). While mouse Th17 cells secrete all the three isoforms IL-17A, IL-17F and IL-

17A/F (142, 144), human CD4+T cells expressed IL-17A/F heterodimer and IL-17F homodimer but almost no IL-17A homodimer (143). *In vitro* functions of the IL-17A/F heterodimer are similar to IL-17A and IL-17F (144). The activity of the IL-17A/F heterodimer was reported to be intermediate of IL-17A and -17F by Wright *et al.* (143), whereas nearly equal to IL-17A homodimers but greater than IL-17F by Liang *et al.* (144).

1.2.4 Other IL-17 cytokine family members

1.2.4a IL-17B and IL-17C

IL-17B and IL-17C share 20-25% sequence identity with IL-17A. The absence of AU-rich repeats in IL-17B resulting in a translation product of more stable message points towards the possibility of a constitutive serum presence of the protein (145). IL-17C was detectable in CD4+ T cells in CIA mice, which suggests that besides IL-17A and IL-17F, expression of IL-17C also takes place at inflammatory sites. IL-17C-induced neutrophil responses were comparable to IL-17A and IL-17F (146) whereas the potency of IL-17B in inducing PMN infiltration was about 10 times less than IL-17A (147). A study by Yamaguchi *et al.* demonstrated that IL-17B and IL-17C but not IL-17A is directly associated with *in vivo* production of TNF- α (148).

1.2.4b IL-17D

IL-17D, similar to IL-17A and IL-17F, stimulates the production of IL-6, IL-8, and GM-CSF in endothelial cells. However, it inhibits the haematopoiesis of myeloid progenitor cells (149).

1.2.4c IL-17E

Human IL-17E, also called IL-25, is a 177 amino acid residues precursor protein (150). IL-17E promotes the expression of the prototypical Th2 genes (146, 151, 152) and appears to be an important mediator of allergic diseases.

1.2.5 (H161R) IL-17F mutant

(H161R) IL-17F mutant is a natural variant of IL-17F, a result of substitution of Histidine by Arginine at amino acid 161 in the third exon. Homozygotes of the (H161R) IL-17F mutant were protected from asthma in a Japanese population (OR 0.06, 95% CI 0.01-0.43, $p = 0.0039$) (153). *In vitro* studies revealed that the (H161R) IL-17F mutant was a competitive inhibitor of the wild-type IL-17F and lacked the ability to activate upstream signaling pathways and induction of cytokine and chemokine secretion in bronchial epithelial cells. Studies in Chinese and European American populations, however, failed to find a similar association between asthma and the IL-17F mutant (154, 155). On the contrary, in a Chinese subpopulation of male asthma patients, the mutant allele was associated with increased risk of susceptibility to the disease. The lack of association in the European American population may be related to a much lower frequency of the mutant, which was only 4.5% as compared to 11.4% in Japanese population.

The association of the (H161R) IL-17F mutant with the risk of susceptibility to various other diseases has been summarised in Table 1.6. In keeping with the observations in asthma, the (H161R) IL-17F mutant was inversely associated with susceptibility to idiopathic thrombocytopenic purpura (ITP) in Japanese; ulcerative colitis in Japanese and Chinese, albeit weakly but not in Caucasian population (156-159). In the Japanese population, there was no association between the mutant and overall susceptibility to psoriasis vulgaris, functional dyspepsia or gastric carcinoma (160-162).

Similar to Japanese asthmatic patients, the (H161R) IL-17F mutant was protective against chronic fatigue syndrome in Europeans and Behcet's disease in the Korean population (163, 164)

whereas, studies in Chinese Han population showed that (H161R) IL-17F mutant was not a major contributor to the pathogenesis of myocardial infarction in men and it did not increase the susceptibility to breast carcinoma in women (165, 166).

Paradowska-Gorycka *et al.* investigated association between (H161R) IL-17F polymorphism in 220 Polish patients with RA and 106 healthy subjects and reported that, although the (H161R) IL-17F mutant did not increase the overall susceptibility to RA, it was associated with a higher number of

tender joints, higher DAS 28 and higher HAQ score implying that (H161R) IL-17F polymorphism might be associated with an increased disease activity in RA (167).

Table 1.6 Association of (H161R IL-17F) mutant with the risk of susceptibility to various diseases

Disease	Population	Disease Association	OR	Reference
Asthma	Japanese	Inverse	CC - 0.06(0.01-0.43), p=0.039 TC - 1.32 (0.95-1.84), p= 0.08	137
Asthma	Chinese male	Direct	1.58 (106-236), p=0.0148	138
Asthma	White women	None	–	139
UC	Chinese	Weak Inverse	TC - 0.96(0.94-0.96)	140
UC	Japanese	Inverse	TT- 1.81(1.01-3.23), p=0.045	141
IBD (UC+CD)	Caucasian	None	–	142
ITP	Japanese	Inverse	TC/CC-0.48(0.27-0.84), p=0.016	143
Ca-breast	Chinese han women	None	–	150
FD	Japanese	None	–	144
Ca-stomach	Japanese	None	–	145
Behcet's Disease	Korean	Inverse	CC - 0% vs 8.3%, p<0.001 TC - 9.6% vs 1.3%, p<0.001	148
CFS	European	Inverse	TC/CC - 8.9% vs 28.5%, OR 4.05, p=0.0018	147
Psoriasis Vulgaris	Japanese	None	–	146
MI	Chinese Han	None	–	149
RA	Polish	None	–	151

OR, odds ratio; CFS, chronic fatigue syndrome, IBD, inflammatory bowel disease; UC, ulcerative colitis; CD, Crohn's disease; RA, rheumatoid arthritis; MI, myocardial infarction; FD, functional dyspepsia; ITP, idiopathic thrombocytopenic purpura.

1.2.6 IL-17 receptor family

The IL-17 receptor family comprises five receptor subunits, IL-17RA to IL-17RE (Table 1.7). The genes encoding human receptors cluster on chromosome 3, except IL-17RA which is located on chromosome 22. All the receptor subunits are single transmembrane domain proteins and contain certain conserved structural motifs, an extracellular fibronectin III-like domain and a cytoplasmic similar expression of fibroblast (SEF)/IL-17R (SEFIR) domain (168). In addition, IL-17RA also contains two extra domains, a TILL [TIR (Toll/IL-1R) like loop] domain close behind the SEFIR domain and a Distal domain in the C-terminus. IL-17RA is a common subunit that forms heterodimeric complexes with other IL-17 receptors.

1.2.6a IL-17RA

IL-17RA mRNA is expressed in virtually all cells and tissues tested. The ubiquitous expression of IL-17RA is consistent with its wide range of effects (169). The expression of IL-17RA is particularly high in hematopoietic tissues (95, 138). In contrast to most cytokines receptors, high levels of IL-17RA seem to be required for an effective response (119, 170). As the signaling strength of IL-17A correlates with cell surface expression levels of IL-17RA, a dynamic regulation of IL-17RA seems to be biologically important. IL-15 and IL-21 upregulate its expression while phosphoinositide 3 kinase (PI3K) limits the expression of IL-17RA in T cells (171, 172). The surface expression of IL-17RA rapidly decreases after it binds to IL-17A due to receptor internalisation. IL-17RA might therefore also limit the signalling by clearing itself from the inflammatory milieu (171). IL-17RA binds to IL-17A with a strong affinity (95), and although weakly to IL-17F, is necessary for signal transduction mediated by IL-17A, IL-17F and IL-17A/F heterodimer.

IL-17RA complex formation

IL-17RA forms heteroreceptor complexes with other IL-17 receptors. It pairs with IL-17RC to induce responses to IL-17A and IL-17F (173). IL-17RA couples with IL-17RB to form IL-17A/B receptor complex (174) and forms a receptor complex with IL-17RD (175). However, no ligand for an IL-17RA/IL-17RD receptor complex has yet been identified.

Studies using fluorescence resonance energy transfer (FRET) showed that formation of IL-17RA complexes is independent of its ligands (176-178). It is not known whether IL-17RC is pre-assembled with IL-17RA to any degree (173). It seems that IL-17RA dimers either dissociate after ligand binding and are replaced by IL-17RA/IL-17RC heterodimers or IL-17RC might be recruited to the IL-17RA dimer to create a trimer or a multimer. Like TNFR, IL-17RA also contains a fibronectin III-like pre-ligand assembly domain (PLAD) (176).

The crystallographic structure of IL-17RA bound to IL-17F showed that it binds to IL-17F in 1:2 stoichiometry. IL-17RA forms an extensive binding interface with IL-17F with the major interaction taking place at three different sites (179). At the sites 1 and 2, IL-17RA D1 binds with strands 2 and 3 of IL-17F whereas site 3 is formed between the IL-17RA D2 F G loop (Cys259–Arg265) and the C-terminal regions of strands 3 and 4 of IL-17F chain A, and the N-terminal extension of IL-17F chain B. Site 3 is rich in charged interactions with nine potential hydrogen bonds and a salt bridge. Once IL-17 is engaged by two fibronectin-type domains of IL-17RA, binding of the first receptor to IL-17 modulates its affinity and specificity of the second receptor-binding event to promote a heterodimeric rather than homodimeric complex formation.

IL-17RA as a common receptor

IL-17RA is able to associate with other IL-17 family members and seems to act as a shared receptor, analogous to those in class I cytokine receptor complexes. IL-17RA is used as a common signaling subunit by at least four ligands. IL-17RA binds both IL-17A and IL-17F, and also IL-17E/IL-17RB receptor complex, and was shown to associate with IL-17RD to form IL-17RA/RD receptor complex. Mapping of the residues conserved among the IL-17 family members onto the IL-17RA-IL-17F complex showed that IL-17RA appears to use a strategy of cross-reactivity based on a subset of conserved and distinct binding sites amongst the several IL-17 family members. IL-17RA contacts the conserved residues with the N-terminal region of the D1 domain and the D2 FG loop domain whereas the IL-17RA C'–C loop interacts mainly with IL-17 residues that differ around the receptor-binding pocket.

Table 1.7 IL-17 receptor family

Family member	Size (aa)	% Homology (to IL-17RA)	% Homology (mouse/human)	Distribution	Ligand	Binding bias	Main functions
IL-17RA	818	100	69	Ubiquitous, high levels in haematopoietic tissues	IL-17A, IL-17F, IL-17E	Prefer IL-17A to IL-17F	Necessary for signal transduction by IL-17A, IL-17F, IL-17E
IL-17RC	791	22	68	Non haematopoietic tissues such as colon, small intestine, lung, prostate	IL-17A, IL-17F	Prefer IL-17F To IL-17A	Complexes with IL-17RA to mediate IL-17 signaling
IL-17RB	502	19.2	76	Th2 cells, various endocrine tissues, kidney, liver	IL-17B, IL-17E	Prefer IL-17B to IL-17E	Pairs with IL-17RA to form a functional receptor complex for IL-17E
IL-17RD	739	–	–	Kidney, heart, small intestine, colon, skeletal muscles, brain, lung, spleen	IL-17A?, FGF?	Interaction with IL-17RA	Mediate IL-17 signaling, inhibit FGF signaling and facilitate EGF signaling
IL-17RE	667	–	–	NA	IL-17C	Prefer IL-17C	Might promote proliferation

IL-17R, Interleukin-17 receptor; FGF, fibroblast growth factor; FGF-R, fibroblast growth factor receptor; EGF, epidermal growth factor; NKT, natural killer T; LTi, lymphoid tissue inducer; THP-1 cells, a human leukemia monocytic cell line; Th, T helper.

1.2.6b IL-17RC

IL-17 receptor C (IL-17 RC, also known as IL-17 RL and IL-17R hom) contains 791 amino acids. The gene for human IL-17RC contains 19 exons and more than 90 splice isoforms of IL-17RC have been identified in human prostate cancer lines (180). The full length IL-17RC isoform occurs 10% of the time, while the three most common isoforms, as a group, occur about 50% of the time. Alternative splicing of IL-17RC appears to regulate ligand specificity. There is a ligand preference of IL-17RC splice isoforms as certain forms bind preferentially to IL-17A or IL-17F. Moreover, some isoforms do not bind either cytokine, suggesting that there might be additional ligands for this receptor subunit (181).

IL-17RC contains a SEFIR domain but not an obvious TILL domain. IL-17RC cannot induce signaling in the absence of IL-17RA and is required for both IL-17A- and IL-17F-mediated signaling. In humans, IL-17RA binds with extremely low affinity to IL-17F but IL-17RC binds to IL-17F with an affinity higher than IL-17A (181). Soluble IL-17RA can efficiently block IL-17A-dependent but not IL-17F-dependent responses in human cells, providing an opportunity to selectively target individual cytokines (181). In mice, IL-17RA binds both IL-17A and IL-17F, whereas IL-17RC binds strongly only to IL-17F. These species dependent differences in receptor binding are important in evaluating IL-17-specific therapeutics in pre-clinical models. There is also species-dependent interaction between the IL-17R subunits. Only mouse IL-17RA can reconstitute IL-17A-dependent signaling in mouse *Il17ra*^{-/-} fibroblasts and co-operation of human but not mouse IL-17RC with human IL-17RA could induce signaling by human IL-17 in these cells (173).

IL-17RA and IL-17RC subunits have reciprocal expression patterns, which indicate tissue-dependent activities (138, 181). In contrast to IL-17RA, expression of IL-17RC is low in haematopoietic tissues whereas seen predominantly in non-immune cells such as prostate, liver, kidney, thyroid and joints (181, 182). Therefore cells with high IL-17RC expression could be highly responsive to IL-17F, whereas those with low IL-17RC expression and high IL-17RA expression might respond better to IL-17A.

1.2.6c Other IL-17 receptors

Recent evidence suggests that IL-17RB pairs with IL-17RA to form a functional receptor complex (174). IL-17 RB binds strongly to IL-17E (150), weakly to IL-17B and does not bind IL-17A, IL-17C and IL-17F.

IL-17RD seems to be the most evolutionary ancient member of the IL-17R family (183). IL-17RD can interact with IL-17RA, although the biological importance of this association remains unclear (175).

IL-17RD has no known ligand.

IL-17RE is highly spliced; six isoforms have been identified in EST databases. Recent studies suggest that its ligand is IL-17C (184).

1.2.7 IL-17-induced signaling pathways

Both IL-17A and IL-17F bind to the IL-17RA and IL-17RC heterodimeric complex to transduce downstream signaling. IL-17 activates many common downstream signaling pathways including nuclear factor kappa light enhancer of activated B cells (NF- κ B), mitogen-activated protein kinases (MAPKs), c-Jun N-terminal kinase (JNK), p38 and extracellular-signal regulated kinase (ERK), CCAAT/enhancer-binding proteins (C/EBPs), phosphoinositide 3-kinase /Janus kinase (PI3K/JAK) and signal transducer and activator of transcription (JAK/STAT) (Fig. 1.4). In addition, IL-17 stabilizes mRNA of some proinflammatory cytokines and chemokines induced by TNF- α (185-188).

The IL-17R family members encode a novel, conserved signalling motif termed: similar expression of fibroblast (SEF)/IL-17R (SEFIR) domain (168). The SEFIR domains of both IL-17RA and IL-17RC are required to activate NF- κ B, MAPK, and C/EBP pathways in response to IL-17A or IL-17F (189, 190).

TRAF6, an adaptor and E3 ubiquitin ligase is essential for IL-17A signaling (191). A cytoplasmic protein, Act1, also known as CIKS (connection to I κ B kinase and stress-activated kinase) contains both SEFIR (192, 193) and a TRAF6 binding motif (194). Act1 directly associates with IL-17RA and IL-17RC via interaction with each SEFIR domain, resulting in the recruitment of TRAF6 and TGF β -activated kinase 1 (TAK1) to activate NF- κ B. In addition to NF- κ B activation, Act1 also mediates IL-

IL-17-induced MAPK activation and C/EBP induction pathways. One report has shown that IL-17 can activate the JAK1/2 and PI3K pathway, which co-ordinates with the NF- κ B-activating pathway of Act1/TRAF6/TAK1 (195).

CXCL1 mRNA stabilization in response to IL-17A is dependent on Act1, but not TRAF6. Recently, inhibitor of κ B kinase I (IKKi) was shown to be important for IL-17-induced phosphorylation of Act1, which is critical for the formation of the Act1–TRAF2–TRAF5 signal complex required to mediate IL-17-induced mRNA stability through dissociation of alternative splicing factor (ASF) from mRNA (186, 187).

IL-17R signaling activates ERK to phosphorylate Thr188 of C/EBP β , which is required for Thr179 phosphorylation of C/EBP β by GSK3 β (glycogen synthase kinase 3 β). The dual phosphorylation of C/EBP β inactivates itself, resulting in the suppression of IL-17-mediated downstream gene induction. TRAF3 in association with Act1 negatively regulates IL-17A-mediated NF- κ B and MAPK activation. (196, 197). A recent study showed that persistent stimulation with IL-17 resulted in β transducin repeat-containing protein (β -TrCP)-mediated ubiquitination of Act1 for its subsequent degradation, and consequently desensitization of IL-17R signaling for the prevention of persistent inflammation (198).

At the downstream of the C-terminus of the IL-17RA, motif TIR-like loop (TILL) (170) bears homology to TIR (Toll/IL-1R) domain of the Toll-like receptor (TLR). The TILL domain is vital for signal transduction by IL-17. Mutations specific to this region, abrogate all IL-17-induced responses. Despite its similarity with TIR domain, IL-17 does not utilize myeloid differentiation primary response protein 88 (MyD88), TIR domain-containing adaptor inducing IFN- β (TRIF), IL-1R-associated kinase 4 (IRAK4) or IRAK1 for cytokine induction (170, 196, 199).

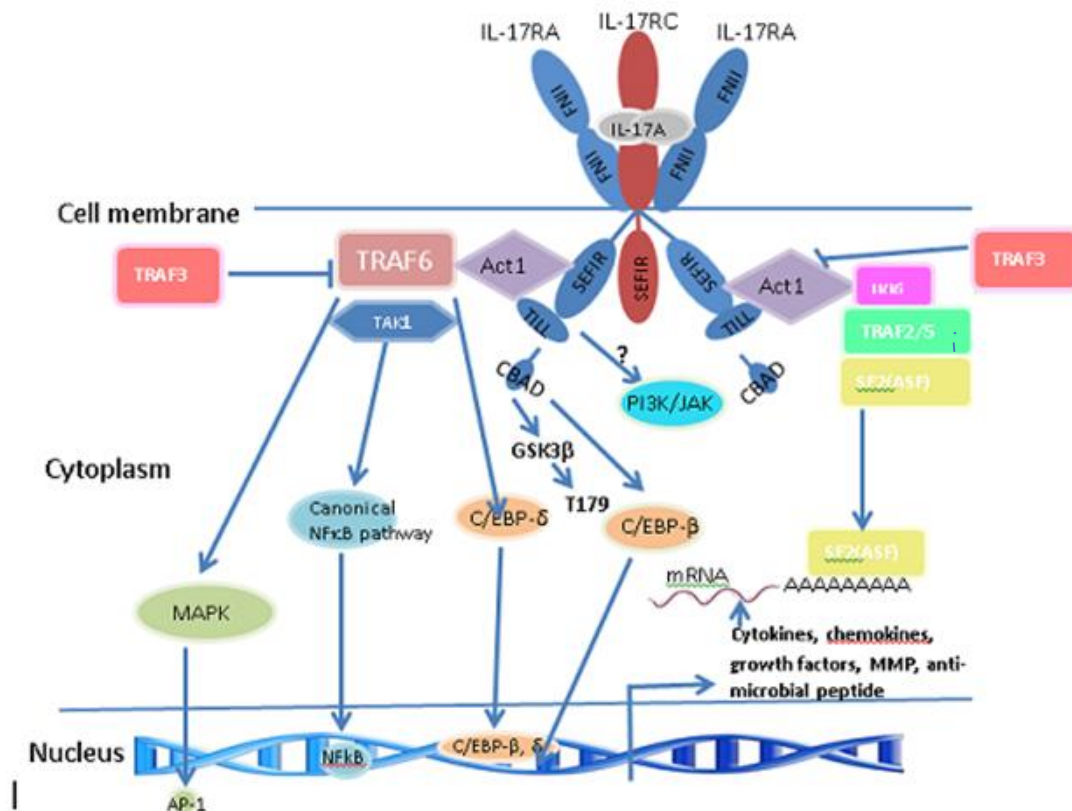


Figure 1.4 IL-17-induced signaling pathways. (a) Both IL-17A and IL-17F bind to a heteroreceptor complex composed of IL-17RA and IL-17RC to transduce downstream signaling. Both IL-17RA and IL-17RC encode SEFIR domains whereas IL-17RA also encodes additional TILL and distal units. IL-17RA and IL-17RC interact with SEFIR domain-containing adaptor Act1, which in turn recruits TRAF6 required for the activation of the NF- κ B, MAPK pathways and induction of C/EBP. The TILL domain of IL-17RA is important for inducible phosphorylation of C/EBP β on threonine 179, which is mediated by GSK3. IL-17 probably also activates the JAK/PI3K pathway. IL-17 mediates TRAF6 independent mRNA stability by formation of another complex Act1-IKKi-TRAF2-TRAF5-SF2 (ASF). In contrast, TRAF3 negatively regulates IL-17R by interfering with the formation of the IL-17R-Act1-TRAF6 complex. TNFR 6, TNFR associated factor 6; IKKi, I κ B kinase i; SF2(ASF), splicing factor 2 (alternative splicing factor); C/EBP, CCAAT enhancer binding protein; GSK3, glycogen synthase kinase 3; CBAD, C-enhancer binding protein activation domain; NF- κ B, nuclear factor kappa light chain enhancer of activated B cells; MAPK, mitogen activated protein kinase; PI3K/JAK, phosphoinositide 3 kinase/Janus kinase; FN, fibronectin III-like domain; SEFIR, similar expression of fibroblast/IL-17R; TILL, Toll/IL-1R (TIR)-like loop.

1.3 Th17 cells

Th17 cells are a subset of CD4⁺ effector T cells that are different from Th1 and Th2 cells (200). Th1 cells mainly produce IFN- γ and are involved in immunity against intracellular pathogens while Th2 cells produce IL-4, IL-10 and IL-13 and are responsible for immunity against parasites and mediation of allergic responses. In contrast to Th1 and Th2 cells, Th17 cells preferentially secrete IL-17A, IL-17F, IL-21, IL-22 and IL-26 (201-203). In healthy individuals, approximately 1% circulating CD4⁺ T cells produce IL-17. Th17 cells play a role in defence against extracellular pathogens (137, 204, 205) and along with Th1 cells are implicated in autoimmune diseases. More recently, a regulatory role of Th17 cells in the form of protection against tissue damage during inflammation has been identified. Evidence now suggests that depending on the microenvironment of various diseases, naïve CD4⁺ T cells can differentiate into either proinflammatory or protective Th17 cells to mediate a diverse set of responses in infection, autoimmunity and immunodeficiency.

1.3.1 Differentiation of Th17 cells

TGF- β and IL-6 are critical for mouse Th17 cell differentiation (204, 206, 207). IL-21, IL-23, IL-1 β and TNF- α provide additional amplificatory signals (204, 206-210). However, IL-6 signaling was dispensable for the induction of pathogenic Th17 cells and induction of EAE in mice lacking Treg cells (211) and more recently, a TGF- β independent differentiation of naïve murine T cells was demonstrated in the presence of IL-6, IL-1 β and IL-23 (212).

Production of IL-17 in humans is dependent on IL-23, IL-1 α , IL-1 β , IL-6 and TGF- β . The combined activity of IL-1 β and IL-23 (or IL-6) is critical in the development of Th17 cells (212, 213). In the absence of IL-1, IL-23 and IL-6 are unable to induce IL-17. It was demonstrated that human IL-17A-producing cells originated from CD161⁺CD4⁺ T cell precursors from human umbilical cord blood (UBC) and post-natal thymus in the presence of both IL-1 β and IL-23 but no other cytokine(s) including TGF- β , IL-6 and IL-21 (214, 215). The CD161⁺CD4⁺ T cell expressed both IL-23R and RORC. IL-23 is required for optimum expansion and activation but not for the differentiation of naïve Th17

cells (216-218). *In vitro*, IL-6 in conjunction with T cell antigen receptor activation induces the expression of IL-21 in naive CD4⁺ T cells, which together with TGF- β , independently of IL-6 can induce expression of IL-17 in mice and humans. In contrast, *in vivo* the absence of IL-21 signaling has little effect on Th17 cell differentiation (208, 219-221).

In initial studies, differentiation of human Th17 cells was shown to be both, TGF- β -independent (222-225) or dependent (226-228). A few earlier reports even indicated that TGF- β actually inhibited Th17 cells (222, 223, 225, 229, 230). In T-bet and STAT6-deficient T cells, IL-6 alone, even in the absence of TGF- β can induce IL-17 production (231). Santarlasci *et al.* showed that addition of TGF- β to IL-1 β and IL-23 increased the relative proportions of CD161⁺ T cells that differentiate into Th17 cells by inhibiting T-bet expression and Th1 development (232). Ichiyama *et al.* demonstrated that TGF- β JNK c-Jun signaling strongly suppressed T Box factor Eomesodermin (Eomes) expression which directs T cell differentiation to Th1 cells and suppresses Th17 development (233). Taken together, all these findings suggest an indirect role of TGF- β in the regulation of Th17 by suppressing Th1 and Th2 cell differentiation. It is yet unknown whether human Th17 cells also produce TGF- β .

The cytokine environment at the time of differentiating Th17 cells determines the pathogenicity of cells (Fig. 1.5). Th17 cells can differentiate in the presence of IL-1 β and IL-6 in combination with TGF- β or alternatively in combination with IL-23 in the absence of TGF- β . The IL-23-differentiated Th17 cells express T-bet, CXCR3, IL-18R1 in addition to IL-17 and could turn into IL-17/IFN- γ double producing cells. On the other hand, the TGF- β -differentiated Th17 cells express IL-17 along with AhR, CCL20, IL-9 and IL-10. The IL-23 differentiated but not the TGF- β differentiated Th17 cells therefore are pathogenic (234, 235). The former subset of Th17 cells often represent a mixed Th1- and Th17-mediated pathology and seem more relevant in terms of autoimmune diseases. In contrast, the Th17 cell population generated in environments with high TGF- β have limited pathogenic potentials but would be useful in host defence (236-238).

Interestingly, *in vitro* TGF- β also induces differentiation of Tregs, cells having properties reciprocal to Th17 cells (239). At lower concentration, together with IL-6 or IL-21 and in the presence of IL-23,

TGF- β induces IL-23R and promotes Th17 differentiation and expansion. In contrast, at higher concentrations, TGF- β inhibits IL-23R, IL-22 and IL-17 expression and favours induction of FoxP3 and Treg differentiation.

Th17 cells also produce IL-22. *In vitro*, IL-22 production was shown to be induced in both Th1 and Th17 conditions, but IL-6 and TGF- β inhibited rather than enhanced IL-22 production in Th17 conditions (226, 240).

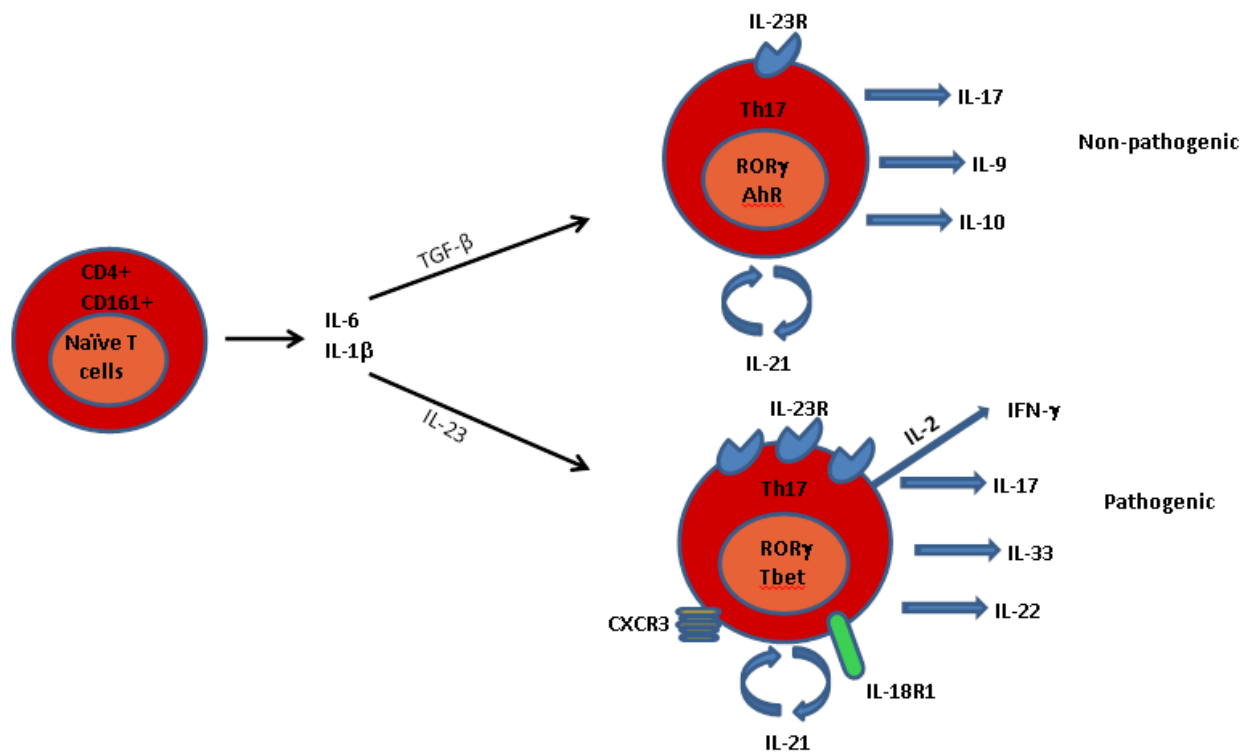


Figure 1.5 Differentiation of pathogenic versus non-pathogenic Th17 cells. Depending on the microenvironment of diseases, naïve T cells can differentiate into either pathogenic or non-pathogenic cells. The naïve T cells can differentiate in the presence of IL-1 β and IL-6 in combination of TGF- β or alternatively with IL-23 in the absence of TGF- β . The T cells generated in the presence of TGF- β express IL-9 and IL-10 in addition to IL-17 and are therefore involved in host defense but have limited role in pathogenicity. In contrast, IL-23 generated Th17 cells express Tbet, CXCR3, IL-18R1 and IL-33 along with IL-17 and can turn into IL-17/IFN- γ cells. This subset of Th17 cells are therefore pathogenic in nature.

1.3.2 Th17 transcriptional regulatory networks

Like other Th lineages, differentiation of Th17 cells is regulated by a complex network of transcription factors which interact with each other at genetic and protein levels (Fig. 1.6). ROR γ t/STAT3 are the key master regulator and the signal transducer and activator of transcription (STAT) proteins that are required for the differentiation of Th17 cells. STAT3 activated by IL-6, IL-21 and IL-23, in conjunction with TCR related transcription factors such as nuclear factor of activated T cells (NFAT) and B-cell activating transcription factor (BATF), induces the expression of ROR γ t. Both ROR γ t and STAT3 bind to multiple sites in the *Il17a/Il17f* locus including the promoters of these cytokines. The transcription of Th17 is negatively regulated by STAT5, eomesodermin (Eomes), vitamin D receptor (VDR) and RA (retinoic acid).

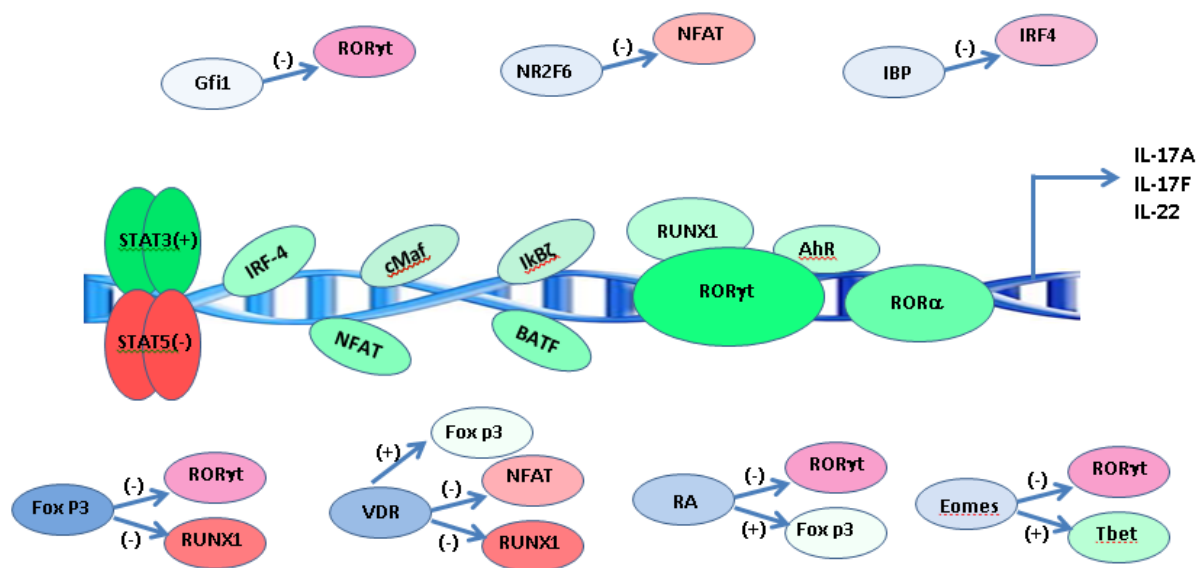


Figure 1.6 Th17 transcriptional regulatory network. IL-6, IL-21 and IL-23 activate STAT3, which in turn is required for the induction of ROR γ t, the Th17 lineage marker. STAT3 is suppressed by STAT5. ROR α , another ROR family member is also unregulated during Th17 differentiation. RUNX1 and AhR synergise with ROR γ t to enhance IL-17 expression while Fox p3, Eomes and RA suppress its activity. The expression of Fox p3 is enhanced by VDR and RA whereas RUNX1 is suppressed by both Foxp3 and VDR. Transcription factors IRF-4, cMaf, I κ B ζ , NFAT and BATF directly bind to *il-17* gene to increase the expression of IL-17.

ROR γ t, retinoic acid receptor-related orphan receptor gamma 2; ROR α , retinoic acid receptor-related orphan receptor alpha; STAT 3; signal transducer and activator of transcription 3; IRF-4, interferon-regulatory factor-4; RUNX 1, runt related transcription factor 1; NFAT, nuclear factor for activated T cells; BATF, B cell activating factor; I κ B ζ , inhibitor kappa B zeta; AhR, aryl hydrocarbon receptor; VDR, vitamin D receptor; RA, retinoic acid; Ets-1, erythroblastosis virus E26 oncogene homolog 1; Eomes, eomesoderm; gfi1, growth factor independent 1; NR2F6, nuclear receptor subfamily 2 group F member 6; IBP. IRF-4 binding protein.

1.3.2a Positive regulators of Th17 transcription

il17a is a direct target gene for ROR γ t (241-245). Forced expression of ROR γ t is sufficient to induce IL-17 expression in the absence of any exogenous cytokines. ROR γ t-deficient mice develop less severe autoimmune diseases and lack Th17 cells in the inflammatory tissues (246, 247). Another ROR family member, ROR α is also upregulated during *in vitro* Th17 cell differentiation (241). Although forced expression of ROR α is sufficient to induce IL-17, ROR α deficiency only selectively impairs IL-17A but not IL-17F expression (241). Both ROR γ t activity and Th17 differentiation, are suppressed by Foxp3 (199, 239, 242, 248, 249).

STAT3 plays an essential role in the differentiation of Th17 cells (208, 210, 250-253). It is activated by IL-6 and IL-23 and binds directly to *il17a* promoter (251), *Il17* locus itself, *Il21*, and *Il23r* and *CCR6* (212, 254, 255). In addition, STAT3 binds to genes encoding transcription factors that are important for Th17 differentiation such as *Rorc*, *Irf4*, *Batf* and *Nfibiz* (254). STAT3 is required for induction of ROR γ t by cytokines and acts together with ROR γ t to induce maximal IL-17 expression (208).

Runt related transcription factor 1 (RUNX1), a transcription factor upregulated during TCR stimulation, is also required for differentiation of Th17 cells (242, 256). Binding of ROR γ t and RUNX1 together to the *il17a* locus leads to increased expression of IL-17. Foxp3 inhibits not only ROR γ t but also RUNX1 activity (242).

Interferon-regulatory factor-4 (IRF-4), a transcription factor previously shown to be important for Th2 cell differentiation, is essential also for Th17 differentiation. IRF-4 regulates expression of IL-21 and IL-23R. IRF-4 deficient T cells show impaired induction of ROR γ t and ROR α and increased expression of Foxp3 (257, 258).

Nuclear factor of activated T cells (NFAT) has been identified as a central regulator of T cell-mediated *IL-17* gene transcription. Two crucial NFAT sites have been identified in the *IL-17a* but not in the *IL-17f* proximal promoter. Inhibition of NFAT activation causes a defect in IL-17A transcription (259, 260).

Activator protein-1 (AP-1 protein) transcription factor, B-cell activating transcription factor (BATF) also plays a critical role in Th17 differentiation. BATF binds conserved intergenic elements in the *Il17a/Il17f* locus and *Il17*, *Il21* and *Il22* promoters. *Batf*^{-/-}T cells fail to induce ROR γ t (246) and IL-21. *Batf*^{-/-} mice have a defect in Th17 differentiation but a normal Th1 and Th2 differentiation.

Th17 cells also express transcription factor proto-oncogene musculoaponeurotic fibrosarcoma oncogene homolog (c-Maf). Lack of c-Maf resulted in a defect in IL-21 production, IL-23R expression and fewer Th17 cells (261).

Inhibitor kappa B zeta (I κ B ζ) encoded by the *Nfkbiz* gene, has recently been shown to be required for Th17 cell development (262). It may act by binding directly to the regulatory region of the *IL-17* gene and synergising with ROR γ t or ROR α . *Nfkbiz*^{-/-} mice have a defect in Th17 development.

Aryl hydrocarbon receptor (AhR) a cytosolic transcription factor (263) is also involved in Th17 cell differentiation creating a link between environmental pollution and inflammation. AhR is required for IL-22 and, to lesser extent, IL-17 expression in Th17-polarizing conditions in the presence of either dioxin or FICZ (264). AhR co-operates with ROR γ t to induce maximal amounts of IL-17 and IL-22 and inhibits TGF- β -induced expression of Foxp3.

1.3.2b Negative regulators of Th17 transcription

IL-2-induced STAT5 is known to inhibit Th17 differentiation potently (265). It displaces STAT3 by directly binding to essentially the same elements in promoter and enhancer on *Il17* gene as STAT3. The balance of activation of STAT3 and STAT5 transcription factors, therefore determines the outcome fate of T cells.

Eomesodermin (Eomes) substantially inhibits ROR γ t and IL-17A expression by directly binding to *Rorc* and *Il17a* promoters and also enhancing *Ifng* promoter activity (233).

IRF-4 binding protein (IBP) sequesters IRF-4 to prevent it from targeting the transcriptional regulatory regions of *il-17* and *il-21* genes (266).

The nuclear orphan receptor NR2F6 directly interferes with the transcriptional activity of the NFAT dependent IL-17A cytokine promoter (267). Growth factor independent 1 (Gfi1) inhibits ROR γ t activity (268).

1,25(OH)₂D₃ via vitamin D receptor (VDR) transcriptionally represses IL-17A expression through multiple mechanisms which include blockage of NFAT, recruitment of histone deacetylase (HDAC), sequestration of Runx1 and a direct induction of Foxp3 (269).

Retinoic acid inhibits Th17 differentiation by down regulating the expression of ROR γ t, and enhancing the expression of Foxp3 (270).

Erythroblastosis virus E26 oncogene homolog 1 (Ets-1) is a negative regulator of Th17 differentiation (271). However, Ets-1 does not bind to the *IL17* promoter. Ets-1-deficient T cells make less IL-2 and have impaired responsiveness in terms of IL-2- mediated inhibition of Th17 differentiation.

1.3.2c Epigenetic control of IL-17 expression

The possibility of an epigenetic regulation of IL-17 expression was raised by an initial observation that the promoters of *IL17* and *IL17F* genes in Th17 cells, but not in Th1 or Th2 cells were histone H3 acetylated and K4 trimethylated (272). Subsequently eight conserved non-coding sequences (CNS) in the *IL17/IL17f* gene locus were identified to be histone H3 acetylated. It was further shown that CNS2, the best studied CNS, could be induced by TGF β and IL-6 and both ROR α and ROR γ t could bind to the ROR response elements (RORE) sites in this region (241). In keeping in with these findings, more recently, RUNX1 factor was shown to cooperate with ROR γ t in activating this element (242).

1.3.3 Plasticity, instability and heterogeneity of Th17 cells

Th17 cells are not terminally differentiated and can be readily converted to other Th effector lineages. It has been suggested that Th17 cells-derived Th17/Th1 or Th1 cells than rather Th17 themselves play a pathogenic role in chronic inflammatory disorders (273, 274).

1.3.3a Th17/Treg cells

IL-17+ Foxp3+ T cells can be detected *in vitro* and *in vivo* in both mice and humans (275, 276). IL-17+Foxp3+ T cells also express CD25 and ROR γ t (277). However, it is not known whether these IL-17+Foxp3+ T cells originate from Th17 or Treg cells (278). Exposure of antigen activated naive CD4+ T cells to TGF- β results in transcriptional up regulation of both Foxp3 and ROR γ t. The double positive Foxp3+ ROR γ t+ T cells are probably a transient population that can differentiate into Treg or Th17 cells. The balance of TGF- β and IL-6 seems to determine the differentiation of Treg/Th17 cells (278-280).

The numbers of Treg and Th17 cells are inversely associated in autoimmune diseases suggesting a dynamic interaction between Treg and Th17 cells (281). Foxp3 expressing Tregs under appropriate conditions can express ROR γ t and, develop capacity to secrete IL-17 or INF- γ (275, 278-280, 282-284). IL-17-secreting Foxp3+ Tregs may either retain or lose their suppressive function. The conversion of human Foxp3+ Tregs into IL-17 producing cells is enhanced in the presence of IL-1 β alone or in combination with IL-23 or IL-6 (275, 285) or in the presence of IL-2, IL-21 and IL-6 (278). It is therefore plausible that reduced numbers of Foxp3 Tregs in patients with autoimmune diseases may occur due to enhanced conversion of these cells into IL-17 secreting cells in the context of an inflammatory environment.

1.3.3b Th17/Th1 cells

Recent evidence suggests that Th17 and Th1 cells might be phenotypically, developmentally and functionally linked in autoimmune diseases. Like Th1, polarized Th17 cells have the capacity to cause

autoimmune diseases although the disease induced by each cell type is distinct in terms of inflammatory infiltrate and preferential tissue location (213, 286-289).

IFN γ +IL-17+ double positive T cells are detectable in both human and mouse inflamed tissues (213, 290, 291). It is possible that IFN γ +IL-17+ T cells can develop from Th1 and/or Th17 cells (292).

The Th1 signature cytokine, IFN- γ , can be expressed by primary Th17 cells in Th17-polarized mouse cells. Th17 cells after multiple rounds of culture *in vitro* begin to produce IFN- γ whereas after transfer *in vivo*, quickly acquire the ability to produce IFN- γ and lose their ability to produce IL-17 (293, 294). In mouse models, under lymphopenic conditions, Th17 cells can re-differentiate into Th1 cells (235). Using the IL-17A reporter mouse model, it was shown that during EAE, a substantial proportion of IFN- γ +T cells was derived from previous IL-17 producing cells (295).

1.3.3c Th17/ Th2 cells

A novel subset of effector T lymphocytes that co-express GATA3 and RORc and that produce both IL-17A and IL-4 has recently been described in both mice and humans (296, 297). Th17/Th2 cells could be produced from either Th17 or Th2 cells. In the presence of an IL-4-rich microenvironment, Th17 lymphocytes could switch toward the Th17/Th2 phenotype whereas, *in vitro*, classical mice Th2 memory cells could be induced into Th17 cells in the presence of IL-1 β , IL-6, and IL-21.

1.4 Targeting IL-17 for the treatment of RA

IL-17 plays a direct role in the pathogenesis of RA (298). The expression of IL-17A, IL-17F, IL-17RA and IL-17RC is augmented in the rheumatoid joint and the levels of IL-17A and IL-17F increased in RA synovial fluid (SF) (299). Serum levels of IL-17 are significantly raised even before the onset of clinical RA (300, 301). IL-17A but not IFN- γ was transiently elevated in SF of RA patients having disease duration less than 3 months suggesting that IL-17 is an important T cell cytokine during early RA (302). The presence of IL-17 in early synovitis SF predicted development of RA and synovial IL-17mRNA expression in early RA predicted progressive joint damage (301, 303).

Development of a cytokine environment that favours Th17 cell generation is an early event in the pathogenesis of RA. IL-17A is predominantly produced in rheumatoid joint by activated CD4+ T cells, though other cells such as $\gamma\delta$ T cells, NKT cells, CD8+T cells, fibroblasts, cells in the subchondral lining and osteoblasts also produce IL-17 (304, 305). Heuber *et al.* reported unexpected finding of predominant production of IL-17A in inflamed RA synovial tissue by mast cells rather than Th17 cells (36). Th17 cells migrate to inflamed joints in response to CCL20 (306) and are activated and expanded via cell contact (307) and cytokines, IL-1 β , IL-6, IL-21 and IL-23 (51, 308-312).

The data now available supports the suggestion that Th17 cells play an important role in driving innate immune inflammation to chronic autoimmune inflammation in RA. Synovial hyperplasia, which occurs at the earliest stages of RA is characterised by the innate immunity cytokine complex of TNF- α , IL-1 β , IL-6, IL-8, IL-15, IL-18 and GM-CSF. The cross-talk between Th17 and RA synoviocytes results in reciprocal activation of both these cells. Th17 promotes uncontrolled growth and invasiveness of RA synoviocytes, which in turn promotes uncontrolled production of IL-6 and IL-15 (313, 314). A persistent stimulation of T lymphocytes by IL-6, IL-15 and TNF- α results in the down regulation of TCR ζ and CD28 expression on synovial T cells (315-318), which in RA signifies transition from antigen-driven to cytokine-driven activation of T cells and conversion from regulatory to inflammatory cytokine production.

IL-17 directly supports both the chronic inflammatory and destructive phase of RA. IL-17 acts as an important effector of chronic synovial inflammation by inducing secretion of other mediators of inflammation, growth factors, adhesion molecules and matrix degrading enzymes (106, 107, 306, 319-322). *In vitro*, IL-17 inhibits both proteoglycan and collagen synthesis, and promotes cartilage destruction (323). IL-17, by increasing the expression of receptor activator of NF- κ B ligand (RANKL) and inhibiting osteoprotegerin supports downstream bone destruction (323-328). The proinflammatory and tissue destructive actions of IL-17 are synergistic to TNF- α and IL-1 β (115).

Exogenous administration of IL-17 exacerbates the onset and severity of experimental arthritis, whereas its neutralisation suppresses disease (327, 329-332). T cells from IL-17 deficient mice showed decreased sensitization to collagen and reduced levels of anti-collagen II antibodies indicating modulation of both cellular and humoral immunity in CIA by IL-17. Inhibition of IL-17 both before and after the onset of arthritis resulted in suppression of synovial inflammation implying that IL-17 contributes to the initiation as well as the effector phase of arthritis (331, 333). Mice deficient in inducible costimulator (ICOS), which is associated with reduced production of IL-17A but a normal Th1 response, were protected against CIA (334). Vaccinating mice with an IL-17-conjugated virus-like particle resulted in high levels of anti-IL-17 antibodies and a lower incidence and severity of CIA (335). Local overexpression of IL-17 enhanced inflammation and erosions in streptococcal cell wall-induced arthritis in both normal and IL-1 β -deficient mice, supporting an IL-1-independent role of IL-17 (332). *Ex vivo* blockage of IL-17A in synergy with TNF- α and IL-1 β was more effective in controlling synovial inflammation and bone resorption (116). A study in TNF- α -deficient mice demonstrated that although TNF- α is required in IL-17-induced joint pathology under naive conditions (336), TNF- α dependency of IL-17 is lost under arthritic conditions (336). Notley *et al.* first reported an unexpected finding of increased number of pathogenic Th1 and Th17 cells in lymph nodes of CIA mice after TNF blockade despite diminished accumulation of Th1/Th17 cells in the joint (337). In keeping with results in murine arthritis, Bose *et al.* showed enhanced expression of activation markers and proliferative response to TCR stimulation of peripheral blood CD4⁺ T cells from patients

of psoriasis and IBD, which occurred concurrently with down regulation of Th7/Th1 cytokines and inflammatory genes in tissue biopsies (338). Moreover, the peripheral CD4+ T cells hyperactivity in these patients did not interfere with responsiveness to anti-TNF therapy.

Phase I/II trials of treatment with anti-IL-17 antibodies have reported beneficial therapeutic effects with no notable side-effects (339-341).

1.5 Targeted therapies

Inhibition of TNF by either monoclonal antibodies or receptor fusion protein in RA has demonstrated outstanding efficacy but unwanted systemic side effects due to the pleiotropic activities of cytokines still remain an issue. These limitations could be overcome by the use of therapies that can target their therapeutic effects to the active disease sites. Immunocytokines and latent cytokines are examples of targeted therapies that have been developed with the aim of localising therapeutic cytokines in this way.

1.5.1 Immunocytokines

An immunocytokine consists of an antigen-specific monoclonal antibody (mAb) and a cytokine, fused into a single molecule in a way that the independent functions of antibody and cytokines are not disturbed. The targeting properties of an immunocytokine mAb enables directing the cytokine to the specific pathology site in order to achieve an effective local concentration in the desired microenvironment, thus minimising the risk of toxicity that could result from the systemic administration of the cytokine. In addition, the large size and inherent stability of the mAb in the complex increases the half-life of the cytokine.

During the past years, several immunocytokines have been developed including mAbs fused to cytokines such as TNF- α , IL-2 and GM-CSF (342-345). Amongst these, Ab-IL-2 fusion proteins are the best characterised. The Ab-IL-2 uses the mAb component to recognize and bind to the tumour, whereas the IL-2 portion activates cells expressing IL-2 receptors, such as CD8⁺T cells and NK cells, inducing the destruction of the tumour cell (346, 347). Dario Nari's group has reported therapeutic efficacy of IL-10 conjugated to the specific components of extracellular matrix in CIA mice. IL-10 when fused to L19, a monoclonal antibody against tenascin C, a specific marker for angiogenesis or F8, a monoclonal antibody to extracellular domain A of fibronectin was effective in inhibiting progression of arthritis in established CIA (348, 349). Hughes *et al.* in our laboratory have demonstrated that anti-ROS modified CII scFv fused to soluble murine TNF receptor II-Fc fusion

protein (mTNFRII-Fc) resulted in significantly reduced inflammation in CIA mice as compared to mTNFRII-Fc alone or mTNFRII-Fc fused to an irrelevant scFv (350).

1.5.2 Latent cytokine

TGF- β , unlike most cytokines is secreted as latent cytokine. TGF- β is produced with an N-terminal region, termed latency associated peptide (LAP). Following disulfide bonding, the LAP serves as a shell that protects C-terminal region, which is the active TGF- β cytokine (351). The non-covalently bound active TGF- β is released from this structure by several mechanisms, including the proteolytic cleavage of LAP, changes in pH or heat (352). For the purpose of targeted therapy, a cytokine can be modified as latent cytokine (Fig. 1.11) by covalently binding the cytokine to the LAP of TGF- β via a MMP sensitive linker (353). This allows formation of a protective shell of LAP around the cytokine, which in turn prevents the interaction of the cytokine with its receptor. The biological activity of a LAP cytokine nonetheless can be released by MMP, which free ups the biologically active cytokine by cleaving the MMP-sensitive linker. Due to the overexpression and localised abundance of MMPs within actively inflamed tissues, therapeutic effects of a LAP-cytokine can be targeted to the actual disease sites. Using this approach, LAP- IFN- β was the first cytokine that was modified as a latent cytokine in our laboratory. *In vitro* LAP- IFN- β did not bind to its cellular receptors and *in vivo* the half-life of LAP-IFN- β was 37-times higher and therapeutic efficacy in CIA mice superior to naïve IFN- β (354). Additional therapeutic agents that were made latent include short anti-inflammatory peptides such as γ - and α -MSH and vasoactive intestinal peptide (VIP) (355).

Latent cytokines can be used in a number of disease conditions in which tissue modelling takes place such as infection, cancer (356), atherosclerosis (357) and autoimmune diseases (358-361). In addition, the cleavable MMP site can be tailored to be sensitive to the MMPs that are expressed predominantly in certain pathological conditions. Furthermore, certain cytokines with important biological functions but high toxicity in clinical trials could be made latent to ensure local action and increase their safety and therapeutic index.

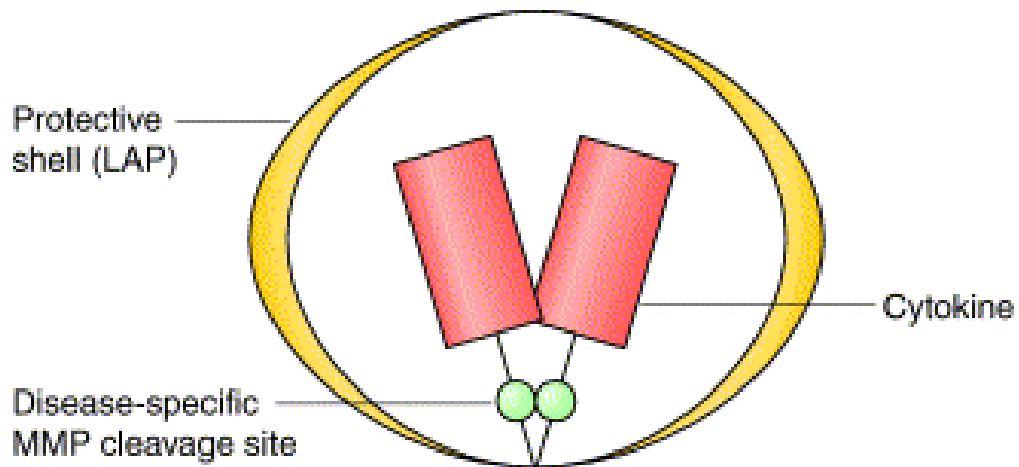


Figure 1.7 Structure of a latent cytokine. A cytokine can be modified as latent cytokine by fusing it with the LAP of TGF- β via a MMP-sensitive linker. The LAP forms a protective shell around the cytokine, which prevents the interaction of the cytokine with its receptors and in turn converts it latent. The biological activity of a latent cytokine can be released by cleavage of the MMP-sensitive linker by MMP and due to the localised overexpression and abundance of MMPs, targeted to the site of active inflammatory pathology. LAP, latency-associated peptide; TGF- β , transforming growth factor- β ; MMP, matrix metalloproteinase. Adams G *et al.* Nature Biotechnology 2003; 21:1314-1320.

1.6 Preclinical *in vivo* testing of new therapies for RA

Preclinical *in vivo* testing of a newly devised therapy is an essential pre-requisite to its safe use in humans. This often involves production of a given therapeutic in large quantities, sufficient to allow multiple administrations to achieve an optimum therapeutic level. *In vitro* expression and purification of large quantities of recombinant therapeutic protein is costly, time consuming and technically difficult especially in the setting of non-industrial research laboratories. These limitations of protein-based therapy can be avoided by administering a given therapeutic in animals under study via *in vivo* gene therapy. Gene-based therapy precludes the need for *in vitro* purification of an investigational therapeutic by allowing its spontaneous *in vivo* expression. Gene therapy, because of its relative ease and low cost can be readily undertaken in research laboratories; thus providing a convenient alternative to protein based drug delivery to establish proof of principle for *in vivo* efficacy of new therapeutic strategies.

1.6.1 Gene therapy as a modality for preclinical testing of new therapies

Gene therapy is defined as transfer of new genetic material to the cells of a living organism for therapeutic purposes. Historically, human gene therapy was mainly focused on the treatment of monogenic diseases with the aim of replacing the defective gene and restoring its functions but in fact has much broader applications. For example, a novel therapeutic can be administered in animal models using gene therapy to assess its preclinical *in vivo* efficacy (Fig. 1.8). A solitary intravenous hydrodynamic delivery of plasmid DNA results in transgene expression that is sustained over weeks. The delivery and expression of a new gene into target cells can be facilitated by using either viral or non-viral vectors. Viral vectors due to their natural ability to enter and integrate their genetic material into target cells offer an excellent efficiency of gene delivery and expression but are difficult to produce and may impose the risk of immunogenicity and insertional mutagenesis. In contrast, non-viral vectors are generally safe and easy to produce but the efficiency of gene transfer is relatively weak.

1.6.1a Viral vectors

Retrovirus, adenovirus and adeno-associated viruses (AAV) are the most widely used vectors for gene therapy applications. Other viruses including pox virus, herpes simplex virus and vaccinia virus have also been investigated.

Retroviruses

Retroviruses are small, enveloped, single stranded RNA viruses with genome capacity of 7-12kb. The retroviruses integrate their DNA into regions of host euchromatin, which provides stable long-term expression of the transgene in the host cell and descendent cells. The use of retroviruses is restricted to mitotic tissues as they cannot infect quiescent cells. The major limitation of retroviruses is the accompanied risk of insertional mutagenesis.

Adenoviruses

Adenoviruses are non-enveloped double stranded linear DNA viruses with a natural tropism for upper respiratory tract and ocular tissue. They can deliver up to an 8 kb cargo. The cargo delivered can be maintained as an episome which may remain transcriptionally active for the life of host cell. Adenoviruses are however highly immunogenic and many people have a pre-existing immune memory that affects its efficacy.

Adeno-associated virus

AAV is a non-pathogenic single stranded DNA virus with a genome of about 4.7kb. Like adenoviruses, they can infect dividing or quiescent cells. Many serotypes are available and they are used actively in clinical research including in RA. In a phase I/II clinical trial, patients treated with intra-articular injection of recombinant AAV containing TNFR-Fc gene reported greater improvement in target joint global visual analogue score at 12 weeks than placebo-treated group. The AAV delivered treatment resulted in site reaction in 12% patients and fatal disseminated histoplasmosis in one patient, that was thought to be unrelated to the study agent (362).

1.6.1b Non-viral methods

Gene constructs if injected directly as naked DNA into skeletal muscles are expressed only at low levels. Physical or chemical methods are usually required to enhance cellular uptake of naked DNA. Physical methods that facilitate the transfer of genes from extracellular to nucleus by creating transient membrane holes/defects using physical forces include local or rapid systemic injection, particle impact, electric pulse, ultrasound and laser irradiation. Chemical vectors such as cationic lipids or polymers form condensed complexes with negatively charged DNA (363), which in turn protect DNA and facilitate cell uptake and intracellular delivery.

Hydrodynamic gene transfer

The method of hydrodynamic gene transfer employs a high pressure as the driving force for the transfer of a gene. Intravenous injection of a large volume, 8-12% of body weight in short time (3-5 seconds) leads to a reversible permeability change in the endothelial lining and the generation of transient pores in hepatocyte membranes allowing the DNA molecules to diffuse internally (364). This is the most efficient non-viral gene transfer method in rodents. Hydrodynamic delivery has been used successfully in monkeys by delivery into skeletal muscle by temporarily blocking the limb circulation with a tourniquet (365).

Electroporation

Electroporation involves use of electric pulses which generate transient pores in cell membranes followed by intracellular electrophoretic DNA movement. Typically, *in vivo* electroporation is conducted by first injecting DNA to the target tissue followed by electric pulses, with varied voltage, pulse duration, and number of cycles, applied from two electrodes. *In vivo* electroporation technique is generally safe, efficient, and can produce good reproducibility and efficiency (366).

Sonoporation

Sonoporation uses ultrasound waves to create plasma membrane defects by acoustic cavitation. Most gene delivery techniques use ultrasound at frequency of 1-3MHz with intensity of 0.5-2.5W/cm² (367). Ultrasound may be combined with contrast agents or microbubbles (368) to

facilitate release of local shock waves that can disrupt the nearby cell membranes and promote transient pore formation to enhance local DNA transfer.

Cationic lipids

Cationic liposome-mediated gene transfer or lipofection is the most extensively investigated and commonly used non-viral gene delivery method. The various lipids used share the common structure of positively charged hydrophilic head and hydrophobic tail that are connected via a linker structure. The positively charged head binds with the negatively charged phosphate of DNA. The positively charged lipids surround the DNA and grant them protection against extra and intracellular nucleases. In addition, liposomes interact with negatively charged molecules of the cell membrane and facilitate their cellular uptake. The cationic lipids are inexpensive to produce and can be engineered to have targeted specificity but have drawbacks of short circulation half-life and acute toxicity.

Cationic polymers

Cationic polymers upon mixing with DNA form nanosized complexes called polyplexes. Amongst cationic polymers, polyethylenimine (PEI) is considered most effective. Upon systemic administration these polyplexes of small particle size aggregate to form larger complexes and accumulate in major tissues including lung and liver. Cationic polyplexes are more stable than lipoplexes but the level of cytokine induction is inferior to the latter (369).

Inorganic nanoparticles

Inorganic nanoparticles are usually prepared from metals (e.g. iron, gold, silver), inorganic salts, or ceramics (370). The small particle size has advantage of bypassing most of the physiological and cellular barriers and produce higher gene expression (371). They can also be transported through the cellular membranes via specific membrane receptor nucleolin which delivers nanoparticles directly to the nucleus, skipping the endosomal-lysosomal degradation (372, 373). Nanoparticles have ability to efficiently transfect post-mitotic cells *in vivo* and *in vitro*, have low or no toxicity and are inert to immune responses.

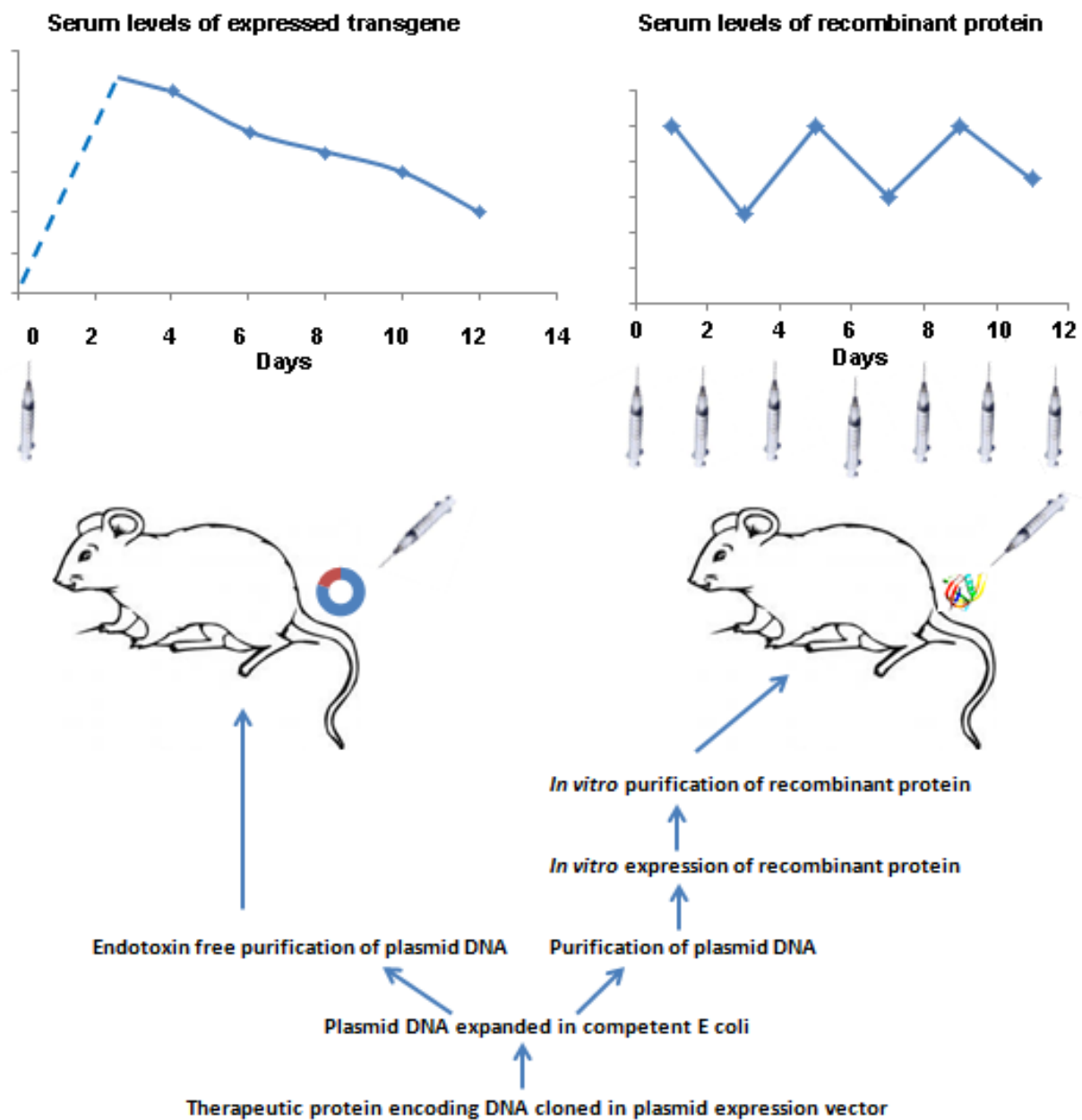


Figure 1.8 Gene therapy as a modality for preclinical *in vivo* testing of new therapies. Gene-based therapy is an expedient alternative to protein-based therapy for preclinical *in vivo* testing of new therapies. The procedure of gene-based therapy is fast, easy and is feasible in the setting of research laboratories. As against, protein-based therapy involves *in vitro* expression and purification of large quantities of recombinant therapeutic protein, a procedure which is technically difficult, time consuming and exceedingly expensive.

1.6.2 Mouse models of experimental arthritis

Animal models of experimental arthritis have been instrumental in studying the RA aetiology, pathophysiology and developing new therapeutic strategies. Induction of chronic inflammatory arthritis in susceptible inbred strains permits *in vivo* study under reproducible controlled conditions. Inflammatory arthritis in animals is stimulated by either overexpression or deletion of target gene, immunisation with putative autoantigens or synthetic chemical challenges. Although the animal models share features with human RA, none reflects all the characteristic articular, systemic, immunological and genetic features of the human disease. A preferential selection of an appropriate animal model that represents the expected outcome in the human clinical situation therefore is extremely important.

Rodent models have been extensively used in RA research. Some of the commonly used mouse models of experimental arthritis and outcome of their responsiveness to IL-17 inhibition are described below.

1.6.2a Collagen induced arthritis mice

Collagen induced arthritis (CIA) is characterised by an autoimmune response-mediated synovitis and cartilage and bone erosion, which closely resemble RA making it the most widely used animal model for RA research.

Mice with H-2^q and H-2^r major histocompatibility complex (MHC) class II haplotype, when immunized with homologous or heterologous native collagen II (CII) develop arthritis (374-377). Both cellular and humoral immunity to CII are necessary for the full development of arthritis in this model (377). An injection of anti-CII antibodies also induces arthritis (378). The development of CIA critically depends on IL-1 (379) and IL-6 (380). While IL-17A (329), TNF (381, 382) and IL-23 are also involved, IFN- γ and IL-4 are involved only marginally. *IL23*^{-/-}-mice but not *IL12 α* ^{-/-}-mice are resistant to disease (383).

Il17a^{-/-}-mice exhibit a significant reduction in the sensitization of T cells following immunization with CII (329). Because both the incidence and the severity score was reduced in *Il17a*^{-/-}-mice with CIA, IL-17 is thought to function at the sensitization as well as the elicitation phase of the arthritis.

1.6.2b Anti-collagen II antibody-induced arthritis mice

Anti-CII Ab-induced arthritis is produced by a mixture of monoclonal anti-CII abs, injected intravenously followed by intraperitoneal injection of LPS. Arthritis is induced within a few days and persists for 2 weeks in BALB/c mice (384, 385). The anti-CII Ab arthritis can also be induced in *scid/scid* mice (386) indicating that both T cells and B cells are not necessary for this disease model. *Il17a*^{-/-} (379) and *Il6*^{-/-}-mice (386) develop full arthritis in this model but development of arthritis is completely suppressed in *tnfr*^{-/-}-mice (386) and significantly suppressed in *Il1ra*^{-/-}-mice (386).

1.6.2c Human T cell-leukemia virus type I transgenic mice

Transgenic mice carrying HTLV-1 tax gene with its own LTR promoter (HTLV-I Tg mice) develop chronic inflammatory polyarthropathy resembling RA (387-389). The expression of IL-1 β , IL-2, IL-6, TNF- α , IFN- γ , and IL-17A is upregulated in transgenic joints (390) and the development of arthritis is greatly suppressed in *Il-17a*^{-/-}, *Il-1 α / β* ^{-/-}, *Il-6*^{-/-}-mice.

1.6.2d IL-1 receptor antagonist deficient mice

IL-1Ra-deficient, *Il1ra*^{-/-} mice develop chronic inflammatory arthropathy (391). The expression of IL-1, IL-17A, IL-6 and TNF- α is augmented in these mice (391, 392). The development of arthritis in *Il1ra*^{-/-}-mice however was completely suppressed in *Il17a*^{-/-}/*Il1ra*^{-/-}-mice until 16 weeks of age while, more than 80% of *Il17a*^{+/+}/*Il1ra*^{-/-} mice develop arthritis at 10 weeks of age (393). Deficiency of TNF- α but not IL-6 led to the suppression of arthritis in these mice (379, 392).

1.6.2e SKG mice

These mice, derived from BALB/c background have a mutation in ζ -associated protein of 70 kDa (ZAP70) (394) and develop autoimmunity and arthritis spontaneously (395). The development of arthritis in SKG mice is completely suppressed by IL-17A or IL-6 deficiency and significantly by IL-1 or TNF- α deficiency (306, 396, 397).

1.6.2f TNF transgenic mice

Transgenic mice carrying a modified human TNF gene under its own promoter and β -globin 3' end, produces a stable TNF mRNA, develop arthritis characterized by subchondral erosions within 4 weeks of age (398). This arthritis develops in a *rag1*^{-/-}-background, which is suggestive of an innate and /or stromal rather than an autoimmune mechanism (399). In this model IL-6 deficiency does not affect the development of arthritis (380) but inhibition of IL-1RI (400) or TNFRI deficiency (399) completely suppresses arthritis development. Role of IL-17 in this animal model has not been determined.

1.6.2g K/BxN mice

K/BxN mice carry a TCR transgene, which is specific for the bovine RNase and also recognizes the MHC class II molecule A(g7) encoded on nucleotide oligomerization domain (NOD) (401). The development of spontaneous arthritis in this model depends on both T cells and B cells (402) and is mediated via antibodies to glucose-6-phosphate isomerase (anti-GPI) (403). Anti-GPI antibody containing immune complexes activate the C5a complement pathway in mast cells to induce secretion of inflammatory cytokines (404, 405). Mast-cell derived IL-1 (405), also TNF but not IL-6 is involved in the development of arthritis in this model (406). Neutralising IL-17A signaling did not affect this model of arthritis (407).

1.6.2h RA/severe combined immunodeficient mice

Severe combined immunodeficient (SCID) mice are deficient in both T and B cell function and widely used as a host for the transplantation of various human tissues since their impaired T and B cell function prevents them from rejecting grafts. Transplantation of RA synovium into SCID mice enables targeting the human RA tissue directly, thereby providing an important step between standard animal models of experimental arthritis and clinical trials.

This humanised arthritis model is used in two variants, each with its own advantages and limitations. In the RA synovial fibroblast (RASf) model, RASf are co-implanted with pieces of cartilage into SCID mice to study the capacity of the RASf to degrade matrix and invade the cartilage (408, 409). The RA synovium/SCID mouse model on the other hand involves transplantation of standardized pieces of RA synovial tissue subcutaneously on the back or under the renal capsule of SCID mice (410, 411). As this model uses the whole RA synovial tissue including various immune cells, it provides an excellent opportunity to investigate multiple cell types within the inflamed synovium and to test new therapies. For example, depletion of human T cells and B cells from the RA synovial grafts confirmed a crucial role for these cells in RA (412, 413) and MTX and anti-TNF treatment in the RA /SCID mouse model resulted in a decrease in the inflammatory cells in the graft (414, 415).

Koenders *et al.* have recently confirmed the validity of the RA synovium /SCID mouse model by examining the effects of commonly prescribed therapies for RA including IL-1 and TNF antagonists, CTLA4-Ig, and anti-CD20 and anti-IL-17 antibodies (416).

1.7 Summary and objectives

IL-17A plays a direct role in the pathogenesis of RA. Exogenous administration of IL-17A exacerbates whereas its neutralisation ameliorates experimental arthritis. Phase I/II clinical studies of inhibition of IL-17 have reported significant improvement in arthritis without notable side effects.

(H161R) IL-17F mutant is a competitive inhibitor of wild-type IL-17F. In a Japanese population, homozygotes of (H161R) IL-17F mutant were protected from asthma. IL-17F shares structural, receptor binding and biological properties with IL-17A but is 30-100% less potent, which is suggestive of an additional inhibition of IL-17A by IL-17F mutant.

Biological activities of cytokine-based therapies can be targeted to the site of active inflammation by modifying a given cytokine as LAP-MMP-cytokine fusion protein.

Hypotheses

1. Human (H161R) IL-17F mutant is an antagonist of IL-17A.
2. (H161R) IL-17F mutant, due to its ability to suppress both IL-17A and IL-17F will be a powerful suppressor of IL-17-induced inflammation in RA.
3. (H161R) IL-17F mutant if modified as LAP-IL-17F mutant would be a highly efficacious targeted therapy for RA.

Aims

1. To confirm that human (H161R) IL-17F mutant is an inhibitor of IL-17A.
2. To construct mouse analogues of human (H161R) IL-17F mutant and characterise their *in vitro* biological properties.
3. To test preclinical *in vivo* therapeutic efficacy of mouse LAP-IL-17F mutant in CIA mice or human LAP-IL-17F mutant in RA synovium/SCID mice model of RA.

CHAPTER II

MATERIAL AND METHODS

2.1 Cloning and expression of IL-17

2.1.1 Harvesting cDNA from mouse splenocytes

2.1.1a Harvesting T cells from mouse spleen

Spleen dissected from NIH Swiss mouse (kindly provided by Dr D. Gould, BJRU) was transported in 20 ml ice-cold complete RPMI medium supplemented with 10% FBS (Invitrogen, Paisley, UK), 2mM L-glutamine and Penicillin (100 units/ml)/Streptomycin (100µg/ml) (Cambrex, Wokingham, UK); cut, mashed and filtered through 70µm BD Falcon cell strainer, washed twice with 50 ml complete RPMI medium and centrifuged at 500rpm (Eppendorf centrifuge 5810R, Hamburg, Germany) for 5 minutes at 4°C. The RBCs were lysed by adding 1ml RBC lysis buffer (0.15M ammonium chloride in 0.01M Tris HCl buffer, pH 7.50), re-filtered through 70 µm BD Falcon cell strainer and washed twice with RPMI. The cell count was performed using haemocytometer. T lymphocytes were activated by incubating the cells with 3 µg/ml Concanavalin A (Con A) in 10ml RPMI in 9cm culture plate at 37°C in 10% CO₂ for 6 hours. The working-surface was cleaned with RNase free water and the plate was transferred on ice; medium aspirated in pre-cooled Eppendorf tubes. 500 µl pre-cooled PBS was added to the adherent cells, the cells were scraped using a scraper and added to collected supernatant, centrifuged at 1200rpm for 5 minutes at 4°C. The pellet was re-washed with 500µl cold PBS and stored at -80°C.

2.1.1b RNA extraction

RNA was extracted in a sterile environment using Ambion RNAqueous®-4PCR kit. The harvested mouse spleen cells were treated with 200µl lysis/binding solution per 10⁶ cells and vortexed. The cell lysate was clarified by centrifugation, mixed with an equal volume of 64% ethanol and RNA was extracted as per the manufacturer's instructions. In brief, the lysate/ethanol mixture was transferred to the filter cartridge, washed twice and RNA was eluted using elution buffer (pre-heated at 70-80°C for 30 minutes). For the removal of DNA, 1µl 10X DNase buffer and 0.1µl DNase 1 was added to each 9µl RNA and incubated for 30 minutes at 37°C. Finally 1µl DNase inactivation solution added and the

extracted RNA stored at -80°C. The extracted total RNA was analysed on 1% agarose gel to confirm the presence of expected ribosomal RNA bands of 28S and 18S.

2.1.1c Reverse transcription with oligo dT primers

The RNA extracted from mouse spleen was heated at 65°C for 5 minutes and transferred on ice immediately. The reaction mixture containing 10X RT buffer (200mM Tris HCl, pH 8.4, 500mM KCL, Gibco BRL), 4µl 25mM MgCl₂, 1µl 10mM dNTP, 1µl oligo dT, 2µl 0.1M DTT, RNase-free water, 0.5µl Moloney murine leukemia virus (M-MLV) reverse transcriptase (200units/µl, Promega, Madison, USA), 1µl RNase inhibitor and RNA in a total volume of 20µl was incubated at 42°C for 60 minutes, 99°C for 5 minutes and 4°C for 5 minutes in a Peltier Technology Thermal cycler (PTC-200, MJ Research Inc., Waltham, MA). The reverse transcribed product containing single-stranded complementary DNA was stored at -20°C.

2.1.2 Cloning of human and mouse full-length IL-17

All primers were ordered from Sigma-Aldrich Inc. (Haverhill, UK). All DNA restriction and modifying enzymes were purchased from New England Biolabs Inc. (Hitchin, UK).

2.1.2a Cloning of human and mouse wild-type full-length IL-17

Human full-length IL-17A (hFL-IL-17A) and IL-17F (hFL-IL-17F) were PCR-amplified using cDNA derived from RT-PCR of CD14⁺ human peripheral blood lymphocytes (PBL) as template (kindly provided by Dr. N Yousaf, BJRU). Mouse full-length IL-17A (mFL-IL-17A) and IL-17F (mFL-IL-17F) were PCR-amplified using NIH Swiss mouse splenocyte cDNA (refer Section 2.1.1) as template employing the protocol described below (Section 2.2.1). The forward and reverse primers are listed in the Table 2.1. Hot-start PCR (Section 2.2.2) was used to amplify mFL-IL-17A. Due to the presence of an additional band, the mFL-IL-17F was gel-purified using PureLink™ Quick Gel Extraction kit. As shown in the Fig. 2.1, the PCR products were digested with BamH1 and Xba1, and cloned in the corresponding sites of the plasmid expression vector pcDNA3 (Invitrogen).

Table 2.1 List of primers used for cloning of human and mouse full-length and LAP- IL-17 constructs

Oligo primer name	Sequence 5'-3'
hFL-IL-17A forward	5'CCGGATCCATGACTCCTGGGAAGACCTCA3'
hLAP-IL-17A forward	5'CGCGGCCGCAGGAATCACAATCCCACGAAT3'
hIL-17A reverse	5'GGTCTAGATTAGGCCACATGGTGGACAATCGG3'
hFL-IL-17F forward	5'CCGGATCCATGACAGTGAAGACCCTGCAT3'
hLAP-IL-17F forward	5'CGCGGCCGCAAAAATCCCCAAAGTAGGAACA3'
hIL-17F reverse	5'GGTCTAGATTACTGCACATGGTGGATGACAGG3'
hIL-17Fmutant oligo forward	5'CCCCTGTCATCCACC G TGTGCAGTAAT3'
hIL-17Fmutant oligo reverse	5'CTAGATTACTGCACA C GGTGGATGACA3'
hLAP-IL-17Fmutant forward	5'CGC /G GCCGCA AAA ATC CCCAAAGTAGGAACA3'
mFL-IL-17A forward	5'CCGGATCCATGAGTCCAGGGAGAGCTTCA3'
mLAP-IL-17A forward	5'CGCGGCCGCAGCAGCGATCATCCCTCCAAGC3'
mIL-17A reverse	5'GGTCTAGAT TTAGGCTGCCTGGCGGACAATCGA
mFL-IL-17F forward	5'CCGGATCCATGAAGTGCACCCGTGAACA3'
mLAP-IL-17F forward	5'CGCGGCCGCACGGAAGAACCCCAAAGCAGGG3'
mIL-17F reverse	5'GGTCTAGATTCAGGCCGCTTGGTGGACAATGGG3'
mFL-IL-17Fmutants forward	5'CCGGATCCATGAAGTGCACCCGTGAAACA3'
mLAP-IL-17Fmutants forward	5'GCCGCACGCCGGAAGAACCCCAAAGCAGGG3'
mIL-17F-mutant 1 reverse	5'GGTCTAGATTCAGGCCGCT C GGTGGACATGGG3'
mIL-17F-mutant 2 reverse	5'GGTCTAGATTCAGGCCGCTTGG C GGACAATGGG
mIL-17F-mutant 3 reverse	5'GGTCTAGATTCAGGCCGCTTGGT G TCA A ATGGGCTTGACACA

The nucleotides marked in red represent the nucleotides that have been substituted in the wild-type IL-17F to create the desired mutations.

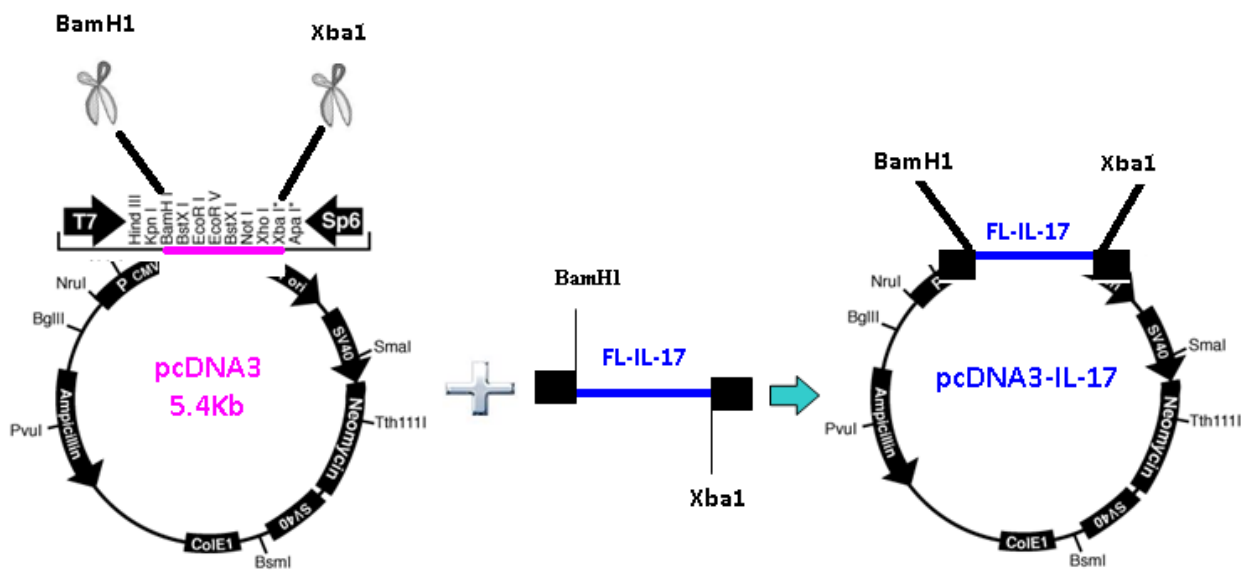


Figure 2.1 Cloning of full-length IL-17 in pcDNA3. Human and mouse full-length IL-17A and IL-17F were constructed by cloning BamHI and XbaI digested full-length IL-17 in the corresponding sites of plasmid expression vector pcDNA3.

2.1.2b Cloning of human full-length (H161R) IL-17F mutant

Annealing complementary oligonucleotides

Previously PCR-amplified hFL-IL-17F fragment (Section 2.1.2a) was digested at BamHI and BSPM1 sites and gel-purified using PureLink™ Quick Gel Extraction kit. Complementary strands of oligonucleotides (Sigma-Aldrich, UK) were custom-ordered and annealed, which contained the desired mutation with codon sequence 5'CCCCTGTCATCCACCGTGTGCAGTAAT3' and anti-codon sequence 5'CTAGATTACTGCACACGGTGGATGACA3') along with BSPM1/Xba1 digestion sites. As shown in the Fig. 2.2, human FL-IL-17F mutant construct was developed by cloning together BamHI/BSPM1-digested FL-IL-17F fragment and annealed complementary oligonucleotides in pcDNA3 (Invitrogen) at the BamHI/Xba1 sites.

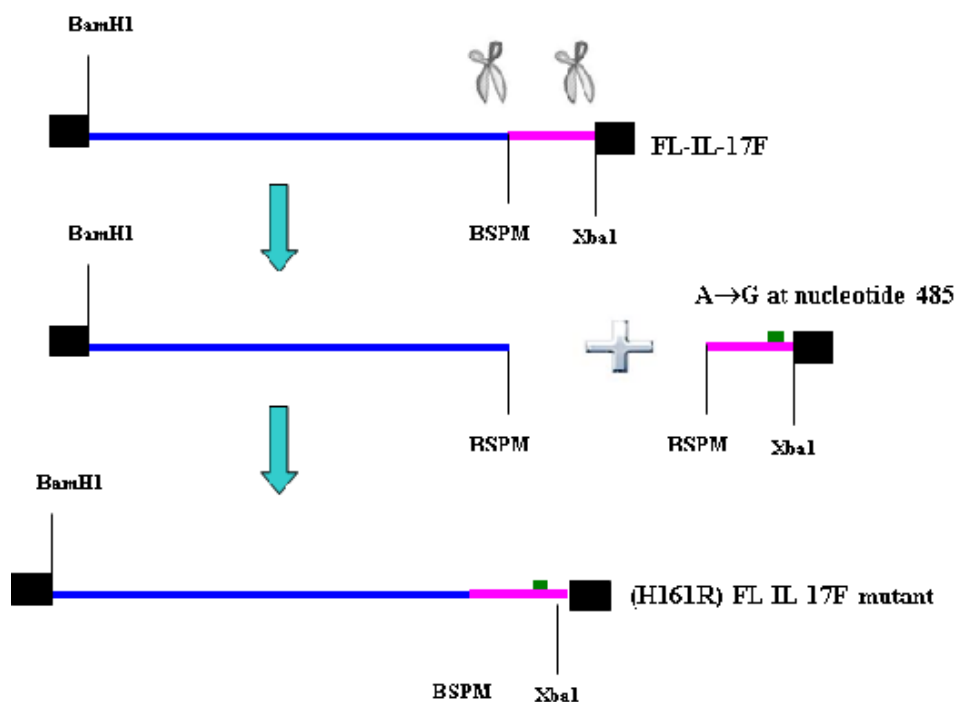


Figure 2.2 Construction of human full-length (H161R) IL-17F mutant. (H161R) IL-17F mutation was created by substituting nucleotide A at position 485 (counted from signal peptide) in full-length IL-17F by G. Previously amplified-type FL-IL-17F (section 2.1.2a) was digested at BSPM and Xba1 sites and the deleted C-terminal end was replaced by annealed complementary oligonucleotides containing the desired point mutation. FL-IL-17F mutant was then cloned in pcDNA3 at BamHI and Xba1 sites.

2.1.2c Cloning of mouse analogues of human (H161R) IL-17F mutant

Human and mouse IL-17F sequences are 77% identical. The (H161R) mutation in human IL-17F is located at the extreme C-terminal end. The amino acid sequence at the C-terminal end in human IL-17F includes HHVQ. In case of the (H161R) mutation, the third last Histidine in human IL-17F is replaced by Arginine. In comparison, the mouse IL-17F is 3 amino acids shorter and contains HQAA at the C-terminal end (Fig. 2.3). Based on these observations, three mouse analogues of human IL-17F mutants were created as follows:

Mouse full-length (Q158R) IL-17F mutant (mFL-IL-17F mutant 1)

The mouse IL-17F mutant 1 consisted of Arginine substitution of Glutamine at amino acid position 158 in wild-type mouse IL-17F. Previously amplified mFL-IL-17F (Section 2.1.2a) was used as template and hot PCR-amplified using the forward and the reverse primers listed in Table 1. The PCR product was digested with BamH1/Xba1 and cloned in the corresponding sites of the expression vector pcDNA3 (Invitrogen).

Mouse full-length (H157R) IL-17F mutant (mFL-IL-17F mutant 2)

Mouse mutant 2 was developed by substituting Histidine at amino acid 157 by Arginine. Previously amplified mFL-IL-17F (Section 2.1.2a) was used as template and hot PCR-amplified using the forward and the reverse primers listed in table 1. The PCR product was digested at BamH1/Xba1 and cloned in the corresponding sites of pcDNA3 (Invitrogen).

Mouse full-length truncated IL-17F mutant (mFL-IL-17F mutant 3)

Mouse IL-17F mutant was developed by substituting Valine at amino acid 156 in wild-type IL-17F by stop codon in order to delete the last four amino acids. Previously amplified mFL-IL-17F (section 2.1.2a) was used as template and hot PCR-amplified using the forward and the reverse primers listed in table 1. The PCR product was digested at BamH1/Xba1 sites and cloned in the corresponding sites of pcDNA3 (Invitrogen).

Human IL-17F (c-terminal end sequence)

SVPIQQETLVVRRKHQGCSVSFQLEKVLVTVGCTCVTPVI**HHVQ**

Mouse IL-17F (c-terminal end sequence)

NSVAIQQEILVLRREPQGCSNSFRLEKMLLVGCTCVKPIV**HQAA**

Figure 2.3 C-terminal sequences of human and mouse IL-17F. Comparison of mouse IL-17F and human IL-17F sequences showed that mouse IL-17F was 3 amino acids shorter and the third last amino acid in mouse IL-17F was Glutamine instead of mutated Histidine in human IL-17F. Mouse IL-17F however contained Histidine immediately preceding Glutamine. Based on these observations, three mouse analogues of human IL-17F mutant were created. Mouse mutant 1 involved substitution of Glutamine at amino acid position 158 by Arginine and mouse mutant 2 included substituting Histidine at 157 by Arginine. Mouse mutant 3 was developed as a truncated mutant by deletion of the last 4 amino acids.

2.1.3 Cloning of human and mouse wild-type and mutated LAP-IL-17

The mature fragments of human and mouse IL-17A, IL-17F and IL-17F mutants were PCR amplified using corresponding full-length IL-17A, IL-17F and IL-17F mutants cDNA (section 2.1.2) as template and the forward and reverse primers as listed in the Table 1. mLAP-IL-17A was amplified using hot-start PCR method (Section 2.1.4a). Due to the presence of an additional band, mLAP-IL-17F was isolated by gel-purification (Section 2.1.5a). The PCR products were digested at Not1 and Xba1 sites and cloned in the corresponding sites of the previously constructed expression vector pcDNA3-LAP-MMP (353) (Fig. 2.4).

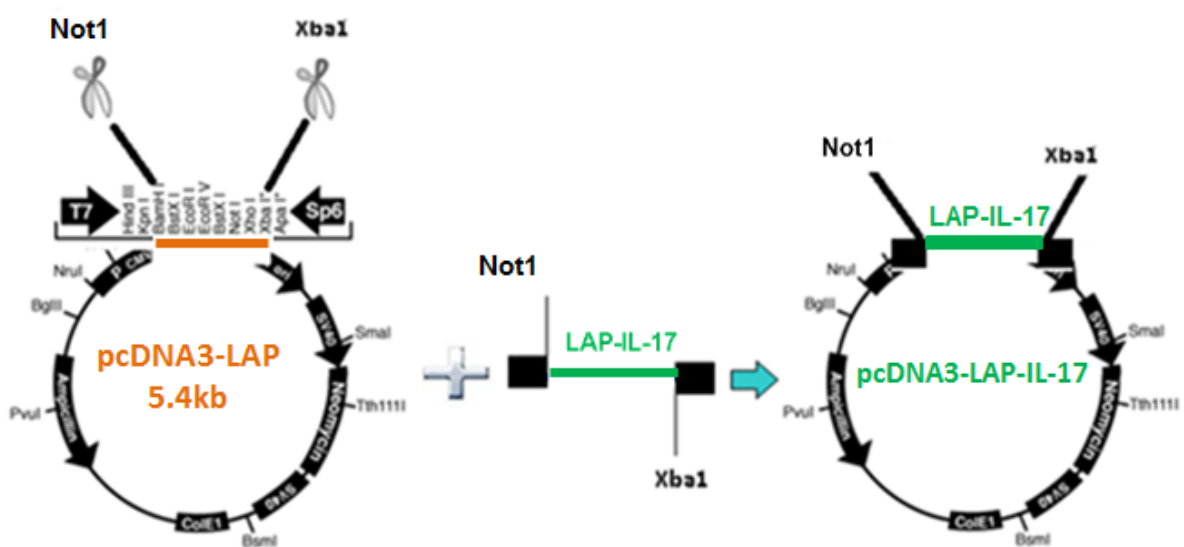


Figure 2.4 Cloning of mature IL-17 in pcDNA3-LAP. Human and mouse LAP-IL-17A, LAP-IL-17F and LAP-IL-17F mutant were constructed by cloning Not1 and Xba1 digested mature IL-17 into the corresponding sites of previously constructed plasmid expression vector pcDNA3-LAP.

2.1.4 Polymerase chain reaction DNA amplification

The PCR reactions containing 200ng DNA template, 0.1µg each forward and reverse primer, 10X Pfu buffer, 2units high-fidelity DNA polymerase, PfuUltra® (Stratagene Inc., CA), 2µl 10mM mixed d-NTP and distilled water to a total volume of 50µl was subjected to a protocol of an initial denaturation step at 95° C for 2 minutes, followed by 34 amplification cycles (denaturation at 95°C for 30 sec, annealing of primers at 60°C for 30 sec and strand amplification at 72°C for 2 min) and a final extension step of annealing at 72°C for 10 minutes using a Peltier Technology Thermal cycler (PTC-200, MJ Research Inc., Waltham, MA). The correct size of the PCR-amplified cDNA fragment was confirmed by agarose gel electrophoresis: 2µl PCR product in 8µl distilled water was mixed with 2µl 6X Bromophenol blue loading dye (30% v/v glycerol in distilled water, 0.25% bromophenol blue, 0.25% xylene blue) and separated on ethidium bromide (0.5µg/ml) containing 1% agarose gel in 0.5X TAE buffer (0.02M Tris-acetate, 0.5mM EDTA, pH 8.0) in parallel with 10µl (2µg) 1Kb Plus DNA ladder (100-12000 bp) (Invitrogen Co., Paisley, UK) at 100V for approximately one hour. The ethidium bromide-bound DNA was visualised under ultraviolet light and the image was captured using a gel documentation system (Uvitec Ltd, Cambridge, UK).

2.1.4a Hot-start PCR

The PCR reaction mixture containing 10X Pfu buffer, 2µl 10mM mixed d-NTP, 0.1µg each forward and the reverse primer, 200ng DNA template was boiled for 5 minutes in screw-capped tubes; transferred on to ice immediately and centrifuged briefly. 2units of high-fidelity DNA polymerase PfuUltra® (Stratagene Inc., La Jolla, CA) were added and PCR-amplification conducted as above (section 2.1.1) except that the annealing temperature was lowered to 52°C.

2.1.4b Phenol: chloroform extraction and sodium acetate precipitation of PCR products

An equal volume of water saturated phenol:chloroform solution was added to PCR mix and vortexed for 30 seconds, centrifuged at 13,000rpm for 5 min using an Eppendorf Microcentrifuge

(541D, Eppendorf, Hamburg, Germany). The top aqueous phase was mixed with 10% sodium acetate 3M, pH 5.2 and 2.5 volumes 100% cold ethanol, incubated at -20°C for 30 min, centrifuged at 13,000 rpm/min for 30 min at room temperature, pellet washed with 500µl 70% ethanol, centrifuged at 13,000rpm for 20 min, recovered DNA resuspended in distilled H₂O, gel-analysed and stored at -20°C.

2.1.5 DNA restriction enzyme digestion

The PCR products and plasmid vectors were digested with 5µl and 10µl respectively of appropriate enzymes, (New England Biolabs, Hitchin, UK) using 10X corresponding buffer ± 100X BSA in a total reaction-volume of 100µl by incubating at 37°C overnight, gel-analysed and stored at -20°C until utilized.

DNA gel purification

100µl digested DNA product or 20µg plasmid vector was loaded in equal amount in 10 different wells of 1% agarose gel and separated at 100V. The DNA band of interest was visualized under ultraviolet transilluminator (Uvitec Ltd), excised from the gel and purified, using PureLink™ Quick Gel extraction kit as per instructions from the manufacturer. In brief, the DNA-containing gel was dissolved in solubilisation buffer, incubated at 50°C for 20 minutes, passed through column, washed; and the purified DNA recovered in distilled water and stored at -20°C.

Annealing complementary strands of oligonucleotides

1µg each of complementary strands of oligonucleotides (1µg/µl) mixed in 10X T4 DNA ligase buffer in a total 50µl volume were annealed by boiling for 5 minutes, followed by slow cooling until the next day and stored at -20°C until cloned.

2.1.6 DNA Ligation

Restriction enzyme digested PCR products were ligated in 10-fold molar excess to the correspondingly digested 1µg plasmid vector in 10X T4 ligase buffer and 1.25µl 400,000 units/ml T4 DNA ligase (New England Biolabs, Ipswich, USA) in a total reaction volume of 25µl by incubating at 4°C overnight.

2.1.7 Transformation of E coli

2.1.7a Preparation of competent E. coli

Fresh E. Coli DH 5α were rendered competent for the uptake of plasmid DNA by using calcium chloride protocol (417). E. coli cells were grown overnight in 5ml LB at 37°C with vigorous shaking. This starter culture was transferred to 500ml pre-warmed LB medium and grown at 37°C with vigorous shaking until optical density (OD) read at 600nm reached values between 0.4 and 0.6. The bacterial culture was pelleted by centrifugation at 4000g for 10 minutes at 4°C using Multispeed Centrifuge (PK 121, ALC International, Milan, Italy) and suspended in 50ml freshly made ice-cold 0.1M MgCl₂. Cells were pelleted again (1500g, 10 min, 4°C), resuspended in 50ml ice-cold 0.1M CaCl₂ and incubated on ice for 20 minutes, re-centrifuged at 1500g for 10 minutes at 4°C. Cells were resuspended in 12.5ml ice cold 0.1M Ca Cl₂ with 14% glycerol, aliquoted, frozen on dry ice and stored at -80°C.

2.1.7b Transformation of competent E. coli DH 5α

25µl DNA ligation product (obtained from step 2.2.7) was mixed with 100µl competent E coli DH 5α (prepared as described below) and incubated on ice for 30 minutes, heat-shocked at 42°C for 2 minutes, incubated on ice for further 2 minutes and grown in 5ml Luria Bertani (1% bactotryptone, 0.5% bacto yeast extract, both from Invitrogen Corp., 0.17M NaCl, pH 7.4) without antibiotic with vigorous shaking at 37°C for 90 minutes. 400µl culture was then plated on a dry LB agar (1.5% w/v) 9

cm plates containing Ampicillin (100µg/ml) (Sigma-Aldrich Inc., UK) and grown at 37°C overnight, individual colonies picked and further analysed.

2.1.8 Extraction of plasmid DNA from *E. coli*

2.1.8a Small scale plasmid DNA extraction (Mini-preps)

The bacterial colonies picked from the LB agar plates were cultured overnight in 5ml LB with 100µg/ml Ampicillin at 37°C shaking. 1.5ml bacterial culture was centrifuged at 5000rpm for 5 minutes at room temperature in an Eppendorf Microcentrifuge. DNA was extracted and purified from the pelleted cells using Purelink™ Quick Plasmid Miniprep Kit, Invitrogen as per the manufacturer's instructions. In brief, the pelleted cells were resuspended in 250µl resuspension buffer with RNase, lysed with 250µl lysis buffer, precipitated with 350µl precipitation buffer. Centrifugation was then carried out at 12,000rpm for 10 min at room temperature. The nucleic acids in the supernatant were transferred to exchange column and centrifuged at 12,000rpm for 1 minute. After washing the column twice, DNA was eluted in distilled water and stored at 4°C. Miniprep-derived DNA from each colony was digested with the restriction enzymes (same as those used for cloning) using 20µl DNA, 10X buffer, 100X BSA and 1µl each enzyme in total 30µl volume and incubated at 37°C for 2 hours, gel-analysed and sequenced at the Genome Centre, Queen Mary, London, UK.

2.1.8b Large scale isolation of plasmid DNA (Maxi-prep)

For large-scale cultures, 1ml of the 5ml starter culture was grown in 500ml LB containing Ampicillin (100µg/ml) with vigorous shaking at 37°C overnight and pelleted by centrifuging at 4000 x g at 4°C for 20 min using Multispeed Centrifuge (PK 121, ALC International, Milan, Italy), then purified using Purelink™ HiPure Plasmid Maxiprep Kit (Invitrogen Corp.) as per the manufacturer's instructions. In brief, the pellet was resuspended in resuspension buffer containing RNase, lysed with lysis buffer, precipitated with precipitation buffer and centrifuged at 4000g for 20 minutes. The supernatant was

transferred to the Maxiprep kit column, washed and DNA eluted in 15ml elution buffer. The eluted DNA was then precipitated with 10.5ml Isopropanol, pelleted by centrifuging at 4000rpm at 4°C for 90 minutes, washed with 70% alcohol, centrifuged at 4000rpm at 4°C for 30 minutes. The pellet was suspended in distilled water and stored at 4°C. Plasmid DNA concentration was determined at 260nm using Pharmacia GeneQuant (Cambridge, UK) spectrophotometer. A sample of the purified plasmid DNA was digested (with enzymes used for cloning) and analysed on 1% agarose gel to confirm the presence of the insert of the correct size.

2.1.9 Expression of IL-17 in mammalian cells

All cell culture reagents were purchased from Cambrex Corp., Wokingham, UK.

293T cell line

The 293T cell line (418) was maintained in complete DMEM medium, supplemented with heat-inactivated 10% fetal bovine serum (FBS), 100U/ml of Penicillin, 100µg/ml of Streptomycin and 2mM L-Glutamine. The cells were detached using Trypsin-versene (Biowhittaker® Lonza, Belgium) for 2 minutes at 37°C before plating. The cells were grown at 37°C in humidified incubator, 10% CO₂ and split 1:10 at 70% confluency. Stocks were prepared by resuspending 1 x 10⁶ cells which had reached 70% confluency in 1ml 10% DMSO in complete DMEM in cryostat tubes, slow frozen first on ice for an hour, then at -80°C overnight and subsequently stored in liquid Nitrogen.

CHO-suspension cell line

CHO-S cells were maintained in L-glutamine containing Gibco® Freestyle™ CHO medium (Invitrogen, UK) in polycarbonate Erlenmeyer flask (Corning Incorp., USA) at 95-125rpm/min at 37°C in 8% CO₂ and split 1:10 at 70% confluency.

2.1.9a Transient transfection of mammalian cells

Calcium phosphate co-precipitation method

293T cells were transiently transfected as described previously (419). 1×10^6 293T cells were seeded in 9cm culture-plates in 10ml complete DMEM and incubated at 37°C in 10% CO₂ overnight. Next day, 20µg plasmid DNA was added to 500µl 2X HBS (280mM NaCl, 50mM HEPES, 1.5mM Na₂HPO₄, pH 7.1) and made upto 950µl with distilled water. 50µl 2.5M CaCl₂ was added drop-wise with constant gentle shaking and incubated for 30 minutes at room temperature. The medium was removed from the 293T cells seeded previous day and the calcium phosphate DNA precipitate was added to the cells and incubated for 30 minutes at room temperature with gentle tilting every 5 minutes. The cells were then topped with 9ml complete DMEM and grown at 37°C in 10% CO₂ overnight. Next day, after removing the medium, 1ml 10% glycerol in serum-free DMEM was added to the cells for 4 minutes with tilting every 30 seconds. The cells were washed twice with 5ml serum-free DMEM and grown in 6ml serum-free DMEM at 37°C in 10% CO₂ for 48 hours. The cell supernatant was collected, centrifuged at 3000rpm for 5 minutes and stored in aliquots at -80°C.

Polyethylene-imine (PEI) co-precipitation method

Human and mouse IL-17A/F, IL-17F/F mutant, IL-17A/F mutant heterodimers were expressed by transient co-transfection of 293T cells using PEI co-precipitation method.

Transient transfection with PEI, linear, MW 25,000 (Polysciences, Inc., Warrington, USA) was conducted in a similar manner to the calcium phosphate co-precipitation method except for the following differences. On day 2, 1ml DNA-PEI mixture was prepared by adding the following in the same order; 940µl Opti-MEM (Invitrogen, UK), DNA 20µg total (varying proportions of FL-IL-17A, IL-17F, IL-17Fmutant and pcDNA3 as described below, 40µl PEI (Polysciences, Inc., Warrington, PA), then vortexed and incubated for 10 minutes at room temperature before adding to the cells and the step of glycerol shock was omitted.

For the expression of heterodimers, total 20µg plasmid DNA was transfected using combinations of varying concentrations of IL-17A, IL-17F, IL-17F mutant and pcDNA3. For example, for the expression

of heterodimer IL-17A/F, IL-17A 15µg, IL-17F 5µg; IL-17A 10µg, IL-17F 10µg; IL-17A 15µg, IL-17F 5µg and IL-17A 5µg, IL-17F 15µg were co-transfected. When a single DNA was transfected, pcDNA3 was used to compensate to a final total of 20µg DNA.

2.1.9b Expression of non-secreted proteins

Some of the proteins may not be secreted but retained within the cells after expression. As mFL-IL-17F mutant 2 could not be detected in 293T cells supernatant, post-transfection the cells were lysed and lysate examined for the expressed protein. 2.5×10^5 /ml 293T cells were incubated in 2ml complete DMEM in a 6-well flat bottom Costar cell culture plate (Corning Incorporated, NY, USA) at 37°C in 10% CO₂ overnight and transfected with 6µg plasmid DNA using calcium phosphate co-precipitation method. Post-transfection, the cells were lysed by incubating with 250µl RIPA buffer, Sigma-Aldrich, UK (containing 150mM NaCl, 1% IGEPAL[®], CA-630, 0.5% sodium deoxycholate, 0.1% SDS, 50mM Tris, pH 8.0) plus 2.5µl protease inhibitor cocktail 8340, Sigma-Aldrich, UK (containing AEBSF i.e. 2-aminoethyl benzenesulfonyl fluoride, 104mM, Aprotinin 80uM, Bestatin 4mM, E-64 1.4mM, leupeptin 2mM, pepstatin A 1.5mM) at 4°C for 30 minutes. The cell lysate was centrifuged at 12,000rpm at 4°C for 20 minutes and collected in pre-cooled tubes and stored at -80°C. The concentration of total protein in the cell lysate was determined by using a Pierce[®] BCA protein assay kit (Thermo Scientific). In brief, 2-fold serial dilutions of cell lysate in serum-free DMEM and 25-2000µg/ml BSA standard in serum free DMEM were incubated with 200µl fresh BCA working reagent (prepared by mixing 50 parts BCA reagent A with 1 part BCA reagent B) in a 96-well Maxisorp, Nunc ELISA plate at 37°C for 30 minutes. The plate was cooled to room temperature before reading with the spectrophotometer set to 562nm. The absorbance measurement of the blank standard was subtracted from the rest of the standards and samples values before deriving the total concentration of proteins in the cell lysates.

2.1.10 Expression and immunoaffinity purification of human IL-17F mutant

2.1.10a Expression of human IL-17F mutant in CHO suspension cells

Human FL- and LAP-IL-17F mutant were expressed by transient transfection of 2 litre culture of CHO-suspension (CHO-S) cells grown at a density of 2×10^6 cells/ml with 800 μ g hFL-IL-17F mutant and LAP-IL-17F mutant plasmid DNA each using PEI co-precipitation method.

The expression of hFL- and LAP-IL-17F mutant protein in the CHO-S cells supernatant was confirmed by Western blot. The expressed hFL- and LAP-IL-17 mutant proteins were purified by immunoaffinity purification.

2.1.10b Binding of anti-human IL-17F antibody to Glycolink column

Oxidation of IL-17F antibody

1mg goat anti-human IL-17F polyclonal antibody (R&D Systems, UK) was diluted in Glycolink coupling buffer, pH 6 to a final volume of 1ml. In a microcentrifuge tube, 2.1mg sodium meta-periodate was added to the 1ml antibody solution while gently pipetting until the powder dissolved (resulting in 10mM periodate). The tube was wrapped in aluminium foil to protect from light and the mixture incubated at room temperature for 30 min.

A 5ml Zeba desalting column was centrifuged at 1000g for 2 minutes at 4°C using a 15ml collection tube and equilibrated by adding 2ml Glycolink coupling buffer and centrifugation, the step repeated twice. The oxidised glycoprotein solution was then slowly applied to the centre of the compact resin bed. The column was centrifuged at 1000g for 2 minutes at 4°C using a 15ml collection tube and the sample collected in 15ml tube, the collected solution contained the oxidised IL-17F antibody.

In the fume hood, 0.2M GlycoLink coupling catalyst was prepared by adding 18 μ l aniline to 1ml Glycolink coupling buffer. The catalyst was vortexed for 10 sec and the total volume added to the oxidised antibody sample (resulting in 0.1M aniline). 100 μ l sample was saved for subsequent determination of coupling efficiency.

Coupling oxidised antibody to Glycolink column

Ensuring that the Glycolink column resin was not allowed to dry at any time, the resin in the column was suspended by end-over-end mixing. The column was centrifuged to remove the storage buffer taking care to avoid drawing of air into the column. 2ml Glycolink coupling buffer was added and the column centrifuged at 1000g for 2 minutes at 4°C using a 15ml collection tube. This step was repeated once. Oxidised antibody sample was added to the GlycoLink column and mixed with resin by end-over-end mixing at RT for 4 hours. The column was centrifuged at 1000g for 2 minutes at 4°C using a new 15ml collection tube to collect non-bound protein. The flow-through was saved and the coupling efficiency determined by comparing the protein concentrations of the non-bound fraction to the starting sample saved previously. The column was washed thrice with 2ml Glycolink coupling buffer and centrifuged. The column was then washed thrice with 2ml wash buffer and centrifuged. The column was equilibrated for storage by adding 2ml PBS with 0.05% sodium azide at pH7-8 and centrifuged at 1000g for 2 minutes at 4°C using a 15ml collection tube. This step was repeated three times. The column resin in 2ml PBS with 0.05% sodium azide, pH7-8 was stored upright at 4°C.

2.1.10c Fast Protein Liquid Chromatography

Immunoaffinity purification of human FL-IL-17F mutant

The CHO-S cells supernatant containing the expressed hFL-IL-17F mutant protein was first dialysed using SnakeSkin Pleated Dialysis Tubing 10,000 MWCO (Thermoscientific, UK) at 4°C in a final total volume of 200 litre 1X PBS allowing buffer exchange for at least 4 hours in a cycle. The dialysed supernatant was filter sterilised using 0.22µm Polyether Sulfone filter system (Corning, USA) and purified by passing it through anti-IL-17F coupled Glycolink column at the rate of 0.5ml/hour at 4°C using FPLC (GE Healthcare, Uppsala, Sweden). Filter sterilised PBS, 0.2M glycine.HCl, pH 2.5-3.0 and 1M sodium phosphate, pH 8-9 were used as binding/wash, elution and neutralisation buffers respectively. Eluted fractions of 1ml were collected after adding 100µl neutralisation buffer to the individual elution tubes. The expression of hFLIL-17F mutant in the eluted fractions was confirmed

by Western blotting and the fractions containing the IL-17F mutant protein were dialysed using Slide-A-Lyzer® Dialysis cassette, 7,000 MWCO, 0.5-3ml capacity, ThermoScientific, Rockford, USA, aliquoted and stored at -80° C.

Immunoaffinity purification of humanLAP-IL-17F mutant

Human LAP-IL-17F mutant protein expressed and secreted in CHO-S cells supernatant was first dialysed using Spectra/Por® 6 dialysis membrane, MWCO, 50,000, Spectrum Laboratories Inc. (Dominguez, CA, USA) in the final total volume of 200 litre 1X PBS at 4°C allowing at least 4 hours of exchange during individual cycles.

The supernatant was filter sterilised and purified by passing it through using HiTrap™ HeparinHP 1ml column (GE Healthcare Bio-Sciences AB, Uppsala, Sweden) at the rate of 0.5ml/hour at 4°C using FPLC. Filter sterilised 20mM Tris HCL, 20mM EDTA, pH 8 was used as binding buffer and 20mM Tris HCL, 20mM EDTA, pH 8 plus 1M NaCl was used as elution buffer.

The heparin column purified hLAP-IL-17F containing CHO-S cell supernatant was subsequently immunoaffinity purified using anti-IL-17F antibody coupled with resin in a 10ml Sephadex column (Column PD-10, Sephadex® G-25M, Pharmacia LKB, Sweden). The column was pre-washed with 5ml 1X PBS at 4°C before running the supernatant at 0.5ml/hour, washed with 10ml PBS and purified LAP-IL-17F mutant eluted with 10ml glycine in fractions of 1ml each in tubes containing 100µl Sodium Phosphate buffer. OD of eluted fractions were estimated at 280nm, the fractions dialysed in 1X PBS using Slide-A-Lyzer® 10K Dialysis Cassette, 10,000 MWCO, Pierce Biotechnology, Rockford, USA, aliquoted and stored at -80°C.

2.2 Characterisation of immunological properties of expressed IL-17 proteins

2.2.1 Western blotting

***In vitro* cleavage of LAP-IL-17 by MMP-1**

200µl 293T cell supernatants transfected with human and mouse LAP-IL-17 proteins were incubated in the presence of MMP buffer 10X (50mM Tris, 5mM CaCl₂, 300mM NaCl, 20µM ZnCl₂, 0.5% Brij-35 and 30% glycerol, pH 7.5) with and without MMP-1 at 1:50 dilution at 37°C overnight. On day 2, EDTA to the final concentration of 2.5mM was added to chelate the zinc and stop the MMP-1 activity.

Sodium dodecyl sulphate-polyacrylamide gel electrophoresis (SDS-PAGE)

Three volumes of transiently transfected 293T cells supernatant or immunoaffinity purified samples were mixed with 1 volume of Laemmli's 4X reducing loading buffer (125mM Tris-HCL, pH 6.8, 0.4M DTT, 10% SDS, 40% glycerol, 0.002% bromophenol blue) (417) and boiled for 5 minutes before loaded onto the gel. 25µl samples were loaded to 1.5mm thick, 4-12% gradient, 10-well NuPAGE® Novex Bis-Tris gel in parallel with 10µl standard (10-250kDa Precision Plus protein standard, Bio-Rad Laboratories Inc., Hemel Hempstead, UK). The gel was run in NuPAGE® MOPS SDS running buffer (Invitrogen, UK) using X cell Sure Lock mini-cell (Invitrogen, UK) at 200V for 50 minutes.

Transfer of electrophoresed proteins to PVDF membrane

The gel was electro-blotted onto a polyvinylidene difluoride membrane (PVDF, Amersham International Plc, UK) by running in NuPAGE® MOPS transfer buffer (Invitrogen, UK) in X cell II™ Blot Module (Invitrogen, UK) at 30V for the minimum of one hour.

Blocking and immunoblotting of PVDF membrane

PVDF membrane was incubated with 25ml 5% non-fat milk (Marvel Premier Foods Plc., St Albans, UK) in PBST (0.005% Tween20 in 1X PBS) with modest shaking for 2 hours at RT, probed with 25µl primary antibody (goat anti-human or -mouse) in 1:1000 dilution in 25ml 5% non-fat milk in PBST by incubating overnight at 4°C; membranes washed thrice, incubated with 1:1000 secondary antibody,

horseradish peroxidase (HRP)-conjugated mouse anti-goat IgG polyclonal antibody (Santa Cruz Biotechnology, Middlesex, UK) in 25ml fresh 5% non-fat dry milk in PBST with mild shaking for 1 hour at RT; washed 4 times, treated with activated enhanced chemiluminescence solution (ECL, Amersham international plc., UK.) for 1 minute and exposed to autoradiography films (Amersham Pharmacia Biotech Inc., Amersham, UK) for approximately 1-10 minutes and the films developed using Agfa Curix 60 processor (Agfa-Gevaert Ltd., Gevaert, Belgium). The expression of the plasmid DNA encoded protein was confirmed by the presence of band of the expected size.

Silver staining of polyacrylamide gel

A sample of the immunoaffinity purified human FL- and LAP-IL-17F mutant each was resolved by SDS-PAGE and stained with Silver stain plus (Bio-Rad, UK) to verify the purity of the proteins. The polyacrylamide gel was first fixed by placing it in a total 400ml fixative enhancer solution (containing 200ml reagent grade methanol, 40ml reagent grade acetic acid, 40ml fixative enhancer concentrate and 120ml deionized water) and subjecting to gentle agitation for 30 min; gel rinsed with 400ml deionized water for 20 min with gentle agitation; stained in a mixture of freshly mixed 35ml deionized water, 5ml silver complex solution, 5ml reduction moderator solution and 5ml image development reagent, and 50ml accelerator solution with gentle agitation until desired staining intensity was reached; the reaction was stopped by placing the gel in 5% acetic acid for a minimum 15 min. The gel was rinsed with deionised water for 5 min and photographed.

2.2.2 Determining quantity of the expressed IL-17 proteins

Antibodies and other reagents

The polyclonal goat anti-human and anti-mouse IL-17A, IL-17F and LAP antibodies were purchased from R & D Systems, UK. The mouse anti-goat IgG-HRP was purchased from Santa Cruz Biotechnology. Recombinant human and mouse IL-17A and IL-17F were purchased from R & D Systems, UK and recombinant LAP was purchased from Sigma-Aldrich, UK.

Concentration of IL-17 containing 293T cell supernatants

Full-length IL-17 proteins

Mouse and human full-length IL-17F and IL-17F mutant expressed in supernatants of transiently transfected 293T cells were concentrated 20-fold using Centricon centrifugal filter device with YM-3 membrane (Millipore Corporation, UK) by centrifuging at 4000g/min at 4°C. Further samples of human FL-IL-17A, FL-IL-17F and FL-IL-17F mutant 293T cells-derived supernatants were concentrated 30-fold using Centricon centrifugal filter device with YM-10 membrane (Millipore Corporation, UK) so as to remove maximum possible impurities.

LAP-IL-17 proteins

Human LAP-IL-17A, LAP- IL-17F and LAP- IL-17F mutant expressed in the supernatant of transiently transfected 293 T cells were concentrated 30-fold using vivaspin 20 centrifugal concentrator MWCO 50,000 (Sigma Aldrich, UK).

2.2.2a Western blot quantitation of IL-17 in 293T cells supernatant

25µl concentrated human and mouse full-length and LAP-IL-17 proteins in serial two-fold dilutions and 100, 50 and 25ng of recombinant human or mouse IL-17A, IL-17F or human LAP were resolved on SDS-PAGE as outlined in Section 2.2.1. The quantity of the 293T-cells expressed proteins were derived by comparing their intensities on film with that of known quantities of standards using image J software.

2.2.2b ELISA quantitation of IL-17 in 293T cells supernatants

96 MicroWell™, MaxiSorp™ surface (Thermo Scientific Nunc, Denmark) plates were coated with 50µl standard (100ng/ml) or 293T cells-derived supernatants in coating buffer (0.1M sodium carbonate buffer, pH 9.6) at 4°C overnight, blocked with 200µl 5% non-fat dry milk in PBST for 2 hours at room temperature, treated with 50µl primary antibody (goat anti-human or mouse IL-17A, IL-17F or LAP) in 1:250 dilution in 5% Marvel for 2 hours, then 100µl secondary antibody (mouse

anti-goat IgG-HRP) in 1:500 dilution in 5% Marvel for 1 hour at room temperature. After each step, the wells were washed thrice with 300µl washing buffer (1X PBS plus 0.005% Tween). Finally, 100µl freshly reconstituted substrate (Tetramethylbenzidin, KPL, Gaithersburg, MD 20878, USA) was added and reaction stopped with 50µl 2M sulphuric acid. The optical density was determined at 450nm using Tecan GENios microplate reader (MTX Lab Systems, Inc., Virginia, USA).

2.2.2c Ultrasensitive ELISA quantitation of immunoaffinity purified IL-17F mutant

An IL-17F ultrasensitive ELISA was developed and standardised by using human IL-17F DuoSet ELISA (R&D Systems, UK) in conjunction with uncoated ELISA plate and 1% PBS or mouse diluents 4 and 5 (MSD, USA) to allow testing of mouse serum samples for the expression of mouse IL-17F mutant and increasing the sensitivity of R&D DuoSet ELISA. The lowest levels of IL-17F or IL-17F mutant that can be detected with DuoSet ELISA are 312.5pg/ml.

The assay was first standardized as follows: On day 1, two separate MSD ELISA plates were coated with 30µl per well 1, 2 and 4µg/ml capture antibody in PBS in duplicates and incubated at 4°C overnight. On day 2, the plates were washed thrice with PBST, blocked with 150µl 3% BSA for 1 hour at 175 rpm at RT. After washing thrice with PBST, one of the plates was incubated with 25µl diluent 4 at 175rpm for 30 minutes. R&D IL-17F standard was 3-fold serially diluted in 1% BSA in PBS or diluent 4 at the starting concentration of 20,000pg/ml. The lowest concentration of IL-17F mutant that could be detected was 27.4pg/ml. The plates were incubated with 25µl/well standard for 2 hours at 175rpm at RT and washed thrice with PBST. 25µl/well 0.1 and 0.5µg/ml detection antibody in 1% BSA in PBS or diluent 5 plus 1µg/ml Streptavidin sulfotag was added and plates incubated for 2 hours at 175rpm at RT, washed thrice with PBST and 150µl 2X Read buffer in deionised water added. The plates were then analysed using Sector® Imager 2400 (Meso Scale Discovery, Rockville, USA).

The quantity of purified FL-and LAP-IL-17F mutant was analysed by human IL-17F ultrasensitive ELISA as described above using 2µg/ml capture and 0.5µg/ml detect antibody in 1% BSA in PBS.

2.3 Characterisation of *in vitro* biological properties of expressed

IL-17 proteins

HFFF2 cells

Human Caucasian foetal foreskin fibroblast cell line, which is derived from foreskin of 14-18 weeks old human foetus were kindly provided by Dr Adrian Churchman, Bart's Institute of Cancer, WHRI. The HFFF2 cells were maintained in complete DMEM at 37°C in 10% CO₂. The cells were passaged when 70% confluent by detaching with Trypsin-versene.

HeLa cells

HeLa cells were maintained in complete DMEM or complete RPMI at 37°C in 10% CO₂.

57A HeLa cells

57A HeLa, a luciferase reporter cell line derived from stable transfection of HeLa cells with NF-κB-responsive luciferase (420) was kindly provided by Dr Apostolos Koutsokeras, BJRU. 57A HeLa cells were maintained in complete DMEM plus 500µg/ml G418 (Geneticin 418) at 37°C in 10% CO₂.

HeLa cells stably transfected with IL-6 promoter-responsive luciferase

HeLa cells were stably transfected with IL-6 promoter-responsive luciferase (kindly provided by Prof Chernajovsky, BJRU) and the cell line was maintained in complete DMEM plus 1µg/ml Blasticidin.

NIH 3T3 cells

The spontaneously immortalised Swiss mouse embryonic fibroblast cell line (421) was maintained in complete DMEM at 37°C in 10% CO₂. The cells were passaged when 70% confluent by detaching with Trypsin-versene.

Raw 264.7 cells stably transfected with NF-κB driven luciferase

Mouse macrophage cells stably transfected with NF-κB-responsive luciferase were kindly provided by Dr S. Vessillier, BJRU. These cells were maintained in complete DMEM plus 200µg/ml G418 at 37°C in 10% CO₂. The cells were passaged when 70% confluent by detaching the adherent cells using sterile cell scraper.

DTF cells stably transfected with IL-6 promoter-responsive luciferase

DTF cells, which are conditionally SV40 large T immortalised DBA/1 fibroblasts (422) were stably transfected with IL-6 promoter-responsive luciferase and maintained in complete DMEM plus 2 µg/ml Blastocidin at 37°C in 10% CO₂. The cells were passaged when 70% confluent by detaching with Trypsin-versene.

2.3.1 Characterisation of *in vitro* biological properties of expressed human IL-17

2.3.1a Determining IL-17RC binding capability of human FL-IL-17F mutant

Mouse polyhistidine monoclonal antibody, recombinant human IL-17A, IL-17F, hIL-17RC, biotinylated anti-human IL-17A and IL-17F antibodies and Streptavidin-HRP were purchased from R&D Systems, UK.

The ability of human FL-IL-17F mutant to bind to human IL-17RC was assessed by functional ELISA as per the manufacturer's instructions. In brief, 96-well ELISA plate (Maxisorp, Nunc, Denmark) was coated with 10 µg/ml mouse anti-polyhistidine in cold PBS (100 µl/well) and incubated at room temperature overnight, blocked with 1% BSA in PBS (300 µl/well) and incubated for 2 hours at 37°C.

In a separate ELISA plate, 50 µl hIL-17RC at the final concentration of 100 ng/ml was mixed with 50 µl 3-fold serially diluted hFL-IL-17A or hFL-IL-17F mutant at the starting final concentration of 2 µg/ml in 0.5% BSA in PBS and incubated at 500 rpm for 2 hours at room temperature. As a control, 50 µl binding buffer instead of the hIL-17RC was added to the human IL-17 dilution wells to check the non-specific binding hIL-17.

After removing the blocking buffer, 100 µl mixture of the hIL-17 and hIL-17RC or the binding buffer was added to each well and incubated at room temperature overnight. Next day after washing with 1% PBST thrice, the plate was incubated with 3 µg/ml goat biotinylated anti-human IL-17 (anti-IL-17A or anti-IL-17F) antibody in binding buffer (100 µl/well) at RT for 2 hours, washed thrice and incubated with 1:200 diluted Streptavidin-HRP (100 µl/well) at RT for 30 minutes. ELISA was developed by adding 100 µl freshly prepared TMB (by mixing 50 µl TMB substrate and reagent each) per well at RT

for 20-30 minutes. The reaction was finally stopped by adding 50µl 2mM Sulphuric acid per well and OD measured at 450nm. The net binding was obtained by subtracting the non-specific binding value from the total binding values.

2.3.1b Fibroblast cells IL-6 induction IL-17 bioassay

Analysis of IL-17 induced secretion of IL-6 in fibroblast cells is the standard bioassay for IL-17 activity (96, 107). Bioactivity of 293T cells expressed human IL-17 was analysed in human foetal foreskin fibroblast and mouse embryonic fibroblast cells.

Evaluation of IL-17 induced secretion of IL-6 in HFFF2 cells

1 x 10⁴ HFFF2 cells in 100µl complete DMEM in 96-well plate were incubated at 37°C in 10% CO₂ until adherent and, stimulated with 100µl/well 100ng/ml rhIL-17(IL-17A and IL-17F), FL-IL17(IL-17A, IL-17F, and IL-17F mutant), and MMP-1-treated and untreated LAP-IL-17 (IL-17A, IL-17F and IL-17F mutant), 10ng/ml rhIL-1β, mock supernatant derived from transient transfection of 293T cells with pcDNA3 alone and complete DMEM in triplicates for 24 hours at 37°C in 10% CO₂ and supernatants analysed using human IL-6 Duoset ELISA (R & D Systems Europe Ltd., Abingdon, UK) as per the manufacturer's instructions.

For competitive inhibition assay, HFFF2 cells were co-stimulated with 293T cells supernatant containing 25ng/ml FL-IL-17A and two-fold serially diluted 25ng/ml FL-IL-17F mutant for 24 hours and supernatant analysed for IL-6 as above.

Evaluation of human IL-17-induced secretion of IL-6 in NIH 3T3 cell

It has been shown that human IL-17A and human IL-17F are able to bind to both mouse IL-17RA and IL-17RC, and stimulate secretion of IL-6 in mouse fibroblast cells (95, 181). Biological effects of expressed human IL-17 proteins in 3T3 cells were analysed as below.

5 x 10³ NIH 3T3 cells in 100 µl complete DMEM in 96-well plate were incubated in 10% CO₂ at 37°C until adherent, stimulated with 100 µl 100ng/ml rhIL-17A and IL-17F , FL-IL17F mutant, and medium alone (complete) DMEM in triplicates in 10% CO₂ at 37°C for 24 hours. The supernatants were

analysed for IL-6 using mouse IL-6 DuoSet ELISA (R & D Systems Europe Ltd., Abingdon, UK) as per the manufacturer's instructions. For competitive inhibition assay, the cells were co-stimulated with two-fold serially diluted 1µg/ml rhIL-17A plus 50µl 293T cells supernatant containing human IL-17F mutant protein.

2.3.1c Epithelial cells IL-6 induction IL-17 bioassay

IL-6 is one of the earliest defined IL-17 gene targets. IL-17 has been shown to induce secretion of IL-6 in endothelial, epithelial and fibroblast cells. Bioactivity of 293T cells-expressed IL-17 in HeLa cells was analysed as described below.

Evaluation of IL-17-induced secretion of IL-6 in HeLa cells

1 x 10⁴ HeLa cells in 100 µl complete DMEM in 96-well plate were incubated at 37°C in 10% CO₂ until adherent, and stimulated with 100µl/well 100ng/ml or 10ng/ml rhIL-17A and IL-17F and 100ng/ml or 10ng/ml immunoaffinity purified IL-17F mutant, 10ng/ml rhIL-1β as positive control and complete DMEM alone at 37°C in 10% CO₂ for 24 hours and the supernatant analysed for IL-6 by human IL-6 DuoSet ELISA (R & D Systems Europe Ltd., Abingdon, UK) as per the manufacturer's instructions.

For competitive inhibition assays, the cells were co-stimulated with 100ng/ml rhIL-17A or IL-17F plus 100ng/ml immunoaffinity purified IL-17F mutant for 24 hours.

IL-6 DuoSet ELISA was carried out as follows: 96-well ELISA plate (Maxisorp, Nunc-Immunoplate, Nunc™, Roskilde, Denmark) was coated with 50µl/well capture antibody (2µg/ml in PBS) overnight at RT, blocked with 200µl 1% BSA (Fisher Scientific, Leicestershire, UK) in PBS for 2 hours at RT, washed with PBST (0.005% Tween® 20 in PBS), incubated with 50µl sample or standard in 1%BSA in PBS for 2 hours at RT, washed thrice with PBST, incubated with 50µl/well detect antibody (0.2µg/ml in 1%BSA in PBS) for 2 hours at RT, washed thrice, incubated with 50µl Streptavidin-HRP diluted 1:200 in 1%BSA in PBS for 20 minutes at room temperature avoiding direct light, washed thrice, incubated with freshly prepared 50µl 1:1 mixture of colour reagent A (H₂O₂) and colour reagent B Tetramethylbenzidine (KPL, Gaithersburg, USA) for 20 minutes at room temperature avoiding direct

light, the reaction stopped with 25µl 2M H₂SO₄ (WWR International Ltd., Poole, England) and OD determined at 450 nm.

2.3.1d Evaluation of biological effects of IL-17F mutant on ERK1/2 signaling

Extracellular signal-related kinase p42/44 (ERK) and p38 MAPK are phosphorylated following IL-17 stimulation (423, 424). The biological effects of immunoaffinity purified IL-17F mutant on ERK1/2 phosphorylation in HeLa cells were analysed as follows:

1 x 10⁶ HeLa cells in 1ml complete DMEM in 12-well culture plate were incubated at 37°C in 10% CO₂ until adherent, washed twice and serum starved in serum-free DMEM for 18 hours and stimulated with either 100ng/ml or 10ng/ml rhIL-17A and IL-17F plus 100ng/ml or 10ng/ml immunoaffinity purified FL-IL-17F mutant in serum free DMEM for 20 minutes and the cell lysates analysed for phosphorylation of ERK1/2 as described below.

The cell lysates were prepared as follows: plates were kept on ice, cells washed twice with ice cold PBS and lysed with 250µl cold lysis buffer (containing 10mM Tris HCl, pH 7.4, 0.1% SDS, 100mM NaCl, sodium deoxycholate 0.5%, EDTA 1mM, EGTA 1mM, Triton X 100 1%, 10% glycerol, 1mM sodium fluoride, 20mM sodium phosphate with freshly added 2mM sodium vanadate, 1mM PMSF and Halt™ protease inhibitor single use cocktail, EDTA free, 100X, Thermo Scientific, Rockford, USA) by incubating for 30 minutes at 4°C. The lysate was centrifuged at 12,000rpm for 20 minutes at 4°C, collected in pre-cooled tubes and stored at -80°C. The concentration of protein in cell lysate was determined by BCA assay as described in Section 2.1.9a.

Analysing ERK1/2 phosphorylation by Western blot

20µg cell lysate proteins were resolved by SDS-PAGE, transferred to PVDF membrane and probed with rabbit P44/P42 MAPK (ERK1/2) antibody (Cell signaling Technology, Inc., Danvers, MA, USA) or rabbit phospho-P44/P42 MAPK (ERK1/2) (Thr202/Tyr204) antibody (Cell signaling Technology, Inc., Danvers, MA, USA) and detected with sheep anti-rabbit IgG (AbD SeroTec, UK) detect antibody.

Analysing ERK1/2 phosphorylation by multiplex ELISA

20µg cell lysate proteins were analysed for total and phosphorylated ERK1/2 using phospho (Thr202/Tyr204; Thr185/Tyr187)/total ERK1/2 whole cell lysate multiplex ELISA (MSD, USA) as per the manufacturer's instructions.

2.3.1e Developing a novel luciferase reporter assay to analyse bioactivity of human IL-17

Cell culture luciferase reporter system

Cell signaling processes leading to specific transcription factor activation can be analysed using reporter gene assays that measure transcription response element (RE) activity. Amongst the available reporters, firefly luciferase is ideal for the study of promoter activity in transfected cells due to its broad dynamic range, sensitivity, ease of quantification, and lack of endogenous activity. By coupling the operative regulatory elements to the expression of luciferase gene, typically by placing the transcription factor DNA binding site just upstream of luciferase gene, the cellular event can be readily detected by a luminescent signal. Luciferase reporter genes can be readily delivered to a variety of cells using approaches such as viral or chemical vectors and electroporation.

Dual luciferase reporter system

In the quantitation of gene expression using firefly luciferase in transiently transfected cultured cells, the experimental reporter gene is often co-transfected with a second reporter gene to correct for experimental variability. Such dual reporters allow comparative measurements within an experimental system. Typically the second reporter is used as an internal control that is coupled to a constitutive promoter that is unperturbed by various experimental conditions, against which the measurement of the experimental reporter is normalized. Sea pansy (*Renilla reniformis*) luciferase possesses distinct evolutionary origins from firefly luciferase and therefore has dissimilar enzyme structures and substrate requirements. Firefly luciferase uses luciferin in the presence of oxygen, ATP and magnesium to produce greenish yellow light at 550-570nm whereas *Renilla* luciferase uses coelenterazine and oxygen to produce a blue light at 480nm. Combining firefly luciferase reporter

systems with those of the Renilla reniformis luciferase therefore allows the sequential measurement of activities of both the luciferases from a single lysate. In this method the substrates for the firefly and Renilla luciferase are added to a sample sequentially and luminescence measured following the addition of each.

57A HeLa cells NF- κ B-promoter-driven luciferase assay

In an attempt to standardise a novel luciferase reporter assay in 57A HeLa cells, 1×10^4 cells in 100 μ l complete DMEM plus 500 μ g/ml G418 were seeded in 96 well plate and incubated at 37°C in 10% CO₂ until adherent, after which the was medium changed to 0.1% FBS-containing DMEM without the antibiotic. The cells were incubated overnight at 37°C in 10% CO₂, washed twice with 0.1% FBS-containing DMEM and stimulated in triplicates with 100 μ l two-fold serially diluted rhIL-17A (500ng/ml), FL- IL-17A , FL- IL-17F, and rhIL-1 β (50ng/ml) for 6 hours. The cell lysates were prepared by washing the cells with PBS twice and lysing with 50 μ l passive lysis buffer (Promega Corp., UK). 10 μ l cell lysate in the presence of 50 μ l substrate was analysed for luciferase activity using MLX microtitre plate luminometer, Dynex Technologies Inc.

As 500ng/ml rhIL-17 failed to induce detectable luciferase activity in 57A HeLa cells, 2ng/ml rmTNF- α was added to enhance its activity. IL-17 activates IL-6 synergistically with many other cytokines including TNF- α , IL-1 β , IFN- γ and IL-22 (114, 115, 121, 425, 426) and IL-17A and IL-17F responsiveness is often evaluated in conjunction with suboptimal concentrations of TNF- α (135).

293T cells IL-6 promoter responsive dual luciferase assay

1.25×10^5 293T cells in 1ml complete DMEM were seeded in 12-well plate and incubated overnight at 37°C in 10% CO₂. The next day cells were transiently co-transfected with 2 μ g pGL2 containing IL-6 promoter responsive luciferase and 0.2 μ g Renilla-CMV using calcium phosphate co-precipitation method, and incubated in 1ml complete DMEM overnight at 37°C in 10% CO₂. On day 3, the cells were washed twice with serum free DMEM and in triplicates stimulated with 500ng/ml rhIL-17, 50ng/ml rhIL-1 β , PMA, PMA+ Ionomycin, 0.5 % FBS containing DMEM for 24 hours at 37°C in 10%

CO₂, washed twice with PBS, lysed with 250µl reporter lysis buffer under moderate agitation for 30 min at RT, lysate centrifuged at 1200rpm for 10 min. 10µl lysate was transferred to luminometer reading plate and analysed by MLX microtitre plate luminometer, Dynex Technologies Inc. using Stop and Glow dual luciferase assay kit. The IL-6 responsive luciferase activity was analysed first in the presence of 50µl luminometer substrate, followed by analysis of Renilla CMV activity in the presence of 50µl Renilla substrate.

Evaluation of IL-17 induced activation of IL-6 promoter-responsive luciferase in HeLa cells

Stable transfection of HeLa cells with pGL2 containing IL-6 promoter responsive luciferase

HeLa cells were stably transfected with plasmid expression vector pGL2 with previously cloned IL-6-promoter responsive luciferase (kindly provided by Prof Yuti Chernajovsky, BJRU) fused to Blasticidin resistant site containing plasmid vector pcDNA6.

Fusion of plasmid vectors pGL2 and pcDNA6

10µg pGL2 and 1µg pcDNA6 were linearized in buffer 4 by restriction digestion at FSP1 site, which cleaved pcDNA6 once and PGL2 twice, albeit within the Ampicillin resistant site; phenol: chloroform extracted; Sodium acetate and Ammonium acetate precipitated and ligated with 5µl T4 ligase in total 150µl volume ligation reaction. The ligation mixture was Ammonium acetate precipitated, resuspended in 100µl H₂O and frozen at -20°C. Efficiency of the ligation was visually confirmed on 1% agar gel.

Estimation of Blasticidin concentration for selection of HeLa cells

2 x 10⁵ HeLa cells in 5ml DMEM were incubated in eight separate 5ml tissue culture flasks in 10% CO₂ at 37°C until adherent. The cells were then treated with DMEM plus Blasticidin in the concentrations of 0, 1, 2, 3, 5, 7, 8 and 10µg/ml and the antibiotic containing medium changed every 3 days. The cells were visually assessed for cell apoptosis on daily basis for determination of the concentration of Blasticidin required for optimum cell selection.

Stable transfection of HeLa cells using calcium phosphate co-precipitation method

0.5 x 10⁶ cells were incubated in complete DMEM in 10% CO₂ at 37°C until adherent, medium changed to fresh complete DMEM, after 6 hours cells were transfected with 50µl ligation mixture of plasmid DNAs pcDNA6 and pGL2 using calcium phosphate co-precipitation method as described in the Section 2.1.9a. Following glycerol shock, the cells were incubated in complete DMEM for 24 hours in 10% CO₂ at 37°C, split into 4 and incubated in complete DMEM plus 2µg/ml Blasticidin at 37°C in 10% CO₂. The antibiotic containing medium was changed every 3-4 days. Blasticidin selected cell clones were expanded to adequate size, ring cloned and individual clones incubated in complete DMEM plus 2µg/ml Blasticidin in 12-wells plates in 10% CO₂ at 37°C until confluent.

Stable transfection of HeLa cells using Fugene 6 transfection reagent

1 x 10⁶ cells in 10ml complete DMEM medium in 9cm culture plate were incubated in 10% CO₂ at 37°C until adherent and transfected with 50µl ligation mixture of pcDNA6 and pGL2 using 18µl Fugene6 (Roche Diagnostics Corporation, Indianapolis, IN) as per the manufacturer's instruction. The cells were incubated for 48 hours in 10% CO₂ at 37°C until ready for passage and antibiotic selection.

Stable transfection of HeLa cells using electroporation

1 x 10⁶ HeLa cells were pelleted by centrifuging the cell suspension at 1000rpm for 10 minutes, mixed with 100µl solution V and ligation mixture of pcDNA6 plus pGL2, transferred to Amaxa cuvette and electroporated using 2 different programmes, O-005 for better viability and I-013 for better efficiency of transfection. The electroporated cells were immediately transferred to 500µl complete DMEM, the cell suspension divided into 3 equal parts and incubated in 6-well plate in 3ml complete DMEM overnight in 10%CO₂ at 37°C. Next day, after trypsinising, the cells were pooled together and incubated in 10ml complete DMEM plus 2µg/ml Blasticidin in 9cm plate in 10%CO₂ at 37°C until ready for ring cloning of Blasticidin selected clones.

Ring cloning

No more than 2 clones per plate were ring cloned. The cells were washed with PBS twice and a sterile ring was placed around the selected clones using sterile paraffin, cells trypsinised with 50µl Trysin-EDTA and individual cell clones transferred to 12-well plate in 2ml complete DMEM plus 2µg/ml Blastcidin and incubated in 10% CO₂ at 37°C until confluent. After adequate expansion, the cell clones were grown in 9cm plates in 10ml complete DMEM plus 2µg/ml Blastcidin in 10% CO₂ at 37°C until 70% confluent. The individual cell clones were then examined for their suitability for the future biological assays.

Assessing biological activity of antibiotic selected clones

1 x 10⁴ HeLa cells stably transfected with IL-6 promoter-responsive luciferase were seeded in 100µl DMEM plus 2µg/ml Blastcidin in 96-well plate and incubated at 37°C in 10% CO₂ until adherent. The cells were serum starved by incubating in 0.5% FBS containing DMEM overnight at 37°C in 10% CO₂ and next day stimulated with 100ng/ml rhIL-17 in 0.5% serum containing DMEM for 24 hours in 10% CO₂ at 37°C. The cell lysates were analysed for the background and IL-17- induced luciferase activity as described in Section 2.3.1d.

2.3.2 Characterisation of *in vitro* biological properties of expressed mouse IL-17 proteins

2.3.2a Determining receptor binding affinity of mouse FL-IL-17F mutants

A functional ELISA to assess the binding of mouse FL-IL-17F mutants to mL-17RC was carried out similar to that for human IL-17F mutant (Section 2.3.1a) except for the following differences: The starting final concentration of mouse IL-17 was 0.3µg/ml and goat biotinylated anti-mouse IL-17F was used at the concentration of 1µg/ml.

2.3.2b Fibroblast cells IL-6 induction mouse IL-17 bioassay

Developing an in-house mouse IL-6 ELISA

Anti-mouse IL-6 antibodies-producing hybridoma cells

Anti-mouse IL-6 capture and detect antibodies producing hybridoma cells, HB10656 and HB10657 were kindly gifted by Dr. Richard Williams, Kennedy Institute, Imperial College, London. The cells were maintained in complete RPMI supplemented with 10% FBS, 100U/ml Penicillin, 100µg/ml Streptomycin and 2mM L-Glutamine. Approximately one litre cell culture supernatant from the cells grown at a final density of $0.5-1 \times 10^6$ cells/ml was collected and stored at -80°C until purified.

Purification of antibodies containing supernatants

The supernatants were filter sterilised prior to purification, using ProSep G columns (Millipore, Schenectady, USA). In brief, Prosep G resin was packed in binding buffer (0.5M glycine in PBS, pH 7.4) in column and equilibrated with a minimum of 100 column volume/hour binding buffer ran through the column for 30-60 minutes. Then the following agents were run through the column at a speed of 1ml/min in the same order. The column was first cleaned with 5 column volumes of 6M Guanidine HCl, regenerated with 10 column volumes of HCl, pH 1.5 followed by 5 column volumes of 1X PBS. Thereafter 5 column volume of binding buffer were passed through the column before running the antibody containing supernatants from the hybridomas. The column was washed with 5 column volumes of binding buffer and protein eluted with 3M potassium thiocyanate in PBS in multiple 1ml fractions. The column was washed with 50-100ml of 1X PBS plus 0.2-1% sodium azide.

The OD of the eluted fractions was determined at 280nm. The eluate was dialysed in 1X PBS using Slide-A-Lyzer dialysis cassettes allowing at least 4 hours of exchange in total 100X volume of the eluate. A fraction of eluate was resolved by SDS-PAGE gel under non-reducing conditions and stained with Commassie Blue. Eluates were aliquoted and stored at -80°C.

Biotinylation of mouse anti- IL-6 detect antibody

The mouse anti-IL-6 antibody was biotinylated using EZ-Link[®] sulfo-NHS-SS-Biotinylation kit (Pierce Biotechnology, Rockford, USA).

10mM Biotin was freshly prepared by dissolving 2.2mg Biotin in 360µl of deionised H₂O. 19.8µl Biotin was added to 1ml detect antibody in PBS (1.5mg/ml) and incubated for 30-60 minutes at RT. The excess Biotin was removed using equilibrated Zeba[™] desalt column and centrifuging at 1000g for 2 minutes. The antibody containing flow through was collected and stored at -80°C.

The level of Biotin incorporation was estimated using HABA assay as follows: 10 mg avidin and 600µl 10mM HABA (4-Hydroxyazobenzene-2-Carboxylic acid) was added to 19.4 ml of PBS and absorbance measured at 500nm to confirm that A₅₀₀ of this solution was between 0.9-1.3 in a 1cm cuvette.

First the absorbance of 180µl HABA/avidin solution in the microplate was measured at 500nm on its own and repeated after adding 20µl biotinylated antibody solution. The degree of biotinylation was reflected by the difference between the two values and calculated as Moles of Biotin per Mole of protein.

Testing immunoactivity of purified anti-IL-6 capture and detect antibodies

On day 1, an ELISA plate was coated with 50µl/well capture antibody in varying concentrations as outlined in Fig. 2.5 and incubated at 4°C overnight. On day 2 after washing thrice with PBST (1%PBS plus 0.05% Tween20), the plate was blocked with 50µl 1% casein for 1 hour at RT; incubated with two-fold serially diluted 50µl/well recombinant mouse IL-6 in PBST at the starting concentration of 20ng/ml for 1 hour at RT, then incubated with 50µl/well biotinylated antibody in PBST in varying dilutions (Fig. 2.5) for 1 hour at RT followed by incubation with 50µl/well Avidin/HRP (1:1000 diluted in PBST) for 1 hour at RT. The plate was washed with PBST thrice after each step. Finally, the plate

was incubated with 50µl substrate (freshly prepared by dissolving 1 tablet Sigma fast™ o-phenylenediamine dihydrochloride in 20 ml distilled water) in the dark for 15 minutes. The reaction was stopped with 10µl/well 20% sulphuric acid and absorbance read at 450nm.

An ELISA to test immunoactivity was repeated by coating 2 separate ELISA plates with 50µl/well 5µg/ml capture antibody and blocking one plate with 1% casein and the 2nd plate without casein, using IL-6 standard at the starting concentration of 5ng/ml and detect antibody in 1:250 and 1:500 dilutions substituting PBST by 1% casein as diluting reagent.

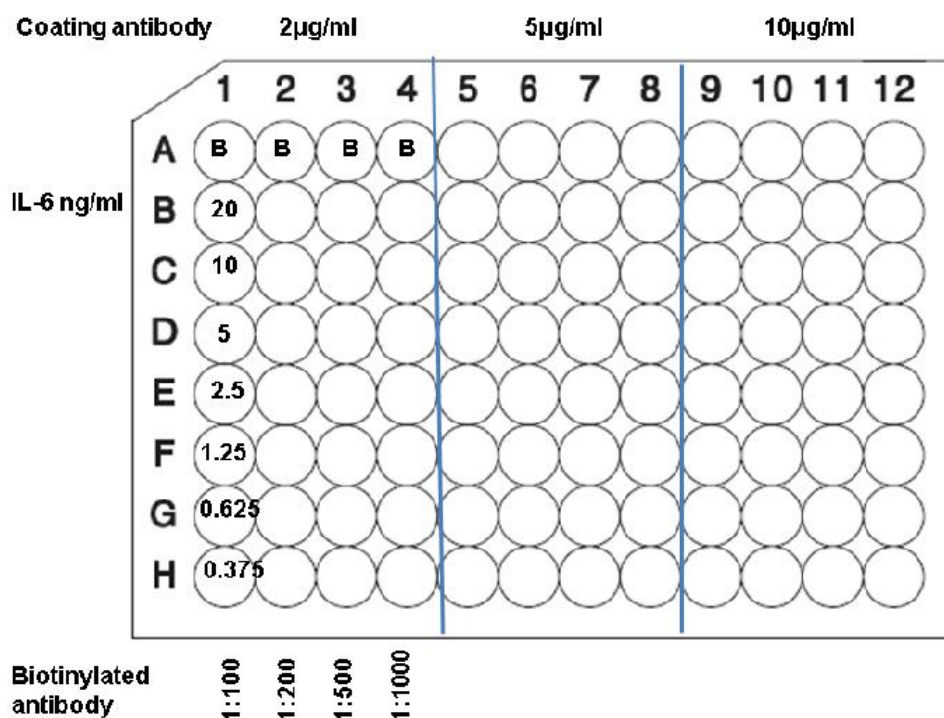


Figure 2.5 Testing immunoactivity of purified mouse anti-IL-6 antibodies. Hybridoma cells derived mouse anti-IL-6 capture and detect antibodies were purified using Prosep G column, detect anti-IL-6 antibody biotinylated and tested for immunoactivity by ELISA. Capture antibody in the concentrations of 2µg/ml, 5µg/ml and 10µg/ml were examined for IL-6 reactivity using two-fold serially diluted IL-6 standard in the starting concentration of 20ng/ml and biotinylated anti-IL-6 detect antibody in 1:100, 1:200, 1:500 and 1:1000 dilution by sandwich ELISA and absorbance read at 450nm.

Mouse IL-17-Induced secretion of IL-6 in NIH 3T3 cells

5 x 10³ cells in 100µl complete DMEM in 96-well plate were incubated in 10% CO₂ at 37°C until adherent and stimulated with 100µl 100ng/ml rIL-17A and -IL-17F; FL-IL-17A, -IL-17F and -IL-17F mutant 1; and MMP-1-treated and untreated LAP-IL-17A, -IL-17F and -IL-17F mutant 1 along with 10ng/ml rTNF-α as positive control, complete DMEM alone in triplicates in 10% CO₂ at 37°C for 24 hours. The supernatants were analysed using mouse IL-6 DuoSet ELISA (R & D Systems Europe Ltd., Abingdon, UK) as per the manufacturer's instructions.

2.3.2c Developing a novel luciferase reporter assay to analyse bioactivity of mouse IL-17

Raw 264.6 cells NF-κB-promoter-driven luciferase assay

1 x 10⁶ raw264.7 NF-κB luc cells (made by Dr. S. Vessillier of BJRU) were incubated in 2ml complete DMEM plus 200µg/ml G418 in 12-well plate at 37°C in 10% CO₂ overnight, stimulated with 1ml/well 500ng/ml rIL-17A, FL- IL-17A and -IL-17F in serum-free DMEM in triplicates at 37°C in 10% CO₂ overnight. For the purpose of positive control, the cells were incubated with 1ml/well 10µg/ml lipopolysaccharide for 4 hours at 37°C in 10% CO₂. The cells were washed with PBS twice, lysed with 100µl cold lysis buffer (200mM NaCl, 20mM Tris HCl, pH 8, 1% Triton X-100) and lysates examined for luciferase activity as described in Section 2.3.1d.

DTF cells IL-6 promoter-responsive luciferase assay

Stable transfection of DTF cells with IL-6 promoter responsive luciferase

DTF cells were stably transfected with pGL2 containing IL-6 promoter responsive luciferase using the same protocol as that was used for transfection of HeLa cells (Section 2.3.1d). The concentration of Blastidicin for optimum selections of DTF cells was determined and the cells stably transfected using calcium phosphate co-precipitation, antibiotic selected clones expanded and screened for biological activity as described above for HeLa cells. One of the antibiotic selected clones which on screening

demonstrated a low background activity along with activation of luciferase in response to rmIL-17A and was further analysed as follows:

2×10^4 DTF cells stably transfected with IL-6 promoter-responsive luciferase were stimulated with 100 μ l/well two-fold serially diluted rmIL-17 (500ng/ml), mouse FL-IL-17A and 17F in 0.1% FBS containing DMEM in triplicates for 6 hours at 37°C in 10% CO₂. The cells were lysed and lysates analysed for luciferase activity as described in the Section 2.3.1d.

As 500ng/ml rmIL-17 failed to activate luciferase in these cells, 2ng/ml recombinant mouse TNF- α was added to enhance the activity of IL-17A.

2.4 Gene therapy in mouse models of inflammation

Preparation of endotoxin-free plasmid DNA

Plasmid DNA encoding human FL-IL-17A, LAP-IL-17A, FL-IL-17F mutant and LAP-IL-17F mutant was extracted and purified using Endofree® Plasmid Mega Kit (Qiagen Ltd, Crawley, UK) as per the manufacturer's instructions. In brief, pellet of sterile 500ml high copy overnight LB bacterial culture obtained by centrifugation at 4000g at 4°C for 20 min using Multispeed Centrifuge (PK 121, ALC International, Milan, Italy) was homogeneously resuspended in 50ml Buffer P1 (50mM Tris HCl, pH 8.0, 10mM EDTA and 100µg/ml RNase A), lysed in 50ml Buffer 2 (200mM NaOH, 1% SDS) by vigorously inverting 5 times and incubating at RT for 5 min, and neutralized with 50ml chilled Buffer P3 (3.0M potassium acetate, pH 5.5) by subjecting it to a thorough mixing by vigorously inverting 5 times. The lysate was added to QIAfilter Mega Cartridge and incubated for 10 min; cleared under a vacuum source and washed with 50ml Buffer FWB2 (1M potassium acetate, pH 5.5) using vacuum. For removal of endotoxins, the cleared lysate was mixed with 12.5ml Buffer ER by inverting the tube 10 times and incubated on ice for 30 min. The ER buffer-treated lysate was applied to a QIAGEN-tip 2500 [pre-equilibrated with 35ml Buffer QBT (750mM NaCl, 50mM MOPS, pH 7.0, 15% isopropanol, 0.15% Triton® X-100)] and allowed to enter the resin by gravity flow, washed with 200ml Buffer QC (1.0M NaCl, 50mM MOPS, pH 7.0, 15% isopropanol). The bound plasmid DNA was eluted with 35ml Buffer QN (1.6M NaCl, 50mM MOPS, pH 7.0, 15% isopropanol), eluted DNA precipitated by adding 24.5ml isopropanol and centrifuging at 4000rpm at 4°C for 90 min. The DNA pellet was washed with endotoxin-free 70% ethanol and centrifuged at 4000rpm at 4°C for 30 min, air-dried for 10-20 min, resuspended in endotoxin-free water (Qiagen Ltd, Crawley, UK) and stored at 4°C. Plasmid DNA concentration was determined at 260nm using Pharmacia GeneQuant spectrophotometer (Cambridge, UK). A sample of the purified plasmid DNA was digested with the enzymes used for cloning and analysed on 1% agarose gel to confirm the presence of insert of the correct size.

C57BL/6 mice

Thirty 6 weeks-old male C57BL/6 mice (20-25g, Charles River UK Limited, UK) were kept under standard conditions and maintained in a 12 h/12 h light/dark cycle at $22 \pm 1^\circ\text{C}$ in accordance with United Kingdom Home Office regulations (Guidance on the Operation of Animals, Scientific Procedures Act 1986) and of the European Union directives.

SCID mice

Four female and 4 male, 6-weeks-old SCID beige mice (Charles River UK Limited) were kept under standard conditions as described above.

Intravenous hydrodynamic delivery of plasmid DNA

Mice were lightly anaesthetized with 4% Isoflurane (IsoFlo[®], Abott Laboratories Ltd, Berkshire, UK) mixed in O₂/NO at 1:1 atmosphere using Boyles' apparatus (British Oxygen Company, London, UK). Mice were injected in the tail vein with 5µg/ml plasmid DNA in normal saline (NS), equating to 10% average mice body weight rapidly over 10-15 seconds. The untreated group of mice were injected with NS alone.

Determining *in vivo* expression of human IL-17 transgene in mice

Collection of serum

Mice were tail bled or terminally bled via cardio-puncture after light anaesthesia. Blood was allowed to clot by storing overnight at 4°C, serum recovered by centrifuging at 14000 rpm at 4°C for 15 minutes and frozen at -80°C.

Harvesting mouse liver tissue

After sacrificing the mice, liver was dissected out and 20mg harvested liver tissue was stabilised by immediately immersing in 200µl RNeasy[®] RNA stabilisation reagent (Qiagen, UK) and stored at -80°C. A separate piece of liver tissue was snap frozen in liquid nitrogen and stored at -80°C until analysed.

Preparation of liver homogenates

Approximately 5mm piece of liver tissue (previously snap frozen in liquid nitrogen and stored at -80°C) was homogenised in 500µl ice cold lysis buffer (20mM Tris HCl, pH 7.4, 150mM NaCl, 1% Triton X-100, 1% BSA, freshly added Halt™ Protease inhibitor, single use cocktail, EDTA free 100X, Thermo scientific, Rockford, USA) in pre-cooled homogenization tubes (Precellys CK14, Bertin Technologies) at 3000rpm, 2 x 20 sec pulses using Precellys™ control device (Stretton Scientific Ltd.). The homogenate was centrifuged at 1500rpm at 4°C for a maximum of 5 min. Protein concentration in the homogenised liver sample was estimated by BCA. The BCA standard and cell lysates were diluted in PBS at least 50-fold to eliminate protein reactivity intrinsic to the lysis buffer due to the presence of 1% BSA.

Ultrasensitive ELISAs

In vivo expression of human IL-17 transgene in mice following systemic gene therapy was analysed by human IL-17A and IL-17F ultrasensitive ELISAs.

Human IL-17A ultrasensitive ELISA

Levels of human IL-17A in mice serum were analysed using human IL-17A ultra-sensitive kit in association with diluents 4 and 5 (Meso Scale Discovery multi-array® System, Gaithersburg, USA) as per the manufacturer's instructions. In brief, 25µl/well diluent 4 in the MSD ELISA plate was incubated at 175 rpm for 30 min at RT; 25µl mouse serum, airpouch lavage fluid or IL-17A standard (concentrations 2.4-10,000pg/ml) in diluent 4 in duplicate were incubated at 175rpm for 2 hours at room temperature; washed 3 times with PBST; 25µl detection antibody solution added and incubated at 175 rpm for 2 hours, washed 3 times with PBST; 150µl 2X read buffer added and the plate was analysed using MSD-sector imager 2400.

Human IL-17F ultrasensitive ELISA

Levels of human full-length and LAP-IL-17F mutant in mice serum, airpouch lavage fluid and liver homogenate samples were analysed using human IL-17F ultrasensitive ELISA using 2µg/ml capture and 0.5µg/ml detect antibody in diluents 4 and 5 as described in the Section 2.2.2c.

2.4.1 Human IL-17A systemic gene therapy in naïve SCID mice

Six-weeks-old SCID beige mice (Charles River UK Ltd.) were divided into two groups of 4 mice each containing 2 female (average weight 17.5g) and 2 male mice (average weight 21.5g). Mice were treated with intravenous hydrodynamically delivered 5µg/ml human full-length IL-17A or LAP-IL-17A plasmid DNA. Blood was collected at 48 hours, 1 week and 2 weeks and serum recovered and stored. Levels of human IL-17 transgene in mice serum were analysed by human IL-17A ultra-sensitive ELISA.

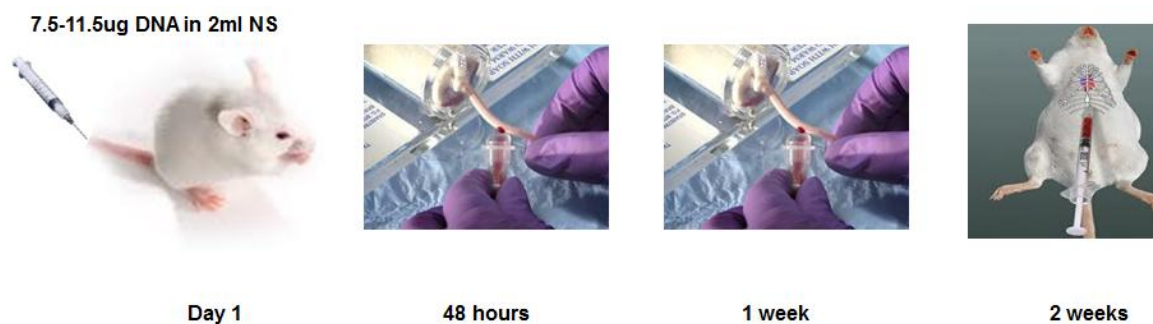


Figure 2.6 Evaluation of *in vivo* expression and pharmacokinetics of human IL-17 systemic gene therapy in naïve SCID mice. Four mice in groups of 2 were treated with intravenous hydrodynamically delivered hIL-17A or hLAP-IL-17A and blood collected at 48 hours, 1 week and 2 weeks. Levels of hIL-17A in mice serum were analysed by IL-17A ultrasensitive ELISA.

2.4.2 Evaluation of human IL-17F mutant systemic gene therapy in mouse airpouch inflammation

Preparation of airpouch and induction of acute inflammation

After lightly anaesthetising C57BL/6 mice, dorsal airpouch were prepared by injecting 2.5ml air subcutaneously on days 1 and 4. On day 5, acute non-specific inflammation was induced by directly injecting 0.5ml 0.5% Carboxy methyl cellulose (CMC 0.5% w/v in sterile PBS) into pouch as previously described by Perretti *et al.* (427, 428).

Hydrodynamic delivery of human IL-17 plasmid DNA

On day 4, mice in groups of five were treated with intravenous hydrodynamically delivered 5µg/ml human FL-IL-17F mutant, LAP-IL-17F mutant DNA, FL-IL-17A, FL-IL-17A plus FL-IL-17F mutant, 1µg/ml LAP-IL-17F mutant and NS alone to investigate *in vivo* expression of human IL-17 transgene. Mouse serum, liver homogenates and airpouch lavage exudate were analysed for the expression of the transgene. The study was terminated at 52 hours post-DNA delivery to allow analysing transgene levels in acutely inflamed airpouch at 4 hours following its systemic expression at 48 hours.

Collection of airpouch lavage fluid

Mice were culled by cervical dislocation. Airpouch was washed thoroughly with 2ml PBS containing 3mM EDTA through a small incision and the recovered lavage fluid was collected in 14ml polypropylene round-bottom FACS tubes (Becton Dickinson, USA), centrifuged at 1500rpm for 10 min at 4°C to separate the exudate from the inflammatory cells. Inflammatory exudate was collected, total volume measured and frozen at -80°C.

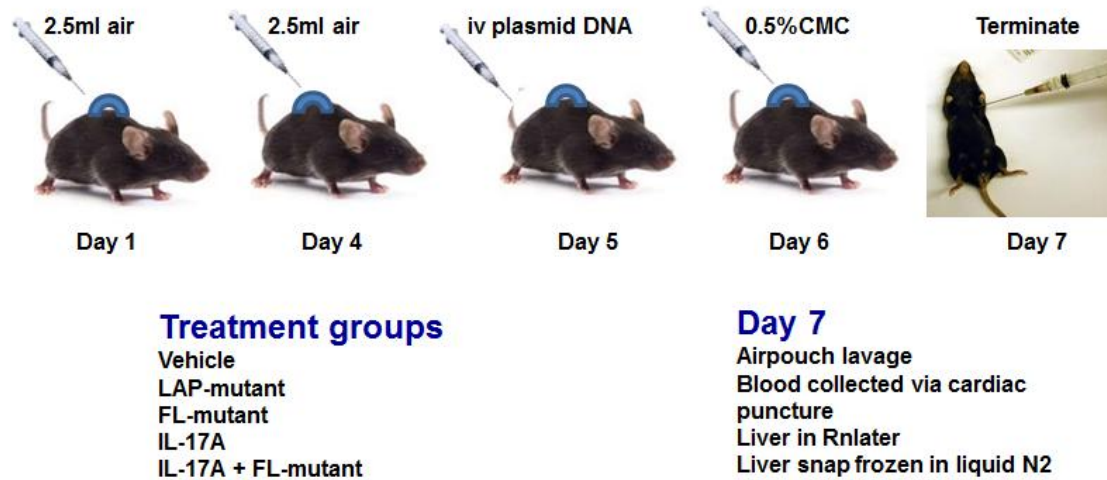


Figure 2.7 Investigation of *in vivo* distribution of human IL-17F mutant gene delivery in mice airpouch. Six mice in each group were treated with intravenous hydrodynamic DNA delivery of hIL-17F mutant plus hIL-17A or hIL-17A, hFL-IL-17F mutant, hLAP-IL-17F mutant (1µg and 5µg/ml) and NS alone 52 hours before the termination of the study. This allowed a 48 hours period for the expression of transgene to take place and then study its distribution on tissues after CMC-induced inflammation for a total 4 hours. Expression of transgene was analysed in serum, airpouch lavage fluid and liver homogenate samples.

Statistical analysis: One way ANOVA and students T test were used to compare the levels of induced cytokines between treatment groups and *p* values less than 0.05 were considered significant. Results are expressed as the mean ± SEM unless stated otherwise.

CHAPTER III

CLONING OF HUMAN, MOUSE AND LATENT

IL-17 ISOFORMS

3.1 Introduction

A new therapeutic agent can be developed and tested rapidly using recombinant DNA technology. Cloning of a therapeutic gene in a suitable expression vector enables its expression in protein form both *in vitro* and *in vivo*, thus allowing an expedient broad preclinical testing. Both viral and non-viral vectors can be used for expression of a gene of interest in mammalian cells. Non-viral or plasmid vectors are safer than viral vectors but require adjunct physical or chemical approaches for an adequate transfection efficiency. Plasmid expression vector pcDNA3 contains all the elements such as CMV promoter with enhancer, T7 site for forward DNA sequencing for expression in relevant E coli host, SV40 origin of replication, Neomycin and Ampicillin drug selection genes for use in eukaryotic and prokaryotic cells respectively, bovine growth hormone (BGH) polyadenylation site to stabilise the mRNA, multiple cloning sites required for efficient cloning in bacteria, and expression in eukaryotic cells (Fig. 3.1). The SP6 site allows for DNA sequencing using a well characterised reverse primer. pcDNA3-LAP encompasses pcDNA3 with a previously cloned LAP of TGF- β (353) .

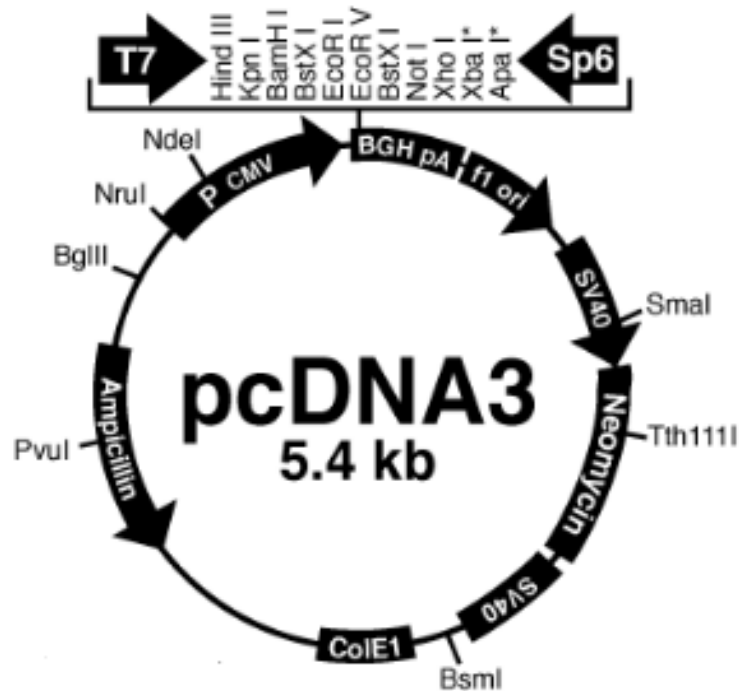


Figure 3.1 Plasmid expression vector pcDNA3. pcDNA3 contains all the elements required for efficient cloning in bacteria, and cloning and translation in eukaryotic cells. CMV promoter/enhancer permits efficient, high level expression of protein, T7 enhancer allows *in vitro* transcription in the sense orientation and sequencing through the insert, SV40 enhancer promoter and origin of replication facilitates high level protein expression and replication of plasmid in cell lines containing large T antigen, SV40 poly functions as transcription terminator, Bovine growth hormone polyA provides efficient transcription termination and mRNA polyadenylation, Neomycin resistant site is utilised for selection of stable transfectants in mammalian cells, Ampicillin resistant site allows selection of vector in *E. coli*, multiple cloning site allows insertion of gene of interest.

IL-17 mRNA was derived from T cells, which produce IL-17 in both human and mouse. Prior to RT-PCR, mRNA extracted from mouse splenic T cells was analysed for integrity. mRNA comprises only 1-3% of total RNA and is not readily detectable even with the most sensitive of methods. Ribosomal RNA (rRNA) however comprises more than 80% of total RNA. mRNA quality has historically been assessed by visual assessment of quality and quantity of rRNA on 1% agarose gel electrophoresis. The majority of rRNA in mammalian system is comprised by the 28S and 18S rRNA and a 28S:18S ratio of 2:1 is taken as indicative of intact RNA.

Human CD14- PBMC and NIH Swiss mouse splenic T cells cDNA was used as template for PCR amplification of human and mouse IL-17. A hot-start PCR was employed if necessary. A manual heating of reaction components prior to adding polymerase to the denaturation temperature of 95° reduces non-specific amplification during the initial set up stages of the PCR. It also permits optimum denaturation of primers especially those with high CpG contents. Non-specific amplification can also be reduced by raising annealing temperature. In the event of presence of more than one band on agarose gel electrophoresis analysis of PCR reaction, band that represented the gene of interest was isolated and purified by gel extraction.

Site-directed mutagenesis

Mutation at a defined site in a DNA molecule can be created using one of the several approaches such as Kunkel's method, cassette mutagenesis, PCR mutagenesis and whole plasmid mutagenesis. In Kunkel's method, mutagenesis template is generated by insertion of wild-type DNA in phagemid such as M13mp18/19 and transforming in *E. coli* that are deficient in DNA repair enzymes (429). Cassette mutagenesis involves insertion of a complementary pair of oligonucleotide containing the mutated gene in plasmid whereas PCR mutagenesis involves amplification of DNA template using single primer that contains the desired mutation. PCR reaction mixture resulting from PCR mutagenesis however contains original unmutated DNA in addition to mutated DNA. PCR mutagenesis could also lead to counter selection of mutants due to presence of mismatch repair system which favors the methylated template DNA. The method of whole plasmid site-directed mutagenesis comprises amplification of entire plasmid using a pair of complementary mutagenic primers followed by elimination of template DNA. This method is highly efficient, relatively simple and commercially available as a kit.

PCR amplified full-length and mature human and mouse wild-type and mutated IL-17 were cloned in pcDNA3 and pcDNA3-LAP at multiple cloning sites. The genes conferring resistance to Ampicillin were utilised for antibiotic selection of transformed *E. coli*. The selected colonies were grown in Ampicillin

containing LB medium and plasmid extracted by alkaline lysis. The confirmation of correctly cloned constructs was attained by gene sequencing using ABI 3730xl capillary sequencer and restriction digestion with enzymes same as those used for cloning.

3.1.1 Aims

1. To harvest mRNA from mouse splenic T cells and RT-PCR it to generate cDNA.
2. To create human (H161R) IL-17F mutant and 3 mouse analogues of human IL-17F mutant.
3. To clone human and mouse full-length and mature IL-17 DNAs in plasmid expression vectors pcDNA3 and pcDNA3-LAP.

3.2 Results

3.2.1 Confirming integrity of mouse splenic T cells mRNA

Mouse IL-17 was amplified using template cDNA derived by reverse transcription of NIH Swiss mouse splenic T cells mRNA. Integrity of mouse spleen extracted RNA was analysed by visual assessment of 28S:18S rRNA ratio on 1% agarose gel. As shown in the figure 3.1, the 28S:18S ratio was approximately 2:1, which confirmed the integrity of mRNA.

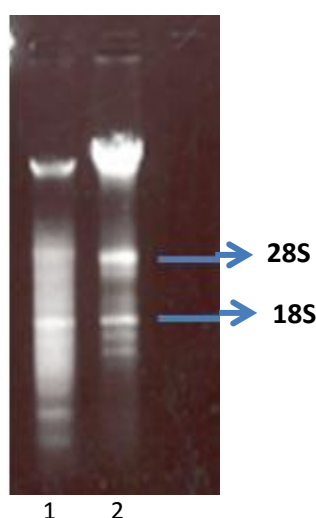


Figure 3.2 Confirming integrity of mouse splenic T cells mRNA. Swiss mouse splenic T cells cDNA was used as template to amplify mouse IL-17. RNA extracted from mouse spleen was analysed for integrity of mRNA by visual analysis of ribosomal RNA on 1% agarose gel electrophoresis. Lane 2 shows presence of 5kb and 2kb sized 28S and 18S ribosomal RNA bands in an approximate ratio of 2:1 indicating intact RNA. Lane 1 shows control RNA extracted from 293T cells.

3.2.2 Cloning of human IL-17

The PCR amplified human full-length IL-17A, IL-17F and IL-17F mutant genes were cloned in pcDNA3 at BamH1 and Xba1 sites. The human (H161R) IL-17F mutant was created by restriction digestion of wild type IL-17F DNA at BSPM1 site and substitution of the deleted C-terminal end with custom ordered complementary oligonucleotides containing the desired mutation. Human LAP-IL-17 constructs were generated by cloning mature IL-17A, IL-17F and IL-17F mutant in pcDNA3-LAP at Not1 and Xba1 sites. Generation of the correct constructs were confirmed by DNA sequencing and restriction enzyme digestion of plasmid DNA (Figs 3.3 and 3.4).

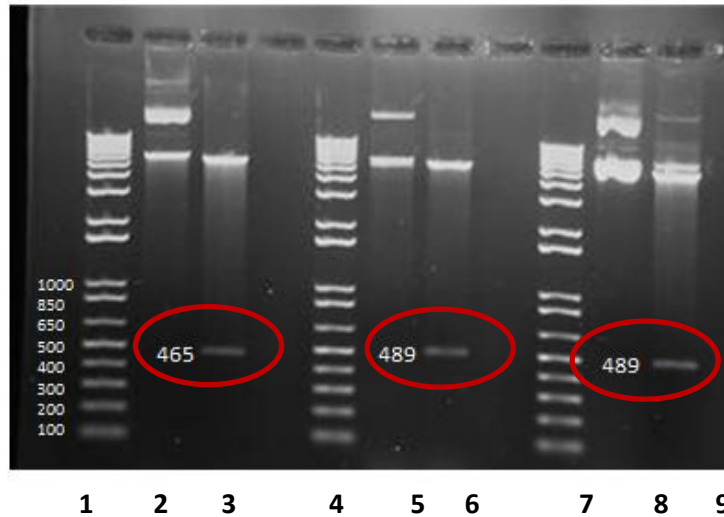


Figure 3.3 Restriction enzyme analysis of human full-length IL-17 on 1% agarose gel confirming the correct cloning of IL-17 in pcDNA3. BamH1 and Xba1 restriction digestion of uncut plasmid DNAs (size 5.4kb, lanes 2, 5 and 8) released the insert and vector fragments of expected size. Lanes 3, 6 and 9 show that the released full-length IL-17A, and IL-17F and IL-17F mutant fragments were of expected 465 and 489 bp size respectively (circled in red) confirming the correct cloning. The 1kb molecular weight DNA ladder was used to assess the size of DNA fragments (lanes 1, 4 and 7).

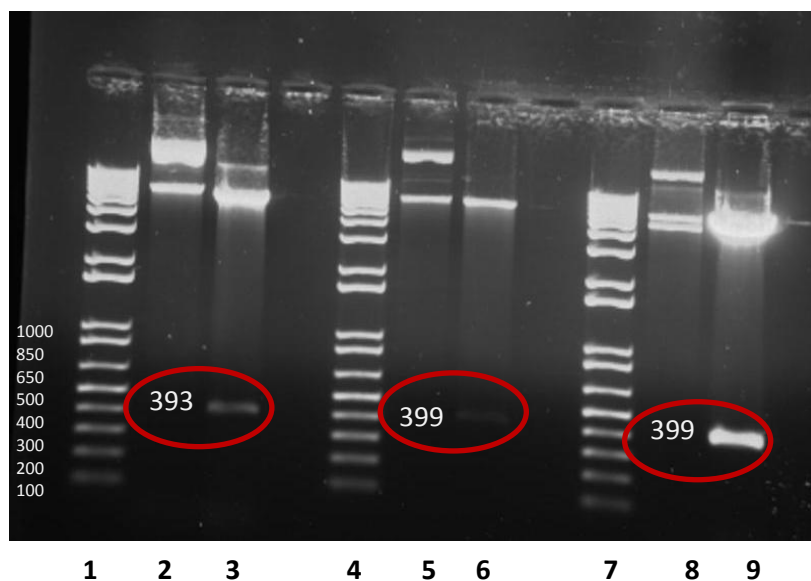


Figure 3.4 Restriction enzyme analysis of human LAP-IL-17 on 1% agarose gel confirming the correct cloning of mature IL-17 in pcDNA3-LAP. Not1 and Xba1 restriction digestion of uncut plasmid DNAs (size 6.1kb, lanes 2, 5 and 8) released the insert and vector fragments of expected size. Lanes 3, 6 and 9 show that the released mature IL-17A, and IL-17F and IL-17F mutant fragments were of expected 393 and 399 bp size respectively (circled in red) confirming the correct cloning. The 1kb molecular weight DNA ladder was used to assess the size of DNA fragments (lanes 1, 4 and 7).

3.2.3 Cloning of mouse IL-17

The PCR amplified mouse full-length and mature wild-type and mutated IL-17 were cloned in pcDNA3 and pcDNA3-LAP similar to that for human IL-17 (Figs 3.5 and 3.6). Three mouse FL-IL-17F mutants namely (Q158R) IL-17F mutant 1, (H157R)IL-17F mutant 2 and a truncated IL-17F mutant 3 were derived by PCR mutagenesis of wild type IL-17F resulting in substitution of nucleotide T at position 464 by C, nucleotide A at 461 by G and codon GGA at 457-59 by stop codon respectively.

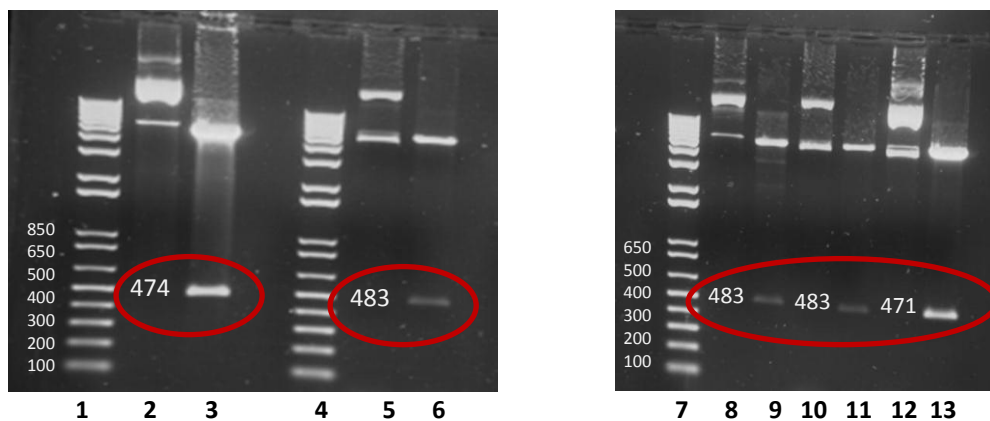


Figure 3.5 Restriction enzyme analysis of mouse full-length IL-17 on 1% agarose gel confirming the correct cloning of IL-17 in pcDNA3. BamH1 and Xba1 restriction digestion of uncut plasmid DNAs (size 5.4kb, lanes 2, 5, 8, 10 and 12) released the insert and vector fragments of expected size. The released full-length IL-17A (lane 3), IL-17F and IL-17F mutants 1 and 2 (lanes 6, 9 and 11) and IL-17F mutant 3(lane 13) fragments were of expected 474, 483 and 471 bp size respectively (circled in red) confirming the correct cloning. The 1kb molecular weight DNA ladder was used to assess the size of DNA fragments (lanes 1, 4 and 7).

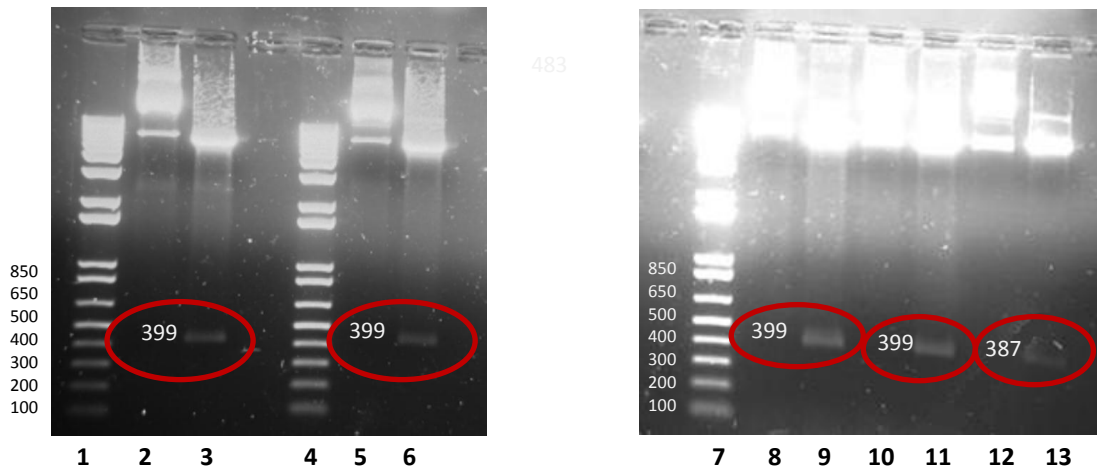


Figure 3.6 Restriction enzyme analysis of mouse LAP-IL-17 on 1% agarose gel confirming the correct cloning of mature IL-17 in pcDNA3-LAP.Not1 and Xba1 restriction digestion of uncut plasmid DNAs (size 6.1kb, lanes 2, 5, 8, 10 and 12) released the insert and vector fragments of expected size. The released mature IL-17A, IL-17F, IL-17F mutants 1 and 2 (lanes 3, 6, 9 and 11) and IL-17F mutant 3 (lane 13) fragments were of expected 399 and 387 bp size respectively (circled in red) confirming the correct cloning. The 1kb molecular weight DNA ladder was used to assess the size of DNA fragments.

3.3 Discussion

Human and mouse full-length and mature wild-type and mutated IL-17 DNA were successfully cloned in plasmid expression vectors pcDNA3 and pcDNA3-LAP. BamH1 and Xba1 restriction sites at multiple cloning sites of pcDNA3 were utilised for cloning of human and mouse wild-type and mutated full-length IL-17 in pcDNA3, whereas Not1 and Xba1 sites were used for cloning of human and mouse wild-type and mutated mature IL-17 in pcDNA3-LAP. The MMP cleavable linker located between the LAP of TGF- β and mature IL-17 cytokine region allows the release of biologically active cytokine at the sites of high MMP activity.

Mouse IL-17 was amplified using mouse splenic T cells cDNA as template. The integrity of mRNA extracted from mouse spleen was analysed by 1% agarose gel electrophoresis and confirmed by presence of 28S:18S rRNA bands in ratio 2:1. Mouse IL-17A and IL-17F mutants were amplified by hot-start PCR due to a relatively high CpG content of the primers. Non-specific PCR amplification of mouse IL-17F DNA could not be eliminated by raising annealing temperature; the correct DNA band was therefore isolated by gel-purification. Alternative splicing of mouse IL-17F has not been reported although human IL-17F has been shown to exist in two forms (131).

Human (H161R) IL-17F mutant was created by substituting nucleotide A at position 485 by G using cassette mutagenesis. The presence of point mutation in IL-17F gene at the extreme C-terminal end and an adjacent BSPM restriction site allowed for an effective insertion of mutation containing complementary oligonucleotides. Mouse IL-17F is 3 amino acids shorter than human IL-17F and contains Glutamine at position equivalent to mutated Histidine in human IL-17F. The first mouse IL-17F mutant analogue was therefore created by Arginine substitution of Glutamine at amino acid position 158 instead of Histidine at 161 in human IL-17F. Amino acid Histidine is however present in mouse IL-17F immediately preceding Glutamine at 158. The second mouse IL-17F mutant therefore comprised Arginine substitution of Histidine at 157. The third Mouse IL-17F mutant was created by deleting the last 4 amino acids in mouse IL-17 to create a truncated form. PCR mutagenesis was used to build the desired point mutations and the deletion mutation in wild-type IL-17F.

Following successful cloning IL-17 proteins were expressed *in vitro* and their immunological and biological properties analysed.

CHAPTER IV

CHARACTERISATION OF IMMUNOLOGICAL PROPERTIES OF THE EXPRESSED IL-17 PROTEINS

4.1 Introduction

Following successful cloning of human and mouse full-length and LAP-IL-17 in plasmid expression vector pcDNA3, IL-17 proteins were expressed *in vitro* under the control of CMV promoter by transient transfection of mammalian cells. Unlike prokaryotes or lower eukaryotes, mammalian cells have capability to conduct elaborate posttranslational modifications, especially N-glycosylation of the complex type, hence are often preferred host to produce human recombinant proteins. 293T cells derived from human embryonic kidney contain large T cell antigen, hence allowing replication of plasmid DNA that contains an SV40 origin of replication such as pcDNA3 and secretion of high quantity of expressed proteins. 293F or Chinese hamster ovary (CHO) suspension cell are currently used for medium scale production of recombinant proteins in our laboratory.

Entry of naked DNA into mammalian cells requires facilitation by natural or synthetic vehicles that can compact DNA, promote binding to the cell membrane, and facilitate entry into the cell. Calcium phosphate and polycation polyethylenimine (PEI) are two very efficient transfection vehicles. Although both calcium phosphate and PEI bind and precipitate efficiently, PEI offers advantages over calcium phosphate for scaled up transfections in terms of simplicity of use and compatibility with serum-free medium. Also, CHO suspension cells are difficult to transfect with calcium phosphate (430). The use of serum-free medium is recommended for the expression of secreted recombinant proteins as it significantly facilitates their recovery and purification. PEI is available as branched and linear polymers with a wide range of molecular weights and polydispersities. Branched 25kDa PEI is more potent in transfection of adherent cells whereas linear 25kDa PEI is more potent for the transfection of suspension-growing 293F and CHO cells (430, 431).

IL-17 proteins expressed and secreted in cell supernatant were separated by sodium dodecyl sulphate polyacrylamide gel electrophoresis (SDS-PAGE) and analysed by Western blotting using specific antibodies. SDS is an anionic detergent that linearizes proteins and imparts a negative charge to linearized proteins in proportion to its mass, thus enabling fractionation of proteins by their approximate size during electrophoresis. SDS-PAGE is commonly done under reducing

condition by addition of another reducing agent such as dithiothreitol (DTT) or 2-mercaptoethanol. This allows further denaturing of proteins by reducing disulfide linkages, which are important to the folding and stability of proteins secreted in the extracellular medium. Under non-reducing SDS-PAGE disulfide bonds of proteins remain intact, hence allow study of its secondary structure.

SDS-PAGE separated proteins are transferred to nitrocellulose or polyvinylidene fluoride (PVDF) membrane and stained with antibodies specific to target protein. Staining antibodies are linked to a reporter enzyme such as horseradish peroxidase (HRP) that on treatment with a chemiluminescent agent produces luminescence in proportion to the amount of protein, which can be recorded on a sensitive sheet of photographic film. Western blot also allows semi-quantitation of proteins by comparing the intensity of band generated with that of known quantity of control.

4.1.1 Fast protein liquid chromatography

FPLC is a form of liquid chromatography that is used to separate or purify proteins and other polymers from complex mixtures. Columns used with an FPLC can separate macromolecules based on size, charge distribution, hydrophobicity, reverse-phase or biorecognition. The chromatographic bed is composed by the gel beads inside the column. In FPLC the pumped solvent velocity is microprocessor-controlled through a software interface to ensure a constant flow rate of solvents. As a result of different components adhering to or diffusing through the gel, the sample mixture gets separated.

4.1.2 Immunoaffinity chromatography

Immunoaffinity chromatography (IAC) is a powerful technique for a selective purification of a target compound that combines the use of liquid chromatography with the specific binding of antibodies or related agents. IAC entails immobilising antibodies onto supports such as agarose, cellulose or synthetic organic compounds. A variety of techniques ranging from covalent attachment to adsorption-based methods can be used to immobilise antibodies. Using covalent attachment,

antibodies can be immobilised by random attachment via amino or carboxyl groups or selectively via modified carbohydrate residues or thiol groups. The easiest is the technique of random attachment but can lead to steric hindrance and a decrease in binding efficiency (432). The target protein is eluted by temporarily lowering the effective strength of antibody binding to the target. One of the common approaches to elution in IAC which has been shown to be effective in dissociating high affinity antibody-antigen complexes includes changing the mobile phase pH usually conducted by applying an acidic buffer (pH 1-3) typically at concentrations of 1.5-8 M to the column (433).

4.1.3 Aims

1. To confirm the correct expression of *in vitro* expressed human and mouse IL-17 proteins and quantitate their amount in transfected cell supernatants.
2. To express human IL-17F mutant at a medium scale and purify by immunoaffinity purification.
3. To confirm *in vitro* cleavage of LAP-IL-17 proteins into intact LAP and IL-17 domains by MMP.

4.2 Results

4.2.1 Confirming the correct expression of IL-17 proteins derived from transient transfection of 293T cells

The correct expression of IL-17 proteins was confirmed by resolving 293T cell supernatants containing IL-17 proteins in reducing SDS-PAGE and immunoblotting with specific antibodies. *In vitro* cleavage of LAP-IL-17 proteins by MMP-1 into intact LAP and IL-17 domains was confirmed by Western blot analysis of MMP-1 pre-treated LAP-IL-17 proteins. Human and mouse full-length IL-17 proteins were immunoblotted with the corresponding anti-IL-17 antibodies whereas LAP-IL-17 proteins were immunoblotted independently with both human anti-LAP antibody and corresponding anti-IL-17 antibodies to target both LAP and IL-17 domain (Figs. 4.2, 4.3 and 4.4).

4.2.1a Determining optimum concentration of MMP-1 required for the complete cleaving of LAP-IL-17 proteins

MMP-1 used in all the experiments was produced in-house via expression in E coli. It was therefore important to determine the optimum dilution of in-house produced MMP-1 that was required for a complete cleaving of LAP-IL-17 proteins. For this, human LAP-IL-17F mutant was selected as representative LAP-IL-17 protein and 25µl 293T cell supernatant containing expressed LAP-IL-17F mutant was pre-incubated with MMP-1 in dilutions ranging from 1:10 to 1:640 at 37°C overnight, resolved with SDS-PAGE and immunoblotted independently with human anti-IL-17F and anti-LAP antibodies. As shown in the Fig.4.1, the bands generated were of the expected molecular weight (uncleaved LAP-IL-17F mutant 58kDa, cleaved IL-17F domain 21kDa and LAP domain 37kDa). Complete cleavage of LAP-IL-17F mutant was seen at MMP-1 dilutions 1:50 or less. For all future experiments including Western blots and biological assays, MMP-1 was used in dilution 1:50 for the pre-treatment of LAP-IL-17 proteins. It has been previously observed in our laboratory that MMP-1 in the final concentration of 30µM results in an adequate cleaving of cell supernatants containing expressed LAP-IL-17 proteins.

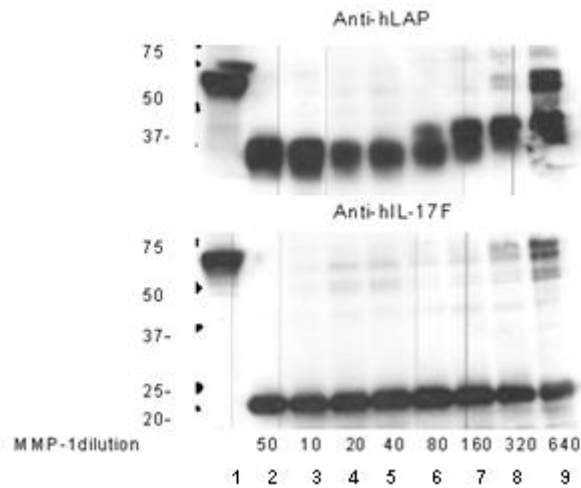


Figure 4.1 Western blot analysis demonstrating optimum dilution of MMP-1 that is required for complete cleaving of LAP-IL-17. MMP-1 pre-incubated (dilutions 1:10 to 1:640) and naïve human LAP-IL-17F mutant was resolved by reducing SDS-PAGE and immunoblotted independently with anti-human IL-17F and -LAP antibodies. Lane 1 shows naïve LAP-IL-17F mutant protein at the expected molecular weight of 58kDa. Bands generated by cleavage of LAP-IL-17F mutant with MMP-1 in dilutions 1:50, 1:10, 1:20 and 1:40 were again of expected molecular weights of 21kDa and 38kDa, representing IL-17F mutant and LAP domains (lanes 2, 3, 4, 5 show the complete cleavage of LAP-IL-17F mutant). MMP-1 in dilutions 1:80 or above (lanes 6, 7, 8, 9) generated bands at molecular weights higher than expected, which is indicative of an incomplete cleavage of LAP-IL-17F mutant. Previous observations in our laboratory have demonstrated that MMP-1 in the final concentration of 30 μ M results in an adequate cleaving of cell supernatants containing expressed LAP-proteins.

4.2.1b Expression of IL-17 homodimers

25 μ l 293T cell supernatants containing human and mouse full-length IL-17 proteins, and naïve plus MMP-1 pre-treated (incubated with 1:50 dilution MMP-1 at 37°C overnight) LAP-IL-17 proteins were resolved by reducing SDS-PAGE and immunoblotted independently with corresponding anti-human or mouse IL-17 and anti-LAP antibodies. Fig. 4.2 shows Western blot analysis of human IL-17 proteins demonstrating bands of the expected molecular weights (human IL-17A 15 and 17kDa, FL-IL-17F and IL-17F mutant proteins 17kDa, naïve LAP-IL-17 proteins 54kDa and LAP domain 34kDa). These results

indicate that human IL-17 proteins were expressed correctly and LAP-IL-17 proteins could be cleaved effectively by MMP-1.

Similarly Western blot analysis of mouse IL-17 proteins (Fig. 4.3) showed the bands of expected molecular size (IL-17A 17 and 21kDa, IL-17F 17kDa and 25kDa and IL-17F mutants 1, 2 and 3 20kDa and 25kDa, and naïve LAP-IL-17 proteins 62kDa). Despite several attempts, *in vitro* expression of mouse FL-IL-17F mutant 2 could not be confirmed in either 293T cells supernatant or whole cell lysates. Interestingly, FL-IL-17F mutant 2 domain released from MMP-1 treated LAP-IL-17F mutant 2 was detectable on Western blot under similar conditions. This suggests that either FL-IL-17F mutant 2 was not translated or was not stable enough to allow detection by Western blot.

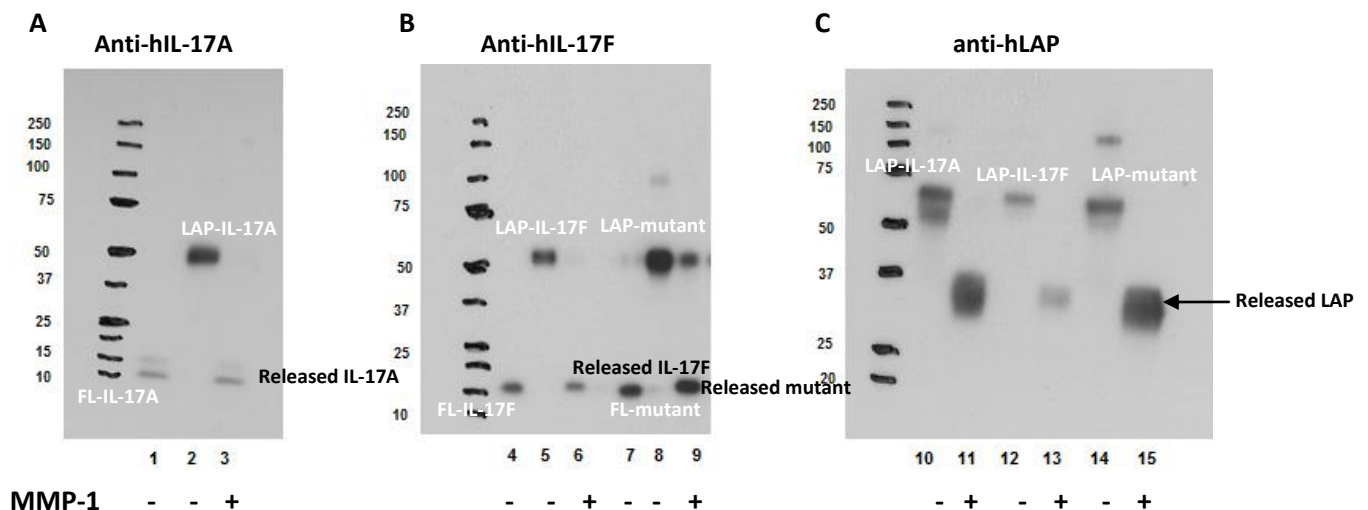


Figure 4.2 Reducing SDS-PAGE resolution and immunoblot analysis of human IL-17 homodimers.

293T cell supernatants containing human full-length and LAP-IL-17 proteins were resolved by reducing SDS-PAGE and immunoblotted with anti-human IL-17A, -IL-17F or -LAP antibodies. LAP-IL-17 proteins were pre-incubated with MMP-1 at final dilution of 1:50 at 37°C overnight.

Panel A, lane 1 shows bands at 15 and 17kDa demonstrating glycosylation of full-length IL-17A. Lane 2 shows LAP-IL-17A protein at the expected molecular weight 58kDa and lane 3 shows bands at 15 and 17kDa IL-17A released from LAP-IL-17A by the action of MMP-1.

Panel B shows 17kDa bands in lanes 4 and 7, which represent full-length IL-17F and IL-17F mutant respectively. Lanes 5 and 8 show LAP-IL-17 and LAP-IL-17F mutant proteins at the expected molecular weight of 58 kDa and lanes 6 and 9 show bands at 17kDa representing IL-17F and IL-17F mutant released from their corresponding LAP-IL-17 proteins by the action of MMP-1.

Panel C shows naïve LAP IL-17A, -IL-17F and -IL-17F mutant in lanes 10, 12 and 14 at the expected molecular weight of 58kDa and the released LAP domain at the expected molecular weight of 37kDa in lanes 11, 13 and 15.

The data is representative of at least three experiments. These results confirmed the correct expression of proteins and cleavage of LAP-IL-17 proteins into intact LAP and IL-17 domains by MMP. Anti-hIL-17A, anti-human IL-17A antibody; anti-hIL-17F, anti-human IL-17F antibody; anti-hLAP, anti-human LAP antibody.

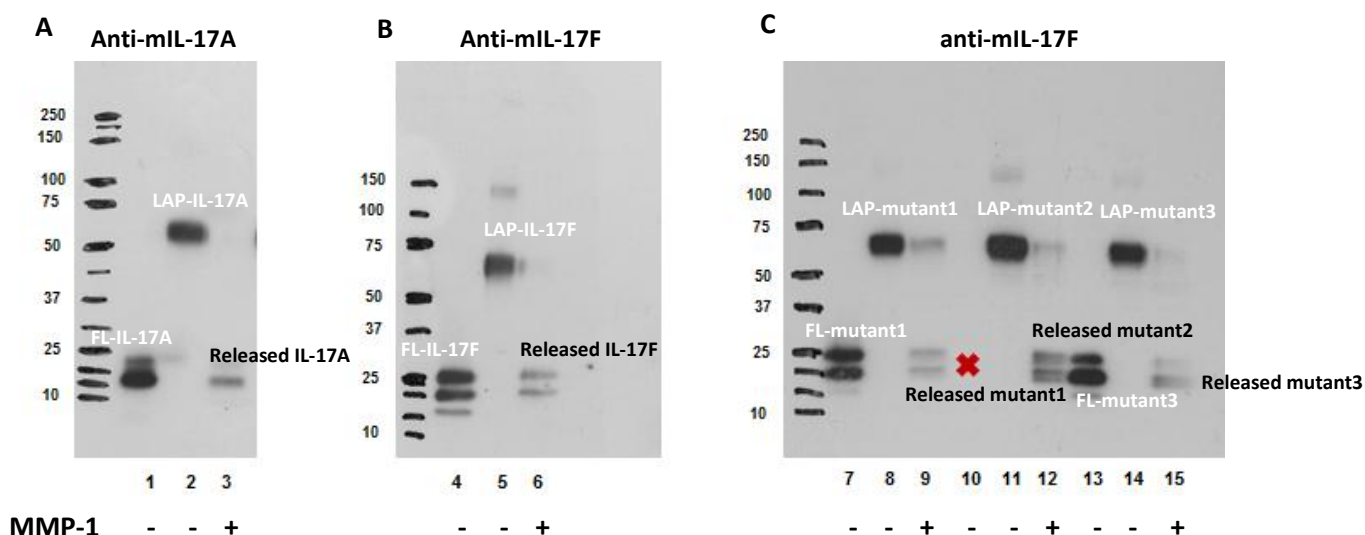


Figure 4.3 Reducing SDS-PAGE resolution and immunoblot analysis of mouse IL-17 homodimers.

293T cell supernatants containing mouse full-length and LAP-IL-17 proteins were resolved by reducing SDS-PAGE and immunoblotted with anti-mouse IL-17A or -IL-17F antibodies. LAP-IL-17 proteins were pre-incubated with MMP-1 at final dilution of 1:50 at 37°C overnight.

Panel A, lane 1 shows bands at 17 and 21kDa demonstrating glycosylation of full-length IL-17A. Lane 2 shows naïve LAP-IL-17A protein at the expected molecular weight of 58kDa and lane 3 shows bands at 17 and 21kDa representing IL-17A released from LAP-IL-17 by the action of MMP-1. The concentrations of FL-IL-17A and LAP-IL-17A in 293T cell supernatants as determined by direct ELISA (Chapter 2, Section 2.2.2b) were 105ng/ml and 415ng/ml respectively.

Panel B shows 17, 21 and 25kDa size bands in lanes 4 which represent full-length IL-17F. Lanes 5 shows LAP-IL-17F at the expected molecular weight of 62kDa and lanes 6 shows bands at 17 and 21kDa representing IL-17F released from LAP-IL-17F by the action of MMP-1. The concentrations of FL-IL-17F and LAP-IL-17F in 293T cell supernatants as determined by direct ELISA (Chapter 2, Section 2.2.2b) were 55ng/ml and 140ng/ml respectively.

Panel C shows 17kDa, 21kDa and 25kDa bands representing glycosylated full-length IL-17F mutant 1 and 3 in lanes 7 and 13 respectively. Expression of full-length IL-17F mutant could not be detected, which is marked with a red cross in lane 10. LAPIL-17F mutants 1, 2 and 3 were expressed at the expected molecular weight of 62kDa as shown in the lanes 8, 11 and 14. Lanes 9, 12 and 15 show 21kDa and 25kDa bands representing IL-17F mutant 1, 2 and 3 domains released from their corresponding LAP-IL-17F mutants by the action of MMP-1. The concentrations of FL-IL-17F mutant 1, -IL-17F mutant 3, LAP-IL-17F mutant 1, -IL-17F mutant 2 and -IL-17F mutant 3 in 293T cell supernatants as determined by direct ELISA (Chapter 2, Section 2.2.2b) were 52ng/ml, 50ng/ml, 300ng/ml, 270ng/ml and 300ng/ml respectively.

The data is representative of at least three experiments. These results confirmed the correct expression of proteins and cleavage of LAP-IL-17 proteins into intact LAP and IL-17 domains by MMP. Anti-mIL-17A, anti-mouse IL-17A antibody; anti-mIL-17F, anti-mouse IL-17F antibody.

4.2.1c LAP-IL-17 proteins are secreted as homodimers

Biological latency of a LAP-cytokine is related to LAP homodimer forming a protective shell around the cytokine, which prevents interaction between the cytokine and its receptor. To confirm that LAP-IL-17 proteins were expressed and secreted as homodimers, 25 μ l 293T cells supernatants containing mouse LAP-IL-17 proteins were resolved by non-reducing SDS-PAGE and immunoblotted with anti-human LAP antibody (Fig. 4.4).

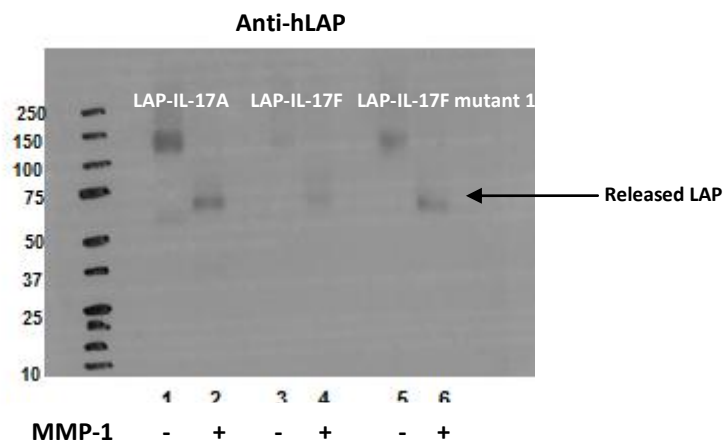


Figure 4.4 LAP-IL-17 proteins are secreted as homodimers. 25 μ l naïve and MMP-1 pre-treated 293T cells supernatants containing mouse LAP -IL-17A, -IL-17F and -IL-17F mutant 1 were resolved by non-reducing SDS-PAGE and immunoblotted with anti-human LAP antibodies. The concentration of LAP-IL-17A, -IL-17F and -IL-17F mutant 1 proteins in 293T cell supernatants as determined by direct ELISA (refer Chapter 2, Section 2.2.2b) was 415ng/ml, 140ng/ml and 300ng/ml respectively. Lanes 1, 3 and 5 show 116kDa bands corresponding to homodimers of LAP-IL-17A, IL-17F and IL-17F mutant 1. MMP-1 pre-treatment of LAP-IL-17 proteins generated 74kDa bands corresponding to LAP homodimers (lanes 2, 4 and 6). The data is representative of at least three experiments. Anti-hLAP, anti-human LAP antibody.

4.2.1d Expression of IL-17 heterodimers

In addition to being secreted as homodimers, human and mouse IL-17A and IL-17F are also secreted as heterodimer of IL-17A/IL-17F (142, 143). This raised the possibility of IL-17F mutant forming a heterodimer with IL-17A and IL-17F, which was investigated by transient co-transfection of 293T

cells with IL-17A or IL-17F plus IL-17F mutant. 293T cells were transiently transfected with total 20µg plasmid DNA in combinations of 15µg/5µg, 10µg/10µg, 5µg/15µg and 1µg/19µg IL-17A or IL-17F/ IL-17F mutant. Additional co-transfections with IL-17A or IL-17F plus empty pcDNA3, and IL-17A plus IL-17F were also examined. 25µl cell supernatant were resolved by reducing SDS-PAGE and immunoblotted independently with anti-IL-17A and anti-IL-17F antibodies. As shown in Figs. 4.5 and 4.6, the bands generated were of the expected molecular size of 17-21kDa. The intensity and thickness of the bands was proportionate to the proportion of DNA utilised for co-transfection. These results showed that human and mouse IL-17A and IL-17F were also expressed as heterodimers of IL-17A and IL-17F. Although heterodimers of mouse IL-17A/IL-17F mutant 1 and IL-17F/IL-17F mutant 1 could be expressed *in vitro*, heterodimers of human IL-17A or IL-17F with IL-17F mutant were not expressed by transient co-transfection of 293T cells.

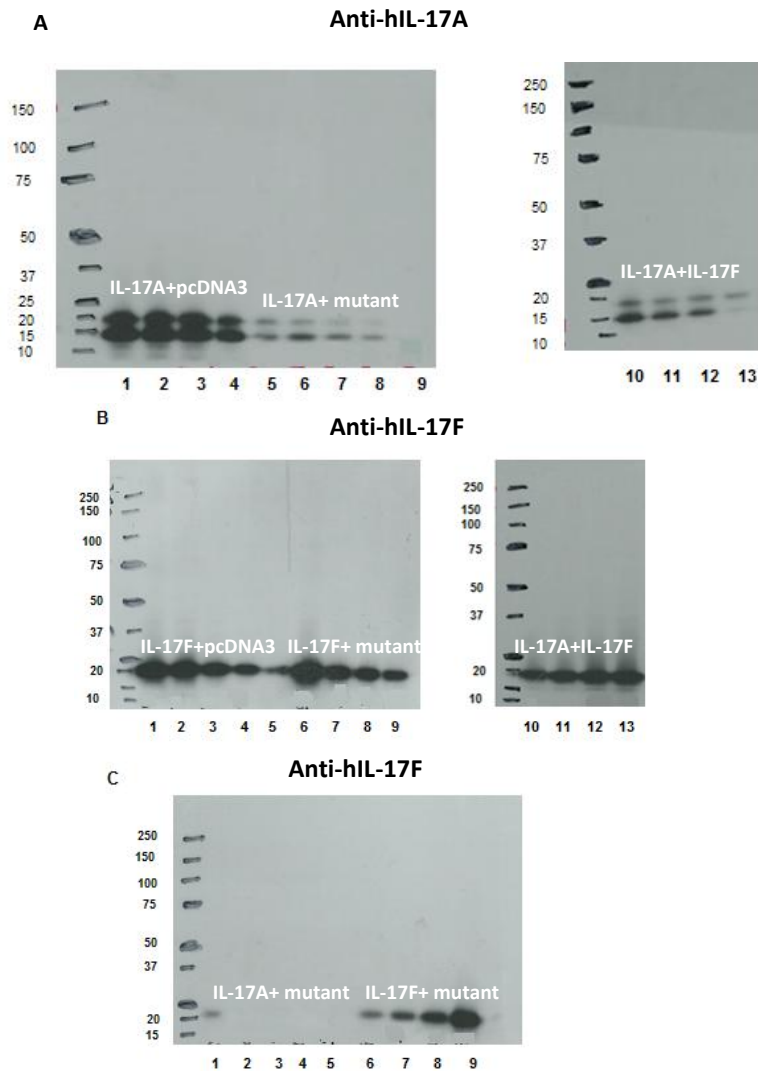


Figure 4.5 Reducing SDS-PAGE resolution and immunoblot analysis of human IL-17 heterodimers. 293T cells were co-transfected with human IL-17A or IL-17F plus IL-17F mutant or empty pcDNA3 or IL-17A plus IL-17F (see text for details). 25 μ l cell supernatants were resolved by reducing SDS-PAGE and immunoblotted independently with anti-human IL-17A and IL-17F antibodies. The bands generated were of expected molecular weight size of 17-21kDa.

Panel A, immunoblotting with anti-human IL-17A shows a progressive decrease in thickness of bands generated by co-transfection with 20 μ g IL-17A plus 0 μ g pcDNA3 (lane 1), 15 μ g IL-17A plus 5 μ g pcDNA3, IL-17F mutant or IL-17F (lanes 2, 6, 10), 10 μ g IL-17A plus 10 μ g pcDNA3, IL-17F or IL-17F mutant (lanes 3, 7, 11), 5 μ g IL-17A plus 15 μ g pcDNA3, IL-17F or IL-17F mutant (lanes 4, 8, 12) and 1 μ g IL-17A plus 19 μ g pcDNA3, IL-17F or IL-17F mutant (lanes 5, 9, 13).

Panel B, immunoblotting with anti-human IL-17F shows a progressive decrease in thickness of bands generated by co-transfection with 20 μ g IL-17F plus 0 μ g pcDNA3 (lane 1), 15 μ g IL-17F plus 5 μ g pcDNA3, IL-17F mutant or IL-17A (lanes 2, 6, 13), 10 μ g IL-17F plus 10 μ g pcDNA3, IL-17F mutant or IL-17A (lanes 3, 7, 12), 5 μ g IL-17F plus 15 μ g pcDNA3, IL-17F mutant or IL-17A (lanes 4, 8, 11) and 1 μ g IL-17F plus 19 μ g pcDNA3, IL-17F mutant or IL-17FA (lanes 5, 9, 10).

Panel C, 293T cell supernatants derived from IL-17A plus IL-17F mutant co-transfection did not generate bands when immunoblotted with anti-human IL-17F (lanes 2 to 5). Supernatants derived from co-transfection with IL-17F plus IL-17F mutant generated bands which corresponded to the quantity of IL-17F utilised for the co-transfection (lanes 6-9). Lane 1 shows band representing IL-17F mutant 20 μ g plus empty pcDNA3. The data is representative of at least three experiments. Anti-hIL-17A, anti-human IL-17A antibody; anti-hIL-17F, anti-human IL-17F antibody.

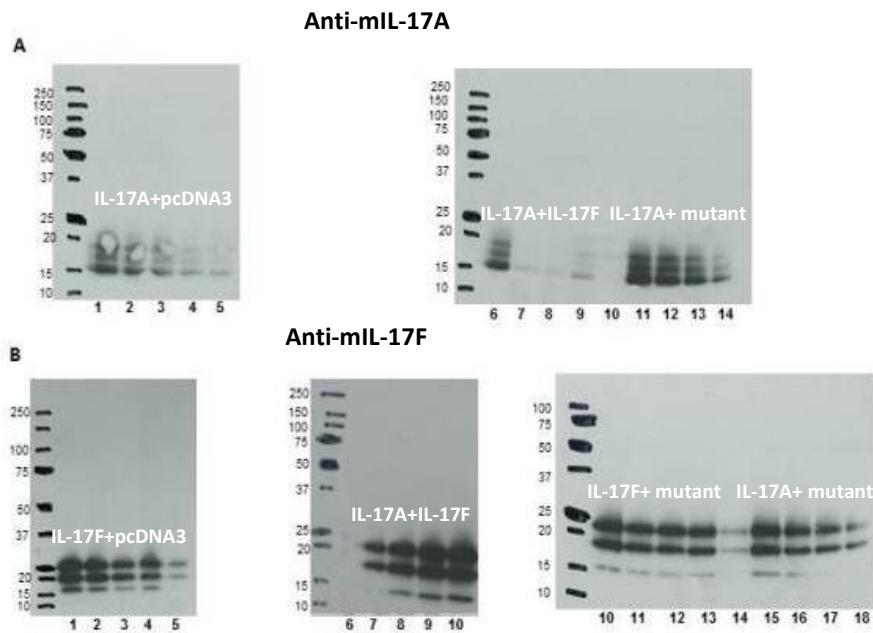


Figure 4.6 Reducing SDS-PAGE resolution and immunoblot analysis of mouse IL-17 heterodimers.

293T cells were co-transfected with mouse IL-17A or IL-17F plus IL-17F mutant or empty pcDNA3, or IL-17A plus IL-17F as described in the text. 25 μ l cell supernatants were resolved by reducing SDS-PAGE and immunoblotted independently with anti-mouse IL-17A and IL-17F antibodies. The bands generated were of expected molecular weight size of 17-21kDa.

Panel A, Blotting with anti-IL-17A antibody shows a progressive decrease in the thickness of band generated from co-transfection with 20 μ g IL-17A plus 0 μ g pcDNA3 (lanes 1), 15 μ g IL-17A plus 5 μ g pcDNA3 or IL-17F mutant (lanes 2, 11), 10 μ g IL-17A plus 10 μ g pcDNA3 or IL-17F mutant (lanes 3, 12), 5 μ g IL-17A plus 15 μ g pcDNA3 or IL-17F mutant (lanes 4, 13) and 1 μ g IL-17A plus 19 μ g pcDNA3, or IL-17F mutant (lanes 5, 14). Lanes 6-9 represent co-transfection with IL-17A plus IL-17F. No band is seen in lanes 7 and 8.

Panel B, Blotting with anti-IL-17F antibody shows a progressive decrease in the thickness of band generated from co-transfection with 20 μ g IL-17F plus 0 μ g pcDNA3 (lane 1, 10), 15 μ g IL-17F plus 5 μ g pcDNA3 or IL-17A (lanes 2, 9), 10 μ g IL-17F plus 10 μ g pcDNA3 or IL-17A (lanes 3, 8), 5 μ g IL-17F plus 15 μ g pcDNA3 or IL-17A (lanes 4, 7) and 1 μ g IL-17F plus 19 μ g pcDNA3 or IL-17FA (lanes 5, 6). Lanes 10 to 13 shows bands of equal size generated by co-transfection of IL-17F and IL-17F mutant together in the quantities of 0/20 μ g, 15/5 μ g, 10/10 μ g and 5/15 μ g. Co-transfection with combined IL-17F mutant and IL-17A in the quantities 19/1 μ g, 15/5 μ g, 10/10 μ g and 5/15 μ g produced bands with a progressive decrease in the thickness and intensity (lanes 15, 16, 17 and 18). The data is representative of at least three experiments. Anti-mIL-17A, anti-mouse IL-17A antibody; anti-mIL-17F, anti-mouse IL-17F antibody.

4.2.1e Efficiency of transfection with PEI is superior to calcium phosphate DNA co-precipitation

As transfection with PEI is more simple and convenient than calcium phosphate co-precipitation, efficiency of the two methods was compared. 1×10^6 293T cells were co-transfected with human IL-17A plus IL-17F plasmid DNAs in combinations of 15 μ g/5 μ g, 10 μ g/10 μ g, 5 μ g/15 μ g and 1 μ g/19 μ g using PEI or calcium phosphate co-precipitation under similar conditions. 25 μ l cell supernatants containing expressed proteins were resolved by reducing SDS-PAGE and immunoblotted independently with anti-human IL-17A and IL-17F antibodies. Efficiency of transfection was determined by comparing the intensity and thickness of the bands. As shown in Fig. 4.7, bands generated with PEI transfection were of greater intensity and thickness than by calcium phosphate suggestive of greater protein expression by PEI method.. This indicates that PEI transfection is superior to calcium phosphate co-precipitation.

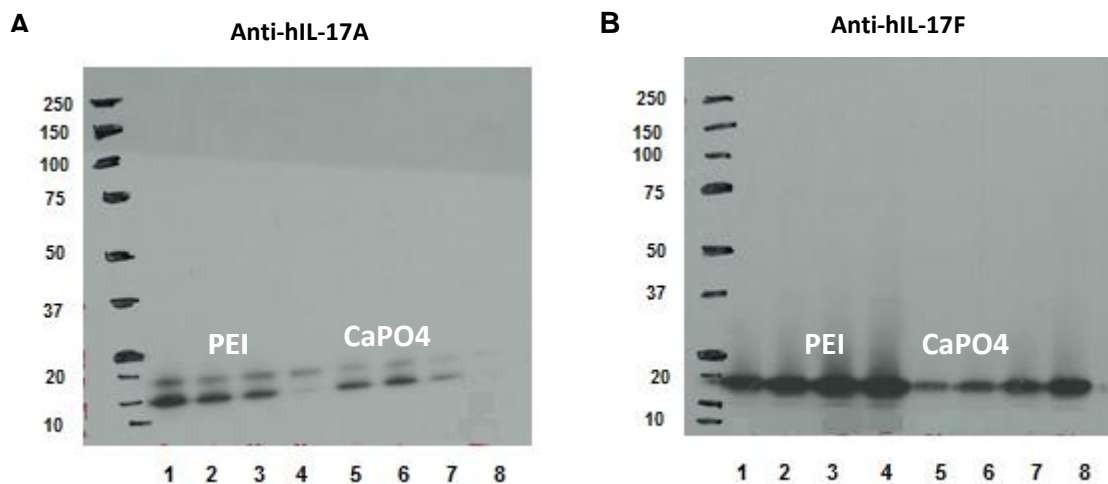


Figure 4.7 Transfection efficiency of PEI is superior to calcium phosphate co-precipitation.

293T cells were transiently co-transfected with human IL-17A plus IL-17F in combinations of 15 μ g/5 μ g, 10 μ g/10 μ g, 5 μ g/15 μ g and 1 μ g/19 μ g using PEI (lanes 1 to 4) or calcium phosphate (lanes 5 to 8). 25 μ l cell supernatants were resolved by reducing SDS-PAGE and immunoblotted independently with anti-human IL-17A (panel A) and IL-17F antibodies (panel B). The bands generated were of expected molecular weight size of 17-21kDa. The intensity and thickness of bands generated by PEI transfection was greater than calcium phosphate co-precipitation indicating PEI transfection is superior to calcium phosphate co-precipitation. Anti-hIL-17A, anti-human IL-17A antibody; anti-hIL-17F, anti-human IL-17F antibody.

4.2.1f Expression of human IL-17F mutant in CHO-S cells

CHO-S cells were used for medium scale expression of human FL- and LAP-IL-17F mutant protein expression for the purpose of immunoaffinity purification. A total 2 litre cell culture of CHO-S cells was transiently transfected by human FL- and LAP-IL-17F mutant in three separate batches each. The correct expression of proteins in cell supernatants was confirmed by Western blot analysis. 25µl supernatant from each of the three batches of FL-IL-17F mutant and MMP-1 untreated and pre-treated LAP-IL-17F mutant were resolved by reducing SDS-PAGE and immunoblotted with anti-human IL-17F antibody (Fig. 4.8).

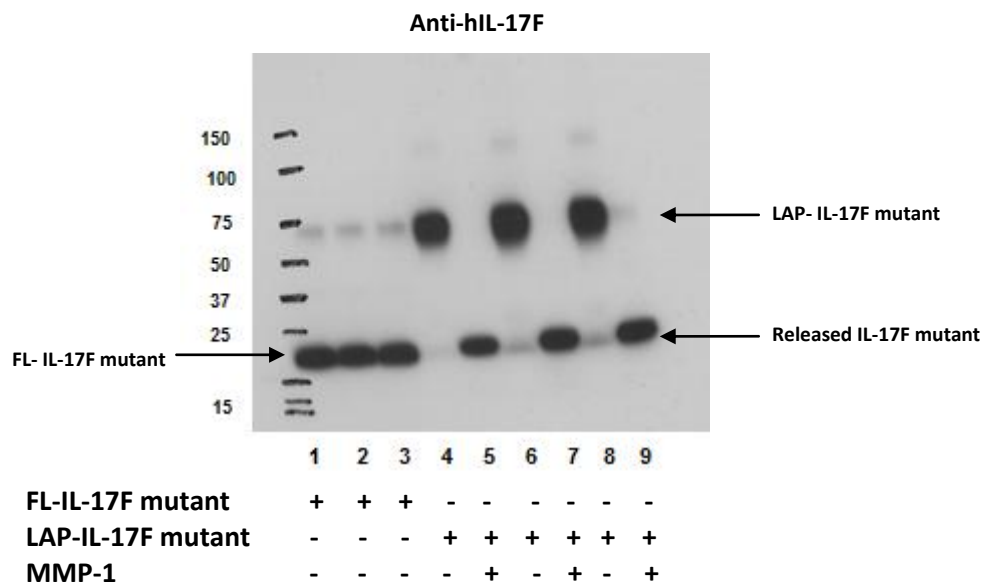


Figure 4.8 Reducing SDS-PAGE resolution and immunoblot analysis of CHO-S expressed human IL-17F mutant. 25µl CHO-S cell supernatants containing FL-IL-17F and MMP-1 pre-treated and untreated LAP-IL-17F mutant from 3 different batches each were resolved by reducing SDS-PAGE and immunoblotted with anti-human IL-17F antibodies. The bands generated were of expected size of 21kDa corresponding to FL-IL-17F mutant (lanes 1, 2, 3) and IL-17F mutant domain released from LAP-IL-17F mutant by the action of MMP-1 (lanes 5, 7 and 9). LAP-IL-17F mutant was expressed at the expected molecular weight of 58kDa (lanes 4, 6, 8). The results confirmed that the proteins were expressed correctly. anti-hIL-17F, anti-human IL-17F antibody.

4.2.2 Immunoaffinity purified human IL-17F mutant was more than 90% pure

Human full-length IL-17F mutant expressed and secreted in CHO-S cells supernatant was purified via FPLC by immunoaffinity purification using 1mg anti-human IL-17F antibody bound to Glycolink column. Human LAP-IL-17F mutant was purified first via FPLC using Heparin column followed by immunoaffinity purification using anti-IL-17F antibody column. Purity of immunoaffinity purified IL-17F mutant was analysed by silver plus staining of 25µl eluates resolved by reducing SDS PAGE (Fig. 4.9). The eluates were also immunoblotted with anti-human IL-17F antibody to confirm that their integrity was retained following the purification procedure.

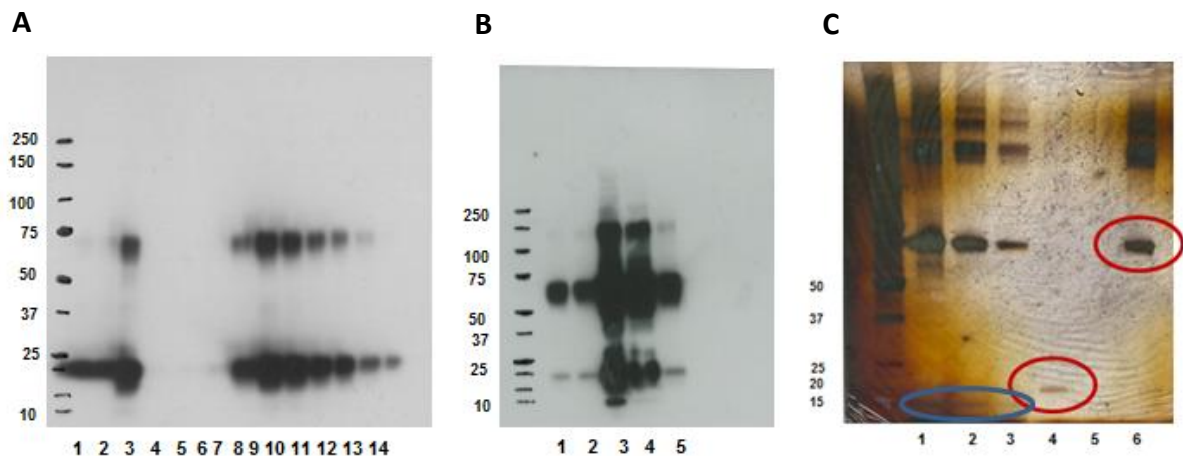


Figure 4.9 Silver plus staining of immunoaffinity purified human IL-17F mutant resolved by reducing SDS PAGE. 25µl eluates of immunoaffinity purified human full-length and LAP-IL-17F mutants and recombinant human IL-17F were resolved by reducing SDS-PAGE and the separated proteins were analysed by Western blot (A and B) and silver plus staining of the polyacrylamide gel (C).

Panel A shows FL-IL-17F eluates generated band of the expected size of 21kDa (lane 1 load, lane 2 flow through, lanes 3, 4, 5, 6, 7, 8, 9, 10, 11, 12 eluates fractions and lanes 13, 14 washes).

Panel B shows LAP-IL-17F eluates at expected molecular weight of 58kDa (lanes 1, 2 eluates, lane 3 flow through, lanes 4, 5 washes).

Panel C shows bands at 15kDa representing 100ng, 50ng and 25ng rhIL-17F (lanes 1, 2, 3, circled in blue) and multiple additional bands. Lanes 4 shows band at 21kDa representing purified glycosylated human FL-IL-17F mutant and only occasional additional bands, which confirmed that purity of FL-IL-17F mutant was more than 95%. Lane 6 shows band at 58kDa molecular weight representing LAP-IL-17F mutant and additional bands that are similar to those present in lanes 1, 2 and 3 indicating that purity of LAP-IL-17F mutant was more than 90%. FL-IL-17F mutant, full-length IL-17F mutant; rhIL-17F; recombinant human IL-17F.

4.2.3 Quantitation of the expressed IL-17 proteins

Quantitation of mouse IL-17 proteins expressed in 293T cells supernatant was carried out by direct ELISA (Table 4.1). 293T cell supernatants containing expressed IL-17 proteins were diluted in carbonated buffer and coated directly on ELISA plates. Bound IL-17 was detected by corresponding anti-mouse IL-17 or anti-human LAP antibodies.

Quantities of expressed human full-length and LAP IL-17 proteins in 30-fold concentrated 293T cell supernatants was determined using Western blot. by comparing the intensity of band generated with that of known quantity of recombinant human IL-17 proteins (Fig. 4.10 and Table 4.2). The concentration of immunoaffinity purified human IL-17F mutant and LAP-IL-17F mutant determined by human IL-17F ultra-sensitive ELISA and was determined as 0.97 μ g/ml and 0.61 μ g/ml respectively.

Table 4.1 ELISA quantitation of 293T cell expressed mouse IL-17 proteins

Protein	(ng/ml)
FL-IL-17A	105
FL-IL-17F	55
FL-IL-17F mutant 1	52
FL-IL-17F mutant 2	-
FL-IL-17F mutant 3	50
LAP-IL-17A	415
LAP-IL-17F	140
LAP-IL-17F mutant 1	300
LAP-IL-17F mutant 2	270
LAP-IL-17F mutant 3	300

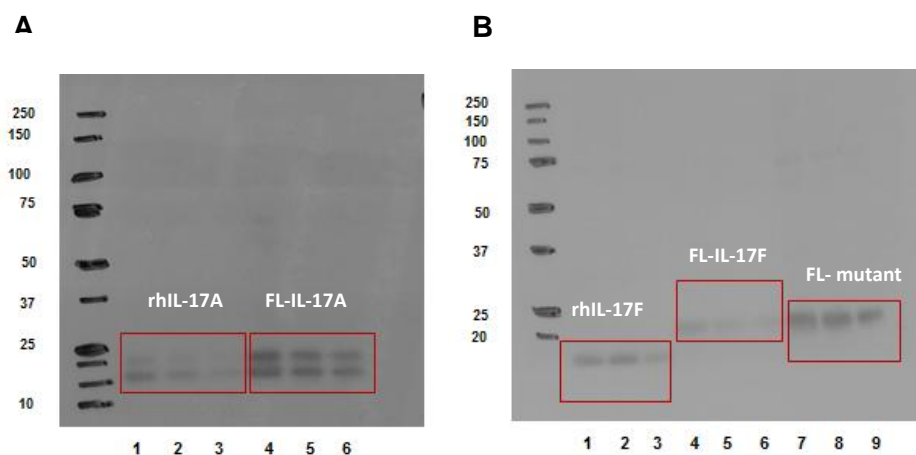


Figure 4.10 Semi-quantitation of expressed human full-length IL-17 proteins by Western blot. Commercial rhIL-17 A and IL-17F proteins and concentrated 25 μ l 293T cell supernatants containing IL-17 proteins were resolved by reducing SDS-PAGE and immunoblotted with anti-human IL-17A (panel A) or IL-17F antibodies (panel B). Density of the bands was analysed by image J software.

(A) Lanes 1, 2 and 3 show bands at 15 and 17kDa corresponding to rhIL-17A 100 ng (density 971, 2936), 50ng (density 557, 1566) and 25ng (density 59, 944) and lanes 4, 5 and 6 show bands generated by 2-fold serially diluted 293T cell supernatants containing IL-17A in the final dilutions of 1:2 (density 6114, 5289), 1:4 (density 4070,4706) and 1:8 (density 2403, 3164).

(B) Lanes 1, 2 and 3 show 17kDa bands generated by rhIL-17F 100ng (density 11606), 50ng (density 15472) and 25ng (6633) and lanes 4, 5, 6, 7, 8 and 9 show bands at 17kDa representing 2-fold serially diluted 293T cell supernatants of IL-17F (density 8933, 6209, 3773) and IL-17F mutant (18137, 19071, 12997) in the final dilutions of 1:2, 1:4 and 1:8. Quantity of the expressed human IL-17 proteins was derived by comparing the densities of bands generated by rhIL-17A and 17F proteins. The data is representative of at least three experiments. rhIL-17A, recombinant human IL-17A; FL-IL-17A, full-length IL-17A; rhIL-17F, recombinant human ILA-17F; FL-IL-17F, full-length

Table 4.2 Western blot quantitation of human IL-17 proteins in 30-fold concentrated 293T cell supernatants

Human IL-17 protein	(μ g/ml)
FL-IL-17A	20
FL-IL-17F	4
FL-IL-17F mutant	53
LAP-IL-17A	50
LAP-IL-17F	21
LAP-IL-17F mutant	95

4.3 Discussion

Western blot analysis confirmed that following transient transfection of 293T cells, IL-17 proteins were correctly expressed *in vitro* and the expressed proteins retained their ability to bind to their corresponding antibodies. IL-17A is a disulfide-linked, homodimeric, variably glycosylated, secreted glycoprotein with a molecular mass of 35 kDa (107). An N-linked glycosylation site on human IL-17A was first identified after purification of the protein revealed two bands, one at 15 kDa and another at 20 kDa. In keeping with this, 293T cells expressed human full-length IL-17A proteins generated similar bands at 15kDa and 20kDa. Human full-length IL-17F and IL-17F mutant and mouse full-length IL-17 proteins were also glycosylated and were confirmed to be expressed correctly.

Biological latency of LAP cytokines is dependent on the release of cytokine domain by the action of MMP. It was therefore essential to first confirm not only the correct expression of LAP-IL-17 proteins but also their ability to undergo cleavage into intact LAP and IL-17 domains by the action of MMP. Western blot analysis confirmed that LAP-IL-17 proteins were expressed correctly and could be cleaved into intact LAP and IL-17 domains by MMP-1. The quantitation analysis of expressed proteins showed that LAP-IL-17 proteins were expressed and secreted in cell supernatants in two to six-fold higher concentrations than full-length IL-17 proteins. These results indicate that modifying a cytokine into LAP-cytokine enhances its *in vitro* expression significantly. Similarly, *in vivo* expression of IL-17 proteins in C57BL/6 and SCID mice (refer Sections 6.2.1 and 6.2.2 and Figs. 6.1 and 6.2) showed a 2.2-fold higher expression of LAP-IL-17F mutant and a 1400-fold higher expression of LAP-IL-17A than their full-length counterparts. A higher *in vitro* and *in vivo* expression of LAP-IL-17 proteins seems to be related to a greater stability of LAP-proteins. The reason for this is not exactly known but we think it is related to either enhanced secretion of LAP proteins and/or a reduction in their degradation due to interference with their ability to bind to their cognate receptors. Our group has previously reported that *in vivo* half-life of LAP-IFN- β in DBA/1 mice was 37-fold higher than naïve IFN- β . These observations imply that LAP-cytokines due to their higher level of expression and prolonged half-life are likely to be superior therapeutics than conventional cytokine-based therapies.

Existence of IL-17A/IL-17F heterodimers has been demonstrated *in vitro* and *in vivo* in both human and mouse. In this study possibility of IL-17F mutant forming a heterodimer with IL-17A and IL-17F was investigated by co-transfection of 293T cells with IL-17A or IL-17F plus IL-17F mutant. Although expression of mouse IL-17A/IL-17F mutant and IL-17F/IL-17F mutant heterodimers could be demonstrated, expression of human IL-17A/IL-17F mutant and IL-17F/IL-17F mutant could not be confirmed. It is possible that either the expressed heterodimers were not stable enough or homodimer formation was preferred over heterodimer formation with the mutant. However, a forced expression of IL-17A/IL-17F mutant heterodimer can be achieved by fusing the genes via a polyglycine linker (143).

Comparison of transfection using PEI with calcium phosphate co-precipitation showed that under similar conditions transfection with PEI resulted in expression and secretion of higher quantities of IL-17 proteins. PEI also offers advantage over calcium phosphate precipitation method in terms of its simplicity. With PEI, the incubation time to form DNA complexes is much shorter, only 10 minutes as against 30 minutes with calcium phosphate, and there is no requirement for osmotic enhancement of DNA uptake with glycerol shock, which is often used as an adjunct with calcium phosphate method.

As the expressed proteins were not tagged, CHO-S cell supernatants containing human full-length IL-17F mutant was purified by immunoaffinity using anti-human IL-17F antibody. The LAP domain of LAP-cytokines binds to heparin (434), hence LAP-IL-17F mutant was first purified using heparin column and then immunoaffinity purified using an anti-IL-17F antibody column. Immunoaffinity purification is a potent technique to separate target protein from a mixture. In this study, purification of human full-length and LAP-IL-17F mutant via FPLC using human anti-IL-17F antibody column yielded proteins which were more than 90% pure.

To summarise, human and mouse IL-17 proteins except mouse IL-17F mutant 2 were successfully expressed *in vitro*. The correct expression of the proteins was confirmed by Western blotting. Immunoaffinity purified human full-length and LAP-IL-17F mutant were more than 90% pure.

CHAPTER V

EVALUATION OF *IN VITRO* BIOLOGICAL ACTIVITY OF IL-17F MUTANT

5.1 Introduction

The process of preclinical testing of an investigational drug requires that its biological activity is first tested *in vitro* on individual cells containing the drug target before *in vivo* examination in animal models. Developing and characterising an *in vitro* system that represents key features of some of the *in vivo* effects of a given therapeutic are paramount to an accurate initial prediction of its future clinical efficacy.

Kawaguchi *et al.* (153) working in asthma reported that (H161R) IL-17F mutant, a natural variant of IL-17F is an antagonist of wild-type IL-17F. The IL-17F mutant blocked IL-17F induced IL-8 production in bronchial epithelial cells in a dose-dependent manner, inhibiting 50% of IL-17F induced IL-8 production at equal concentrations. This inhibition reached 100% when the concentration of IL-17F mutant was increased to 5-fold that of IL-17F, which suggested that (H161R) IL-17F mutant is a competitive inhibitor of IL-17F and the loss of its biological function was not a result of its inability to bind to the IL-17F receptor. However, at that time, the receptor for IL-17F had not been identified. It has now been shown that human IL-17A and IL-17F bind to IL-17RA/RC, a heteroreceptor complex of IL-17RA and IL-17RC to mediate their biological effects (173, 181). Although isoform and species specific differences exist in the binding affinities of the individual receptor components (189), both IL-17RA and IL-17RC are essential for the biological activity of IL-17A and IL-17F (136, 435, 436).

IL-17 induces secretion of pro-inflammatory cytokines, chemokines and growth factors in stromal cells such as endothelial, epithelial and fibroblast cells (96). IL-17 activates common signaling pathways such as NF- κ B, MAPKs, C/EBPs and PI3K/JAK pathways (95, 114, 195, 437-439). Kawaguchi *et al.* (153) in their study showed that IL-17F mutant lacked the ability to activate ERK1/2 phosphorylation in bronchial epithelial cells

Human IL-17 has also been shown to induce biological response in murine cells. Human IL-17 induces secretion of IL-6 in mouse stromal cells (440, 441). It has also been demonstrated that human IL-17A and IL-17F are able to bind to mouse IL-17RA and IL-17RC (181).

5.1.1 Aims

1. Examine *in vitro* biological activity of human and mouse IL-17F mutants.
2. Develop a novel luciferase reporter system to assess biological activity of human and mouse IL-17.

5.2 Results

5.2.1 Human IL-17F mutant lacks the ability to induce secretion of IL-6 in human and mouse fibroblast cells

Biological activity of human IL-17 is most commonly evaluated by assessing production of IL-6 by IL-17 stimulated human foreskin fibroblasts and mouse embryonic fibroblasts. These bioassays were therefore used to assess *in vitro* biological activity of human IL-17F mutant. First, the biological activity of full-length IL-17F mutant was assessed by analysing induction of IL-6 secretion in HFFF2 and 3T3 cells in comparison with commercial recombinant or 293T cell expressed full-length IL-17A and IL-17F as positive controls (Figs. 5.1A and 5.1B). The results demonstrated that unlike IL-17A and IL-17F, IL-17F mutant was unable to induce the secretion of IL-6 in these cells, which confirmed that IL-17F mutant lacked the ability to stimulate secretion of IL-6 in both human and mouse fibroblast cells.

5.2.2 Human IL-17F mutant inhibits IL-17A induced IL-6 secretion in human and mouse fibroblast cells

After establishing that IL-17F mutant was unable to induce IL-6 secretion in fibroblast cells,, the hypothesis that IL-17F mutant is an inhibitor of IL-17A was tested by co-stimulating HFFF2 and 3T3 cells together with IL-17A and IL-17F mutant. HFFF2 cells were co-stimulated with rhIL-17A at a constant concentration of 25ng/ml plus 2-fold serially diluted 293T cell supernatants containing IL-17F mutant at the starting concentration of 25ng/ml (Fig. 5.2A). 3T3 cells were co-stimulated with a constant 50µl volume of 293T cells supernatant containing human full-length IL-17F mutant plus 2-fold serially diluted 1µg/ml rhIL-17A (Fig. 5.2B). In equal concentrations of 25ng/ml, IL-17F mutant led to a 62% decrease in IL-17A induced secretion of IL-6 in HFFF2 cells. Keeping the concentration of IL-17A constant at 25ng/ml and serially decreasing the concentration of added IL-17F mutant led to a progressive increase in IL-17A induced secretion of IL-6 confirming that IL-17F mutant competitively inhibited IL-17A. In keeping with results in human fibroblast cells, human IL-17F mutant was also

able to inhibit human IL-17A induced IL-6 secretion in 3T3 cells. Taken together these results confirm the hypothesis that the human IL-17F mutant is an inhibitor of IL-17A.

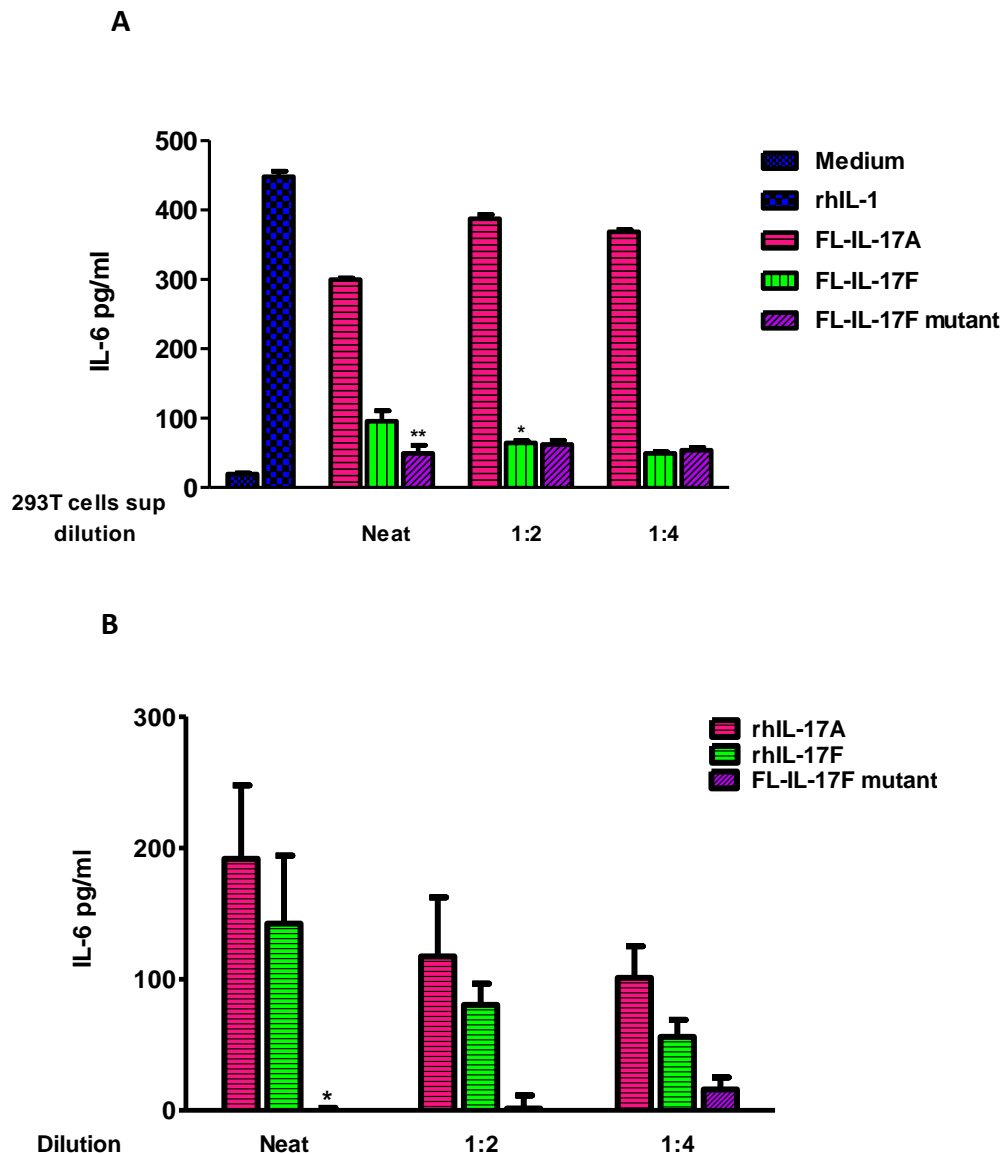


Figure 5.1 Human IL-17F mutant is unable to induce secretion of IL-6 in HFFF2 and 3T3 cells. (A) 1×10^4 HFFF2 cells and (B) 5×10^3 3T3 cells were stimulated with 2-fold serial dilution of 293T cells supernatants containing the expressed human full-length IL-17F mutant in parallel with (A) 293T cells expressed FL-IL-17A and -IL-17F proteins or (B) commercial rhIL-17A and IL-17F at the starting concentration of $1 \mu\text{g/ml}$. HFFF2 cells were also stimulated with rhIL-1 β 10ng/ml as a positive control. Twenty four hours post-stimulation the induced secretion of human IL-6 in HFFF2 cells and mouse IL-6 in 3T3 cells was analysed by ELISA. Unlike IL-17A and IL-17F, IL-17F mutant was unable to induce the secretion of IL-6. IL-17A induced a significantly higher secretion of IL-6 in HFFF2 but not in 3T3 cells. * ($p < 0.05$), ** ($p < 0.005$); HFFF2, human foetal foreskin fibroblasts; 3T3 cells, mouse foetal fibroblasts; rhIL-1, recombinant human IL-1; rhIL-17A, recombinant human IL-17A; rhIL-17F, recombinant human IL-17F; FL-IL-17A, full-length IL-17A; FL-IL-17F, full-length IL-17F; FL-IL-17F mutant, full-length IL-17F mutant.

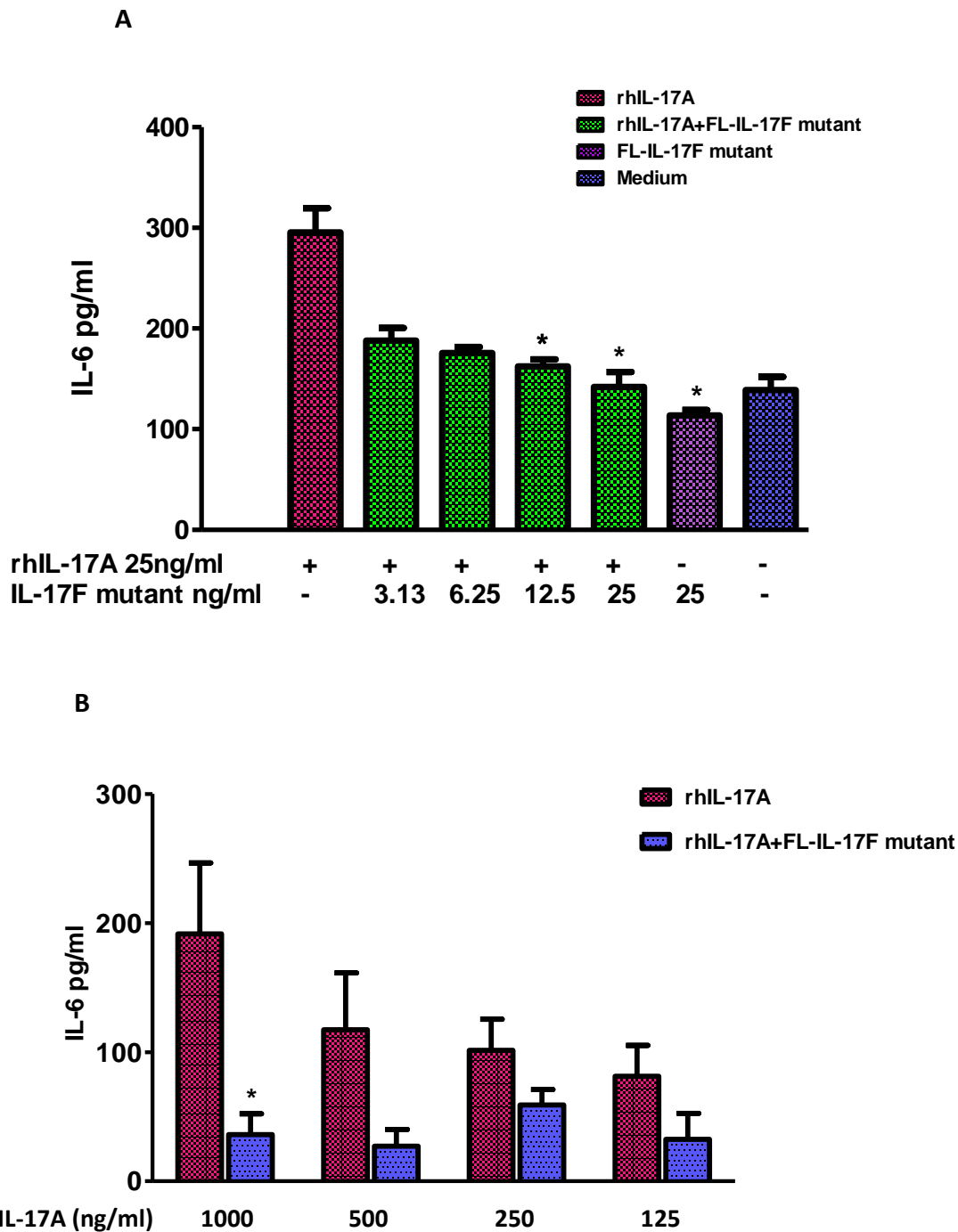


Figure 5.2 Human IL-17F mutant inhibits IL-17A induced IL-6 secretion in HFFF2 and 3T3 cells. (A) 1×10^4 HFFF2 cells were co-stimulated with 25ng/ml rhIL-17A and two-fold serially diluted 293T cell supernatant containing 25ng/ml FL-IL-17F mutant and **(B)** 5×10^3 3T3 cells were co-stimulated with two-fold serially diluted 1 μ g/ml rhIL-17A with or without 50 μ l 293T cells supernatants containing human IL-17F mutant and analysed for induced secretion of IL-6 by ELISA. **(A)** In equal concentrations of 25ng/ml FL-IL-17F mutant led to a 62% decrease in IL-17A induced IL-6 secretion. A serial reduction in the concentration of added IL-17F mutant led to the corresponding increase in the induced secretion of IL-6 by IL-17A. **(B)** Similar to HFFF2 cells, human IL-17F mutant inhibited IL-17 induced IL-6 secretion in 3T3 cells. Taken together, these findings imply that IL-17F mutant is an inhibitor of IL-17A. * $p < 0.05$; HFFF2 cells, human foetal foreskin fibroblast cells; 3T3 cells, mouse embryonic fibroblasts; rhIL-17A, recombinant human IL-17A; FL-IL-17F mutant, full-length IL-17F mutant; medium, complete DMEM.

5.2.3 In vitro biological effects of IL-17F mutant are specific to its biological activity

Transiently transfected 293T cell supernatants, in addition to the expressed proteins also contain multiple other substances including impurities and non-specific inhibitors. It was therefore possible that one of the non-specific inhibitors rather than IL-17F mutant was responsible for the apparent IL-17A inhibition by the mutant. The specificity of biological activity of IL-17F mutant was therefore assessed in several ways. For example, by examining capability of IL-17F mutant to bind to IL-17 receptor, by repeating the assays of biological activity using immunoaffinity purified IL-17F mutant and additionally assessing whether biological effects of IL-17F mutant could be reversed in the presence of a neutralising anti-IL-17F antibody. In addition, modulation of ERK1/2 signaling by IL-17F mutant was also analysed.

5.2.3a IL-17F mutant binds to IL-17RC

Human IL-17A and IL-17F bind to IL-17RA/IL-17RC, a heteroreceptor complex and require both the receptor components to mediate their biological activity. Human IL-17F however binds to IL-17RC with a much stronger affinity than IL-17RA whereas human IL-17A binds to both IL-17RA and IL-17RC with an equal affinity (181). Based on these observations, ability of IL-17F mutant to bind to IL-17RC was assessed using a commercially available functional ELISA (described in detail in Chapter 2, Section 2.3.1a). As high concentrations of IL-17F mutant were required for the assays, 293T cells supernatants containing IL-17F mutant and full-length IL-17A (used as control) were first 30-fold concentrated using a Centricon centrifugal filter device (refer Chapter 2, Section 2.2.2). The results confirmed that human IL-17F mutant was able to bind to IL-17RC although the strength of its binding to IL-17RC was 1.4-fold less than full-length IL-17A (Fig.5.3). This finding provided an initial circumstantial evidence for the specificity of biological activity of IL-17F mutant.

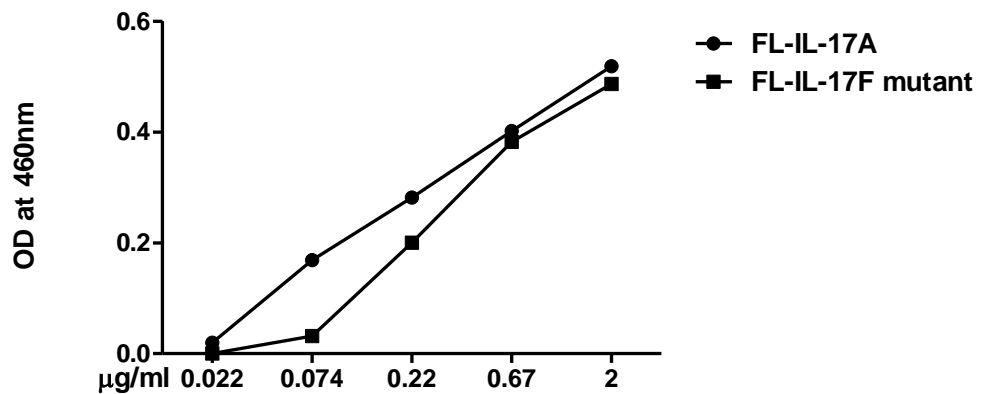


Figure 5.3 Human IL-17F mutant binds to IL-17RC. A competitive binding inhibition assay of 30-fold concentrated 293T cell supernatants containing human FL- IL-17F mutant and - IL-17A to human IL-17RC was performed using functional ELISA (Chapter 2, Section 2.3.1a). In brief, a mixture of hIL-17RC at the final concentration of 100ng/ml or binding buffer (control) and 3-fold serially diluted human FL-IL-17A or FL-IL-17F mutant at the starting final concentration of 2µg/ml were incubated at 500rpm for 2 hours at room temperature and captured with 10µg/ml anti-polyhistidine and detected with 3µg/ml anti-human IL-17A or IL-17F antibody. The results confirmed that IL-17F mutant was able to bind to IL-17RC but its strength of binding to the receptor was 1.4-fold less than IL-17A. FL-IL-17A, full-length IL-17A; FL- IL-17F mutant, full-length IL-17F mutant; OD, optical density.

5.2.3b Immunoaffinity purified IL-17F mutant is unable to stimulate IL-6 secretion and ERK1/2 activation in HeLa cells

In order to confirm the specificity of biological activity of IL-17F mutant, unwanted impurities including non-specific inhibitors were eliminated from the transiently transfected CHO-S cell supernatant containing IL-17F mutant by immunoaffinity purification (Chapter 4, Section 4.2.2).

Besides fibroblasts, IL-17 also induces the secretion of IL-6 in epithelial cells (442). IL-17 has been shown to induce IL-6 and also upregulate ERK1/2 phosphorylation in HeLa, a human cervical epithelial cell carcinoma cell line (443). HeLa instead of HFFF2 cells were used for this part of the study mainly because growth and expansion of HFFF2 cells was very slow. HeLa cells were stimulated with immunoaffinity purified IL-17F mutant and induced secretion of IL-6 and ERK1/2 activation in cell lysates were analysed (Chapter 2, Sections 2.3.1b and 2.3.1c). Based on a time course analysis

study by Kawaguchi *et al.* which showed that IL-17 induced phosphorylation of ERK1/2 in primary bronchial epithelial cells reached a maximum at approximately 20 minutes and returned to baseline levels by 60 minutes (444), ERK1/2 phosphorylation was analysed after stimulation of HeLa cells for 20 minutes.

As shown in the Fig. 5.4A, immunoaffinity purified IL-17F mutant failed to induce the secretion of IL-6 in HeLa cells. Furthermore, unlike recombinant IL-17A and IL-17F, after 20 minutes of stimulation, immunoaffinity purified IL-17F mutant was unable to activate ERK1/2 phosphorylation (Fig. 5.4B). These findings taken together with the results of experiments described in the Sections 5.2.1 and 5.2.3a confirmed that inability of IL-17F mutant to stimulate IL-6 secretion in epithelial or fibroblasts was specific to its biological activity and not merely due to the lack of binding to IL-17R or presence of non-specific inhibitor(s) in 293T cell supernatants.

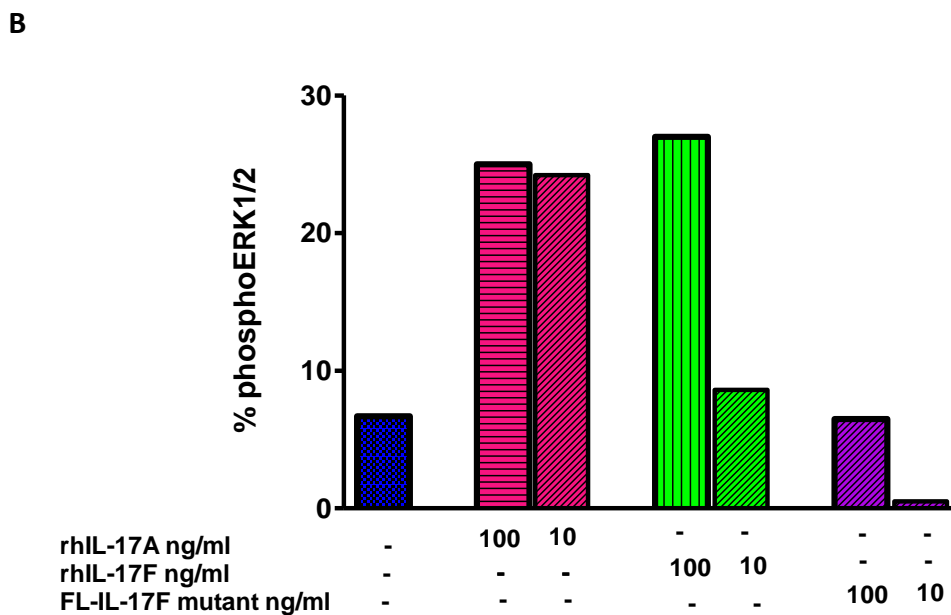
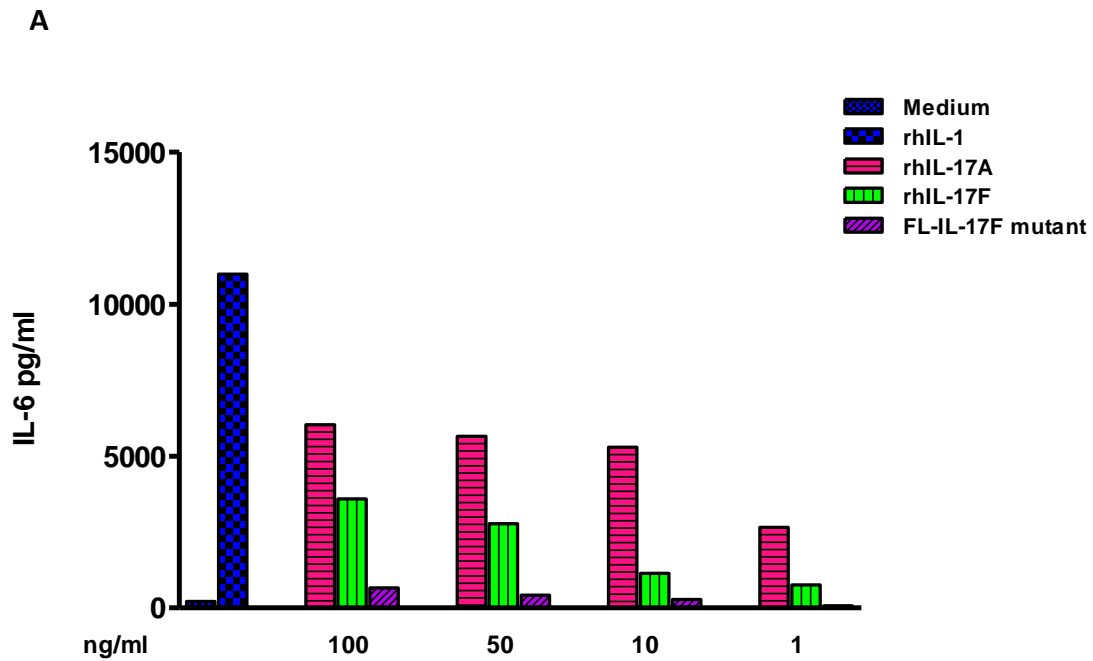


Figure 5.4 Immunoaffinity purified IL-17F mutant is unable to induce IL-6 secretion and ERK1/2 activation in HeLa cells. (A) and (B) 1×10^4 HeLa cells were stimulated with 100ng/ml and 10ng/ml immunoaffinity purified IL-17F mutant in parallel with rhIL-17A and IL-17F and analysed for secretion of IL-6 and activation of ERK1/2. 10ng/ml rhIL-1 was used as a positive control. Unlike IL-17A and IL-17F, immunoaffinity purified IL-17F mutant was unable to induce secretion of IL-6 and phosphorylate ERK1/2 in HeLa cells. PhosphoERK1/2 data represents percentage of total ERK1/2 that was phosphorylated (refer Chapter 2, Section 2.3.1d). Both these assays have been done only once and the graphs therefore do not contain error bars. rhIL-17A, recombinant human IL-17A; rhIL-17F, recombinant human IL-17F; rhIL-1, recombinant human IL-1; IL-17F mutant, immunoaffinity purified human full-length IL-17F mutant; medium, complete RPMI.

5.2.3c Inhibition of IL-17A by immunoaffinity purified IL-17F mutant is reversed by a neutralising anti-IL-17F antibody

The biological specificity of IL-17F mutant was further confirmed by assessing whether its biological effects could be reversed in the presence of a neutralising anti-IL-17F antibody. HeLa cells were co-stimulated with rhIL-17A plus immunoaffinity purified IL-17F mutant with or without 10µg/ml neutralising anti-IL-17F antibody. In equal concentration of 100ng/ml, IL-17F mutant led to a 72% decrease in IL-17A induced IL-6 secretion and this could be reversed by a neutralising anti-IL-17F antibody (Fig. 5.5). These findings confirmed that inhibition of IL-17A induced IL-6 secretion by IL-17F mutant is specific to its biological activity..

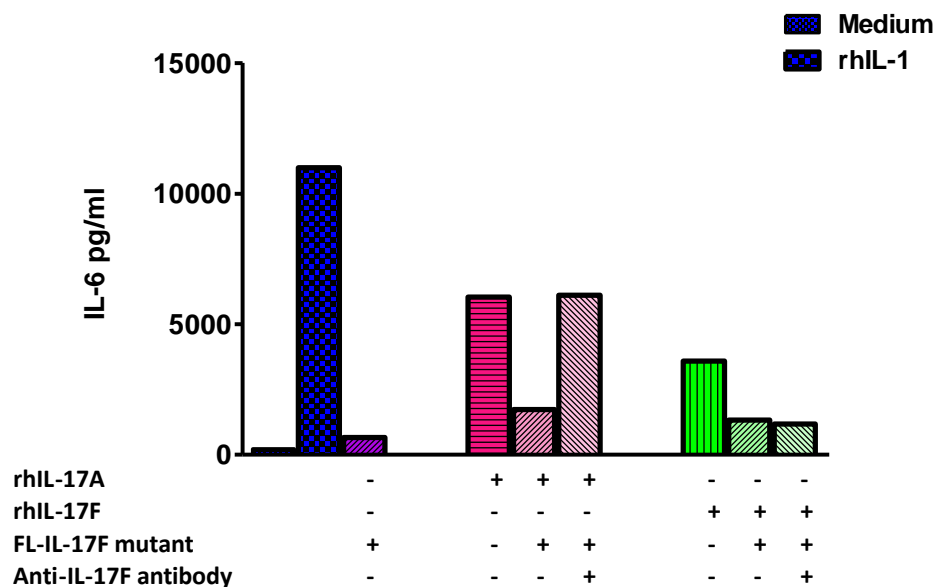


Figure 5.5 Inhibition of IL-17A by immunoaffinity purified IL-17F mutant is reversed by a neutralising anti-IL-17F antibody. HeLa cells were co-stimulated with 100ng/ml rhIL-17A or IL-17F plus immunoaffinity purified IL-17F mutant with or without 10µg/ml neutralising anti-IL-17F antibody. 10ng/ml rhIL-1 was used as a positive control. IL-17F mutant led to a 72% decrease in IL-17A induced IL-6 secretion and this decrease in IL-6 was reversed by a neutralising anti-IL-17F antibody, thus confirming that the inhibition of IL-17A by IL-17F mutant is specific to its the biological activity. rhIL-17A, recombinant human IL-17A; rhIL-17F, recombinant human IL-17F; rhIL-1, recombinant human IL-1; IL-17F mutant, immunoaffinity purified human full-length IL-17F mutant; medium, complete RPMI.

5.2.4 Treatment with MMP-1 releases IL-17 activity from latent LAP-IL-17 molecules

In order to investigate the release of biological activity of LAP-IL-17 proteins, HFFF2 cells were stimulated with untreated or MMP-1 treated 293T cell supernatants containing the expressed human LAP-IL-17 proteins for 24 hours and analysed for the induced secretion of IL-6. As shown in the Fig. 5.6, IL-6 secretion was significantly higher when cells were stimulated with MMP-1 pre-treated than untreated LAP-IL-17 proteins. These results indicate that the biological activity of LAP-IL-17 is released in the presence of MMP. The unexpected finding of stimulation of IL-6 secretion by MMP-1 pre-treated LAP-IL-17F mutant seems to be related to LPS contamination of in-house MMP-1 that was expressed in *E. coli*.

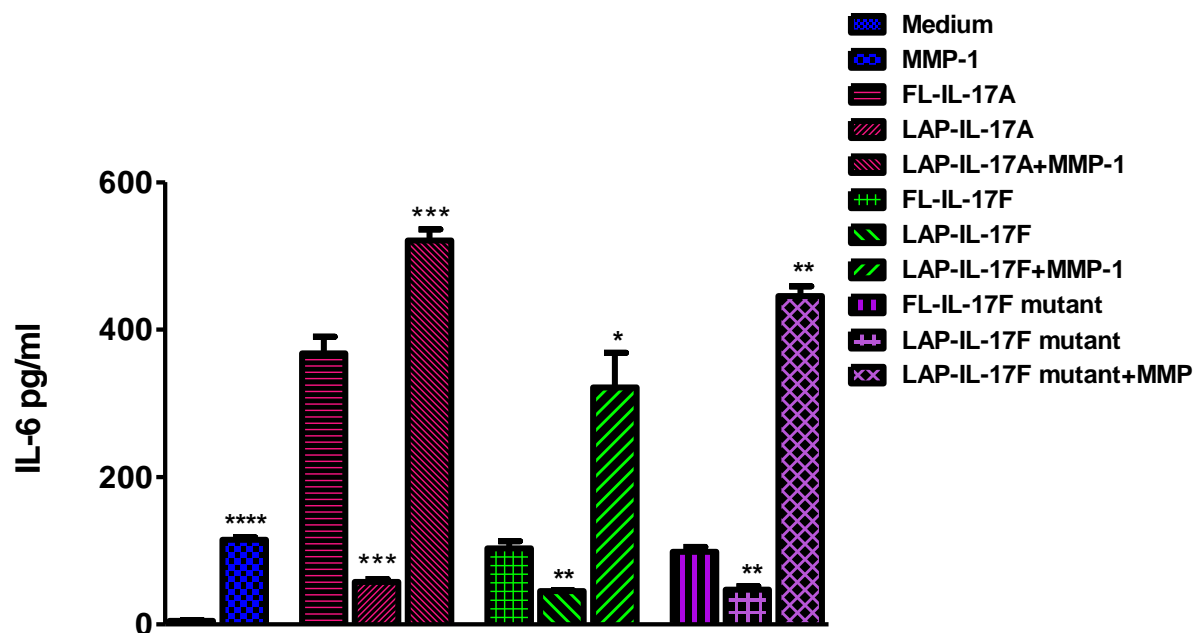


Figure 5.6 Biological latency of human LAP-IL-17 proteins is released by MMP. 1×10^4 HFFF2 cells were stimulated with MMP-1 treated and untreated 293T cells supernatants containing human LAP-IL-17 proteins and analysed for IL-6 secretion by ELISA. MMP-1 treatment of LAP-IL-17 proteins resulted in a significant increase in the secretion of IL-6 than untreated LAP-IL-17 proteins implying that biological activity of LAP-IL-17 proteins is released by the action of MMP. * $p < 0.05$, ** $p < 0.005$, *** $p < 0.0005$; HFFF2, human foetal foreskin fibroblasts; FL-IL-17A, full-length IL-17A; FL-IL-17F, full-length IL-17F; MMP-1, matrix metalloprotease 1; medium, complete Dulbecco's modified eagle medium.

5.2.5 IL-17 is unable to activate luciferase in 57A HeLa cells

IL-17 activates transcription factor NF- κ B in HeLa cells (443). As 57A HeLa cells contain NF- κ B dependent luciferase (420), it was attempted to standardise a luciferase reporter assay in response to IL-17 in these cells.

Activation of luciferase in 57A HeLa cells could not be induced even with 500ng/ml rhIL-17A (data not shown). Based on a study by Ruddy M *et al.*, which reported a synergistic enhancement of IL-17 induced IL-6 secretion in osteoclast cells with 0.2 to 2ng/ml TNF- α (114), an amplification of IL-17 induced luciferase activation was attempted by co-stimulating 57A HeLa cells with IL-17A plus 2ng/ml mouse TNF- α . However, even with TNF- α amplification, activation of luciferase could not be induced (Fig 5.7) and therefore a luciferase reporter assay as a readout for the biological activity of IL-17 could not be standardised in HeLa cells.

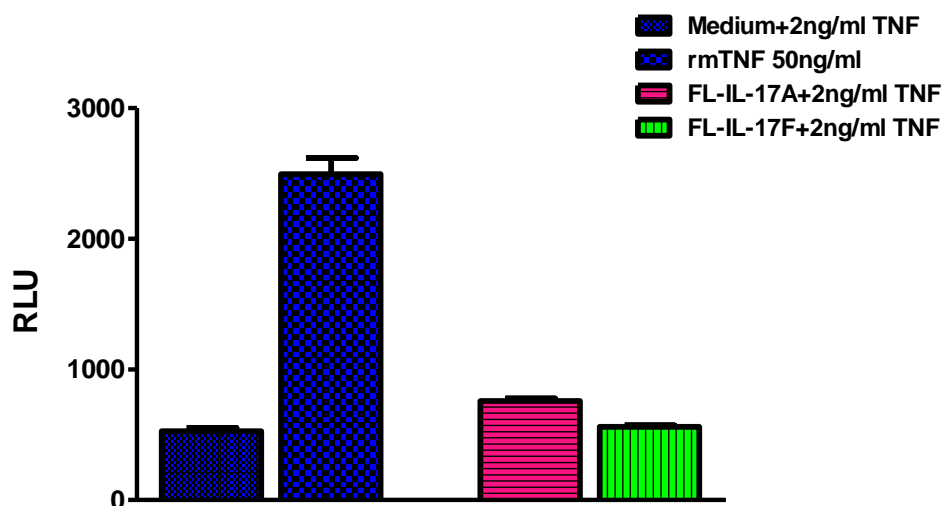


Figure 5.7 IL-17 is unable to activate luciferase in 57A cells. 57A HeLa cells were co-stimulated with 293T cell supernatants containing expressed FL-IL-17A and -IL-17F plus 2ng/ml mTNF- α in an attempt to amplify IL-17 induced activation of luciferase. Combination of IL-17A and suboptimal concentration of TNF- α did not induce activation of luciferase in 57A HeLa cells. FL-IL-17A, full-length IL-17A; FL-IL-17F, full-length IL-17F; mTNF, mouse TNF- α ; RLU, relative luminescent units.

5.2.6 IL-17 was unable to activate IL-6 promoter responsive luciferase in epithelial cells

As IL-17 stimulated production of IL-6 in HeLa cells (Section 5.2.3b) it was decided to attempt and develop an IL-6 promoter responsive luciferase reporter system in response to IL-17 in HeLa cells. In addition, ability of IL-17 to activate IL-6 promoter responsive luciferase in 293T cells was also examined (Chapter 2, Section 2.3.1g). This system however produced a very high background activity.

For developing an IL-6 promoter responsive luciferase assay in HeLa cells, the cells were stably transfected with a plasmid expression vector containing IL-6 promoter responsive luciferase (Chapter 2, Section 2.3.1g). However, none of the eleven clones selected with Blasticidin were responsive to IL-17.

5.2.7 Mouse IL-17F mutant 1 but not IL-17F mutant 3 binds to IL-17RC

Of the three mouse analogues of human IL-17F mutant that were constructed, only mouse IL-17F mutant 1 and mutant 3 were further analysed. Mouse IL-17F mutant 2 could not be expressed *in vitro* and therefore could not be further examined.

Ability of mouse IL-17F mutants to bind to mouse IL-17 receptor was first assessed. Mouse IL-17F binds to both mouse IL-17RC and IL-17RA. IL-17RC binding affinities of mouse IL-17F mutants 1 and 3 were analysed using a commercially available functional ELISA (Chapter 2, Section 2.3.2a). The results showed that mouse IL-17F mutant 1 but not mutant 3 could bind to IL-17RC (Fig. 5.8). The binding strength of IL-17F mutant 1 to IL-17RC was 1.75-fold higher than commercial rIL-17F, which in turn was 1.73-fold higher than 293T cells expressed full-length IL-17F. These results showed that mouse IL-17F mutant 1 but not mutant 3 was able to bind to mouse IL-17RC.

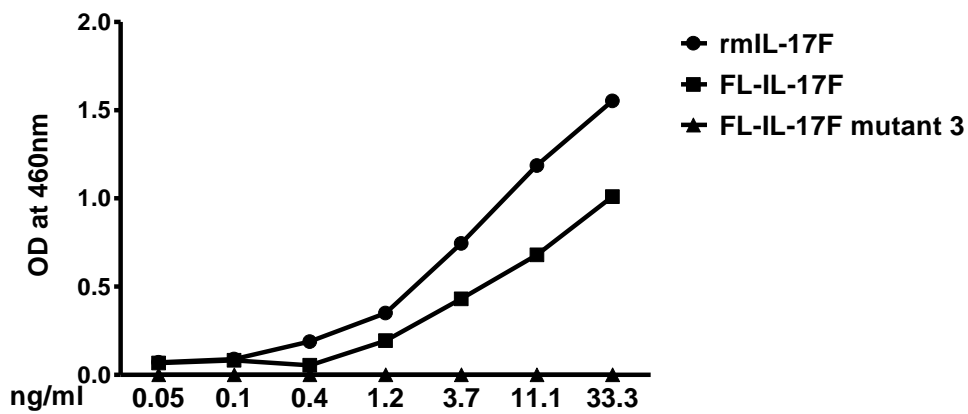
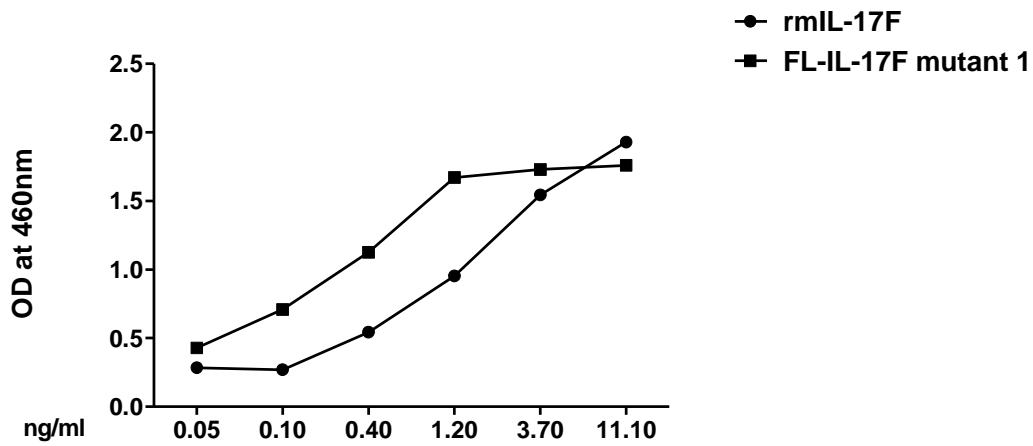


Figure 5.8 Mouse IL-17F mutant 1 but not IL-17F mutant 3 binds to IL-17RC. Ability of mouse FL-IL-17F mutants 1 and 3 to mouse IL-17RC was analysed by functional ELISA determining competitive binding inhibition as described in Chapter 2, Section 2.3.2a. IL-17F mutant 1 but not IL-17F mutant 3 could to bind to IL-17RC. The strength of binding of IL-17F mutant 1 to IL-17RC was 1.75-fold higher than rmlL-17F, which in turn was 1.73-fold higher than 293T cells expressed FL-IL-17F. FL-IL-17F; full-length IL-17F; rmlL-17F, recombinant mouse IL-17F; FL-IL-17F mutant 1, full-length IL-17F mutant 1; FL-IL-17F mutant 3, full-length IL-17F mutant 3; OD, optical density.

5.2.8 Mouse IL-17F mutant 1 is an agonist of IL-17

Mouse IL-17F mutants 2 and 3 were not further examined because the mutant 2 could not be expressed *in vitro* and the mutant 3 was unable to bind to IL-17RC.

Similar to human IL-17, mouse IL-17 stimulates secretion of IL-6 in stromal cells (445). Biological activity of IL-17F mutant 1 was assessed by stimulating mouse embryonic fibroblasts, 3T3 cells and analysing the induced secretion of IL-6. Mouse IL-17F mutant 1 unexpectedly resulted in stimulation of IL-6 secretion in 3T3 cells, which was significantly higher than that induced by IL-17A and IL-17F, $p < 0.005$ (Fig. 5.9). These results imply that mouse IL-17F mutant 1 is an agonist rather than antagonist of IL-17.

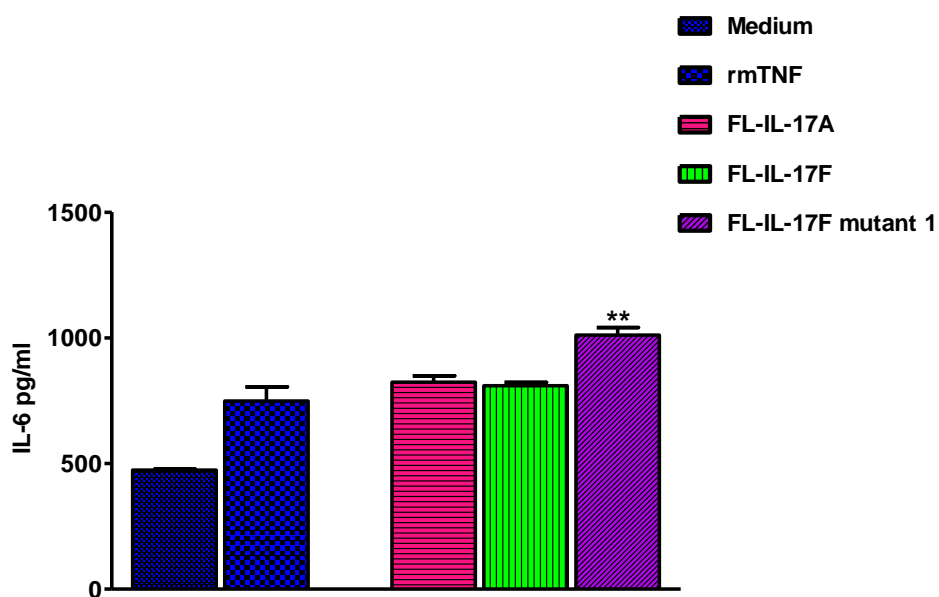


Figure 5.9 Mouse IL-17F mutant 1 is an agonist of IL-17. 5×10^3 3T3 cells were stimulated with 293T cell supernatant containing the expressed mouse full-length IL-17F mutant in parallel with IL-17A and IL-17F and the induced secretion of IL-6 was analysed by ELISA. 25ng/ml rmTNF- α was used as a positive control. IL-17F mutant 1 unexpectedly stimulated the secretion of IL-6, which was significantly higher than that induced by IL-17A and IL-17F ($p < 0.005$). ** $p < 0.005$; 3T3, mouse embryonic fibroblasts; FL-IL-17A, full-length IL-17A; FL-IL-17F, full-length IL-17F; FL-IL-17F mutant 1, full-length IL-17F mutant 1; mTNF, mouse TNF- α ; medium, complete DMEM.

5.2.9 Biological latency of mouse LAP-IL-17 proteins is released by MMP

Release of biological activity of mouse LAP-IL-17 proteins was assessed using the protocol same as that was used for human LAP-IL-17 proteins. 3T3 cells were stimulated with 293T cell supernatants containing mouse full-length IL-17 proteins, untreated or MMP-1 treated LAP-IL-17 proteins and analysed for the induced secretion of IL-6 (Fig. 5.10). Untreated LAP-IL-17A and -IL-17F proteins although induced a secretion of IL-6 that was higher than that induced by medium alone, it was significantly less than that induced by their corresponding full-length IL-17 proteins. MMP-1 treatment of LAP-IL-17A and IL-17F proteins resulted in a significant increase in the secretion of IL-6. These results confirmed that biological activity of LAP-IL-17 proteins can be released by MMP.

Interestingly, IL-6 secretion induced by untreated LAP-IL-17F mutant 1 was significantly higher than that induced by full-length IL-17F mutant 1, which further increased with MMP-1 treatment ($p < 0.0005$).

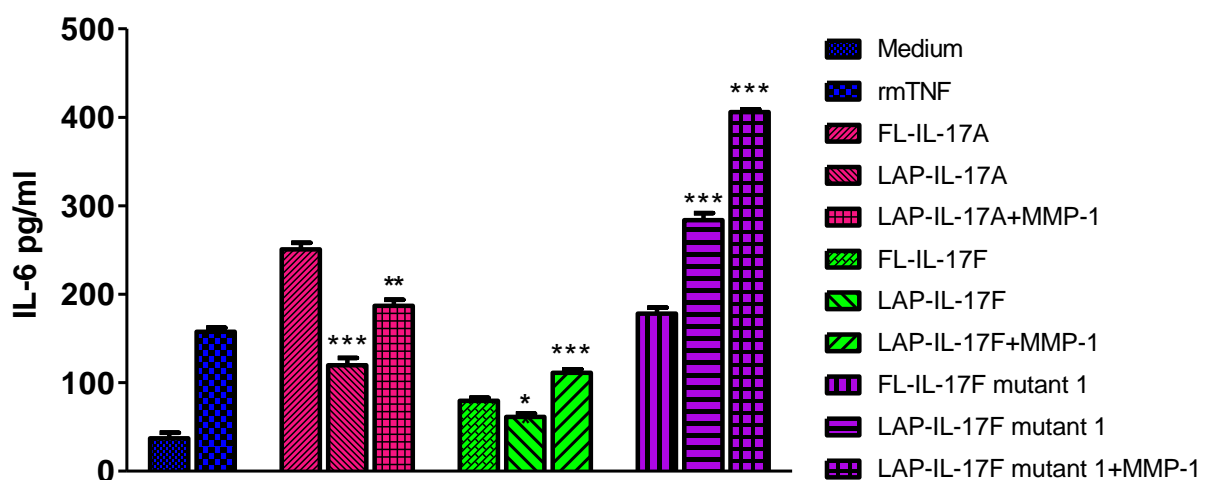


Figure 5.10 Biological activity of mouse LAP-IL-17 proteins is released by MMP. 5×10^3 3T3 cells were stimulated with 293T cell supernatants containing the expressed mouse full-length IL-17 proteins, and untreated or MMP-1 treated LAP-IL-17 proteins and induced secretion of IL-6 was analysed by ELISA. 10ng/ml rmTNF- α was used as a positive control. MMP-1 treatment of LAP-IL-17 proteins resulted in a significant increase in the induced IL-6 secretion implying that biological activity of LAP-IL-17 proteins is released by MMP. Stimulation of IL-6 secretion by MMP-1 untreated LAP-IL-17 proteins seems to be related to the presence of endogenous MMP-1 in 293T cells supernatants. * $p < 0.05$; ** $p < 0.005$; *** $p < 0.0005$; 3T3, mouse embryonic fibroblasts; FL-IL-17A, full-length IL-17A; FL-IL-17F, full-length IL-17F; FL-IL-17F mutant 1; full-length IL-17F mutant 1; rmTNF, recombinant mouse TNF- α ; medium, complete Dulbecco's modified eagle medium.

5.2.10 A novel IL-6 promoter responsive luciferase reporter system to assess biological activity of mouse IL-17 is developed and standardised

Murine IL-17 induces production of a number of cytokines and chemokines in macrophage cells (446). Jovanovic *et al.* have shown that IL-17 induces NF- κ B in human macrophage cells (106). Raw 264.7 cells, a mouse macrophage cell line which was previously selected in G418 to express an NF- κ B driven luciferase construct (kindly provided by Dr. Vessillier, BJRU) were stimulated with mouse IL-17 proteins for 24 hours and the cell lysates were analysed for luciferase activity. The results showed that IL-17 did not activate luciferase in these cells although lipopolysaccharide (LPS) used as a positive control was able to activate luciferase in these cells (data not shown). A NF- κ B driven luciferase reporter assay as a readout for biological activity of mouse IL-17 therefore could not be developed in Raw 264.7 cells.

Development and standardisation of a IL-6 promoter responsive luciferase assay was therefore attempted. First, DBA/1 mouse fibroblast cells were stably transfected with a plasmid expression vector containing IL-6 promoter responsive luciferase (Chapter 2, Section 2.3.2c). However, stimulation of these cells even with 500ng/ml rmlIL-17A did not result in the activation of IL-6 promoter responsive luciferase (data not shown). The cells were then stimulated with IL-17 in combination with a small amount of TNF- α to see whether synergistic activity of these two cytokines could lead to stimulation of IL-6 promoter responsive luciferase.

As shown in the Fig. 5.11, addition of 2ng/ml rmTNF- α to mouse IL-17A and IL-17F led to a synergistic activation of IL-6 promoter responsive luciferase in DTF cells. Although, not used here, a checkerboard experiment using different concentrations of TNF- α and IL-17 would have ideal to demonstrate the synergistic activation of IL-6 by TNF- α and IL-17 together. As luciferase reporter assays are sensitive yet simple and efficient assay systems, use of herewith developed and standardised novel IL-6 promoter responsive cell culture luciferase reporter system would allow an easy testing of biological activity of mouse IL-17.

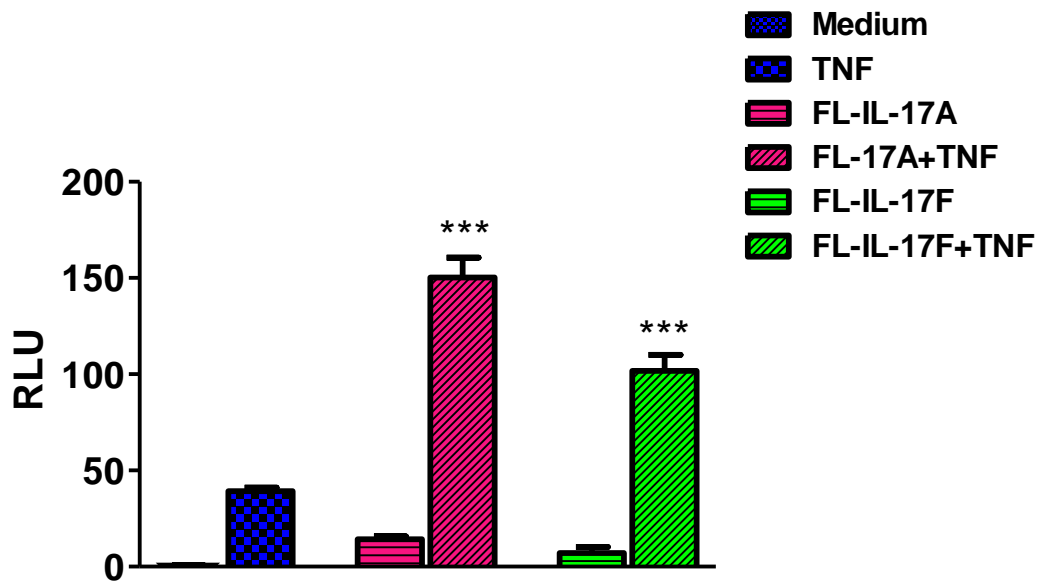


Figure 5.11 DTF cells stably transfected with IL-6 promoter driven luciferase are responsive to mouse IL-17A plus 2ng/ml TNF- α . DTF cells were stably transfected with pGL2 containing IL-6 promoter responsive luciferase under Blasticidin selection (Chapter 2, Section 2.3.2c). The stably transfected DTF cells were stimulated with 293T cells supernatants containing expressed mouse FL-IL-17A or -IL-17F alone or in combination with 2ng/ml rmTNF- α for 6 hours and cell lysates analysed for luciferase activity. Addition of suboptimal concentrations of rmTNF- α resulted in a synergistic amplification of induction of luciferase activation by IL-17A and IL-17F. *** $p < 0.0005$; FL-IL-17A, full-length IL-17A; FL-IL-17F, full-length IL-17F, medium, 0.5% FBS containing DMEM; RLU, relative luminescent unit.

5.3. Discussion

In vitro functional assays showed that in equal concentrations, human (H161R) IL-17F mutant reduced IL-17A induced secretion of IL-6 by more than 50% in HFFF2, 3T3 and HeLa cells. The inhibition of IL-17A by IL-17F mutant was reversed in the presence of a neutralising anti-IL-17F antibody. Although not used in this experiment, use of a control IgG to demonstrate that reversal of IL-17A induced reduction in secreted IL-6 was achieved by anti-IL-17F neutralising antibody but not the control IgG would have been highly desirable to further confirm the specificity of biological activity of IL-17F mutant. The mutant on its own was unable to induce secretion of IL-6 in all the three cell lines and lacked the ability to activate ERK1/2 in HeLa cells. Taken together these results confirm the hypothesis that human (H161R) IL-17F mutant is an inhibitor of IL-17A. Inhibition of IL-17F but not IL-17A by IL-17F mutant has been previously reported (153). This study for the first time demonstrates an additional inhibition of IL-17A by the mutant. IL-17A is the major proinflammatory IL-17 cytokine and 30-100 times more potent than IL-17F (143). An inhibition of IL-17A by IL-17F mutant is likely to result in a therapeutically effective suppression of IL-17 mediated inflammation in RA and similar autoimmune conditions. All the three mouse analogues of human IL-17F mutant that were developed for *in vivo* investigation proved unsuitable for testing in CIA mice. The RA synovium/SCID model would have allowed direct targeting of human RA tissue by human IL-17F mutant but suitable RA synovial samples could not be obtained.

This part of the study also demonstrated that IL-17F mutant is able to bind to IL-17RC. IL-17A and IL-17F bind to a heteroreceptor complex IL-17RA/RC and require both the receptor to mediate their signaling effects (136, 435, 436). In contrast to IL-17RC, which binds both IL-17A and IL-17F with a high affinity, IL-17RA binds IL-17A effectively but binds IL-17F with 1000-fold lower affinity (447). Binding of IL-17F mutant to IL-17RA was not examined. However, irrespective of whether or not IL-17F mutant binds to IL-17RA, demonstration of its binding to IL-17RC suggests that the mutant would be able to inhibit both IL-17A and IL-17F mediated signaling effects. While, either anti-IL-17RA or anti-IL-17RC antibody resulted in a significant reduction in *in vitro* biological activity of IL-17A and

IL-17F (447), a soluble form of IL-17RC but not IL-17RA blocked binding of both IL-17A and IL-17F, and inhibited the signaling effects in response to both the cytokines (181). It has been shown that in the absence of IL-17RC, IL-17A and IL-17F are unable to activate downstream pathways (173, 181). IL-17F mutant would compete with both IL-17A and IL-17F for binding to IL-17RC and therefore would inhibit both IL-17A and IL-17F mediated signaling effects.

The receptor binding assays of mouse IL-17F mutants showed rather unexpected results (IL-17F mutant 2 due to undetectable expression *in vitro* was not examined). Interestingly, the strength of affinity of the mouse IL-17F mutant 1 s analysed by a competitive binding inhibition ELISA was 1.75-fold higher than wild-type IL-17F whereas mouse IL-17F mutant 3 did not bind to IL-17RC at all. These changes in receptor binding affinity of mouse IL-17F mutants seem to be related to the fact that the mutations involved an important receptor binding site of IL-17F (179). Substitution of Glutamine by Arginine in mouse IL-17F mutant 1 caused a gain of function mutation resulting in enhancement of its receptor binding affinity, whereas deletion of the last 4 amino acids in the truncated IL-17F mutant 3 resulted in the loss of receptor binding affinity. In line with the results of receptor binding, mouse IL-17F mutant 1 stimulated rather than inhibited IL-6 secretion from 3T3 cells. All the three mouse analogues of human IL-17F mutant thus displayed either immunological or biological properties that were contrary to those expected.

The functional assays demonstrated that MMP-1 pre-treated LAP-IL-17 proteins induced significantly higher secretion of IL-6 than naïve LAP-IL-17 proteins, thus confirming *in vitro* release of biological latency of human and mouse LAP-IL-17 by MMP. Stimulation of fibroblast cells with MMP-1 pre-treated LAP-IL-17F mutant unexpectedly resulted in induction than inhibition of IL-6 secretion, which seems to be related to LPS contamination of in-house MMP-1 that was expressed in *E. coli*. Also, the biological activity of naïve LAP proteins was higher than that induced by medium alone. 293T cells contain endogenous MMPs, which seem to be responsible for partial release of biological activity of naïve LAP-IL-17 proteins. The LAP cytokine approach was pioneered in our laboratory first using IFN- β and since has been validated for a number of other cytokines and small molecules including MSH- α

and VIP (355). Use of LAP-cytokine allows targeting of biological effects of cytokine-based therapies to the sites, where MMPs are overexpressed. In addition, LAP-cytokine approach offers other advantages such as significant enhancement in *in vitro* and *in vivo* expression of a given cytokine as shown in this study and a significant prolongation of *in vivo* half-life as shown previously. Half-life of LAP-IFN- β was thirty-seven fold higher than naive IFN- β and its therapeutic efficacy was superior to IFN- β in CIA mice (353). Similarly, *in vivo* therapeutic effects of LAP-MSH were superior to free MSH in a peritonitis mouse model (355).

A novel IL-6 promoter responsive luciferase reporter system to analyse biological activity of mouse IL-17 was developed and standardised. DTF cells (DBA/1 mouse fibroblasts) were stably transfected with IL-6 promoter responsive luciferase. Although not used in this study, a checkerboard experiment using different concentrations of rmTNF- α and IL-17A or IL-17F would have been ideal to demonstrate the observed synergy between IL-17A and TNF- α . The cells demonstrated a synergistic activation of luciferase in response to mouse IL-17A and IL-17F in combination with 2ng/ml TNF- α but not when stimulated by IL-17A or IL-17F alone. It has been shown that IL-17 induces secretion of IL-6 primarily by activating the transcription factor C/EBP- δ and β , having a minimal activity on NF- κ B, but in combination with TNF- α , even in suboptimal concentrations can induce a much greater secretion of IL-6 by synergistically activating C/EBP- δ and β (114). In addition, stabilisation of mRNA of IL-6 and other TNF- α target genes by IL-17 further enhances the synergism between the two cytokines (185).

Development and standardisation of an IL-6 promoter driven luciferase reporter system in 293T and HeLa cells to assess biological activity of human IL-17 was not successful. Similarly, standardisation of a NF- κ B responsive luciferase reporter system in 57A HeLa cells (420) and Raw 264.7 cells (mouse macrophage cells stably transfected with NF- κ B driven luciferase) to assess biological activity of human and mouse IL-17 could not be achieved. All these cell lines failed to activate luciferase in response to IL-17. Shen *et al.* have previously reported a lack of NF- κ B-linked luciferase activity in response to IL-17 in a number of mammalian cell lines (135).

To conclude, *in vitro* biological assays confirmed the hypothesis that human IL-17F mutant is an inhibitor of IL-17A. The study also demonstrated that *in vitro* biological activity of LAP-IL-17 proteins can be released by MMP. A novel IL-6 promoter responsive luciferase reporter system to assess biological activity of mouse IL-17 was successfully developed and standardised.

CHAPTER VI

EVALUATION OF *IN VIVO* EXPRESSION OF HUMAN IL-17 TRANSGENE IN MOUSE MODELS OF INFLAMMATION

6.1 Introduction

In vitro studies in primary cells or cell lines, although extremely important, they do not fully reproduce the situation *in vivo*, which is much more complex and less well defined. It is therefore important to test preclinical efficacy of an investigational therapy *in vivo* in animal models of disease before clinical testing in humans. CIA in mice bears close resemblance to RA (448, 449) and is well recognised for its robustness in predicting efficacy of anti-TNF therapy (450). This model of RA was initially selected for *in vivo* testing of IL-17F mutant but could not be pursued due to unexpected *in vitro* properties of the mouse analogues of human IL-17F mutant that were constructed for this purpose. Mouse IL-17F mutant 1 displayed IL-17 agonist rather than antagonist activity whereas *in vitro* expression of IL-17F mutant 2 could not be detected at all. The third mouse IL-17F mutant failed to bind to mouse IL-17RC.

The RA synovium/SCID mouse model of RA provides a unique opportunity to directly examine efficacy of therapeutics of human origin in mice implanted with human RA synovium. Koenders *et al.* (416) have confirmed the validity of this model in predicting therapeutic efficacy of currently used biological therapies for RA. Investigation of IL-17 inhibition in this model showed that a significant response to anti-IL-17 treatment was seen only in the mice which were transplanted with RA synovium enriched in CD3+T cells, implying that the responsiveness to anti-IL-17 is dependent on the presence of CD3+ T cells in a RA joint.

Mouse stromal cells secrete IL-6 in response to human IL-17 (440, 445). In keeping with these observations, as described in Chapter 5, Section 5.2.1, 3T3 cells were responsive to human IL-17 and produced IL-6 when stimulated with human IL-17A and IL-17F. As in human fibroblast and epithelial cells, human IL-17F mutant was unable to induce secretion of IL-6 in 3T3 cells and inhibited human IL-17A induced secretion of IL-6 in these cells (Chapter 5, sections 5.2.1 and 5.2.2).

Murine airpouch model is considered a model of synovial-like tissue inflammation (451). Airpouch pouch cavity formed by subcutaneous injection of sterile air into the back of a mouse is lined with cells that resembles the synovial membrane after 6 days (452). Injection of non-specific irritants such

as Carboxymethyl cellulose (CMC) into an air pouch induces an acute inflammatory response that can be readily evaluated by analysing the volume of exudate produced, the infiltration of cells, and the release of inflammatory mediators.

Amongst non-viral approaches to gene transfer, intravenous hydrodynamic delivery (364) results in highest gene transfer and expression and seems to be well tolerated in rodents despite rapid injection of a relatively large volume of normal saline. In comparison with other physical and chemical methods, the procedure of intravenous hydrodynamic delivery is relatively simple and does not require special equipment or chemical adjuncts. Intravenous administration of plasmid DNA in normal saline in volume equivalent to 10% body weight rapidly over 3-5 seconds alters transmembrane permeability of hepatocytes by creating transient pores and allows uptake of injected DNA by liver cells. DNA transferred to hepatocytes then becomes available for translation and expression into its protein and is eventually secreted into the circulation. Due to its high efficiency and a non-viral nature of delivery, hydrodynamic gene delivery is under active investigation for human use. Hydrodynamic limb vein delivery in large research animals has demonstrated an efficiency that is comparable to small research animals (365) and holds a good promise for human use. A therapeutic gene can be delivered to an isolated limb by infusing plasmid DNA into a limb vein and facilitating gene transfer by the placement of a proximal tourniquet, which in turn will result in a transient increase in vascular pressure and aid extravasation of plasmid DNA (453).

After demonstrating that human IL-17F mutant but none of the three cloned mouse IL-17F mutants were able to inhibit IL-17A *in vitro*, it was decided to examine *in vivo* therapeutic efficacy of human IL-17F mutant in RA synovium/SCID mice model of RA. As a preliminary to this, *in vivo* expression of intravenous hydrodynamically delivered human full-length and LAP-IL-17A plasmid DNA and its pharmacokinetics over the two weeks period was first examined in naïve SCID mice. IL-17A instead of IL-17F mutant was used for this part of the study as a commercial ELISA to analyse expression of human IL-17F in mouse serum was not available. It was also believed that due to the

striking similarities between IL-17A and IL-17F, the necessary information about *in vivo* expression of human IL-17F mutant transgene in mouse serum required for the future definitive experiment could be well obtained by using IL-17A in the preliminary experiment.

As *in vitro* assays also demonstrated that human IL-17F mutant inhibited IL-17A induced secretion of IL-6 not only in human but also mouse fibroblast cells, it was also decided to examine *in vivo* therapeutic efficacy of human IL-17F mutant in CIA mice. Although an immune response to human IL-17F mutant would be inevitable in mice, the short duration, approximately 10 days of post-treatment assessment would have still allowed the completion of CIA experiment. As a preliminary to this, *in vivo* expression of human full-length and LAP-IL-17F mutant was first examined in C57BL/6 mice. In addition, airpouch were created over the dorsum of these mice and acute non-specific inflammation induced in the pouch to enable investigation of therapeutic transgene expression at the site of actual inflammation. After successful development and standardisation of an ultrasensitive ELISA (Chapter 2, Section 2.2.2c) to analyse expression of human IL-17F in mouse serum, systemic gene therapy with human IL-17F mutant was used for this part of the experiment. As mouse airpouch model offers an opportunity to examine acute inflammatory response, number of neutrophils in airpouch lavage fluid, and levels of KC and IL-6 in mouse airpouch lavage exudate and serum were also analysed as a preliminary to investigation of therapeutic efficacy of human IL-17F mutant in CIA mice. The results however showed that the numbers of neutrophils and levels of KC and IL-6 in IL-17F mutant treated group were not different than the control group of normal saline treated mice (data not shown). CIA experiment therefore was not pursued.

6.1.1 Aims

1. To evaluate systemic expression and pharmacokinetics of intravenous hydrodynamically delivered human IL-17A gene therapy in naïve SCID mice.
2. To examine expression of intravenous hydrodynamically delivered human IL-17F mutant gene therapy in serum and airpouch exudate in C57BL/6 mice.

6.2 Results

6.2.1 Expression of human FL- and LAP-IL-17A transgenes in naïve SCID mice

Pharmacokinetics and *in vivo* expression of intravenous hydrodynamically delivered human full-length- and LAP-IL-17 plasmid DNA were studied in naïve SCID mice as a preliminary to assessing *in vivo* therapeutic efficacy of human IL-17F gene therapy in RA synovium/SCID model of RA. Due to the need to use human RA tissue in RA/SCID model, it was essential to confirm that intravenous hydrodynamic plasmid-based gene therapy with human IL-17 led to an adequate *in vivo* transgene expression in SCID mice and that the expression of transgene was sustained for at least one week, before conducting the final study. Human IL-17A instead of IL-17F mutant was used for this part of the study as a commercial ELISA sensitive enough to detect human IL-17A but not human IL-17F in mouse serum was available. It was believed that due to the striking structural and functional similarities between IL-17A and IL-17F, the expression and pharmacokinetic characteristics of IL-17F mutant would be well represented by IL-17A.

Previous observations in our laboratory have shown that 5µg/ml plasmid DNA delivered via intravenous hydrodynamic tail injection in mice resulted in a transgene expression that was first detected at 48 hours and lasted over several weeks. On the basis of these findings, naïve SCID mice were treated with intravenous hydrodynamically delivered 5µg/ml human full-length and LAP-IL-17A plasmid DNA and levels of transgene expression in mouse serum analysed at 48 hours, 1 week and 2 weeks. The treatment had to be discontinued prematurely in 2 female mice due to technical difficulties. One of these female mice received 8.5µg FL-IL-17A in 1.5ml NS and another received only 3.5µg LAP-IL-17A in 0.7ml NS. Two mice (one male and one female) from the LAP-IL-17A treated group died unexpectedly; the male mouse died at the time of intravenous injection of the plasmid DNA and the female mouse died 30 hours post-LAP-IL-17A injection from unknown causes. The results (Fig. 6.1) showed that the levels of human LAP- IL-17A transgene in mice serum were 1400-fold higher than full-length IL-17A. The serum levels of both full-length and LAP-IL-17A declined to 20% and 2% of the baseline at the end of the first and second week respectively.

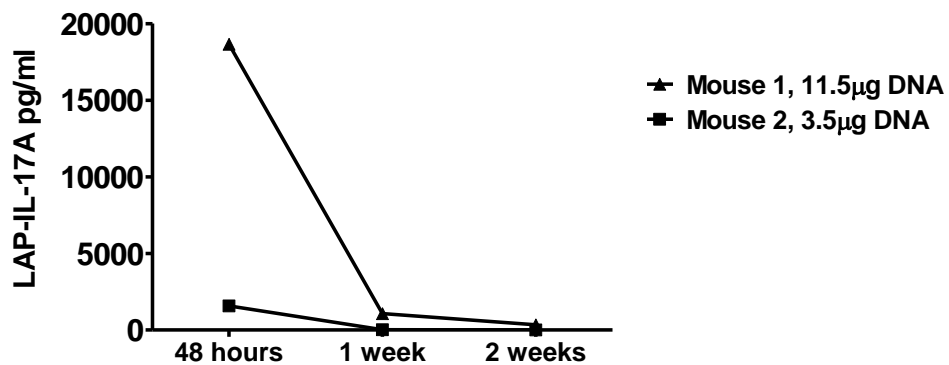
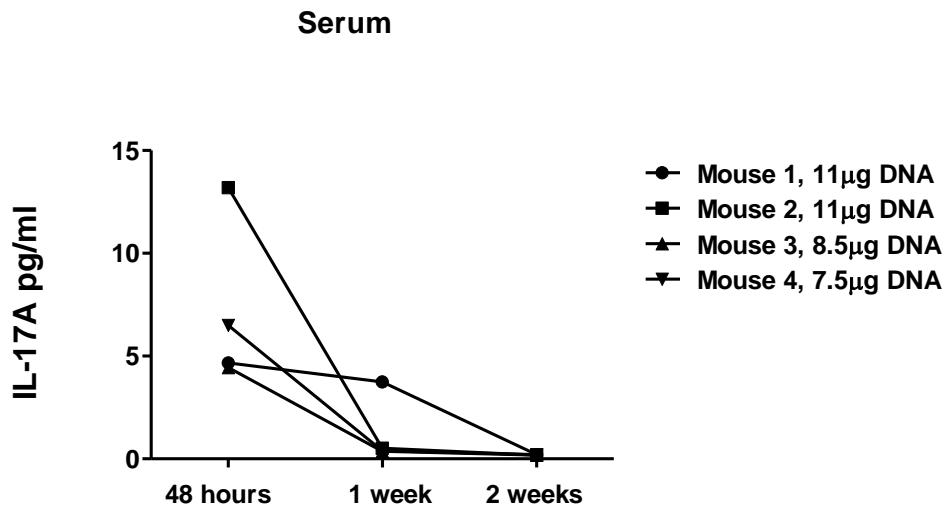


Figure 6.1 Expression of human IL-17 transgene in naïve SCID mice. Naïve SCID mice (n=4) were treated with intravenous hydrodynamic human full-length or LAP-IL-17A gene therapy and levels of expressed transgenes in individual mouse serum were analysed at 48 hours, 1 week and 2 weeks by ELISA. The expression of LAP-IL-17A was 1400- fold higher than full-length IL-17A and the levels of expressed transgenes declined to 20% and 2% of the baseline levels at 1 and 2 weeks period respectively. IL-17A, full-length IL-17A.

6.2.2 Expression of human FL- and LAP-IL-17 transgenes in C57BL/6 mice

Thirty C57BL/6 mice were injected dorsally to develop an airpouch and treated with intravenous hydrodynamically delivery 5µg/ml human IL-17F mutant or control plasmid DNAs. Expression of transgene was analysed at 52 hours post-plasmid DNA administration.

Expression of human full-length IL-17A and IL-17F mutant, administered either alone or in combination, and LAP-IL-17F mutant, administered in two different doses of 1µg/ml and 5µg/ml in mouse serum, airpouch lavage exudate and liver homogenates was analysed by human IL-17A and a modified human IL-17F ultrasensitive ELISA. An ultrasensitive ELISA was developed and standardised for detection of human IL-17F in mouse serum by using human IL-17F Duoset ELISA (R&D Systems, UK) in conjunction with uncoated ELISA plate and mouse diluents 4 and 5 (MSD, USA) (Chapter 2, section 2.2.2c). As seen in the Fig. 6.2, levels of human full-length IL-17F mutant in mouse serum and airpouch lavage exudate were 1000-fold higher than full-length IL-17A. The concentrations of expressed transgene in mouse serum following co-administration of full-length IL-17A plus IL-17F mutant in an equal concentration of 2.5µg/ml were 7700-fold higher and in airpouch lavage exudate 134-fold higher on detection with anti-human IL-17F than anti-human IL-17A antibody. The levels of expressed LAP-IL-17F mutant in mice serum were 2.2-fold higher than full-length IL-17F mutant. Administration of LAP-IL-17F mutant in two different doses of 1µg/ml and 5µg/ml led to a dose-dependent expression of LAP-IL-17F mutant transgene in mice serum, airpouch lavage exudate and liver homogenate samples. The levels of LAP-IL-17F mutant in mouse serum, airpouch lavage exudate and liver homogenates following treatment with 5µg/ml LAP-IL-17F mutant were 5.2, 3 and 2.4-fold higher than the treatment with 1µg/ml LAP-IL-17F mutant. Interestingly, only 0.35% serum LAP-IL-17F mutant was expressed in airpouch lavage exudate as against a 4.5% expression of serum full-length IL-17F mutant in airpouch lavage exudate.

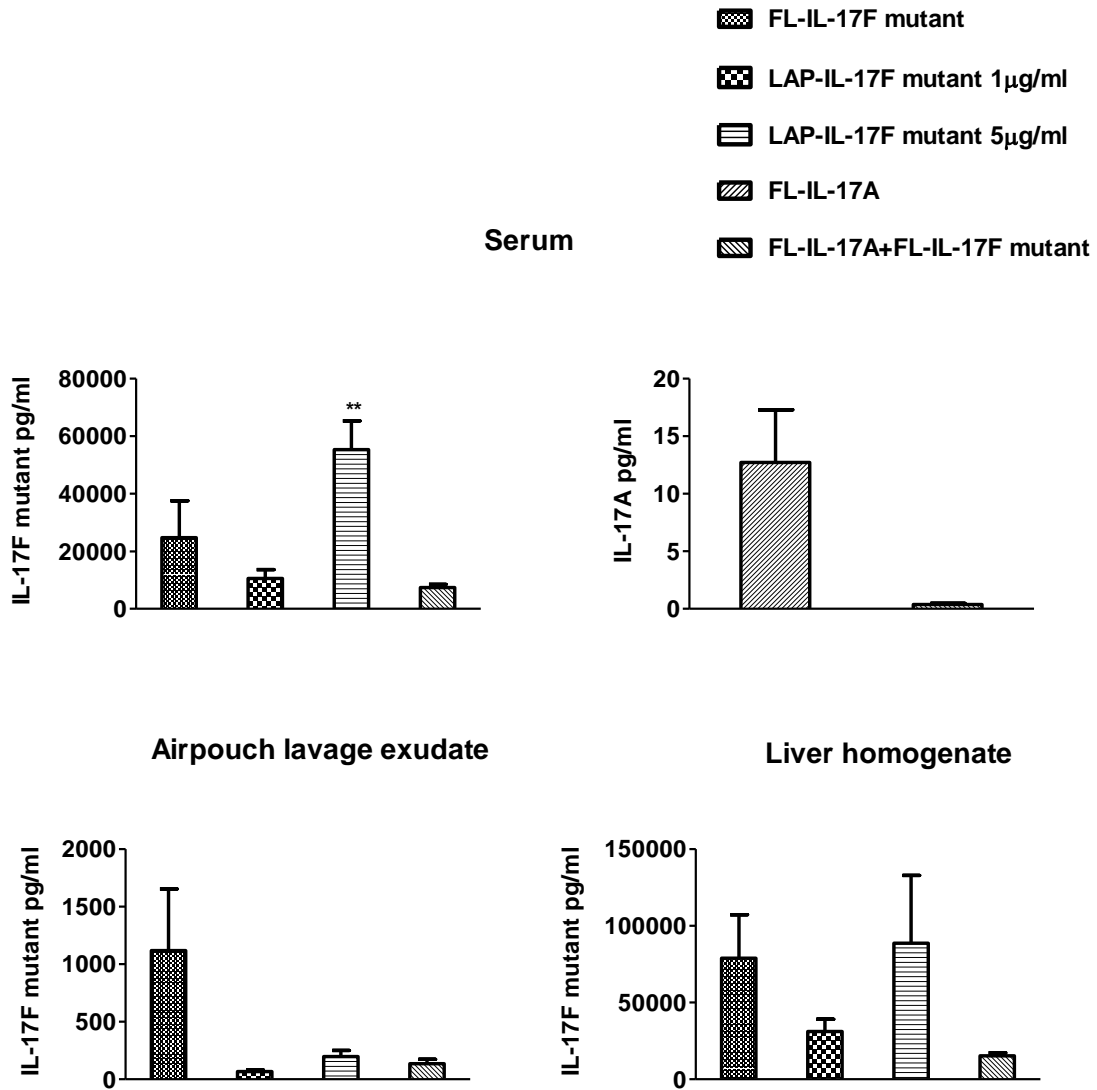


Figure 6.2 Expression of human IL-17 transgene in C57BL/6 mice. 52 hours post- hydrodynamic gene delivery, levels of human IL-17 transgenes expressed *in vivo* were analysed in mouse serum, airpouch lavage fluid and liver homogenates by ELISA. Expression of IL-17A in liver homogenates was not examined. Levels of IL-17F mutant in serum and airpouch lavage exudate were significantly higher than IL-17A ($p < 0.05$). Administration of 5µg/ml LAP-IL-17F mutant in comparison with 1µg/ml resulted in a significant higher expression of transgene in serum, airpouch exudate and liver homogenates ($p < 0.005$). Levels of transgene detected in serum following co-administration of IL-17A plus IL-17F mutant were significantly higher when detected with anti-human IL-17F than anti-human IL-17A antibody. Levels of LAP-IL-17F mutant and FL-IL-17F mutant in airpouch lavage exudate were only 0.35% and 4.5% of their serum levels. FL-IL-17A, full-length IL-17A; FL-IL-17F mutant, full-length IL-17F mutant, IL-17A/IL-17F mutant, IL-17A/IL-17F heterodimer.

6.3 Discussion

Intravenous hydrodynamic injection of human full-length and LAP- IL-17 plasmid DNA constructs via tail vein in SCID and C57BL/6 mice resulted in a detectable expression of human IL-17 transgenes at protein level in mice serum and airpouch lavage exudate. These findings support the previous reports of a high efficiency of gene transfer achieved with this relatively simple non-viral method of gene delivery (454, 455).

The levels of expressed IL-17 transgene however declined rapidly and progressively over the two week study period. The expression of transgene was 20% of the baseline at the end of first week and only 2% of the baseline after 2 weeks. Longevity of transgene expression is influenced by the methylation status of the plasmid vectors (456). Expression vectors produced in bacteria such as pcDNA3 contain numerous methylated CpG dinucleotides, which may generate a proinflammatory cytokine response by activating TLR 9 (457) and cause a rapid decline in the level of expressed transgene as seen in this study.

It was thus demonstrated that systemic gene therapy with human full-length and LAP-IL-17 led to a successful expression of human IL-17 transgene in naïve SCID and C57BL/6 mice although the transgene levels declined rapidly over the two weeks period. The results also showed that human IL-17F mutant was unable to suppress mouse airpouch inflammation as assessed by analysing the number of neutrophils and levels of KC and IL-6 in airpouch lavage fluid (data not shown). It was therefore decided to further investigate *in vivo* therapeutic efficacy of human IL-17F mutant in RA synovium/SCID mice model of RA. Although the levels of transgene declined rapidly, the very fact that these could still be detected in mouse serum at the end of two weeks would have still allowed the completion of the study, which required post-treatment assessment over one week period. Due to difficulty in obtaining suitable RA synovium samples and SCID mice, this experiment however could not be conducted.

In vivo expression of IL-17F mutant transgene in serum and airpouch lavage exudate in C57BL/6 mice was 1000-fold higher than IL-17A. Similarly, serum and airpouch exudate levels of expressed

transgene following co-administration of IL-17A plus IL-17F mutant were 7700-and 135-fold higher when detected with anti-human IL-17F antibody than anti-human IL-17A antibody. These results imply that IL-17F mutant had a longer half-life *in vivo* and was more stable than IL-17A. It is also possible that the majority of the transgene expression following co-administration of IL-17A plus IL-17F mutant was either in the form of IL-17F mutant homodimers or expressed as IL-17A/IL-17F mutant heterodimer which was better detected with anti-IL-17F than anti-IL-17A antibody. A preferred expression of IL-17F over IL-17A has been previously reported. Wright *et al.* (143) have shown that activated human CD4+ T cells secreted minimal IL-17A but 10-fold or greater IL-17F and Liang *et al.* (144) have reported a higher expression of IL-17F than IL-17A from naïve mouse CD4+ T cells.

In vivo expression of LAP-IL-17A in SCID mice was 1400-fold higher than full-length IL-17A whereas expression of LAP-IL-17F mutant was 2.2-fold higher than full-length IL-17F mutant in C57BL/6 mice. Similarly, *in vitro* expression of LAP-IL-17A, IL-17F and IL-17F mutant proteins was two to six-folds higher than corresponding full-length IL-17. These results imply that modification of a cytokine as LAP-cytokine significantly enhances both its *in vitro* and *in vivo* expression. A significant prolongation of *in vivo* half-life of LAP-IFN- β in the order of 37-fold higher than naïve IFN- β in CIA mice has been previously reported (353). A LAP-cytokine approach therefore offers advantage of a superior expression and a prolonged half-life over naïve cytokine and a potential for reduction in the dose and frequency of administration of a cytokine based therapy.

The local expression of transgenes in airpouch lavage exudate was only slight in comparison to the systemic expression. The levels of LAP-IL-17F mutant in airpouch lavage exudate were only 0.35% of its serum level as against airpouch lavage exudate levels of full-length IL-17F mutant, which were 4.5% of its systemic levels. The less efficient migration of LAP-IL-17F locally into acutely inflamed airpouch does not seem to be related to its size. The molecular weight of LAP-IL-17F mutant homodimer is approximately 108kDa, much lower than that of immunoglobulins, which are able to easily migrate through vascular endothelium. It will be of interest to investigate whether

thrombospondin in the basal surface of endothelial cells (458, 459) interacted with LAP domain (460) of LAP-IL-17F mutant and prevented its migration through the local vasculature.

Although this study has helped in arriving at some important conclusions such as confirmation of efficiency of intravenous hydrodynamic plasmid injection via tail vein in achieving an effective *in vivo* transgene expression in mice and significantly enhanced *in vivo* expression of LAP-IL-17 in comparison to full-length IL-17, some of the key experiments to essentially investigate *in vivo* therapeutic efficacy of IL-17F mutant could not be conducted. After a successful *in vivo* expression of human full-length and LAP-IL-17 transgenes in naïve SCID mice, a further confirmation of therapeutic effectiveness of IL-17F mutant could not be carried out due to difficulties in obtaining suitable RA synovial samples. Although both human IL-17F mutant and LAP-IL-17F mutant could also be successfully expressed in C57BL/6 mice, a preliminary analysis of therapeutic efficacy of human IL-17F mutant did not show expected results. Rather, no difference between the treatment and untreated group was observed. The levels of KC, IL-6 and degree of neutrophilia were almost similar in treatment group, positive control treated with human IL-17A and a control group of mice treated with normal saline alone. One would have liked to examine therapeutic efficacy of human IL-17F mutant in CIA mice, if the preliminary experiments in mouse airpouch model of inflammation were successful. It would therefore be highly desirable to examine *in vivo* therapeutic efficacy of human IL-17F mutant in RA synovium/SCID mice model.

CHAPTER VII

GENERAL DISCUSSION

RA was defined as a Th1 mediated disease until the discovery of Th17 cells. Both Th1 and Th17 cells have been recognised in RA and the research in this important field continues. A recent study by van Hamburg *et al.* showed that Th17 but not Th1 cells cooperated with RASF in a proinflammatory feedback loop underscoring the importance of Th17 cells (461). In treatment-naïve, early RA patients, serum and SF IL-17A levels were shown to correlate strongly with DAS28, ACPA, RF and histopathology score (462). Increased levels of IL-17 mRNA in synovium are predictive of more severe joint damage progression (303). Phase I/II clinical trials of humanised anti-IL-17 monoclonal antibodies in RA have demonstrated therapeutic efficacy without notable side effects (339, 341). Likewise, in phase II clinical trials of psoriasis, neutralisation of IL-17 by a humanised anti-IL-17 monoclonal antibody or human anti-IL-17 receptor antibody resulted in significant clinical improvement (463, 464). IL-17 in these studies was inhibited using either an anti-IL-17 or anti-IL-17R monoclonal antibody similar to using anti-TNF and other cytokine inhibiting therapies in RA (41, 465-468). These therapies, however, cause a non-targeted inhibition of cytokines that are also needed for other important immune functions. This approach results in a state of generalised immune suppression and consequently increases the risk of systemic infections. Such unwanted side-effects of a cytokine-based therapy can be avoided by modifying a cytokine as a latent cytokine (353). A non-covalent fusion of a cytokine with LAP of TGF- β via a MMP-sensitive linker allows targeting biological actions of a pleiotropic cytokine to the site of active inflammation, prolongs its half-life and enhances its overall therapeutic efficacy (353). The aim of this study was to develop a novel latent IL-17 antagonist for targeted therapy of RA and examine its preclinical therapeutic efficacy in CIA mice via plasmid- based systemic gene therapy.

Kawaguchi *et al.* (153) in their study of IL-17F polymorphism reported that (H161R) IL-17F mutant was an antagonist of IL-17F and protective against asthma in a Japanese population. The fact that IL-17F is structurally and functionally similar to IL-17A but biologically 30-100 times less potent, (143, 144, 469) suggested to us that the protective effect of IL-17F mutant in asthma was due to additional inhibition of IL-17A. We therefore hypothesised that (H161R) IL-17F mutant is also an inhibitor of IL-

17A. We further hypothesised that IL-17F mutant, if modified as LAP- IL-17F mutant would be superior to conventional IL-17 or IL-17R inhibiting therapies in RA.

Plasmid expression vectors encoding human full-length and LAP-IL-17F mutant were constructed and the proteins expressed *in vitro*. The results of *in vitro* biological assays showed that IL-17A induced secretion of IL-6 was inhibited by IL-17F mutant. The mutant lacked the ability to induce secretion of IL-6 in HFFF2, 3T3 and HeLa cells, and activate phosphorylation of ERK1/2 in HeLa cells. These biological effects were specific to the biological activity of IL-17F mutant as confirmed by demonstrating that IL-17F mutant was able to bind to IL-17 receptor and its ability to inhibit IL-17A was reversed in the presence of a neutralising anti-IL-17F antibody. Taken together, these findings confirmed the hypothesis that IL-17F mutant is an inhibitor of IL-17A (manuscript in preparation). The findings that IL-17F mutant was able to bind to IL-17RC but inhibited IL-17A induced secretion of IL-6 in fibroblast and epithelial cells suggest that IL-17F mutant is a receptor antagonist of IL-17A. Furthermore, as this novel inhibitor of IL-17A is a cytokine variant and not a monoclonal antibody or receptor fusion protein, it offers an opportunity for modifying it as LAP-IL-17F mutant for targeted therapy of RA.

The targeted activity of LAP-cytokines is dependent on MMPs, which releases its biological activity by cleaving the linker that binds the cytokine to LAP. The release of biological activity of expressed LAP-IL-17 proteins by MMP was confirmed *in vitro* by demonstrating that naïve LAP-cytokines induced significantly less secretion of IL-6 than their corresponding full-length proteins but when pre-incubated with MMP-1, resulted in a significant increase in the induced secretion of IL-6. Use of LAP-IL-17F mutant in the treatment of RA is expected to provide superior therapeutic efficacy than inhibition of IL-17 via monoclonal antibodies or receptor fusion proteins. Our group has previously demonstrated that biological activity of LAP-IFN- β could be released by pre-incubation with synovial fluid from RA or osteoarthritis patients. The half-life of LAP-IFN- β was 37 fold higher than naive IFN- β and it was effective in ameliorating established CIA in mice (353). The LAP cytokine approach since first used for IFN- β in our laboratory has been validated for a number of other cytokines and small

molecules including MSH- α and VIP (355). *In vivo* therapeutic effects of LAP-MSH were superior to free MSH in a peritonitis mouse model (355). Therapeutic efficacy of LAP-cytokines in the treatment of RA and similar autoimmune conditions, due to their targeted biological activity, prolonged half-life and significantly enhanced *in vitro* and *in vivo* expression (as shown in this study) is expected to be superior to conventional cytokine inhibiting therapies.

All the three mouse analogues of human IL-17F mutant, which were developed for the purpose of *in vivo* testing in CIA mice, exhibited unexpected immunological or biological activities. Mouse IL-17F mutant 1 did not inhibit but stimulated IL-6 secretion in fibroblast cells, *in vitro* expression of mouse IL-17F mutant 2 could not be detected in either transfected cells supernatant or lysate, and mouse IL-17F mutant 3 failed to bind to mouse IL-17RC. The crystal structure of human IL-17F bound to IL-17RA revealed that one of the major receptor bindings sites of IL-17F is located at its C-terminal end (179). It seems that the site-specific point and deletion mutations, which are located within this important receptor binding region of IL-17F were significant enough to alter the receptor binding affinities. A total lack of expression of mouse IL-17F mutant 2 *in vitro* points towards the possibility of severe compromise of its stability.

Thus, only the human IL-17F mutant construct could be assessed *in vivo*. RA synovium/SCID mice model allows a direct testing of therapeutics of human origin in SCID mice implanted with human RA synovium (410, 411). As a preliminary to investigating *in vivo* therapeutic efficacy of human IL-17F mutant in this model of RA, expression and pharmacokinetics of intravenous hydrodynamically delivered human full-length and LAP-IL-17A in naïve SCID were studied. *In vivo* expression of LAP-IL-17A in mice serum was 1400-fold higher than full-length IL-17A. Similarly, *in vivo* expression of LAP-IL-17F mutant in C57BL/6 mice serum was 2.2-fold higher than FL-IL-17F mutant and *in vitro* expression of LAP-IL-17 proteins was two-six-fold higher than their corresponding full-length IL-17 proteins. An enhanced expression of LAP-cytokines, as shown in this study, in conjunction with a significantly prolonged half-life (353) would help decreasing the dose and frequency of therapy.

The levels of transgene expression in SCID mice declined rapidly. The serum levels of both FL-and LAP-IL-17A were only 20% and 2% of the baseline at the end of first and second week respectively. The levels of the expressed transgene however still would have been adequate to evaluate therapeutic response after a week's treatment in RA/SCID mice. The rapid decline in transgene expression in mice seems to be related to generation of a proinflammatory TLR induced response to CpG dinucleotides in pcDNA3 plasmid DNA (456, 457). Transgene expression could also be reduced by the CpG methylation of the promoter region in the plasmid expression vector (470).

In vivo expression of intravenous hydrodynamically delivered human IL-17F mutant transgene at the site of inflammation was examined in C57BL/6 mouse airpouch inflammation. The local expression of human full-length and LAP-IL-17F mutant transgenes was negligible in comparison to their systemic levels. Interestingly, expression of IL-17F mutant in C57BL/6 mouse serum and airpouch lavage exudate was 1000-fold higher than IL-17A. Also, concentrations of expressed transgene following co-administration of IL-17A plus IL-17F mutant were 7700-fold higher in mouse serum and at least 134-fold higher in airpouch lavage exudate on detection with anti-IL-17F antibody than anti-IL-17A antibody. Although this difference may be related to a superior detection of IL-17A/IL-17F mutant heterodimer by anti-IL-17F than anti-IL-17A detection antibody, it is more likely to be related to a better stability of IL-17F mutant than IL-17A. It is also possible that co-administration of IL-17A plus IL-17F mutant resulted in a preferred expression of IL-17F mutant homodimers. Wright *et al.* (143) have previously shown that activated human CD4⁺ T cells secreted minimal IL-17A but 10-fold or greater IL-17F. Similarly, Liang *et al.* (144) have demonstrated a higher expression of IL-17F than IL-17A in naïve mouse CD4⁺T cells.

After demonstrating successful *in vivo* transgene expression of human IL-17 in mice following systemic gene therapy, an experiment to investigate *in vivo* therapeutic efficacy of human IL-17F mutant in RA synovium/SCID mice was planned but could not be conducted due to difficulty in obtaining suitable RA synovium samples. The readouts for *in vivo* therapeutic efficacy of IL-17F mutant included histopathology of implanted synovium for the severity of inflammation, mRNA

levels of KC, IL-6, IL-8, IL-1 β and TNF- α in the synovial tissue and proteins levels of KC, IL-6, IL-8, IL-1 β and TNF- α in mouse serum, which would have been compared between FL-IL-17F mutant, LAP-IL-17F mutant, FL-IL-17A treated group (as a positive control) and untreated group.

A novel IL-6 promoter responsive reporter system was developed and standardised to assess biological activity of mouse IL-17. DTF (DBA/1 mouse fibroblasts) cells were stably transfected with IL-6 promoter responsive luciferase. A combination of mouse IL-17A or IL-17F and 2ng/ml TNF- α but not IL-17A or IL-17F alone induced an activation of luciferase in these cells. It has been previously reported that IL-17 induces IL-6 secretion primarily by activating the transcription factor C/EBP- δ and β , having a minimal activity on NF- κ B but IL-17 in combination with even suboptimal concentrations of TNF- α , can induce a much greater secretion of IL-6 by synergistically activating C/EBP- δ and β (114). Unlike DTF cells, an IL-6 promoter responsive luciferase reporter system in HeLa and 293T cells did not demonstrate luciferase activation in response to human IL-17. Similarly, human and mouse IL-17 were unable to activate NF- κ B driven luciferase in 57A HeLa (420) and Raw 264.7 cells, previously transfected with NF- κ B driven luciferase. A lack of NF- κ B-linked luciferase activity in response to IL-17 in a number of mammalian cell lines has been previously reported (135).

In conclusion, this study for the first time demonstrates that human (H161R) IL-17F mutant is an inhibitor of IL-17A. It was also demonstrated that modification of a cytokine as LAP-cytokine enhances its *in vitro* and *in vivo* expression. A novel IL-6 promoter responsive luciferase reporter system to assess biological activity of mouse IL-17 was developed and standardised. Lastly, intravenous hydrodynamic gene therapy delivered via tail vein in mice resulted in detectable levels of transgene in mouse serum, thus confirming that this method of *in vivo* gene transfer is highly efficient.

CHAPTER VIII

FUTURE STUDIES

The aim of this study was to develop a novel latent IL-17 antagonist for targeted therapy of RA. The study has for the first time demonstrated that (H161R) IL-17F mutant, a natural inhibitor of human IL-17F is an additional inhibitor of IL-17A. The study has also confirmed that LAP-IL-17F mutant was biologically latent and that its biological activity can be released by the action of MMP. Taken together, the results of the study support the proposition that LAP-IL-17F mutant is likely to be an effective targeted therapy for RA. It will therefore be important to substantiate the findings of this study by examining biological effects of IL-17F mutant *ex vivo* in RA synovial explants and *in vivo* in a suitable preclinical model of RA. A direct *in vivo* testing of therapeutics of human origin is possible in SCID mice implanted with RA synovium (410, 411). The RA synovium/SCID therefore would be an ideal rodent model to study preclinical *in vivo* therapeutic efficacy of IL-17F mutant. As responsiveness to IL-17 targeted therapies in RA is dependent on rich infiltration of CD3+T cells in RA synovium (416), it will be important to pre-screen RA synovial samples before engrafting in mice. For a rapid preclinical testing, human IL-17F mutant can be delivered via intravenous hydrodynamic gene therapy. Therapeutic efficacy of the therapy can be assessed by analysing synovial inflammation, levels of IL-6 and IL-8 mRNA in engrafted synovium and IL-6 and IL-8 proteins in mice serum.

Although gene therapy is an easy and quick method to test preclinical *in vivo* therapeutic efficacy of investigational and new therapies, it has its own limitations. For example, some of the problems encountered in the study were varied levels of transgene expression despite administration of equal quantity of plasmid DNA, and a rapid decline in the levels of expressed transgenes. Moreover, gene therapy in humans is still in experimental stages. Therefore it will be desirable to also assess preclinical *in vivo* therapeutic efficacy of IL-17F mutant delivered via protein-based therapy.

IL-17F binds only weakly to IL-17RA. The binding affinity of human IL-17A to IL-17RA is 1000 stronger than that of IL-17F (181). This suggests that a heterodimer of IL-17A/IL-17F mutant would bind to IL-17RA more strongly than IL-17F mutant homodimer and therefore mediate a more potent inhibition of IL-17A than IL-17F mutant homodimer. A forced expression of IL-17A/IL-17F mutant heterodimer

can be achieved by fusing IL-17A to IL-17F mutant via a polyglycine linker (143). *In vitro* biological actions and *in vivo* therapeutic efficacy of expressed IL-17A/IL-17 F mutant then be analysed using the assays same as those used for IL-17F mutant homodimer.

Finally, if human IL-17F mutant homodimer and/or IL-17A/IL-17F heterodimer are proven to be effective in preclinical models of RA, the findings can be translated and integrated with clinical research.

APPENDIX

DNA sequence of human and mouse IL-17 constructs

Shown below are the open reading frames (ORF) of DNA sequences of human and mouse full-length and LAP-IL-17 constructs. One letter code translation is shown for each ORF where * indicates termination of the translation.

A1. Human FL-IL-17A

```

    <SdeAI  >Bbr7I
    <MlyI   >BbsI
    >BspD6I >AjuI
    <PleI   >CchII
    |       ||
    ATG ACT CCT GGG AAG ACC TCA TTG GTG TCA CTG CTA CTG CTG CTG AGC CTG GAG GCC ATA < 60
    M  T  P  G  K  T  S  L  V  S  L  L  L  L  L  S  L  E  A  I
    |       |       |       |       |
    10      20      30      40      50

                                Bsp509I
                                PfoI
                                ApoI
                                >DraRI <AquIV
    GTG AAG GCA GGA ATC ACA ATC CCA CGA AAT CCA GGA TGC CCA AAT TCT GAG GAC AAG AAC < 120
    V  K  A  G  I  T  I  P  R  N  P  G  C  P  N  S  E  D  K  N
    |       |       |       |       |       |       |       |
    70      80      90     100     110

                                >RdeGBIII
    NciI   <NlaCI
    EcoHI  HpyCH4III HincII
    |       |       |       |
    TTC CCC CGG ACT GTG ATG GTC AAC CTG AAC ATC CAT AAC CGG AAT ACC AAT ACC AAT CCC < 180
    F  P  R  T  V  M  V  N  L  N  I  H  N  R  N  T  N  T  N  P
    |       |       |       |       |
    130     140     150     160     170

                                >BsrDI
    Sse8647I
    |
    AAA AGG TCC TCA GAT TAC TAC AAC CGA TCC ACC TCA CCT TGG AAT CTC CAC CGC AAT GAG < 240
    K  R  S  S  D  Y  Y  N  R  S  T  S  P  W  N  L  H  R  N  E
    |       |       |       |       |       |       |       |
    190     200     210     220     230

                                StyI
                                MslI
    <SimI   EcoRV
    |       |
    GAC CCT GAG AGA TAT CCC TCT GTG ATC TGG GAG GCA AAG TGC CGC CAC TTG GGC TGC ATC < 300
    D  P  E  R  Y  P  S  V  I  W  E  A  K  C  R  H  L  G  C  I
    |       |       |       |       |
    250     260     270     280     290

                                <TstI
                                BglI
                                <BsaXI
                                TauI
                                <CchIII
    HpyCH4IV
    TaiI
    <PlaDI  >PsrI
    |       |       |
    AAC GCT GAT GGG AAC GTG GAC TAC CAC ATG AAC TCT GTC CCC ATC CAG CAA GAG ATC CTG < 360
    N  A  D  G  N  V  D  Y  H  M  N  S  V  P  I  Q  Q  E  I  L
    |       |       |       |       |
    310     320     330     340     350

    HhaI
    HinPII
    GlaI
    FspI
    |       |
    GTC CTG CGC AGG GAG CCT CCA CAC TGC CCC AAC TCC TTC CGG CTG GAG AAG ATA CTG GTG < 420
    V  L  R  R  E  P  P  H  C  P  N  S  F  R  L  E  K  I  L  V
    |       |       |       |       |
    370     380     390     400     410

    BtgI
    <TspGWI <BsgI
    ||       |

                                <CstMI
                                >BsrI
                                <BaeI
    |       |
    DraIII
    PflMI
    ||       |
  
```

TCC GTG GGC TGC ACC TGT GTC ACC CCG ATT GTC CAC CAT GTG GCC TAA < 468
 S V G C T C V T P I V H H V A *
 430 440 450 460

Signal peptide starts from nucleotide 1, mature peptide starts from nucleotide 136.

A2. Human LAP-IL-17A

HindIII

|
 AAG CTT ATG CCG CCC TCC GGG CTG CGG CTG CTG CCG CTG CTG CTA CCG CTG CTG TGG CTA < 60
 K L M P P S G L R L L P L L L P L L W L
 10 20 30 40 50

KroI
 NaeI
 >BspMI
 >AarI <BcgI >ApyPI
 BsaHI
 NgoMIV

CTG GTG CTG ACG CCT GGC CCG CCG GCC GCG GGA CTA TCC ACC tgc AAG ACT ATC GAC ATG < 120
 L V L T P G P P A A G L S T C K T I D M
 70 80 90 100 110

>CdiI
 <Bsp24I

GAG CTG GTG AAG CGG AAG CGC ATC GAG GCC ATC CGC GGC CAG ATC CTG TCC AAG CTG CGG < 180
 E L V K R K R I E A I R G Q I L S K L R
 130 140 150 160 170

CTC GCC AGC CCC CCG AGC CAG GGG GAG GTG CCG CCC GGC CCG CTG CCC GAG GCC GTG CTC < 240
 L A S P P S Q G E V P P G P L P E A V L
 190 200 210 220 230

BsrGI

GCC CTG TAC AAC AGC ACC CGC GAC CGG GTG GCC GGG GAG AGT GCA GAA CCG GAG CCC GAG < 300
 A L Y N S T R D R V A G E S A E P E P E
 250 260 270 280 290

Bsu36I
 AleI
 >RleAI

CCT GAG GCC GAC TAC TAC GCC AAG GAG GTC ACC CGC GTG CTA ATG GTG GAA ACC CAC AAC < 360
 P E A D Y Y A K E V T R V L M V E T H N
 310 320 330 340 350

>Tth111II

GAA ATC TAT GAC AAG TTC AAG CAG AGT ACA CAC AGC ATA TAT ATG TTC TTC AAC ACA TCA < 420
 E I Y D K F K Q S T H S I Y M F F N T S
 370 380 390 400 410

>UcoMSI
 SacI
 Eco53kI
 KpnI
 Acc65I
 SmaI
 XmaI

GAG CTC CGA GAA GCG GTA CCT GAA CCC GTG TTG CTC TCC CGG GCA GAG CTG CGT CTG CTG < 480
 E L R E A V P E P V L L S R A E L R L L
 430 440 450 460 470

<BpuEI
 SmlI
 MseI
 PmlI
 BsaAI

AGG CTC AAG TTA AAA GTG GAG CAG CAC GTG GAG CTG TAC CAG AAA TAC AGC AAC AAT TCC < 540
 R L K L K V E Q H V E L Y Q K Y S N N S
 490 500 510 520 530

>AlfI

>RdeGBII

TGG CGA TAC CTC AGC AAC CGG CTG CTG GCA CCC AGC GAC TCG CCA GAG TGG TTA TCT TTT < 600
 W R Y L S N R L L A P S D S P E W L S F
 550 560 570 580 590

<AquII

GAT GTC ACC GGA GTT GTG CGG CAG TGG TTG AGC CGT GGA GGG GAA ATT GAG GGC TTT CGC < 660
 D V T G V V R Q W L S R G G E I E G F R
 610 620 630 640 650

HaeII

LpnI

CTT AGC GCC CAC TGC TCC TGT GAC AGC AGG GAT AAC ACA CTG CAA GTG GAC ATC AAC GGG < 720
 L S A H C S C D S R D N T L Q V D I N G
 670 680 690 700 710

>NmeAIII

TTC ACT ACC GGC CGC CGA GGT GAC CTG GCC ACC ATT CAT GGC ATG AAC CGG CCT TTC CTG < 780
 F T T G R R G D L A T I H G M N R P F L
 730 740 750 760 770

ApaI

PspOMI

BstXI

BaeGI

EcoRI

>EciI

CTT CTC ATG GCC ACC CCG CTG GAG AGG GCC CAG CAT CTG CAA AGC GAA TTC GGG GGA GGC < 840
 L L M A T P L E R A Q H L Q S E F G G G
 790 800 810 820 830

>AjuI

>Bbr7I

>BbsI

>CchII

BamHI

>BsrBI

<PspOMII

NotI

GGA TCC CCG CTC GGG CTT TGG GCG GGA GGG GGC TCA GCG GCC GCA ATG ACT CCT GGG AAG < 900
 G S P L G L W A G G G S A A A M T P G K
 850 860 870 880 890

<SdeOSI

<NgoAVIII

ACC TCA TTG GTG TCA CTG CTA CTG CTG CTG AGC CTG GAG GCC ATA GTG AAG GCA GGA ATC < 960
 T S L V S L L L L S L E A I V K A G I
 910 920 930 940 950

<NlaCI

PfoI

>DraRI

<AquIV

HpyCH4III

ACA ATC CCA CGA AAT CCA GGA TGC CCA AAT TCT GAG GAC AAG AAC TTC CCC CGG ACT GTG <
 1020
 T I P R N P G C P N S E D K N F P R T V
 970 980 990 1000 1010

HincII

Sse8647I

ATG GTC AAC CTG AAC ATC CAT AAC CGG AAT ACC AAT ACC AAT CCC AAA AGG TCC TCA GAT <
 1080
 M V N L N I H N R N T N T N P K R S S D
 1030 1040 1050 1060 1070

<SimI

EcoRV

TAC TAC AAC CGA TCC ACC TCA CCT TGG AAT CTC CAC CGC AAT GAG GAC CCT GAG AGA TAT <
 1140
 Y Y N R S T S P W N L H R N E D P E R Y
 1090 1100 1110 1120 1130

<BsaXI

<TstI

<CchIII

>PsrI

```

CCC TCT GTG ATC TGG GAG GCA AAG TGC CGC CAC TTG GGC TGC ATC AAC GCT GAT GGG AAC <
1200
P S V I W E A K C R H L G C I N A D G N
      1150      1160      1170      1180      1190

                                FspI
                                |
GTG GAC TAC CAC ATG AAC TCT GTC CCC ATC CAG CAA GAG ATC CTG GTC CTG CGC AGG GAG <
1260
V D Y H M N S V P I Q Q E I L V L R R E
      1210      1220      1230      1240      1250

                                <BaeI
                                |
                                <TspGWI
                                |
CCT CCA CAC TGC CCC AAC TCC TTC CGG CTG GAG AAG ATA CTG GTG TCC GTG GGC TGC ACC <
1320
P P H C P N S F R L E K I L V S V G C T
      1270      1280      1290      1300      1310

                                DraIII
                                PflMI
                                | |
TGT GTC ACC CCG ATT GTC CAC CAT GTG GCC TAA < 1353
C V T P I V H H V A *
      1330      1340      1350

```

Signal peptide of LAP from nucleotide 7, mature peptide of IL-17A from nucleotide 886.

A3. Human FL-IL-17F

```

                                NcoI
                                >GsaI BtgI ScaI
                                >BseYI >RdeGBIII <ApyPI
                                | | | | |
ATG ACA GTG AAG ACC CTG CAT GGC CCA GCC ATG GTC AAG TAC TTG CTG CTG TCG ATA TTG < 60
M T V K T L H G P A M V K Y L L L S I L
      10      20      30      40      50

                                >AceIII
                                |
GGG CTT GCC TTT CTG AGT GAG GCG GCA GCT CGG AAA ATC CCC AAA GTA GGA CAT ACT TTT < 120
G L A F L S E A A A R K I P K V G H T F
      70      80      90      100      110

                                EcoNI
                                >Sth132I
                                >FauI >SdeAI HindIII
                                | | | | |
TTC CAA AAG CCT GAG AGT TGC CCG CCT GTG CCA GGA GGT AGT ATG AAG CTT GAC ATT GGC < 180
F Q K P E S C P P V P G G S M K L D I G
      130      140      150      160      170

                                SelI
                                BstUI
                                HhaI HpyCH4IV
                                HinP1I TaiI
                                GlaI BsaAI >CdiI >BplI >BsrBI
                                | | | | |
ATC ATC AAT GAA AAC CAG CGC GTT TCC ATG TCA CGT AAC ATC GAG AGC CGC TCC ACC TCC < 240
I I N E N Q R V S M S R N I E S R S T S
      190      200      210      220      230

                                VpaK11AI
                                AvaII
                                Psp03I Acc65I

```


GCC CTG TAC AAC AGC ACC CGC GAC CGG GTG GCC GGG GAG AGT GCA GAA CCG GAG CCC GAG < 300
 A L Y N S T R D R V A G E S A E P E P E
 250 260 270 280 290

Bsu36I >**CstMI** **AleI** >**RleAI**
 | | | |
 CCT GAG GCC GAC TAC TAC GCC AAG GAG GTC ACC CGC GTG CTA ATG GTG GAA ACC CAC AAC < 360
 P E A D Y Y A K E V T R V L M V E T H N
 310 320 330 340 350

>**Tth111II** >**PlaDI**
 | |
 GAA ATC TAT GAC AAG TTC AAG CAG AGT ACA CAC AGC ATA TAT ATG TTC TTC AAC ACA TCA < 420
 E I Y D K F K Q S T H S I Y M F F N T S
 370 380 390 400 410

>**UcoMSI**
Eco53kI **XmaI**
SacI **SmaI**
 | |
 GAG CTC CGA GAA GCG GTA CCT GAA CCC GTG TTG CTC TCC CGG GCA GAG CTG CGT CTG CTG < 480
 E L R E A V P E P V L L S R A E L R L L
 430 440 450 460 470

MseI **PmlI**
 | |
 AGG CTC AAG TTA AAA GTG GAG CAG CAC GTG GAG CTG TAC CAG AAA TAC AGC AAC AAT TCC < 540
 R L K L K V E Q H V E L Y Q K Y S N N S
 490 500 510 520 530

>**AlfI** >**RdeGBII** <**MlyI**
 <**HinfI** <**PleI**
 | | | |
 TGG CGA TAC CTC AGC AAC CGG CTG CTG GCA CCC AGC GAC TCG CCA GAG TGG TTA TCT TTT < 600
 W R Y L S N R L L A P S D S P E W L S F
 550 560 570 580 590

GAT GTC ACC GGA GTT GTG CGG CAG TGG TTG AGC CGT GGA GGG GAA ATT GAG GGC TTT CGC < 660
 D V T G V V R Q W L S R G G E I E G F R
 610 620 630 640 650

LpnI
HaeII
 |
 CTT AGC GCC CAC TGC TCC TGT GAC AGC AGG GAT AAC ACA CTG CAA GTG GAC ATC AAC GGG < 720
 L S A H C S C D S R D N T L Q V D I N G
 670 680 690 700 710

>**NmeAIII**
 |
 TTC ACT ACC GGC CGC CGA GGT GAC CTG GCC ACC ATT CAT GGC ATG AAC CGG CCT TTC CTG < 780
 F T T G R R G D L A T I H G M N R P F L
 730 740 750 760 770

PspOMI
ApaI
BaeGI
 >**BpmI** >**Eco57MI** >**EciI**
 | | | |
 CTT CTC ATG GCC ACC CCG CTG GAG AGG GCC CAG CAT CTG CAA AGC GAA TTC GGG GGA GGC < 840
 L L M A T P L E R A Q H L Q S E F G G G
 790 800 810 820 830

BamHI <**PspOMII** **BlpI** **NotI** >**TstI**
 | | | |
 GGA TCC CCG CTC GGG CTT TGG GCG GGA GGG GGC TCA GCG GCC GCA CGG AAA ATC CCC AAA < 900

G S P L G L W A G G G S A A A R K I P K
 850 860 870 880 890

EcoNI

|
 GTA GGA CAT ACT TTT TTC CAA AAG CCT GAG AGT TGC CCG CCT GTG CCA GGA GGT AGT ATG < 960
 V G H T F F Q K P E S C P P V P G G S M
 910 920 930 940 950

>BplI

|
 AAG CTT GAC ATT GGC ATC ATC AAT GAA AAC CAG CGC GTT TCC ATG TCA CGT AAC ATC GAG <
 1020
 K L D I G I I N E N Q R V S M S R N I E
 970 980 990 1000 1010

AvaII
Psp03I
VpaK11AI
KflI
PpuMI **AgeI**

|| |
 AGC CGC TCC ACC TCC CCC TGG AAT TAC ACT GTC ACT TGG GAC CCC AAC CGG TAC CCC TCG <
 1080
 S R S T S P W N Y T V T W D P N R Y P S
 1030 1040 1050 1060 1070

<BmrI **>BbsI**
>Bbr7I

| |
 GAA GTT GTA CAG GCC CAG TGT AGG AAC TTG GGC TGC ATC AAT GCT CAA GGA AAG GAA GAC <
 1140
 E V V Q A Q C R N L G C I N A Q G K E D
 1090 1100 1110 1120 1130

PshAI
<BsmAI **>AquIV**
<BsaI **BspEI**

| | |
 ATC TCC ATG AAT TCC GTT CCC ATC CAG CAA GAG ACC CTG GTC GTC CGG AGG AAG CAC CAA <
 1200
 I S M N S V P I Q Q E T L V V R R K H Q
 1150 1160 1170 1180 1190

<MmeI **<HpyAV** **<NgoAVIII**
>RpaI **<SdeOSI**

| | |
 GGC TGC TCT GTT TCT TTC CAG TTG GAG AAG GTG CTG GTG ACT GTT GGC TGC ACC TGC GTC <
 1260
 G C S V S F Q L E K V L V T V G C T C V
 1210 1220 1230 1240 1250

DraIII

|
 ACC CCT GTC ATC CAC CAT GTG CAG TAA < 1287
 T P V I H H V Q *
 1270 1280

Signal peptide of LAP from nucleotide 7, mature peptide of IL-17F from nucleotide 886.

A5. Human FL-IL-17F mutant

```

                                NcoI
                                >GsaI  BtgI      ScaI
                                >BseYI  >RdeGBIII
                                |          |          |
ATG ACA GTG AAG ACC CTG CAT GGC CCA GCC ATG GTC AAG TAC TTG CTG CTG TCG ATA TTG < 60
M  T  V  K  T  L  H  G  P  A  M  V  K  Y  L  L  L  S  I  L
                                |          |          |
                                10          20          30          40          50

                                >AceIII
                                |
GGG CTT GCC TTT CTG AGT GAG GCG GCA GCT CGG AAA ATC CCC AAA GTA GGA CAT ACT TTT < 120
G  L  A  F  L  S  E  A  A  A  R  K  I  P  K  V  G  H  T  F
                                |          |          |          |
                                70          80          90          100          110

                                EcoNI
                                >FauI
                                >Sth132I  >SdeAI      HindIII
                                |          |          |
TTC CAA AAG CCT GAG AGT TGC CCG CCT GTG CCA GGA GGT AGT ATG AAG CTT GAC ATT GGC < 180
F  Q  K  P  E  S  C  P  P  V  P  G  G  S  M  K  L  D  I  G
                                |          |          |          |
                                130          140          150          160          170

                                Sell
                                BstUI
                                GlaI
                                HhaI
                                HinPII
                                |          |          |          |
ATC ATC AAT GAA AAC CAG CGC GTT TCC ATG TCA CGT AAC ATC GAG AGC CGC TCC ACC TCC < 240
I  I  N  E  N  Q  R  V  S  M  S  R  N  I  E  S  R  S  T  S
                                |          |          |          |
                                190          200          210          220          230

                                AvaII
                                Psp03I
                                VpaK11AI
                                >BsmFI
                                PssI
                                KflI
                                EcoO109I
                                PpuMI
                                |          |          |          |
                                250          260          270          280          290

                                BanI
                                KpnI
                                Acc65I
                                AgeI
                                >NmeDI
                                BsrFI
                                |          |          |          |
                                300          310          320          330          340

                                BsrGI
                                <BmrI
                                |          |
                                350          360

                                <BpuEI
                                SmlI
                                |          |
                                370          380

                                MslI
                                |          |
                                390          400

                                EcoRI
                                ApoI
                                <TspGWI
                                |          |
                                410          420

                                PshAI
                                <BsaI
                                <BsmAI
                                >BccI
                                |          |          |          |
GTT CCC ATC CAG CAA GAG ACC CTG GTC GTC CGG AGG AAG CAC CAA GGC TGC TCT GTT TCT < 420
V  P  I  Q  Q  E  T  L  V  V  R  R  K  H  Q  G  C  S  V  S
                                |          |          |          |
                                370          380          390          400          410

                                <MmeI
                                >RpaI
                                |          |
                                430          440

                                <HpyAV
                                |
                                450

                                >AarI
                                MwoI
                                |          |
                                460          470

                                <HgaI
                                >BspMI
                                <SdeOSI
                                |          |          |
                                480          490          500

                                DraIII
                                |
                                510

```

CGT GTG CAG TAA < 492
 R V Q *
 490

Signal peptide from nucleotide 1, mature peptide from nucleotide 91.

A6. Human LAP-IL-17F mutant

BglI

AAG CTT ATG CCG CCC TCC GGG CTG CGG CTG CTG CCG CTG CTG CTA CCG CTG CTG TGG CTA < 60
 K L M P P S G L R L L P L L L P L L W L
 10 20 30 40 50

NaeI
NgoMIV
BsaHI | **KroI** | **<BcgI** | **>ApyPI**
 CTG GTG CTG ACG CCT GGC CCG CCG GCC GCG GGA CTA TCC ACC tgc AAG ACT ATC GAC ATG < 120
 L V L T P G P P A A G L S T C K T I D M
 70 80 90 100 110

<Bsp24I
 GAG CTG GTG AAG CGG AAG CGC ATC GAG GCC ATC CGC GGC CAG ATC CTG TCC AAG CTG CGG < 180
 E L V K R K R I E A I R G Q I L S K L R
 130 140 150 160 170

CTC GCC AGC CCC CCG AGC CAG GGG GAG GTG CCG CCC GGC CCG CTG CCC GAG GCC GTG CTC < 240
 L A S P P S Q G E V P P G P L P E A V L
 190 200 210 220 230

GCC CTG TAC AAC AGC ACC CGC GAC CGG GTG GCC GGG GAG AGT GCA GAA CCG GAG CCC GAG < 300
 A L Y N S T R D R V A G E S A E P E P E
 250 260 270 280 290

Bsu36I | **>CstMI** | **AleI** | **>RleAI**
 CCT GAG GCC GAC TAC TAC GCC AAG GAG GTC ACC CGC GTG CTA ATG GTG GAA ACC CAC AAC < 360
 P E A D Y Y A K E V T R V L M V E T H N
 310 320 330 340 350

>Tth111II | **>PlaDI**
 GAA ATC TAT GAC AAG TTC AAG CAG AGT ACA CAC AGC ATA TAT ATG TTC TTC AAC ACA TCA < 420
 E I Y D K F K Q S T H S I Y M F F N T S
 370 380 390 400 410

SacI
Eco53kI
>UcoMSI | **SmaI**
XmaI
 GAG CTC CGA GAA GCG GTA CCT GAA CCC GTG TTG CTC TCC CGG GCA GAG CTG CGT CTG CTG < 480
 E L R E A V P E P V L L S R A E L R L L
 430 440 450 460 470

MseI | **PmlI**
 AGG CTC AAG TTA AAA GTG GAG CAG CAC GTG GAG CTG TAC CAG AAA TAC AGC AAC AAT TCC < 540
 R L K L K V E Q H V E L Y Q K Y S N N S
 490 500 510 520 530


```

E V V Q A Q C R N L G C I N A Q G K E D
1090 1100 1110 1120 1130

PshAI
<BsmAI >AquIV
<BsaI BspEI
| | | |
ATC TCC ATG AAT TCC GTT CCC ATC CAG CAA GAG ACC CTG GTC GTC CGG AGG AAG CAC CAA <
1200
I S M N S V P I Q Q E T L V V R R K H Q
1150 1160 1170 1180 1190

>RpaI <NgoAVIII
<MmeI <HpyAV <SdeOSI
| | | |
GGC TGC TCT GTT TCT TTC CAG TTG GAG AAG GTG CTG GTG ACT GTT GGC TGC ACC TGC GTC <
1260
G C S V S F Q L E K V L V T V G C T C V
1210 1220 1230 1240 1250

DraIII
|
ACC CCT GTC ATC CAC CGT GTG CAG TAA < 1287
T P V I H R V Q *
1270 1280

```

Signal peptide of LAP from nucleotide 7, mature peptide of IL-17F mutant from nucleotide 886.

A7. Mouse FL-IL-17A

```

<SdeOSI >BsmAI
| |
ATG AGT CCA GGG AGA GCT TCA TCT GTG TCT CTG ATG CTG TTG CTG CTG CTG AGC CTG GCG < 60
M S P G R A S S V S L M L L L L L S L A
10 20 30 40 50

SfcI >Hin4I >Tth111III >DraRI
| | | |
GCT ACA GTG AAG GCA GCA GCG ATC ATC CCT CAA AGC TCA GCG TGT CCA AAC ACT GAG GCC < 120
A T V K A A A I I P Q S S A C P N T E A
70 80 90 100 110

<CchII HincII MseI
<AquIV Hpy166II
| | | |
AAG GAC TTC CTC CAG AAT GTG AAG GTC AAC CTC AAA GTC TTT AAC TCC CTT GGC GCA AAA < 180
K D F L Q N V K V N L K V F N S L G A K
130 140 150 160 170

SacI <HphI
Eco53kI <SspD5I
BanII >SdeAI MaeIII
>UcoMSI Tsp45I
Bsp1286I PssI HpyCH4IV
BsiHKAI EcoO109I TaiI
| | | |
GTG AGC TCC AGA AGG CCC TCA GAC TAC CTC AAC CGT TCC ACG TCA CCC TGG ACT CTC CAC < 240
V S S R R P S D Y L N R S T S P W T L H
190 200 210 220 230

>BbsI >Bbr7I EcoRV >AfeI
>BsrDI BsaBI <TstI LpnI
| | | | HaeII
| | | |

```

CGC AAT GAA GAC CCT GAT AGA TAT CCC TCT GTG ATC TGG GAA GCT CAG TGC CGC CAC CAG < 300
 R N E D P D R Y P S V I W E A Q C R H Q
 250 260 270 280 290

ApoI
NlaIII
FaiI
FatI Tsp509I
CviAII

<MaqI >CdpI >CjePI EcoRI
 | | | |
 CGC TGT GTC AAT GCG GAG GGA AAG CTG GAC CAC CAC ATG AAT TCT GTT CTC ATC CAG CAA < 360
 R C V N A E G K L D H H M N S V L I Q Q
 310 320 330 340 350

<EarI
 <AlwI >AclI
 BstYI BslI NlaIV <AceIII
 || | | | |
 GAG ATC CTG GTC CTG AAG AGG GAG CCT GAG AGC TGC CCC TTC ACT TTC AGG GTC GAG AAG < 420
 E I L V L K R E P E S C P F T F R V E K
 370 380 390 400 410

>BspMI
 >AarI
 AleI
 HpyCH4V
 <RleAI <BsgI <EciI
 | | | | |
 ATG CTG GTG GGT GTG GGC TGC ACC TGC GTG GCC TCG ATT GTC CGC CAG GCA GCC TAA < 477
 M L V G V G C T C V A S I V R Q A A *
 430 440 450 460 470

Signal peptide from nucleotide 1, mature peptide from nucleotide 76.

A8. Mouse LAP-IL-17A

HindIII BglI >BsrI
 | | |
 AAG CTT ATG CCG CCC TCC GGG CTG CGG CTG CTG CCG CTG CTG CTA CCG CTG CTG TGG CTA < 60
 K L M P P S G L R L L P L L L P L L W L
 10 20 30 40 50

KroI
 NgoMIV
 BsaHI NaeI >BsmFI <BcgI >ApyPI
 | | | | |
 CTG GTG CTG ACG CCT GGC CCG CCG GCC GCG GGA CTA TCC ACC tgc AAG ACT ATC GAC ATG < 120
 L V L T P G P P A A G L S T C K T I D M
 70 80 90 100 110

>CdiI >BccI <Bsp24I
 | | |
 GAG CTG GTG AAG CCG AAG CGC ATC GAG GCC ATC CGC GGC CAG ATC CTG TCC AAG CTG CGG < 180
 E L V K R K R I E A I R G Q I L S K L R
 130 140 150 160 170

CTC GCC AGC CCC CCG AGC CAG GGG GAG GTG CCG CCC GGC CCG CTG CCC GAG GCC GTG CTC < 240
 L A S P P S Q G E V P P G P L P E A V L
 190 200 210 220 230

BsrGI
 |

GCC CTG TAC AAC AGC ACC CGC GAC CGG GTG GCC GGG GAG AGT GCA GAA CCG GAG CCC GAG < 300
 A L Y N S T R D R V A G E S A E P E P E
 250 260 270 280 290

Bsu36I | | **>CstMI** |
 CCT GAG GCC GAC TAC TAC GCC AAG GAG GTC ACC CGC GTG CTA ATG GTG GAA ACC CAC AAC < 360
 P E A D Y Y A K E V T R V L M V E T H N
 310 320 330 340 350

| **>PlaDI** |
 GAA ATC TAT GAC AAG TTC AAG CAG AGT ACA CAC AGC ATA TAT ATG TTC TTC AAC ACA TCA < 420
 E I Y D K F K Q S T H S I Y M F F N T S
 370 380 390 400 410

KpnI | **SmaI**
Acc65I | **XmaI**
 GAG CTC CGA GAA GCG GTA CCT GAA CCC GTG TTG CTC TCC CGG GCA GAG CTG CGT CTG CTG < 480
 E L R E A V P E P V L L S R A E L R L L
 430 440 450 460 470

SmlI | **PmlI**
<BpuEI | **BsaAI**
 AGG CTC AAG TTA AAA GTG GAG CAG CAC GTG GAG CTG TAC CAG AAA TAC AGC AAC AAT TCC < 540
 R L K L K V E Q H V E L Y Q K Y S N N S
 490 500 510 520 530

>AlfI | **>RdeGBII** |
 TGG CGA TAC CTC AGC AAC CGG CTG CTG GCA CCC AGC GAC TCG CCA GAG TGG TTA TCT TTT < 600
 W R Y L S N R L L A P S D S P E W L S F
 550 560 570 580 590

<AquII |
 GAT GTC ACC GGA GTT GTG CGG CAG TGG TTG AGC CGT GGA GGG GAA ATT GAG GGC TTT CGC < 660
 D V T G V V R Q W L S R G G E I E G F R
 610 620 630 640 650

CTT AGC GCC CAC TGC TCC TGT GAC AGC AGG GAT AAC ACA CTG CAA GTG GAC ATC AAC GGG < 720
 L S A H C S C D S R D N T L Q V D I N G
 670 680 690 700 710

>NmeAIII |
 TTC ACT ACC GGC CGC CGA GGT GAC CTG GCC ACC ATT CAT GGC ATG AAC CGG CCT TTC CTG < 780
 F T T G R R G D L A T I H G M N R P F L
 730 740 750 760 770

BaeGI |
ApaI |
BstXI | **PspOMI** |
 CTT CTC ATG GCC ACC CCG CTG GAG AGG GCC CAG CAT CTG CAA AGC GAA TTC GGG GGA GGC < 840
 L L M A T P L E R A Q H L Q S E F G G G
 790 800 810 820 830

BamHI | **>BsrBI** | **<PspOMII** | **NotI** |
 GGA TCC CCG CTC GGG CTT TGG GCG GGA GGG GGC TCA GCG GCC GCA GCA GCG ATC ATC CCT < 900
 G S P L G L W A G G G S A A A A I I P
 850 860 870 880 890

| **<CchII** |
>DraRI | **<AquIV** | **HincII** |
 CAA AGC TCA GCG TGT CCA AAC ACT GAG GCC AAG GAC TTC CTC CAG AAT GTG AAG GTC AAC < 960

Q S S A C P N T E A K D F L Q N V K V N
 910 920 930 940 950

CTC AAA GTC TTT AAC TCC CTT GGC GCA AAA GTG AGC TCC AGA AGG CCC TCA GAC TAC CTC <
 1020

L K V F N S L G A K V S S R R P S D Y L
 970 980 990 1000 1010

>Bbr7I
 >BbsI
 EcoRV

HpyCH4III >BmgBI >BsrDI BsaBI

| | | | |

AAC CGT TCC ACG TCA CCC TGG ACT CTC CAC CGC AAT GAA GAC CCT GAT AGA TAT CCC TCT <
 1080

N R S T S P W T L H R N E D P D R Y P S
 1030 1040 1050 1060 1070

<TstI AfeI <MaqI >CdpI

| | | |

GTG ATC TGG GAA GCT CAG TGC CGC CAC CAG CGC TGT GTC AAT GCG GAG GGA AAG CTG GAC <
 1140

V I W E A Q C R H Q R C V N A E G K L D
 1090 1100 1110 1120 1130

<EarI
 >AclI

| |

CAC CAC ATG AAT TCT GTT CTC ATC CAG CAA GAG ATC CTG GTC CTG AAG AGG GAG CCT GAG <
 1200

H H M N S V L I Q Q E I L V L K R E P E
 1150 1160 1170 1180 1190

AGC TGC CCC TTC ACT TTC AGG GTC GAG AAG ATG CTG GTG GGT GTG GGC TGC ACC TGC GTG <
 1260

S C P F T F R V E K M L V G V G C T C V
 1210 1220 1230 1240 1250

GCC TCG ATT GTC CGC CAG GCA GCC TAA < 1287
 A S I V R Q A A *
 1270 1280

Signal peptide of LAP from nucleotide 7, mature peptide of IL-17A from nucleotide 886.

GCC TGA < 486
A *

Signal peptide from nucleotide 1, mature peptide from nucleotide 76.

A10. Mouse LAP-IL-17F

```
HindIII      BglI
|            |
AAG CTT ATG CCG CCC TCC GGG CTG CGG CTG CTG CCG CTG CTG CTA CCG CTG CTG TGG CTA < 60
K  L  M  P  P  S  G  L  R  L  L  P  L  L  L  P  L  L  W  L
                    10          20          30          40          50

                    KroI
                    NgoMIV
                    NaeI
                    >BspMI
                    >AarI <BcgI >ApyPI
BsaHI
|            |            |            |            |
CTG GTG CTG ACG CCT GGC CCG CCG GCC GCG GGA CTA TCC ACC tgc AAG ACT ATC GAC ATG < 120
L  V  L  T  P  G  P  P  A  A  G  L  S  T  C  K  T  I  D  M
                    70          80          90          100         110

                    <StsI
                    <FokI
                    <BtsCI
                    >CdiI >BccI <Bsp24I
|            ||           |
GAG CTG GTG AAG CGG AAG CGC ATC GAG GCC ATC CGC GGC CAG ATC CTG TCC AAG CTG CGG < 180
E  L  V  K  R  K  R  I  E  A  I  R  G  Q  I  L  S  K  L  R
                    130         140         150         160         170

CTC GCC AGC CCC CCG AGC CAG GGG GAG GTG CCG CCC GGC CCG CTG CCC GAG GCC GTG CTC < 240
L  A  S  P  P  S  Q  G  E  V  P  P  G  P  L  P  E  A  V  L
                    190         200         210         220         230

BsrGI
|
GCC CTG TAC AAC AGC ACC CGC GAC CGG GTG GCC GGG GAG AGT GCA GAA CCG GAG CCC GAG < 300
A  L  Y  N  S  T  R  D  R  V  A  G  E  S  A  E  P  E  P  E
                    250         260         270         280         290

Bsu36I      >CstMI      AleI      >RleAI
|            |            |            |
CCT GAG GCC GAC TAC TAC GCC AAG GAG GTC ACC CGC GTG CTA ATG GTG GAA ACC CAC AAC < 360
P  E  A  D  Y  Y  A  K  E  V  T  R  V  L  M  V  E  T  H  N
                    310         320         330         340         350

                    >Tth111II      >PlaDI
|            |
GAA ATC TAT GAC AAG TTC AAG CAG AGT ACA CAC AGC ATA TAT ATG TTC TTC AAC ACA TCA < 420
E  I  Y  D  K  F  K  Q  S  T  H  S  I  Y  M  F  F  N  T  S
                    370         380         390         400         410

SacI
Eco53kI      Acc65I      SmaI
>UcoMSI      KpnI      XmaI
|            |            |
GAG CTC CGA GAA GCG GTA CCT GAA CCC GTG TTG CTC TCC CGG GCA GAG CTG CGT CTG CTG < 480
E  L  R  E  A  V  P  E  P  V  L  L  S  R  A  E  L  R  L  L
                    430         440         450         460         470

<BpuEI      MseI
|            |
AGG CTC AAG TTA AAA GTG GAG CAG CAC GTG GAG CTG TAC CAG AAA TAC AGC AAC AAT TCC < 540
R  L  K  L  K  V  E  Q  H  V  E  L  Y  Q  K  Y  S  N  N  S
                    490         500         510         520         530
```

```

                                     <MlyI
                                     >BspD6I
                                     <PleI
                                     |
          >AlfI                         >RdeGBII
          |                               |
TGG CGA TAC CTC AGC AAC CGG CTG CTG GCA CCC AGC GAC TCG CCA GAG TGG TTA TCT TTT < 600
W  R  Y  L  S  N  R  L  L  A  P  S  D  S  P  E  W  L  S  F
          550                   560                   570                   580                   590

GAT GTC ACC GGA GTT GTG CGG CAG TGG TTG AGC CGT GGA GGG GAA ATT GAG GGC TTT CGC < 660
D  V  T  G  V  V  R  Q  W  L  S  R  G  G  E  I  E  G  F  R
          610                   620                   630                   640                   650

HaeII
LpnI
|
CTT AGC GCC CAC TGC TCC TGT GAC AGC AGG GAT AAC ACA CTG CAA GTG GAC ATC AAC GGG < 720
L  S  A  H  C  S  C  D  S  R  D  N  T  L  Q  V  D  I  N  G
          670                   680                   690                   700                   710

          >NmeAIII
          |
TTC ACT ACC GGC CGC CGA GGT GAC CTG GCC ACC ATT CAT GGC ATG AAC CGG CCT TTC CTG < 780
F  T  T  G  R  R  G  D  L  A  T  I  H  G  M  N  R  P  F  L
          730                   740                   750                   760                   770

                                     PspOMI
                                     ApaI
                                     BaeGI
                                     PssI
          BstXI                         EcoO109I                         >EciI
          |                               ||                               |
CTT CTC ATG GCC ACC CCG CTG GAG AGG GCC CAG CAT CTG CAA AGC GAA TTC GGG GGA GGC < 840
L  L  M  A  T  P  L  E  R  A  Q  H  L  Q  S  E  F  G  G  G
          790                   800                   810                   820                   830

BamHI                         <PspOMII                         BlpI      NotI
|                               |                               |           |
GGA TCC CCG CTC GGG CTT TGG GCG GGA GGG GGC TCA GCG GCC GCA CGG AAG AAC CCC AAA < 900
G  S  P  L  G  L  W  A  G  G  G  S  A  A  A  R  K  N  P  K
          850                   860                   870                   880                   890

GCA GGG GTT CCT GCC TTG CAG AAG GCT GGG AAC TGT CCT CCC CTG GAG GAT AAC ACT GTG < 960
A  G  V  P  A  L  Q  K  A  G  N  C  P  P  L  E  D  N  T  V
          910                   920                   930                   940                   950

          TfiI
          |
HincII      BstBI                         >TstI
          |       |                               |
AGA GTT GAC ATT CGA ATC TTC AAC CAA AAC CAG GGC ATT TCT GTC CCA CGT GAA TTC CAG <
1020
R  V  D  I  R  I  F  N  Q  N  Q  G  I  S  V  P  R  E  F  Q
          970                   980                   990                   1000                   1010

                                     <BsaI
                                     SciI
                                     XhoI
          NcoI                         >NlaCI       <BsmAI       AgeI
          |                               |           |           |
AAC CGC TCC AGT TCC CCA TGG GAT TAC AAC ATC ACT CGA GAC CCC CAC CGG TTC CCC TCA <
1080
N  R  S  S  S  P  W  D  Y  N  I  T  R  D  P  H  R  F  P  S
          1030                   1040                   1050                   1060                   1070

          <BmrI                         >BbsI
          |                               |
          >Bbr7I
          |

```

GAG ATC GCT GAG GCC CAG TGC AGA CAC TCA GGC TGC ATC AAT GCC CAG GGT CAG GAA GAC <
 1140
 E I A E A Q C R H S G C I N A Q G Q E D
 1090 1100 1110 1120 1130

Hpy99I **Psp03I**
VpaK11AI
AvaII

AGC ACC ATG AAC TCC GTC GCC ATT CAG CAA GAA ATC CTG GTC CTT CGG AGG GAG CCC CAG <
 1200
 S T M N S V A I Q Q E I L V L R R E P Q
 1150 1160 1170 1180 1190

>RpaI
<AcuI **<MmeI**

GGC TGT TCT AAT TCC TTC AGG TTG GAG AAG ATG CTC CTA AAA GTT GGC TGC ACC TGT GTC <
 1260
 G C S N S F R L E K M L L K V G C T C V
 1210 1220 1230 1240 1250

AAG CCC ATT GTC CAC CAA GCG GCC TGA < 1287
 K P I V H Q A A *
 1270 1280

Signal peptide of LAP from nucleotide 7, mature peptide of IL-17F from nucleotide 886.

A11. Mouse FL-IL-17F mutant 1(Q158R mutation)

ApaI
BaeGI **>Sth132I**
BsiHKAI **>RdeGBIII**

ATG AAG TGC ACC CGT GAA ACA GCC ATG GTC AAG TCT TTG CTA CTG TTG ATG TTG GGA CTT < 60
 M K C T R E T A M V K S L L L L M L G L
 10 20 30 40 50

AluI
>AceIII **>SdeAI**

GCC ATT CTG AGG GAG GTA GCA GCT CGG AAG AAC CCC AAA GCA GGG GTT CCT GCC TTG CAG < 120
 A I L R E V A A R K N P K A G V P A L Q
 70 80 90 100 110

<GsaI **HincII** **BstBI** **AgsI**
<BseYI **HinfI** **TfiI**

AAG GCT GGG AAC TGT CCT CCC CTG GAG GAT AAC ACT GTG AGA GTT GAC ATT CGA ATC TTC < 180
 K A G N C P P L E D N T V R V D I R I F
 130 140 150 160 170

HpyCH4IV
TaiI
BsaAI
>TstI **ApoI**
PmlI **EcoRI** **>BsrBI**

AAC CAA AAC CAG GGC ATT TCT GTC CCA CGT GAA TTC CAG AAC CGC TCC AGT TCC CCA TGG < 240
 N Q N Q G I S V P R E F Q N R S S S P W
 190 200 210 220 230

<BsmAI
Nli3877I **Sth302II**

BsrGI
|
GCC CTG TAC AAC AGC ACC CGC GAC CGG GTG GCC GGG GAG AGT GCA GAA CCG GAG CCC GAG < 300
A L Y N S T R D R V A G E S A E P E P E
250 260 270 280 290

Bsu36I >**CstMI** **AleI** >**RleAI**
| | | |
CCT GAG GCC GAC TAC TAC GCC AAG GAG GTC ACC CGC GTG CTA ATG GTG GAA ACC CAC AAC < 360
P E A D Y Y A K E V T R V L M V E T H N
310 320 330 340 350

>**Tth111II** >**PlaDI**
| |
GAA ATC TAT GAC AAG TTC AAG CAG AGT ACA CAC AGC ATA TAT ATG TTC TTC AAC ACA TCA < 420
E I Y D K F K Q S T H S I Y M F F N T S
370 380 390 400 410

SacI
Eco53kI **Acc65I** **SmaI**
>**UcoMSI** **KpnI** **XmaI**
| | |
GAG CTC CGA GAA GCG GTA CCT GAA CCC GTG TTG CTC TCC CGG GCA GAG CTG CGT CTG CTG < 480
E L R E A V P E P V L L S R A E L R L L
430 440 450 460 470

<**BpuEI** **MseI**
| |
AGG CTC AAG TTA AAA GTG GAG CAG CAC GTG GAG CTG TAC CAG AAA TAC AGC AAC AAT TCC < 540
R L K L K V E Q H V E L Y Q K Y S N N S
490 500 510 520 530

>**AlfI** >**RdeGBII** <**MlyI**
| | | >**BspD6I**
| | | <**PleI**
TGG CGA TAC CTC AGC AAC CGG CTG CTG GCA CCC AGC GAC TCG CCA GAG TGG TTA TCT TTT < 600
W R Y L S N R L L A P S D S P E W L S F
550 560 570 580 590

GAT GTC ACC GGA GTT GTG CGG CAG TGG TTG AGC CGT GGA GGG GAA ATT GAG GGC TTT CGC < 660
D V T G V V R Q W L S R G G E I E G F R
610 620 630 640 650

HaeII
LpnI
|
CTT AGC GCC CAC TGC TCC TGT GAC AGC AGG GAT AAC ACA CTG CAA GTG GAC ATC AAC GGG < 720
L S A H C S C D S R D N T L Q V D I N G
670 680 690 700 710

>**NmeAIII**
|
TTC ACT ACC GGC CGC CGA GGT GAC CTG GCC ACC ATT CAT GGC ATG AAC CGG CCT TTC CTG < 780
F T T G R R G D L A T I H G M N R P F L
730 740 750 760 770

PspOMI
ApaI
BaeGI
PssI
BstXI **EcoO109I** >**EciI**
| | | |
CTT CTC ATG GCC ACC CCG CTG GAG AGG GCC CAG CAT CTG CAA AGC GAA TTC GGG GGA GGC < 840
L L M A T P L E R A Q H L Q S E F G G G
790 800 810 820 830

BamHI <**PspOMII** **BlpI** **NotI**
| | | |


```

GGA TCC CCG CTC GGG CTT TGG GCG GGA GGG GGC TCA GCG GCC GCA CGG AAG AAC CCC AAA < 900
G  S  P  L  G  L  W  A  G  G  G  S  A  A  A  R  K  N  P  K
                850                860                870                880                890

GCA GGG GTT CCT GCC TTG CAG AAG GCT GGG AAC TGT CCT CCC CTG GAG GAT AAC ACT GTG < 960
A  G  V  P  A  L  Q  K  A  G  N  C  P  P  L  E  D  N  T  V
                910                920                930                940                950

                TfiI
      HincII  BstBI                                >TstI
      |      |      |                                |
AGA GTT GAC ATT CGA ATC TTC AAC CAA AAC CAG GGC ATT TCT GTC CCA CGT GAA TTC CAG <
1020
R  V  D  I  R  I  F  N  Q  N  Q  G  I  S  V  P  R  E  F  Q
                970                980                990                1000                1010

                <BsaI
                SciI
                XhoI
      NcoI                                >NlaCI  <BsmAI  AgeI
      |      |      |                                |      |      |      |
AAC CGC TCC AGT TCC CCA TGG GAT TAC AAC ATC ACT CGA GAC CCC CAC CGG TTC CCC TCA <
1080
N  R  S  S  S  P  W  D  Y  N  I  T  R  D  P  H  R  F  P  S
                1030                1040                1050                1060                1070

                <BmrI                                >BbsI
                |                                >Bbr7I
                |                                |
GAG ATC GCT GAG GCC CAG TGC AGA CAC TCA GGC TGC ATC AAT GCC CAG GGT CAG GAA GAC <
1140
E  I  A  E  A  Q  C  R  H  S  G  C  I  N  A  Q  G  Q  E  D
                1090                1100                1110                1120                1130

                Psp03I
                VpaK11AI
                AvaII
      Hpy99I                                |
      |      |      |                                |
AGC ACC ATG AAC TCC GTC GCC ATT CAG CAA GAA ATC CTG GTC CTT CGG AGG GAG CCC CAG <
1200
S  T  M  N  S  V  A  I  Q  Q  E  I  L  V  L  R  R  E  P  Q
                1150                1160                1170                1180                1190

                >RpaI
      <AcuI  <MmeI
      |      |
GGC TGT TCT AAT TCC TTC AGG TTG GAG AAG ATG CTC CTA AAA GTT GGC TGC ACC TGT GTC <
1260
G  C  S  N  S  F  R  L  E  K  M  L  L  K  V  G  C  T  C  V
                1210                1220                1230                1240                1250

AAG CCC ATT GTC CAC CAA GCG GCC TGA < 1287
K  P  I  V  H  Q  A  A  *
                1270                1280

```

Signal peptide of LAP from nucleotide 7, mature peptide of IL-17F mutant 1 from nucleotide 886.

A14. Mouse LAP-IL-17F mutant 2 (H157R mutation)

HindIII | **BglI**
 AAG CTT ATG CCG CCC TCC GGG CTG CGG CTG CTG CCG CTG CTG CTA CCG CTG CTG TGG CTA < 60
 K L M P P S G L R L L P L L L P L L W L
 10 20 30 40 50

BsaHI | **KroI** | **NaeI** | **NgoMIV** | **>BspMI** | **>AarI** | **<BcgI** | **>ApyPI**
 CTG GTG CTG ACG CCT GGC CCG CCG GCC GCG GGA CTA TCC ACC tgc AAG ACT ATC GAC ATG < 120
 L V L T P G P P A A G L S T C K T I D M
 70 80 90 100 110

<BtsCI | **<StsI** | **<FokI** | **>CdiI** | **>BccI** | **<Bsp24I**
 GAG CTG GTG AAG CGG AAG CGC ATC GAG GCC ATC CGC GGC CAG ATC CTG TCC AAG CTG CGG < 180
 E L V K R K R I E A I R G Q I L S K L R
 130 140 150 160 170

CTC GCC AGC CCC CCG AGC CAG GGG GAG GTG CCG CCC GGC CCG CTG CCC GAG GCC GTG CTC < 240
 L A S P P S Q G E V P P G P L P E A V L
 190 200 210 220 230

BsrGI
 GCC CTG TAC AAC AGC ACC CGC GAC CGG GTG GCC GGG GAG AGT GCA GAA CCG GAG CCC GAG < 300
 A L Y N S T R D R V A G E S A E P E P E
 250 260 270 280 290

Bsu36I | **>CstMI** | **AleI** | **>RleAI**
 CCT GAG GCC GAC TAC TAC GCC AAG GAG GTC ACC CGC GTG CTA ATG GTG GAA ACC CAC AAC < 360
 P E A D Y Y A K E V T R V L M V E T H N
 310 320 330 340 350

>Tth111II | **>PlaDI**
 GAA ATC TAT GAC AAG TTC AAG CAG AGT ACA CAC AGC ATA TAT ATG TTC TTC AAC ACA TCA < 420
 E I Y D K F K Q S T H S I Y M F F N T S
 370 380 390 400 410

Eco53kI | **>UcoMSI** | **Acc65I** | **SmaI**
SacI | **KpnI** | **XmaI**
 GAG CTC CGA GAA GCG GTA CCT GAA CCC GTG TTG CTC TCC CGG GCA GAG CTG CGT CTG CTG < 480
 E L R E A V P E P V L L S R A E L R L L
 430 440 450 460 470

<BpuEI | **MseI**
 AGG CTC AAG TTA AAA GTG GAG CAG CAC GTG GAG CTG TAC CAG AAA TAC AGC AAC AAT TCC < 540
 R L K L K V E Q H V E L Y Q K Y S N N S
 490 500 510 520 530

>AlfI | **>RdeGBII** | **<MlyI** | **>BspD6I** | **<PleI**
 TGG CGA TAC CTC AGC AAC CGG CTG CTG GCA CCC AGC GAC TCG CCA GAG TGG TTA TCT TTT < 600
 W R Y L S N R L L A P S D S P E W L S F
 550 560 570 580 590

GAT GTC ACC GGA GTT GTG CGG CAG TGG TTG AGC CGT GGA GGG GAA ATT GAG GGC TTT CGC < 660
 D V T G V V R Q W L S R G G E I E G F R
 610 620 630 640 650

HaeII

LpnI

CTT AGC GCC CAC TGC TCC TGT GAC AGC AGG GAT AAC ACA CTG CAA GTG GAC ATC AAC GGG < 720
 L S A H C S C D S R D N T L Q V D I N G
 670 680 690 700 710

>NmeAIII

TTC ACT ACC GGC CGC CGA GGT GAC CTG GCC ACC ATT CAT GGC ATG AAC CGG CCT TTC CTG < 780
 F T T G R R G D L A T I H G M N R P F L
 730 740 750 760 770

ApaI

PspOMI

BaeGI

PssI

BstXI

EcoO109I

CTT CTC ATG GCC ACC CCG CTG GAG AGG GCC CAG CAT CTG CAA AGC GAA TTC GGG GGA GGC < 840
 L L M A T P L E R A Q H L Q S E F G G G
 790 800 810 820 830

BamHI

<PspOMII

BlpI

NotI

GGA TCC CCG CTC GGG CTT TGG GCG GGA GGG GGC TCA GCG GCC GCA CGG AAG AAC CCC AAA < 900
 G S P L G L W A G G G S A A A R K N P K
 850 860 870 880 890

GCA GGG GTT CCT GCC TTG CAG AAG GCT GGG AAC TGT CCT CCC CTG GAG GAT AAC ACT GTG < 960
 A G V P A L Q K A G N C P P L E D N T V
 910 920 930 940 950

TfiI

HincII

BstBI

>TstI

AGA GTT GAC ATT CGA ATC TTC AAC CAA AAC CAG GGC ATT TCT GTC CCA CGT GAA TTC CAG <
 1020
 R V D I R I F N Q N Q G I S V P R E F Q
 970 980 990 1000 1010

<BsaI

XhoI

SciI

NcoI

>NlaCI

<BsmAI

AgeI

AAC CGC TCC AGT TCC CCA TGG GAT TAC AAC ATC ACT CGA GAC CCC CAC CGG TTC CCC TCA <
 1080
 N R S S S P W D Y N I T R D P H R F P S
 1030 1040 1050 1060 1070

>Bbr7I

>BbsI

<BmrI

GAG ATC GCT GAG GCC CAG TGC AGA CAC TCA GGC TGC ATC AAT GCC CAG GGT CAG GAA GAC <
 1140
 E I A E A Q C R H S G C I N A Q G Q E D
 1090 1100 1110 1120 1130

AvaII

Psp03I

VpaK11AI

Hpy99I

```

AGC ACC ATG AAC TCC GTC GCC ATT CAG CAA GAA ATC CTG GTC CTT CGG AGG GAG CCC CAG <
1200
S T M N S V A I Q Q E I L V L R R E P Q
      1150      1160      1170      1180      1190

          >RpaI
          <AcuI  <MmeI
          |      |
GGC TGT TCT AAT TCC TTC AGG TTG GAG AAG ATG CTC CTA AAA GTT GGC TGC ACC TGT GTC <
1260
G C S N S F R L E K M L L K V G C T C V
      1210      1220      1230      1240      1250

AAG CCC ATT GTC CGC CAA GCG GCC TGA < 1287
K P I V R Q A A *
      1270      1280

```

Signal peptide of LAP from nucleotide 7, mature peptide of IL-17F mutant 2 from nucleotide 886.

A15. Mouse FL-IL-17F mutant 3 (deletion of the last 4 amino acids)

```

          ApaLI
          BaeGI >Sth132I
          BsiHKAI
          |      |
ATG AAG TGC ACC CGT GAA ACA GCC ATG GTC AAG TCT TTG CTA CTG TTG ATG TTG GGA CTT < 60
M K C T R E T A M V K S L L L M L G L
      10      20      30      40      50

          AluI
          >AceIII
          ||
GCC ATT CTG AGG GAG GTA GCA GCT CGG AAG AAC CCC AAA GCA GGG GTT CCT GCC TTG CAG < 120
A I L R E V A A R K N P K A G V P A L Q
      70      80      90      100      110

          HinfI
          TfiI
          |      |      |
          <GsaI
          <BseYI
          |
AAG GCT GGG AAC TGT CCT CCC CTG GAG GAT AAC ACT GTG AGA GTT GAC ATT CGA ATC TTC < 180
K A G N C P P L E D N T V R V D I R I F
      130      140      150      160      170

          HpyCH4IV
          TaiI
          BsaAI
          PmlI ApoI
          >TstI EcoRI
          ||      |
AAC CAA AAC CAG GGC ATT TCT GTC CCA CGT GAA TTC CAG AAC CGC TCC AGT TCC CCA TGG < 240
N Q N Q G I S V P R E F Q N R S S S P W
      190      200      210      220      230

          <BsaI
          AvaI
          XhoI
          SciI
          Nli3877I
          HpaII
          Sth302II
          BsrFI
          AgeI
          MboI
          DpnI <BbvCI
          Asi256I AoxI

```



```

GCA GGG GTT CCT GCC TTG CAG AAG GCT GGG AAC TGT CCT CCC CTG GAG GAT AAC ACT GTG < 960
A  G  V  P  A  L  Q  K  A  G  N  C  P  P  L  E  D  N  T  V
          910          920          930          940          950

          TfiI
    HincII  BstBI                                >TstI
    |      |      |      |      |      |      |      |      |
AGA GTT GAC ATT CGA ATC TTC AAC CAA AAC CAG GGC ATT TCT GTC CCA CGT GAA TTC CAG <
1020
R  V  D  I  R  I  F  N  Q  N  Q  G  I  S  V  P  R  E  F  Q
          970          980          990          1000          1010

          <BsaI
          XhoI
          SciI
    NcoI          >NlaCI          <BsmAI          AgeI
    |      |      |      |      |      |      |      |
AAC CGC TCC AGT TCC CCA TGG GAT TAC AAC ATC ACT CGA GAC CCC CAC CGG TTC CCC TCA <
1080
N  R  S  S  S  P  W  D  Y  N  I  T  R  D  P  H  R  F  P  S
          1030          1040          1050          1060          1070

          <BmrI          >BbsI
          >Bbr7I
GAG ATC GCT GAG GCC CAG TGC AGA CAC TCA GGC TGC ATC AAT GCC CAG GGT CAG GAA GAC <
1140
E  I  A  E  A  Q  C  R  H  S  G  C  I  N  A  Q  G  Q  E  D
          1090          1100          1110          1120          1130

          AvaII
          VpaK11AI
          Psp03I
    Hpy99I
    |      |      |      |      |      |      |      |
AGC ACC ATG AAC TCC GTC GCC ATT CAG CAA GAA ATC CTG GTC CTT CGG AGG GAG CCC CAG <
1200
S  T  M  N  S  V  A  I  Q  Q  E  I  L  V  L  R  R  E  P  Q
          1150          1160          1170          1180          1190

          >RpaI
    <AcuI  <MmeI
    |      |
GGC TGT TCT AAT TCC TTC AGG TTG GAG AAG ATG CTC CTA AAA GTT GGC TGC ACC TGT GTC <
1260
G  C  S  N  S  F  R  L  E  K  M  L  L  K  V  G  C  T  C  V
          1210          1220          1230          1240          1250

AAG CCC ATT TGA < 1272
K  P  I  *
          1270

```

Signal peptide of LAP from nucleotide 7, mature peptide of IL-17F mutant 3 from nucleotide 886.

Scientific communications

Oral Presentations

Human (H161R) IL-17F mutant is a dual antagonist of IL-17A and IL-17F. Sixth Gene Therapy Meeting, May 2011, London, UK

Development of a latent IL-17 antagonist for targeted therapy of rheumatoid arthritis. North West London Rheumatology Club, June 2010, London, UK

Poster Presentations

G Mittal, R Mageed, Y Chernajovsky. Human (H161R) IL-17F mutant is a dual antagonist of IL-17A and IL-17F. British Society of Rheumatology AGM, April 2011, Brighton, UK.

G Mittal, R Mageed, Y Chernajovsky. Human (H161R) IL-17F mutant is a dual antagonist of IL-17A and IL-17F. William Harvey Research Day, St Bartholomew's Hospital, October 2010, London, UK.

Publications

L. Mullen, G. Adams, R. Fatah, D. Gould, A. Rigby, M. Sclanders, A. Koutsokeras, **G. Mittal**, S. Vessillier & Y. Chernajovsky. Development of latent cytokine fusion proteins in Fusion protein technologies for biopharmaceuticals: Applications and Challenges, S.R. Schmidt (Ed.) Wiley-Blackwell (in Press), 2012

Lisa Mullen, Anne Rigby, Michelle Sclanders, Gill Adams, **Gayatri Mittal**, Julia Colston, Rewas Fatah, Maria Subang, Julie Foster, Philippa Francis-West, Mario Köster, Hansjörg Hauser, Lorna Layward, Sandrine Vessillier, Alex Annenkov, Sarah Al-Izki, Gareth Pryce, Chris Bolton, David Baker, David J. Gould and Yuti Chernajovsky. Aggrecanase-released cytokine confers arthritis-specific drug delivery (submitted).

Mittal, G., Vessillier, S., Mullen, L., Mageed, R.A. and Chernajovsky, Y. Development of a latent IL-17 antagonist for targeted therapy of RA (in preparation).

References

1. Berkanovic E, Hurwicz ML. Rheumatoid arthritis and comorbidity. *J Rheumatol*. 1990;17(7):888-92.
2. Myasoedova E, Davis JM, 3rd, Crowson CS, Gabriel SE. Epidemiology of rheumatoid arthritis: rheumatoid arthritis and mortality. *Curr Rheumatol Rep*. 2010;12(5):379-85.
3. Lanchbury JS. The HLA association with rheumatoid arthritis. *Clin Exp Rheumatol*. 1992;10(3):301-4.
4. Gregersen PK, Silver J, Winchester RJ. The shared epitope hypothesis. An approach to understanding the molecular genetics of susceptibility to rheumatoid arthritis. *Arthritis Rheum*. 1987;30(11):1205-13.
5. Plenge RM, Cotsapas C, Davies L, Price AL, de Bakker PI, Maller J, et al. Two independent alleles at 6q23 associated with risk of rheumatoid arthritis. *Nat Genet*. 2007;39(12):1477-82.
6. Remmers EF, Plenge RM, Lee AT, Graham RR, Hom G, Behrens TW, et al. STAT4 and the risk of rheumatoid arthritis and systemic lupus erythematosus. *N Engl J Med*. 2007;357(10):977-86.
7. Plenge RM, Seielstad M, Padyukov L, Lee AT, Remmers EF, Ding B, et al. TRAF1-C5 as a risk locus for rheumatoid arthritis--a genomewide study. *N Engl J Med*. 2007;357(12):1199-209.
8. Begovich AB, Carlton VE, Honigberg LA, Schrodi SJ, Chokkalingam AP, Alexander HC, et al. A missense single-nucleotide polymorphism in a gene encoding a protein tyrosine phosphatase (PTPN22) is associated with rheumatoid arthritis. *Am J Hum Genet*. 2004;75(2):330-7.
9. Gregersen PK, Amos CI, Lee AT, Lu Y, Remmers EF, Kastner DL, et al. REL, encoding a member of the NF-kappaB family of transcription factors, is a newly defined risk locus for rheumatoid arthritis. *Nat Genet*. 2009;41(7):820-3.
10. Irigoyen P, Lee AT, Wener MH, Li W, Kern M, Batliwalla F, et al. Regulation of anti-cyclic citrullinated peptide antibodies in rheumatoid arthritis: contrasting effects of HLA-DR3 and the shared epitope alleles. *Arthritis Rheum*. 2005;52(12):3813-8.
11. Sigurdsson S, Padyukov L, Kurreeman FA, Liljedahl U, Wiman AC, Alfredsson L, et al. Association of a haplotype in the promoter region of the interferon regulatory factor 5 gene with rheumatoid arthritis. *Arthritis Rheum*. 2007;56(7):2202-10.
12. Lorentzen JC, Flornes L, Eklow C, Backdahl L, Ribbhammar U, Guo JP, et al. Association of arthritis with a gene complex encoding C-type lectin-like receptors. *Arthritis Rheum*. 2007;56(8):2620-32.
13. Symmons DP, Bankhead CR, Harrison BJ, Brennan P, Barrett EM, Scott DG, et al. Blood transfusion, smoking, and obesity as risk factors for the development of rheumatoid arthritis: results from a primary care-based incident case-control study in Norfolk, England. *Arthritis Rheum*. 1997;40(11):1955-61.
14. Klareskog L, Stolt P, Lundberg K, Kallberg H, Bengtsson C, Grunewald J, et al. A new model for an etiology of rheumatoid arthritis: smoking may trigger HLA-DR (shared epitope)-restricted immune reactions to autoantigens modified by citrullination. *Arthritis Rheum*. 2006;54(1):38-46.
15. Hyrich KL, Inman RD. Infectious agents in chronic rheumatic diseases. *Curr Opin Rheumatol*. 2001;13(4):300-4.
16. Wegner N, Wait R, Sroka A, Eick S, Nguyen KA, Lundberg K, et al. Peptidylarginine deiminase from *Porphyromonas gingivalis* citrullinates human fibrinogen and alpha-enolase: implications for autoimmunity in rheumatoid arthritis. *Arthritis Rheum*. 2010;62(9):2662-72.
17. Blass S, Engel JM, Burmester GR. The immunologic homunculus in rheumatoid arthritis. *Arthritis Rheum*. 1999;42(12):2499-506.
18. Gravallese EM. Bone destruction in arthritis. *Ann Rheum Dis*. 2002;61 Suppl 2:ii84-6.

19. Haringman JJ, Gerlag DM, Zwinderman AH, Smeets TJ, Kraan MC, Baeten D, et al. Synovial tissue macrophages: a sensitive biomarker for response to treatment in patients with rheumatoid arthritis. *Ann Rheum Dis*. 2005;64(6):834-8.
20. Feldmann M, Brennan FM, Maini RN. Role of cytokines in rheumatoid arthritis. *Annu Rev Immunol*. 1996;14:397-440.
21. Feldmann M, Maini RN. The role of cytokines in the pathogenesis of rheumatoid arthritis. *Rheumatology (Oxford)*. 1999;38 Suppl 2:3-7.
22. Aupperle KR, Boyle DL, Hendrix M, Seftor EA, Zvaifler NJ, Barbosa M, et al. Regulation of synoviocyte proliferation, apoptosis, and invasion by the p53 tumor suppressor gene. *Am J Pathol*. 1998;152(4):1091-8.
23. Inazuka M, Tahira T, Horiuchi T, Harashima S, Sawabe T, Kondo M, et al. Analysis of p53 tumour suppressor gene somatic mutations in rheumatoid arthritis synovium. *Rheumatology (Oxford)*. 2000;39(3):262-6.
24. Kullmann F, Judex M, Neudecker I, Lechner S, Justen HP, Green DR, et al. Analysis of the p53 tumor suppressor gene in rheumatoid arthritis synovial fibroblasts. *Arthritis Rheum*. 1999;42(8):1594-600.
25. Yamanishi Y, Hiyama K, Maeda H, Ishioka S, Murakami T, Hiyama E, et al. Telomerase activity in rheumatoid synovium correlates with the mononuclear cell infiltration level and disease aggressiveness of rheumatoid arthritis. *J Rheumatol*. 1998;25(2):214-20.
26. Kinne RW, Boehm S, Iftner T, Aigner T, Vornehm S, Weseloh G, et al. Synovial fibroblast-like cells strongly express jun-B and C-fos proto-oncogenes in rheumatoid- and osteoarthritis. *Scand J Rheumatol Suppl*. 1995;101:121-5.
27. Ritchlin C. Fibroblast biology. Effector signals released by the synovial fibroblast in arthritis. *Arthritis Res*. 2000;2(5):356-60.
28. Brennan FM, Hayes AL, Ciesielski CJ, Green P, Foxwell BM, Feldmann M. Evidence that rheumatoid arthritis synovial T cells are similar to cytokine-activated T cells: involvement of phosphatidylinositol 3-kinase and nuclear factor kappaB pathways in tumor necrosis factor alpha production in rheumatoid arthritis. *Arthritis Rheum*. 2002;46(1):31-41.
29. Panayi GS, Corrigan VM, Pitzalis C. Pathogenesis of rheumatoid arthritis. The role of T cells and other beasts. *Rheum Dis Clin North Am*. 2001;27(2):317-34.
30. Tak PP, van der Lubbe PA, Cauli A, Daha MR, Smeets TJ, Kluin PM, et al. Reduction of synovial inflammation after anti-CD4 monoclonal antibody treatment in early rheumatoid arthritis. *Arthritis Rheum*. 1995;38(10):1457-65.
31. Muirden KD, Mills KW. Do lymphocytes protect the rheumatoid joint? *Br Med J*. 1971;4(5781):219-21.
32. Nakken B, Munthe LA, Konttinen YT, Sandberg AK, Szekanecz Z, Alex P, et al. B-cells and their targeting in rheumatoid arthritis--current concepts and future perspectives. *Autoimmun Rev*. 2011;11(1):28-34.
33. Macaulay AE, DeKruyff RH, Umetsu DT. Antigen-primed T cells from B cell-deficient JHD mice fail to provide B cell help. *J Immunol*. 1998;160(4):1694-700.
34. Cascao R, Rosario HS, Souto-Carneiro MM, Fonseca JE. Neutrophils in rheumatoid arthritis: More than simple final effectors. *Autoimmun Rev*. 2010;9(8):531-5.
35. Nigrovic PA, Lee DM. Synovial mast cells: role in acute and chronic arthritis. *Immunol Rev*. 2007;217:19-37.
36. Hueber AJ, Asquith DL, Miller AM, Reilly J, Kerr S, Leipe J, et al. Mast cells express IL-17A in rheumatoid arthritis synovium. *J Immunol*. 2010;184(7):3336-40.
37. McMurray RW. Adhesion molecules in autoimmune disease. *Semin Arthritis Rheum*. 1996;25(4):215-33.
38. Houssiau FA. Cytokines in rheumatoid arthritis. *Clin Rheumatol*. 1995;14 Suppl 2:10-3.

39. Kudo O, Sabokbar A, Pocock A, Itonaga I, Fujikawa Y, Athanasou NA. Interleukin-6 and interleukin-11 support human osteoclast formation by a RANKL-independent mechanism. *Bone*. 2003;32(1):1-7.
40. Kurihara N, Bertolini D, Suda T, Akiyama Y, Roodman GD. IL-6 stimulates osteoclast-like multinucleated cell formation in long term human marrow cultures by inducing IL-1 release. *J Immunol*. 1990;144(11):4226-30.
41. Singh JA, Beg S, Lopez-Olivo MA. Tocilizumab for rheumatoid arthritis: a Cochrane systematic review. *J Rheumatol*. 2011;38(1):10-20.
42. Feldmann M, Brennan FM, Maini RN. Rheumatoid arthritis. *Cell*. 1996;85(3):307-10.
43. Hess A, Axmann R, Rech J, Finzel S, Heindl C, Kreitz S, et al. Blockade of TNF-alpha rapidly inhibits pain responses in the central nervous system. *Proc Natl Acad Sci U S A*. 2011;108(9):3731-6.
44. McInnes IB, Schett G. Cytokines in the pathogenesis of rheumatoid arthritis. *Nat Rev Immunol*. 2007;7(6):429-42.
45. Brennan FM, McInnes IB. Evidence that cytokines play a role in rheumatoid arthritis. *J Clin Invest*. 2008;118(11):3537-45.
46. Clark W, Jobanputra P, Barton P, Burls A. The clinical and cost-effectiveness of anakinra for the treatment of rheumatoid arthritis in adults: a systematic review and economic analysis. *Health Technol Assess*. 2004;8(18):iii-iv, ix-x, 1-105.
47. Firestein GS, Zvaifler NJ. How important are T cells in chronic rheumatoid synovitis? *Arthritis Rheum*. 1990;33(6):768-73.
48. Volin MV, Koch AE. Interleukin-18: a mediator of inflammation and angiogenesis in rheumatoid arthritis. *J Interferon Cytokine Res*. 2011;31(10):745-51.
49. Kunisch E, Chakilam S, Gandesiri M, Kinne RW. IL-33 regulates TNF-alpha dependent effects in synovial fibroblasts. *Int J Mol Med*. 2012;29(4):530-40.
50. Xiangyang Z, Lutian Y, Lin Z, Liping X, Hui S, Jing L. Increased levels of interleukin-33 associated with bone erosion and interstitial lung diseases in patients with rheumatoid arthritis. *Cytokine*. 2012;58(1):6-9.
51. Niu X, He D, Zhang X, Yue T, Li N, Zhang JZ, et al. IL-21 regulates Th17 cells in rheumatoid arthritis. *Hum Immunol*. 2010;71(4):334-41.
52. Yuan FL, Li X, Sun JM, Xu RS. Emerging role of IL-23 in rheumatoid arthritis. *Clin Rheumatol*. 2011;30(8):1135-6.
53. Pickens SR, Chamberlain ND, Volin MV, Pope RM, Talarico NE, Mandelin AM, 2nd, et al. Characterization of interleukin-7 and interleukin-7 receptor in the pathogenesis of rheumatoid arthritis. *Arthritis Rheum*. 2011;63(10):2884-93.
54. Miranda-Carus ME, Balsa A, Benito-Miguel M, Perez de Ayala C, Martin-Mola E. IL-15 and the initiation of cell contact-dependent synovial fibroblast-T lymphocyte cross-talk in rheumatoid arthritis: effect of methotrexate. *J Immunol*. 2004;173(2):1463-76.
55. Gracie JA, Forsey RJ, Chan WL, Gilmour A, Leung BP, Greer MR, et al. A proinflammatory role for IL-18 in rheumatoid arthritis. *J Clin Invest*. 1999;104(10):1393-401.
56. Hsu YH, Li HH, Hsieh MY, Liu MF, Huang KY, Chin LS, et al. Function of interleukin-20 as a proinflammatory molecule in rheumatoid and experimental arthritis. *Arthritis Rheum*. 2006;54(9):2722-33.
57. Ikeuchi H, Kuroiwa T, Hiramatsu N, Kaneko Y, Hiromura K, Ueki K, et al. Expression of interleukin-22 in rheumatoid arthritis: potential role as a proinflammatory cytokine. *Arthritis Rheum*. 2005;52(4):1037-46.
58. Joosten LA, Netea MG, Kim SH, Yoon DY, Oppers-Walgreen B, Radstake TR, et al. IL-32, a proinflammatory cytokine in rheumatoid arthritis. *Proc Natl Acad Sci U S A*. 2006;103(9):3298-303.
59. Perper SJ, Browning B, Burkly LC, Weng S, Gao C, Giza K, et al. TWEAK is a novel arthritogenic mediator. *J Immunol*. 2006;177(4):2610-20.

60. Koch AE, Kunkel SL, Harlow LA, Johnson B, Evanoff HL, Haines GK, et al. Enhanced production of monocyte chemoattractant protein-1 in rheumatoid arthritis. *J Clin Invest.* 1992;90(3):772-9.
61. Haringman JJ, Gerlag DM, Smeets TJ, Baeten D, van den Bosch F, Bresnihan B, et al. A randomized controlled trial with an anti-CCL2 (anti-monocyte chemoattractant protein 1) monoclonal antibody in patients with rheumatoid arthritis. *Arthritis Rheum.* 2006;54(8):2387-92.
62. Amin AR, Attur M, Abramson SB. Nitric oxide synthase and cyclooxygenases: distribution, regulation, and intervention in arthritis. *Curr Opin Rheumatol.* 1999;11(3):202-9.
63. Brooks PM. Clinical management of rheumatoid arthritis. *Lancet.* 1993;341(8840):286-90.
64. Cattell V, Jansen A. Inducible nitric oxide synthase in inflammation. *Histochem J.* 1995;27(10):777-84.
65. Clancy RM, Amin AR, Abramson SB. The role of nitric oxide in inflammation and immunity. *Arthritis Rheum.* 1998;41(7):1141-51.
66. Weinberg JB. Nitric oxide synthase 2 and cyclooxygenase 2 interactions in inflammation. *Immunol Res.* 2000;22(2-3):319-41.
67. Brennan FM, Maini RN, Feldmann M. Role of pro-inflammatory cytokines in rheumatoid arthritis. *Springer Semin Immunopathol.* 1998;20(1-2):133-47.
68. Trabandt A, Gay RE, Fassbender HG, Gay S. Cathepsin B in synovial cells at the site of joint destruction in rheumatoid arthritis. *Arthritis Rheum.* 1991;34(11):1444-51.
69. Nguyen Q, Mort JS, Roughley PJ. Cartilage proteoglycan aggregate is degraded more extensively by cathepsin L than by cathepsin B. *Biochem J.* 1990;266(2):569-73.
70. Hughes CE, Caterson B, Fosang AJ, Roughley PJ, Mort JS. Monoclonal antibodies that specifically recognize neoepitope sequences generated by 'aggrecanase' and matrix metalloproteinase cleavage of aggrecan: application to catabolism in situ and in vitro. *Biochem J.* 1995;305 (Pt 3):799-804.
71. Gravalles EM, Harada Y, Wang JT, Gorn AH, Thornhill TS, Goldring SR. Identification of cell types responsible for bone resorption in rheumatoid arthritis and juvenile rheumatoid arthritis. *Am J Pathol.* 1998;152(4):943-51.
72. Diarra D, Stolina M, Polzer K, Zwerina J, Ominsky MS, Dwyer D, et al. Dickkopf-1 is a master regulator of joint remodeling. *Nat Med.* 2007;13(2):156-63.
73. Katsikis PD, Chu CQ, Brennan FM, Maini RN, Feldmann M. Immunoregulatory role of interleukin 10 in rheumatoid arthritis. *J Exp Med.* 1994;179(5):1517-27.
74. Fava R, Olsen N, Keski-Oja J, Moses H, Pincus T. Active and latent forms of transforming growth factor beta activity in synovial effusions. *J Exp Med.* 1989;169(1):291-6.
75. Engelmann H, Aderka D, Rubinstein M, Rotman D, Wallach D. A tumor necrosis factor-binding protein purified to homogeneity from human urine protects cells from tumor necrosis factor toxicity. *J Biol Chem.* 1989;264(20):11974-80.
76. Seckinger P, Isaaz S, Dayer JM. A human inhibitor of tumor necrosis factor alpha. *J Exp Med.* 1988;167(4):1511-6.
77. Cope AP, Aderka D, Doherty M, Engelmann H, Gibbons D, Jones AC, et al. Increased levels of soluble tumor necrosis factor receptors in the sera and synovial fluid of patients with rheumatic diseases. *Arthritis Rheum.* 1992;35(10):1160-9.
78. Combe B, Landewe R, Lukas C, Bolosiu HD, Breedveld F, Dougados M, et al. EULAR recommendations for the management of early arthritis: report of a task force of the European Standing Committee for International Clinical Studies Including Therapeutics (ESCIIT). *Ann Rheum Dis.* 2007;66(1):34-45.
79. Pincus T, Yazici Y, Sokka T, Aletaha D, Smolen JS. Methotrexate as the "anchor drug" for the treatment of early rheumatoid arthritis. *Clin Exp Rheumatol.* 2003;21(5 Suppl 31):S179-85.
80. Kremer JM. Toward a better understanding of methotrexate. *Arthritis Rheum.* 2004;50(5):1370-82.

81. O'Dell JR, Haire CE, Erikson N, Drymalski W, Palmer W, Eckhoff PJ, et al. Treatment of rheumatoid arthritis with methotrexate alone, sulfasalazine and hydroxychloroquine, or a combination of all three medications. *N Engl J Med.* 1996;334(20):1287-91.
82. Kremer JM, Genovese MC, Cannon GW, Caldwell JR, Cush JJ, Furst DE, et al. Concomitant leflunomide therapy in patients with active rheumatoid arthritis despite stable doses of methotrexate. A randomized, double-blind, placebo-controlled trial. *Ann Intern Med.* 2002;137(9):726-33.
83. Lee YH, Woo JH, Rho YH, Choi SJ, Ji JD, Song GG. Meta-analysis of the combination of TNF inhibitors plus MTX compared to MTX monotherapy, and the adjusted indirect comparison of TNF inhibitors in patients suffering from active rheumatoid arthritis. *Rheumatol Int.* 2008;28(6):553-9.
84. Saag KG, Teng GG, Patkar NM, Anuntiyo J, Finney C, Curtis JR, et al. American College of Rheumatology 2008 recommendations for the use of nonbiologic and biologic disease-modifying antirheumatic drugs in rheumatoid arthritis. *Arthritis Rheum.* 2008;59(6):762-84.
85. Jain R, Lipsky PE. Treatment of rheumatoid arthritis. *Med Clin North Am.* 1997;81(1):57-84.
86. Guidelines for the management of rheumatoid arthritis. American College of Rheumatology Ad Hoc Committee on Clinical Guidelines. *Arthritis Rheum.* 1996;39(5):713-22.
87. Nixon RM, Bansback N, Brennan A. Using mixed treatment comparisons and meta-regression to perform indirect comparisons to estimate the efficacy of biologic treatments in rheumatoid arthritis. *Stat Med.* 2007;26(6):1237-54.
88. Kaine J, Gladstein G, Strusberg I, Robles M, Louw I, Gujrathi S, et al. Evaluation of abatacept administered subcutaneously in adults with active rheumatoid arthritis: impact of withdrawal and reintroduction on immunogenicity, efficacy and safety (phase IIB ALLOW study). *Ann Rheum Dis.* 2012;71(1):38-44.
89. Cragg MS, Walshe CA, Ivanov AO, Glennie MJ. The biology of CD20 and its potential as a target for mAb therapy. *Curr Dir Autoimmun.* 2005;8:140-74.
90. Smolen JS, Keystone EC, Emery P, Breedveld FC, Betteridge N, Burmester GR, et al. Consensus statement on the use of rituximab in patients with rheumatoid arthritis. *Ann Rheum Dis.* 2007;66(2):143-50.
91. Pesu M, Laurence A, Kishore N, Zwillich SH, Chan G, O'Shea JJ. Therapeutic targeting of Janus kinases. *Immunol Rev.* 2008;223:132-42.
92. Kremer JM, Bloom BJ, Breedveld FC, Coombs JH, Fletcher MP, Gruben D, et al. The safety and efficacy of a JAK inhibitor in patients with active rheumatoid arthritis: Results of a double-blind, placebo-controlled phase IIa trial of three dosage levels of CP-690,550 versus placebo. *Arthritis Rheum.* 2009;60(7):1895-905.
93. Bajpai M, Chopra P, Dastidar SG, Ray A. Spleen tyrosine kinase: a novel target for therapeutic intervention of rheumatoid arthritis. *Expert Opin Investig Drugs.* 2008;17(5):641-59.
94. Weinblatt ME, Kavanaugh A, Genovese MC, Musser TK, Grossbard EB, Magilavy DB. An oral spleen tyrosine kinase (Syk) inhibitor for rheumatoid arthritis. *N Engl J Med.* 2010;363(14):1303-12.
95. Yao Z, Fanslow WC, Seldin MF, Rousseau AM, Painter SL, Comeau MR, et al. Herpesvirus Saimiri encodes a new cytokine, IL-17, which binds to a novel cytokine receptor. *Immunity.* 1995;3(6):811-21.
96. Fossiez F, Djossou O, Chomarat P, Flores-Romo L, Ait-Yahia S, Maat C, et al. T cell interleukin-17 induces stromal cells to produce proinflammatory and hematopoietic cytokines. *J Exp Med.* 1996;183(6):2593-603.
97. Shin HC, Benbernou N, Esnault S, Guenounou M. Expression of IL-17 in human memory CD45RO+ T lymphocytes and its regulation by protein kinase A pathway. *Cytokine.* 1999;11(4):257-66.
98. Stark MA, Huo Y, Burcin TL, Morris MA, Olson TS, Ley K. Phagocytosis of apoptotic neutrophils regulates granulopoiesis via IL-23 and IL-17. *Immunity.* 2005;22(3):285-94.

99. Rachitskaya AV, Hansen AM, Horai R, Li Z, Villasmil R, Luger D, et al. Cutting edge: NKT cells constitutively express IL-23 receptor and ROR γ and rapidly produce IL-17 upon receptor ligation in an IL-6-independent fashion. *J Immunol.* 2008;180(8):5167-71.
100. Coury F, Annels N, Rivollier A, Olsson S, Santoro A, Speziani C, et al. Langerhans cell histiocytosis reveals a new IL-17A-dependent pathway of dendritic cell fusion. *Nat Med.* 2008;14(1):81-7.
101. Cua DJ, Tato CM. Innate IL-17-producing cells: the sentinels of the immune system. *Nature reviews. Immunology.* 2010;10(7):479-89.
102. Molet S, Hamid Q, Davoine F, Nutku E, Taha R, Page N, et al. IL-17 is increased in asthmatic airways and induces human bronchial fibroblasts to produce cytokines. *J Allergy Clin Immunol.* 2001;108(3):430-8.
103. Ferretti S, Bonneau O, Dubois GR, Jones CE, Trifilieff A. IL-17, produced by lymphocytes and neutrophils, is necessary for lipopolysaccharide-induced airway neutrophilia: IL-15 as a possible trigger. *J Immunol.* 2003;170(4):2106-12.
104. Spriggs MK. Interleukin-17 and its receptor. *J Clin Immunol.* 1997;17(5):366-9.
105. Broxmeyer HE. Is interleukin 17, an inducible cytokine that stimulates production of other cytokines, merely a redundant player in a sea of other biomolecules? *J Exp Med.* 1996;183(6):2411-5.
106. Jovanovic DV, Di Battista JA, Martel-Pelletier J, Jolicoeur FC, He Y, Zhang M, et al. IL-17 stimulates the production and expression of proinflammatory cytokines, IL-6 and TNF- α , by human macrophages. *J Immunol.* 1998;160(7):3513-21.
107. Yao Z, Painter SL, Fanslow WC, Ulrich D, Macduff BM, Spriggs MK, et al. Human IL-17: a novel cytokine derived from T cells. *J Immunol.* 1995;155(12):5483-6.
108. Schwarzenberger P, Huang W, Ye P, Oliver P, Manuel M, Zhang Z, et al. Requirement of endogenous stem cell factor and granulocyte-colony-stimulating factor for IL-17-mediated granulopoiesis. *J Immunol.* 2000;164(9):4783-9.
109. Schwarzenberger P, La Russa V, Miller A, Ye P, Huang W, Zieske A, et al. IL-17 stimulates granulopoiesis in mice: use of an alternate, novel gene therapy-derived method for in vivo evaluation of cytokines. *J Immunol.* 1998;161(11):6383-9.
110. Ye P, Rodriguez FH, Kanaly S, Stocking KL, Schurr J, Schwarzenberger P, et al. Requirement of interleukin 17 receptor signaling for lung CXC chemokine and granulocyte colony-stimulating factor expression, neutrophil recruitment, and host defense. *J Exp Med.* 2001;194(4):519-27.
111. Yu JJ, Ruddy MJ, Wong GC, Sfintescu C, Baker PJ, Smith JB, et al. An essential role for IL-17 in preventing pathogen-initiated bone destruction: recruitment of neutrophils to inflamed bone requires IL-17 receptor-dependent signals. *Blood.* 2007;109(9):3794-802.
112. Witowski J, Pawlaczyk K, Breborowicz A, Scheuren A, Kuzlan-Pawlaczyk M, Wisniewska J, et al. IL-17 stimulates intraperitoneal neutrophil infiltration through the release of GRO α chemokine from mesothelial cells. *J Immunol.* 2000;165(10):5814-21.
113. Ruddy MJ, Shen F, Smith JB, Sharma A, Gaffen SL. Interleukin-17 regulates expression of the CXC chemokine LIX/CXCL5 in osteoblasts: implications for inflammation and neutrophil recruitment. *J Leukoc Biol.* 2004;76(1):135-44.
114. Ruddy MJ, Wong GC, Liu XK, Yamamoto H, Kasayama S, Kirkwood KL, et al. Functional cooperation between interleukin-17 and tumor necrosis factor- α is mediated by CCAAT/enhancer-binding protein family members. *J Biol Chem.* 2004;279(4):2559-67.
115. Chabaud M, Fossiez F, Taupin JL, Miossec P. Enhancing effect of IL-17 on IL-1-induced IL-6 and leukemia inhibitory factor production by rheumatoid arthritis synoviocytes and its regulation by Th2 cytokines. *J Immunol.* 1998;161(1):409-14.
116. Chabaud M, Miossec P. The combination of tumor necrosis factor α blockade with interleukin-1 and interleukin-17 blockade is more effective for controlling synovial inflammation and bone resorption in an ex vivo model. *Arthritis Rheum.* 2001;44(6):1293-303.

117. Huang W, Na L, Fidel PL, Schwarzenberger P. Requirement of interleukin-17A for systemic anti-*Candida albicans* host defense in mice. *J Infect Dis*. 2004;190(3):624-31.
118. van Beelen AJ, Zelinkova Z, Taanman-Kueter EW, Muller FJ, Hommes DW, Zaat SA, et al. Stimulation of the intracellular bacterial sensor NOD2 programs dendritic cells to promote interleukin-17 production in human memory T cells. *Immunity*. 2007;27(4):660-9.
119. Shen F, Hu Z, Goswami J, Gaffen SL. Identification of common transcriptional regulatory elements in interleukin-17 target genes. *J Biol Chem*. 2006;281(34):24138-48.
120. Kao CY, Chen Y, Thai P, Wachi S, Huang F, Kim C, et al. IL-17 markedly up-regulates beta-defensin-2 expression in human airway epithelium via JAK and NF-kappaB signaling pathways. *J Immunol*. 2004;173(5):3482-91.
121. Liang SC, Tan XY, Luxenberg DP, Karim R, Dunussi-Joannopoulos K, Collins M, et al. Interleukin (IL)-22 and IL-17 are coexpressed by Th17 cells and cooperatively enhance expression of antimicrobial peptides. *J Exp Med*. 2006;203(10):2271-9.
122. Chen Y, Thai P, Zhao YH, Ho YS, DeSouza MM, Wu R. Stimulation of airway mucin gene expression by interleukin (IL)-17 through IL-6 paracrine/autocrine loop. *J Biol Chem*. 2003;278(19):17036-43.
123. Matusiewicz D, Kivisakk P, He B, Kostulas N, Ozenci V, Fredrikson S, et al. Interleukin-17 mRNA expression in blood and CSF mononuclear cells is augmented in multiple sclerosis. *Mult Scler*. 1999;5(2):101-4.
124. Albanesi C, Scarponi C, Cavani A, Federici M, Nasorri F, Girolomoni G. Interleukin-17 is produced by both Th1 and Th2 lymphocytes, and modulates interferon-gamma- and interleukin-4-induced activation of human keratinocytes. *J Invest Dermatol*. 2000;115(1):81-7.
125. Kebir H, Kreymborg K, Ifergan I, Dodelet-Devillers A, Cayrol R, Bernard M, et al. Human TH17 lymphocytes promote blood-brain barrier disruption and central nervous system inflammation. *Nat Med*. 2007;13(10):1173-5.
126. Yagi Y, Andoh A, Inatomi O, Tsujikawa T, Fujiyama Y. Inflammatory responses induced by interleukin-17 family members in human colonic subepithelial myofibroblasts. *J Gastroenterol*. 2007;42(9):746-53.
127. Schnyder-Candrian S, Togbe D, Couillin I, Mercier I, Brombacher F, Quesniaux V, et al. Interleukin-17 is a negative regulator of established allergic asthma. *J Exp Med*. 2006;203(12):2715-25.
128. Yi T, Zhao D, Lin CL, Zhang C, Chen Y, Todorov I, et al. Absence of donor Th17 leads to augmented Th1 differentiation and exacerbated acute graft-versus-host disease. *Blood*. 2008;112(5):2101-10.
129. Ogawa A, Andoh A, Araki Y, Bamba T, Fujiyama Y. Neutralization of interleukin-17 aggravates dextran sulfate sodium-induced colitis in mice. *Clin Immunol*. 2004;110(1):55-62.
130. Yang XO, Chang SH, Park H, Nurieva R, Shah B, Acero L, et al. Regulation of inflammatory responses by IL-17F. *J Exp Med*. 2008;205(5):1063-75.
131. Kawaguchi M, Onuchic LF, Li XD, Essayan DM, Schroeder J, Xiao HQ, et al. Identification of a novel cytokine, ML-1, and its expression in subjects with asthma. *J Immunol*. 2001;167(8):4430-5.
132. Hymowitz SG, Filvaroff EH, Yin JP, Lee J, Cai L, Risser P, et al. IL-17s adopt a cystine knot fold: structure and activity of a novel cytokine, IL-17F, and implications for receptor binding. *EMBO J*. 2001;20(19):5332-41.
133. Starnes T, Robertson MJ, Sledge G, Kelich S, Nakshatri H, Broxmeyer HE, et al. Cutting edge: IL-17F, a novel cytokine selectively expressed in activated T cells and monocytes, regulates angiogenesis and endothelial cell cytokine production. *J Immunol*. 2001;167(8):4137-40.
134. Kawaguchi M, Kokubu F, Odaka M, Watanabe S, Suzuki S, Ieki K, et al. Induction of granulocyte-macrophage colony-stimulating factor by a new cytokine, ML-1 (IL-17F), via Raf I-MEK-ERK pathway. *J Allergy Clin Immunol*. 2004;114(2):444-50.

135. Shen F, Gaffen SL. Structure-function relationships in the IL-17 receptor: implications for signal transduction and therapy. *Cytokine*. 2008;41(2):92-104.
136. McAllister F, Henry A, Kreindler JL, Dubin PJ, Ulrich L, Steele C, et al. Role of IL-17A, IL-17F, and the IL-17 receptor in regulating growth-related oncogene-alpha and granulocyte colony-stimulating factor in bronchial epithelium: implications for airway inflammation in cystic fibrosis. *J Immunol*. 2005;175(1):404-12.
137. Aujla SJ, Chan YR, Zheng M, Fei M, Askew DJ, Pociask DA, et al. IL-22 mediates mucosal host defense against Gram-negative bacterial pneumonia. *Nat Med*. 2008;14(3):275-81.
138. Ishigame H, Kakuta S, Nagai T, Kadoki M, Nambu A, Komiyama Y, et al. Differential roles of interleukin-17A and -17F in host defense against mucoepithelial bacterial infection and allergic responses. *Immunity*. 2009;30(1):108-19.
139. Saijo S, Ikeda S, Yamabe K, Kakuta S, Ishigame H, Akitsu A, et al. Dectin-2 recognition of alpha-mannans and induction of Th17 cell differentiation is essential for host defense against *Candida albicans*. *Immunity*. 2010;32(5):681-91.
140. Nakae S, Komiyama Y, Nambu A, Sudo K, Iwase M, Homma I, et al. Antigen-specific T cell sensitization is impaired in IL-17-deficient mice, causing suppression of allergic cellular and humoral responses. *Immunity*. 2002;17(3):375-87.
141. Aggarwal S, Ghilardi N, Xie MH, de Sauvage FJ, Gurney AL. Interleukin-23 promotes a distinct CD4 T cell activation state characterized by the production of interleukin-17. *J Biol Chem*. 2003;278(3):1910-4.
142. Chang SH, Dong C. A novel heterodimeric cytokine consisting of IL-17 and IL-17F regulates inflammatory responses. *Cell Res*. 2007;17(5):435-40.
143. Wright JF, Guo Y, Quazi A, Luxenberg DP, Bennett F, Ross JF, et al. Identification of an interleukin 17F/17A heterodimer in activated human CD4+ T cells. *J Biol Chem*. 2007;282(18):13447-55.
144. Liang SC, Long AJ, Bennett F, Whitters MJ, Karim R, Collins M, et al. An IL-17F/A heterodimer protein is produced by mouse Th17 cells and induces airway neutrophil recruitment. *J Immunol*. 2007;179(11):7791-9.
145. Shaw G, Kamen R. A conserved AU sequence from the 3' untranslated region of GM-CSF mRNA mediates selective mRNA degradation. *Cell*. 1986;46(5):659-67.
146. Hurst SD, Muchamuel T, Gorman DM, Gilbert JM, Clifford T, Kwan S, et al. New IL-17 family members promote Th1 or Th2 responses in the lung: in vivo function of the novel cytokine IL-25. *J Immunol*. 2002;169(1):443-53.
147. Hoshino H, Lotvall J, Skoogh BE, Linden A. Neutrophil recruitment by interleukin-17 into rat airways in vivo. Role of tachykinins. *Am J Respir Crit Care Med*. 1999;159(5 Pt 1):1423-8.
148. Yamaguchi Y, Fujio K, Shoda H, Okamoto A, Tsuno NH, Takahashi K, et al. IL-17B and IL-17C are associated with TNF-alpha production and contribute to the exacerbation of inflammatory arthritis. *J Immunol*. 2007;179(10):7128-36.
149. Starnes T, Broxmeyer HE, Robertson MJ, Hromas R. Cutting edge: IL-17D, a novel member of the IL-17 family, stimulates cytokine production and inhibits hemopoiesis. *J Immunol*. 2002;169(2):642-6.
150. Lee J, Ho WH, Maruoka M, Corpuz RT, Baldwin DT, Foster JS, et al. IL-17E, a novel proinflammatory ligand for the IL-17 receptor homolog IL-17Rh1. *J Biol Chem*. 2001;276(2):1660-4.
151. Pan G, French D, Mao W, Maruoka M, Risser P, Lee J, et al. Forced expression of murine IL-17E induces growth retardation, jaundice, a Th2-biased response, and multiorgan inflammation in mice. *J Immunol*. 2001;167(11):6559-67.
152. Angkasekwinai P, Park H, Wang YH, Chang SH, Corry DB, Liu YJ, et al. Interleukin 25 promotes the initiation of proallergic type 2 responses. *J Exp Med*. 2007;204(7):1509-17.

153. Kawaguchi M, Takahashi D, Hizawa N, Suzuki S, Matsukura S, Kokubu F, et al. IL-17F sequence variant (His161Arg) is associated with protection against asthma and antagonizes wild-type IL-17F activity. *J Allergy Clin Immunol.* 2006;117(4):795-801.
154. Qian F, Zhang Q, Zhou L, Ma G, Jin G, Huang Q, et al. Association between polymorphisms in IL17F and male asthma in a Chinese population. *J Investig Allergol Clin Immunol.* 2012;22(4):257-63.
155. Ramsey CD, Lazarus R, Camargo CA, Jr., Weiss ST, Celedon JC. Polymorphisms in the interleukin 17F gene (IL17F) and asthma. *Genes Immun.* 2005;6(3):236-41.
156. Chen B, Zeng Z, Hou J, Chen M, Gao X, Hu P. Association of interleukin-17F 7488 single nucleotide polymorphism and inflammatory bowel disease in the Chinese population. *Scand J Gastroenterol.* 2009;44(6):720-6.
157. Arisawa T, Tahara T, Shibata T, Nagasaka M, Nakamura M, Kamiya Y, et al. The influence of polymorphisms of interleukin-17A and interleukin-17F genes on the susceptibility to ulcerative colitis. *J Clin Immunol.* 2008;28(1):44-9.
158. Seiderer J, Elben I, Diegelmann J, Glas J, Stallhofer J, Tillack C, et al. Role of the novel Th17 cytokine IL-17F in inflammatory bowel disease (IBD): upregulated colonic IL-17F expression in active Crohn's disease and analysis of the IL17F p.His161Arg polymorphism in IBD. *Inflamm Bowel Dis.* 2008;14(4):437-45.
159. Saitoh T, Tsukamoto N, Koiso H, Mitsui T, Yokohama A, Handa H, et al. Interleukin-17F gene polymorphism in patients with chronic immune thrombocytopenia. *Eur J Haematol.* 2011;87(3):253-8.
160. Arisawa T, Tahara T, Shibata T, Nagasaka M, Nakamura M, Kamiya Y, et al. Genetic polymorphisms of molecules associated with inflammation and immune response in Japanese subjects with functional dyspepsia. *Int J Mol Med.* 2007;20(5):717-23.
161. Shibata T, Tahara T, Hirata I, Arisawa T. Genetic polymorphism of interleukin-17A and -17F genes in gastric carcinogenesis. *Hum Immunol.* 2009;70(7):547-51.
162. Shibata S, Saeki H, Tsunemi Y, Kato T, Nakamura K, Kakinuma T, et al. IL-17F single nucleotide polymorphism is not associated with psoriasis vulgaris or atopic dermatitis in the Japanese population. *J Dermatol Sci.* 2009;53(2):163-5.
163. Metzger K, Fremont M, Roelant C, De Meirleir K. Lower frequency of IL-17F sequence variant (His161Arg) in chronic fatigue syndrome patients. *Biochem Biophys Res Commun.* 2008;376(1):231-3.
164. Jang WC, Nam YH, Ahn YC, Lee SH, Park SH, Choe JY, et al. Interleukin-17F gene polymorphisms in Korean patients with Behcet's disease. *Rheumatol Int.* 2008;29(2):173-8.
165. Pei F, Han Y, Zhang X, Yan C, Huang M, Deng J, et al. Association analysis of the IL-17F His161Arg polymorphism in myocardial infarction. *Coron Artery Dis.* 2009;20(8):513-7.
166. Wang L, Jiang Y, Zhang Y, Wang Y, Huang S, Wang Z, et al. Association analysis of IL-17A and IL-17F polymorphisms in Chinese Han women with breast cancer. *PLoS One.* 2012;7(3):e34400.
167. Paradowska-Gorycka A, Wojtecka-Lukasik E, Trefler J, Wojciechowska B, Lacki JK, Maslinski S. Association between IL-17F gene polymorphisms and susceptibility to and severity of rheumatoid arthritis (RA). *Scand J Immunol.* 2010;72(2):134-41.
168. Novatchkova M, Leibbrandt A, Werzowa J, Neubuser A, Eisenhaber F. The STIR-domain superfamily in signal transduction, development and immunity. *Trends Biochem Sci.* 2003;28(5):226-9.
169. Yao Z, Spriggs MK, Derry JM, Strockbine L, Park LS, VandenBos T, et al. Molecular characterization of the human interleukin (IL)-17 receptor. *Cytokine.* 1997;9(11):794-800.
170. Maitra A, Shen F, Hanel W, Mossman K, Tocker J, Swart D, et al. Distinct functional motifs within the IL-17 receptor regulate signal transduction and target gene expression. *Proc Natl Acad Sci U S A.* 2007;104(18):7506-11.

171. Lindemann MJ, Hu Z, Benczik M, Liu KD, Gaffen SL. Differential regulation of the IL-17 receptor by gamma-cytokines: inhibitory signaling by the phosphatidylinositol 3-kinase pathway. *J Biol Chem*. 2008;283(20):14100-8.
172. Zeng R, Spolski R, Finkelstein SE, Oh S, Kovanen PE, Hinrichs CS, et al. Synergy of IL-21 and IL-15 in regulating CD8+ T cell expansion and function. *J Exp Med*. 2005;201(1):139-48.
173. Toy D, Kugler D, Wolfson M, Vanden Bos T, Gurgel J, Derry J, et al. Cutting edge: interleukin 17 signals through a heteromeric receptor complex. *J Immunol*. 2006;177(1):36-9.
174. Rickel EA, Siegel LA, Yoon BR, Rottman JB, Kugler DG, Swart DA, et al. Identification of functional roles for both IL-17RB and IL-17RA in mediating IL-25-induced activities. *J Immunol*. 2008;181(6):4299-310.
175. Rong Z, Wang A, Li Z, Ren Y, Cheng L, Li Y, et al. IL-17RD (Sef or IL-17RLM) interacts with IL-17 receptor and mediates IL-17 signaling. *Cell Res*. 2009;19(2):208-15.
176. Kramer JM, Hanel W, Shen F, Isik N, Malone JP, Maitra A, et al. Cutting edge: identification of a pre-ligand assembly domain (PLAD) and ligand binding site in the IL-17 receptor. *J Immunol*. 2007;179(10):6379-83.
177. Kramer JM, Gaffen SL. Interleukin-17: a new paradigm in inflammation, autoimmunity, and therapy. *J Periodontol*. 2007;78(6):1083-93.
178. Kramer JM, Yi L, Shen F, Maitra A, Jiao X, Jin T, et al. Evidence for ligand-independent multimerization of the IL-17 receptor. *J Immunol*. 2006;176(2):711-5.
179. Ely LK, Fischer S, Garcia KC. Structural basis of receptor sharing by interleukin 17 cytokines. *Nat Immunol*. 2009;10(12):1245-51.
180. Haudenschild DR, Curtiss SB, Moseley TA, Reddi AH. Generation of interleukin-17 receptor-like protein (IL-17RL) in prostate by alternative splicing of RNA. *Prostate*. 2006;66(12):1268-74.
181. Kuestner RE, Taft DW, Haran A, Brandt CS, Brender T, Lum K, et al. Identification of the IL-17 receptor related molecule IL-17RC as the receptor for IL-17F. *J Immunol*. 2007;179(8):5462-73.
182. Haudenschild D, Moseley T, Rose L, Reddi AH. Soluble and transmembrane isoforms of novel interleukin-17 receptor-like protein by RNA splicing and expression in prostate cancer. *J Biol Chem*. 2002;277(6):4309-16.
183. Pancer Z, Mayer WE, Klein J, Cooper MD. Prototypic T cell receptor and CD4-like coreceptor are expressed by lymphocytes in the agnathan sea lamprey. *Proc Natl Acad Sci U S A*. 2004;101(36):13273-8.
184. Song X, Zhu S, Shi P, Liu Y, Shi Y, Levin SD, et al. IL-17RE is the functional receptor for IL-17C and mediates mucosal immunity to infection with intestinal pathogens. *Nat Immunol*. 2011;12(12):1151-8.
185. Hartupée J, Liu C, Novotny M, Li X, Hamilton T. IL-17 enhances chemokine gene expression through mRNA stabilization. *J Immunol*. 2007;179(6):4135-41.
186. Sun D, Novotny M, Bulek K, Liu C, Li X, Hamilton T. Treatment with IL-17 prolongs the half-life of chemokine CXCL1 mRNA via the adaptor TRAF5 and the splicing-regulatory factor SF2 (ASF). *Nat Immunol*. 2011;12(9):853-60.
187. Bulek K, Liu C, Swaidani S, Wang L, Page RC, Gulen MF, et al. The inducible kinase IKKi is required for IL-17-dependent signaling associated with neutrophilia and pulmonary inflammation. *Nat Immunol*. 2011;12(9):844-52.
188. Sonder SU, Saret S, Tang W, Sturdevant DE, Porcella SF, Siebenlist U. IL-17-induced NF-kappaB activation via CIKS/Act1: physiologic significance and signaling mechanisms. *J Biol Chem*. 2011;286(15):12881-90.
189. Ho AW, Gaffen SL. IL-17RC: a partner in IL-17 signaling and beyond. *Semin Immunopathol*. 2010;32(1):33-42.
190. Hu Y, Shen F, Crellin NK, Ouyang W. The IL-17 pathway as a major therapeutic target in autoimmune diseases. *Ann N Y Acad Sci*. 2011;1217:60-76.

191. Schwandner R, Yamaguchi K, Cao Z. Requirement of tumor necrosis factor receptor-associated factor (TRAF)6 in interleukin 17 signal transduction. *J Exp Med*. 2000;191(7):1233-40.
192. Li X, Commane M, Nie H, Hua X, Chatterjee-Kishore M, Wald D, et al. Act1, an NF-kappa B-activating protein. *Proc Natl Acad Sci U S A*. 2000;97(19):10489-93.
193. Leonardi A, Chariot A, Claudio E, Cunningham K, Siebenlist U. CIKS, a connection to Ikappa B kinase and stress-activated protein kinase. *Proc Natl Acad Sci U S A*. 2000;97(19):10494-9.
194. Kanamori M, Kai C, Hayashizaki Y, Suzuki H. NF-kappaB activator Act1 associates with IL-1/Toll pathway adaptor molecule TRAF6. *FEBS Lett*. 2002;532(1-2):241-6.
195. Huang F, Kao CY, Wachi S, Thai P, Ryu J, Wu R. Requirement for both JAK-mediated PI3K signaling and ACT1/TRAF6/TAK1-dependent NF-kappaB activation by IL-17A in enhancing cytokine expression in human airway epithelial cells. *J Immunol*. 2007;179(10):6504-13.
196. Chang SH, Park H, Dong C. Act1 adaptor protein is an immediate and essential signaling component of interleukin-17 receptor. *J Biol Chem*. 2006;281(47):35603-7.
197. Qian Y, Liu C, Hartupee J, Altuntas CZ, Gulen MF, Jane-Wit D, et al. The adaptor Act1 is required for interleukin 17-dependent signaling associated with autoimmune and inflammatory disease. *Nat Immunol*. 2007;8(3):247-56.
198. Shi P, Zhu S, Lin Y, Liu Y, Liu Y, Chen Z, et al. Persistent stimulation with interleukin-17 desensitizes cells through SCFbeta-TrCP-mediated degradation of Act1. *Sci Signal*. 2011;4(197):ra73.
199. Yang XO, Nurieva R, Martinez GJ, Kang HS, Chung Y, Pappu BP, et al. Molecular antagonism and plasticity of regulatory and inflammatory T cell programs. *Immunity*. 2008;29(1):44-56.
200. Dong C, Flavell RA. Cell fate decision: T-helper 1 and 2 subsets in immune responses. *Arthritis Res*. 2000;2(3):179-88.
201. Park H, Li Z, Yang XO, Chang SH, Nurieva R, Wang YH, et al. A distinct lineage of CD4 T cells regulates tissue inflammation by producing interleukin 17. *Nat Immunol*. 2005;6(11):1133-41.
202. Harrington LE, Hatton RD, Mangan PR, Turner H, Murphy TL, Murphy KM, et al. Interleukin 17-producing CD4+ effector T cells develop via a lineage distinct from the T helper type 1 and 2 lineages. *Nat Immunol*. 2005;6(11):1123-32.
203. Langrish CL, Chen Y, Blumenschein WM, Mattson J, Basham B, Sedgwick JD, et al. IL-23 drives a pathogenic T cell population that induces autoimmune inflammation. *J Exp Med*. 2005;201(2):233-40.
204. Mangan PR, Harrington LE, O'Quinn DB, Helms WS, Bullard DC, Elson CO, et al. Transforming growth factor-beta induces development of the T(H)17 lineage. *Nature*. 2006;441(7090):231-4.
205. Zheng Y, Valdez PA, Danilenko DM, Hu Y, Sa SM, Gong Q, et al. Interleukin-22 mediates early host defense against attaching and effacing bacterial pathogens. *Nat Med*. 2008;14(3):282-9.
206. Bettelli E, Carrier Y, Gao W, Korn T, Strom TB, Oukka M, et al. Reciprocal developmental pathways for the generation of pathogenic effector TH17 and regulatory T cells. *Nature*. 2006;441(7090):235-8.
207. Veldhoen M, Hocking RJ, Atkins CJ, Locksley RM, Stockinger B. TGFbeta in the context of an inflammatory cytokine milieu supports de novo differentiation of IL-17-producing T cells. *Immunity*. 2006;24(2):179-89.
208. Zhou L, Ivanov II, Spolski R, Min R, Shenderov K, Egawa T, et al. IL-6 programs T(H)-17 cell differentiation by promoting sequential engagement of the IL-21 and IL-23 pathways. *Nat Immunol*. 2007;8(9):967-74.
209. Korn T, Bettelli E, Gao W, Awasthi A, Jager A, Strom TB, et al. IL-21 initiates an alternative pathway to induce proinflammatory T(H)17 cells. *Nature*. 2007;448(7152):484-7.
210. Nurieva R, Yang XO, Martinez G, Zhang Y, Panopoulos AD, Ma L, et al. Essential autocrine regulation by IL-21 in the generation of inflammatory T cells. *Nature*. 2007;448(7152):480-3.

211. Korn T, Mitsdoerffer M, Croxford AL, Awasthi A, Dardalhon VA, Galileos G, et al. IL-6 controls Th17 immunity in vivo by inhibiting the conversion of conventional T cells into Foxp3+ regulatory T cells. *Proc Natl Acad Sci U S A*. 2008;105(47):18460-5.
212. Ghoreschi K, Laurence A, Yang XP, Tato CM, McGeachy MJ, Konkel JE, et al. Generation of pathogenic T(H)17 cells in the absence of TGF-beta signalling. *Nature*. 2010;467(7318):967-71.
213. Annunziato F, Cosmi L, Santarlasci V, Maggi L, Liotta F, Mazzinghi B, et al. Phenotypic and functional features of human Th17 cells. *J Exp Med*. 2007;204(8):1849-61.
214. Cosmi L, De Palma R, Santarlasci V, Maggi L, Capone M, Frosali F, et al. Human interleukin 17-producing cells originate from a CD161+CD4+ T cell precursor. *J Exp Med*. 2008;205(8):1903-16.
215. Annunziato F, Cosmi L, Liotta F, Maggi E, Romagnani S. Human Th17 cells: are they different from murine Th17 cells? *Eur J Immunol*. 2009;39(3):637-40.
216. Kryczek I, Wei S, Vatan L, Escara-Wilke J, Szeliga W, Keller ET, et al. Cutting edge: opposite effects of IL-1 and IL-2 on the regulation of IL-17+ T cell pool IL-1 subverts IL-2-mediated suppression. *J Immunol*. 2007;179(3):1423-6.
217. Stockinger B, Veldhoen M. Differentiation and function of Th17 T cells. *Curr Opin Immunol*. 2007;19(3):281-6.
218. Watanabe H, Gehrke S, Contassot E, Roques S, Tschopp J, Friedmann PS, et al. Danger signaling through the inflammasome acts as a master switch between tolerance and sensitization. *J Immunol*. 2008;180(9):5826-32.
219. Coquet JM, Chakravarti S, Smyth MJ, Godfrey DI. Cutting edge: IL-21 is not essential for Th17 differentiation or experimental autoimmune encephalomyelitis. *J Immunol*. 2008;180(11):7097-101.
220. Ivanov, II, Frutos Rde L, Manel N, Yoshinaga K, Rifkin DB, Sartor RB, et al. Specific microbiota direct the differentiation of IL-17-producing T-helper cells in the mucosa of the small intestine. *Cell Host Microbe*. 2008;4(4):337-49.
221. Sonderegger I, Kisielow J, Meier R, King C, Kopf M. IL-21 and IL-21R are not required for development of Th17 cells and autoimmunity in vivo. *Eur J Immunol*. 2008;38(7):1833-8.
222. Acosta-Rodriguez EV, Napolitani G, Lanzavecchia A, Sallusto F. Interleukins 1beta and 6 but not transforming growth factor-beta are essential for the differentiation of interleukin 17-producing human T helper cells. *Nat Immunol*. 2007;8(9):942-9.
223. Evans HG, Suddason T, Jackson I, Taams LS, Lord GM. Optimal induction of T helper 17 cells in humans requires T cell receptor ligation in the context of Toll-like receptor-activated monocytes. *Proc Natl Acad Sci U S A*. 2007;104(43):17034-9.
224. van Beelen AJ, Teunissen MB, Kapsenberg ML, de Jong EC. Interleukin-17 in inflammatory skin disorders. *Curr Opin Allergy Clin Immunol*. 2007;7(5):374-81.
225. Wilson NJ, Boniface K, Chan JR, McKenzie BS, Blumenschein WM, Mattson JD, et al. Development, cytokine profile and function of human interleukin 17-producing helper T cells. *Nat Immunol*. 2007;8(9):950-7.
226. Volpe E, Servant N, Zollinger R, Bogiatzi SI, Hupe P, Barillot E, et al. A critical function for transforming growth factor-beta, interleukin 23 and proinflammatory cytokines in driving and modulating human T(H)-17 responses. *Nat Immunol*. 2008;9(6):650-7.
227. Yang L, Anderson DE, Baecher-Allan C, Hastings WD, Bettelli E, Oukka M, et al. IL-21 and TGF-beta are required for differentiation of human T(H)17 cells. *Nature*. 2008;454(7202):350-2.
228. Manel N, Unutmaz D, Littman DR. The differentiation of human T(H)-17 cells requires transforming growth factor-beta and induction of the nuclear receptor RORgamma. *Nat Immunol*. 2008;9(6):641-9.
229. Chen Z, Tato CM, Muul L, Laurence A, O'Shea JJ. Distinct regulation of interleukin-17 in human T helper lymphocytes. *Arthritis Rheum*. 2007;56(9):2936-46.

230. Lyakh L, Trinchieri G, Provezza L, Carra G, Gerosa F. Regulation of interleukin-12/interleukin-23 production and the T-helper 17 response in humans. *Immunol Rev.* 2008;226:112-31.
231. Das J, Ren G, Zhang L, Roberts AI, Zhao X, Bothwell AL, et al. Transforming growth factor beta is dispensable for the molecular orchestration of Th17 cell differentiation. *J Exp Med.* 2009;206(11):2407-16.
232. Santarasci V, Maggi L, Capone M, Frosali F, Querci V, De Palma R, et al. TGF-beta indirectly favors the development of human Th17 cells by inhibiting Th1 cells. *Eur J Immunol.* 2009;39(1):207-15.
233. Ichiyama K, Sekiya T, Inoue N, Tamiya T, Kashiwagi I, Kimura A, et al. Transcription factor Smad-independent T helper 17 cell induction by transforming-growth factor-beta is mediated by suppression of eomesodermin. *Immunity.* 2011;34(5):741-54.
234. Yang Y, Weiner J, Liu Y, Smith AJ, Huss DJ, Winger R, et al. T-bet is essential for encephalitogenicity of both Th1 and Th17 cells. *J Exp Med.* 2009;206(7):1549-64.
235. Jager A, Dardalhon V, Sobel RA, Bettelli E, Kuchroo VK. Th1, Th17, and Th9 effector cells induce experimental autoimmune encephalomyelitis with different pathological phenotypes. *J Immunol.* 2009;183(11):7169-77.
236. Gutcher I, Donkor MK, Ma Q, Rudensky AY, Flavell RA, Li MO. Autocrine transforming growth factor-beta1 promotes in vivo Th17 cell differentiation. *Immunity.* 2011;34(3):396-408.
237. Li MO, Wan YY, Flavell RA. T cell-produced transforming growth factor-beta1 controls T cell tolerance and regulates Th1- and Th17-cell differentiation. *Immunity.* 2007;26(5):579-91.
238. Veldhoen M, Hocking RJ, Flavell RA, Stockinger B. Signals mediated by transforming growth factor-beta initiate autoimmune encephalomyelitis, but chronic inflammation is needed to sustain disease. *Nat Immunol.* 2006;7(11):1151-6.
239. Zhou L, Lopes JE, Chong MM, Ivanov II, Min R, Victora GD, et al. TGF-beta-induced Foxp3 inhibits T(H)17 cell differentiation by antagonizing RORgamma function. *Nature.* 2008;453(7192):236-40.
240. Zheng Y, Danilenko DM, Valdez P, Kasman I, Eastham-Anderson J, Wu J, et al. Interleukin-22, a T(H)17 cytokine, mediates IL-23-induced dermal inflammation and acanthosis. *Nature.* 2007;445(7128):648-51.
241. Yang XO, Pappu BP, Nurieva R, Akimzhanov A, Kang HS, Chung Y, et al. T helper 17 lineage differentiation is programmed by orphan nuclear receptors ROR alpha and ROR gamma. *Immunity.* 2008;28(1):29-39.
242. Zhang F, Meng G, Strober W. Interactions among the transcription factors Runx1, RORgamma and Foxp3 regulate the differentiation of interleukin 17-producing T cells. *Nat Immunol.* 2008;9(11):1297-306.
243. Eberl G, Marmon S, Sunshine MJ, Rennert PD, Choi Y, Littman DR. An essential function for the nuclear receptor RORgamma(t) in the generation of fetal lymphoid tissue inducer cells. *Nat Immunol.* 2004;5(1):64-73.
244. Egawa T, Eberl G, Taniuchi I, Benlagha K, Geissmann F, Hennighausen L, et al. Genetic evidence supporting selection of the Valpha14i NKT cell lineage from double-positive thymocyte precursors. *Immunity.* 2005;22(6):705-16.
245. Sun Z, Unutmaz D, Zou YR, Sunshine MJ, Pierani A, Brenner-Morton S, et al. Requirement for RORgamma in thymocyte survival and lymphoid organ development. *Science.* 2000;288(5475):2369-73.
246. Ivanov II, McKenzie BS, Zhou L, Tadokoro CE, Lepelley A, Lafaille JJ, et al. The orphan nuclear receptor RORgamma directs the differentiation program of proinflammatory IL-17+ T helper cells. *Cell.* 2006;126(6):1121-33.
247. Leppkes M, Becker C, Ivanov II, Hirth S, Wirtz S, Neufert C, et al. RORgamma-expressing Th17 cells induce murine chronic intestinal inflammation via redundant effects of IL-17A and IL-17F. *Gastroenterology.* 2009;136(1):257-67.

248. Lochner M, Peduto L, Cherrier M, Sawa S, Langa F, Varona R, et al. In vivo equilibrium of proinflammatory IL-17⁺ and regulatory IL-10⁺ Foxp3⁺ ROR γ ⁺ T cells. *J Exp Med*. 2008;205(6):1381-93.
249. Ichiyama K, Yoshida H, Wakabayashi Y, Chinen T, Saeki K, Nakaya M, et al. Foxp3 inhibits ROR γ -mediated IL-17A mRNA transcription through direct interaction with ROR γ . *J Biol Chem*. 2008;283(25):17003-8.
250. Wei L, Laurence A, Elias KM, O'Shea JJ. IL-21 is produced by Th17 cells and drives IL-17 production in a STAT3-dependent manner. *J Biol Chem*. 2007;282(48):34605-10.
251. Chen Z, Laurence A, Kanno Y, Pacher-Zavisin M, Zhu BM, Tato C, et al. Selective regulatory function of Socs3 in the formation of IL-17-secreting T cells. *Proc Natl Acad Sci U S A*. 2006;103(21):8137-42.
252. Mathur AN, Chang HC, Zisoulis DG, Stritesky GL, Yu Q, O'Malley JT, et al. Stat3 and Stat4 direct development of IL-17-secreting Th cells. *J Immunol*. 2007;178(8):4901-7.
253. Milner JD, Brenchley JM, Laurence A, Freeman AF, Hill BJ, Elias KM, et al. Impaired T(H)17 cell differentiation in subjects with autosomal dominant hyper-IgE syndrome. *Nature*. 2008;452(7188):773-6.
254. Durant L, Watford WT, Ramos HL, Laurence A, Vahedi G, Wei L, et al. Diverse targets of the transcription factor STAT3 contribute to T cell pathogenicity and homeostasis. *Immunity*. 2010;32(5):605-15.
255. Yang XP, Ghoreschi K, Steward-Tharp SM, Rodriguez-Canales J, Zhu J, Grainger JR, et al. Opposing regulation of the locus encoding IL-17 through direct, reciprocal actions of STAT3 and STAT5. *Nat Immunol*. 2011;12(3):247-54.
256. Ono M, Yaguchi H, Ohkura N, Kitabayashi I, Nagamura Y, Nomura T, et al. Foxp3 controls regulatory T-cell function by interacting with AML1/Runx1. *Nature*. 2007;446(7136):685-9.
257. Huber M, Brustle A, Reinhard K, Guralnik A, Walter G, Mahiny A, et al. IRF4 is essential for IL-21-mediated induction, amplification, and stabilization of the Th17 phenotype. *Proc Natl Acad Sci U S A*. 2008;105(52):20846-51.
258. Brustle A, Heink S, Huber M, Rosenplanter C, Stadelmann C, Yu P, et al. The development of inflammatory T(H)-17 cells requires interferon-regulatory factor 4. *Nat Immunol*. 2007;8(9):958-66.
259. Liu XK, Lin X, Gaffen SL. Crucial role for nuclear factor of activated T cells in T cell receptor-mediated regulation of human interleukin-17. *J Biol Chem*. 2004;279(50):52762-71.
260. Chen Z, Laurence A, O'Shea JJ. Signal transduction pathways and transcriptional regulation in the control of Th17 differentiation. *Semin Immunol*. 2007;19(6):400-8.
261. Bauquet AT, Jin H, Paterson AM, Mitsdoerffer M, Ho IC, Sharpe AH, et al. The costimulatory molecule ICOS regulates the expression of c-Maf and IL-21 in the development of follicular T helper cells and TH-17 cells. *Nat Immunol*. 2009;10(2):167-75.
262. Okamoto K, Iwai Y, Oh-Hora M, Yamamoto M, Morio T, Aoki K, et al. IkappaBzeta regulates T(H)17 development by cooperating with ROR nuclear receptors. *Nature*. 2010;464(7293):1381-5.
263. Nguyen LP, Bradfield CA. The search for endogenous activators of the aryl hydrocarbon receptor. *Chem Res Toxicol*. 2008;21(1):102-16.
264. Veldhoen M, Hirota K, Westendorf AM, Buer J, Dumoutier L, Renaud JC, et al. The aryl hydrocarbon receptor links TH17-cell-mediated autoimmunity to environmental toxins. *Nature*. 2008;453(7191):106-9.
265. Laurence A, Tato CM, Davidson TS, Kanno Y, Chen Z, Yao Z, et al. Interleukin-2 signaling via STAT5 constrains T helper 17 cell generation. *Immunity*. 2007;26(3):371-81.
266. Chen Q, Yang W, Gupta S, Biswas P, Smith P, Bhagat G, et al. IRF-4-binding protein inhibits interleukin-17 and interleukin-21 production by controlling the activity of IRF-4 transcription factor. *Immunity*. 2008;29(6):899-911.

267. Hermann-Kleiter N, Gruber T, Lutz-Nicoladoni C, Thuille N, Fresser F, Labi V, et al. The nuclear orphan receptor NR2F6 suppresses lymphocyte activation and T helper 17-dependent autoimmunity. *Immunity*. 2008;29(2):205-16.
268. Ichiyama K, Hashimoto M, Sekiya T, Nakagawa R, Wakabayashi Y, Sugiyama Y, et al. Gfi1 negatively regulates T(h)17 differentiation by inhibiting ROR γ activity. *Int Immunol*. 2009;21(7):881-9.
269. Joshi S, Pantalena LC, Liu XK, Gaffen SL, Liu H, Rohowsky-Kochan C, et al. 1,25-dihydroxyvitamin D(3) ameliorates Th17 autoimmunity via transcriptional modulation of interleukin-17A. *Mol Cell Biol*. 2011;31(17):3653-69.
270. Elias KM, Laurence A, Davidson TS, Stephens G, Kanno Y, Shevach EM, et al. Retinoic acid inhibits Th17 polarization and enhances FoxP3 expression through a Stat-3/Stat-5 independent signaling pathway. *Blood*. 2008;111(3):1013-20.
271. Moisan J, Grenningloh R, Bettelli E, Oukka M, Ho IC. Ets-1 is a negative regulator of Th17 differentiation. *J Exp Med*. 2007;204(12):2825-35.
272. Akimzhanov AM, Yang XO, Dong C. Chromatin remodeling of interleukin-17 (IL-17)-IL-17F cytokine gene locus during inflammatory helper T cell differentiation. *J Biol Chem*. 2007;282(9):5969-72.
273. Cosmi L, Cimaz R, Maggi L, Santarasci V, Capone M, Borriello F, et al. Evidence of the transient nature of the Th17 phenotype of CD4+CD161+ T cells in the synovial fluid of patients with juvenile idiopathic arthritis. *Arthritis Rheum*. 2011;63(8):2504-15.
274. Annunziato F, Romagnani S. The transient nature of the Th17 phenotype. *Eur J Immunol*. 2010;40(12):3312-6.
275. Beriou G, Costantino CM, Ashley CW, Yang L, Kuchroo VK, Baecher-Allan C, et al. IL-17-producing human peripheral regulatory T cells retain suppressive function. *Blood*. 2009;113(18):4240-9.
276. Kryczek I, Banerjee M, Cheng P, Vatan L, Szeliga W, Wei S, et al. Phenotype, distribution, generation, and functional and clinical relevance of Th17 cells in the human tumor environments. *Blood*. 2009;114(6):1141-9.
277. Ratajczak P, Janin A, Peffault de Latour R, Leboeuf C, Desveaux A, Keyvanfar K, et al. Th17/Treg ratio in human graft-versus-host disease. *Blood*;116(7):1165-71.
278. Voo KS, Wang YH, Santori FR, Boggiano C, Arima K, Bover L, et al. Identification of IL-17-producing FOXP3+ regulatory T cells in humans. *Proc Natl Acad Sci U S A*. 2009;106(12):4793-8.
279. Koenen HJ, Smeets RL, Vink PM, van Rijssen E, Boots AM, Joosten I. Human CD25^{high}Foxp3^{pos} regulatory T cells differentiate into IL-17-producing cells. *Blood*. 2008;112(6):2340-52.
280. Ayyoub M, Deknuydt F, Raimbaud I, Dousset C, Leveque L, Bioley G, et al. Human memory FOXP3+ Tregs secrete IL-17 ex vivo and constitutively express the T(H)17 lineage-specific transcription factor ROR γ t. *Proc Natl Acad Sci U S A*. 2009;106(21):8635-40.
281. Oukka M. Interplay between pathogenic Th17 and regulatory T cells. *Ann Rheum Dis*. 2007;66 Suppl 3:iii87-90.
282. Zhou X, Bailey-Bucktrout SL, Jeker LT, Penaranda C, Martinez-Llordella M, Ashby M, et al. Instability of the transcription factor Foxp3 leads to the generation of pathogenic memory T cells in vivo. *Nat Immunol*. 2009;10(9):1000-7.
283. Weaver CT, Hatton RD. Interplay between the TH17 and TReg cell lineages: a (co-)evolutionary perspective. *Nat Rev Immunol*. 2009;9(12):883-9.
284. Nistala K, Wedderburn LR. Th17 and regulatory T cells: rebalancing pro- and anti-inflammatory forces in autoimmune arthritis. *Rheumatology (Oxford)*. 2009;48(6):602-6.
285. Deknuydt F, Bioley G, Valmori D, Ayyoub M. IL-1 β and IL-2 convert human Treg into T(H)17 cells. *Clin Immunol*. 2009;131(2):298-307.

286. Awasthi A, Riol-Blanco L, Jager A, Korn T, Pot C, Galileos G, et al. Cutting edge: IL-23 receptor gfp reporter mice reveal distinct populations of IL-17-producing cells. *J Immunol.* 2009;182(10):5904-8.
287. Bai H, Cheng J, Gao X, Joyee AG, Fan Y, Wang S, et al. IL-17/Th17 promotes type 1 T cell immunity against pulmonary intracellular bacterial infection through modulating dendritic cell function. *J Immunol.* 2009;183(9):5886-95.
288. Lin Y, Ritchea S, Logar A, Slight S, Messmer M, Rangel-Moreno J, et al. Interleukin-17 is required for T helper 1 cell immunity and host resistance to the intracellular pathogen *Francisella tularensis*. *Immunity.* 2009;31(5):799-810.
289. Damsker JM, Hansen AM, Caspi RR. Th1 and Th17 cells: adversaries and collaborators. *Ann N Y Acad Sci.* 2010;1183:211-21.
290. Kebir H, Ifergan I, Alvarez JI, Bernard M, Poirier J, Arbour N, et al. Preferential recruitment of interferon-gamma-expressing TH17 cells in multiple sclerosis. *Ann Neurol.* 2009;66(3):390-402.
291. Brucklacher-Waldert V, Stuermer K, Kolster M, Wolthausen J, Tolosa E. Phenotypical and functional characterization of T helper 17 cells in multiple sclerosis. *Brain.* 2009;132(Pt 12):3329-41.
292. Boniface K, Blumenschein WM, Brovont-Porth K, McGeachy MJ, Basham B, Desai B, et al. Human Th17 cells comprise heterogeneous subsets including IFN-gamma-producing cells with distinct properties from the Th1 lineage. *J Immunol.* 2010;185(1):679-87.
293. Bending D, De la Pena H, Veldhoen M, Phillips JM, Uyttenhove C, Stockinger B, et al. Highly purified Th17 cells from BDC2.5NOD mice convert into Th1-like cells in NOD/SCID recipient mice. *J Clin Invest.* 2009;119(3):565-72.
294. Shi G, Cox CA, Vistica BP, Tan C, Wawrousek EF, Gery I. Phenotype switching by inflammation-inducing polarized Th17 cells, but not by Th1 cells. *J Immunol.* 2008;181(10):7205-13.
295. Hirota K, Duarte JH, Veldhoen M, Hornsby E, Li Y, Cua DJ, et al. Fate mapping of IL-17-producing T cells in inflammatory responses. *Nat Immunol.* 2011;12(3):255-63.
296. Cosmi L, Maggi L, Santarlasci V, Capone M, Cardilicchia E, Frosali F, et al. Identification of a novel subset of human circulating memory CD4(+) T cells that produce both IL-17A and IL-4. *J Allergy Clin Immunol.* 2010;125(1):222-30 e1-4.
297. Wang YH, Voo KS, Liu B, Chen CY, Uygungil B, Spoede W, et al. A novel subset of CD4(+) T(H)2 memory/effector cells that produce inflammatory IL-17 cytokine and promote the exacerbation of chronic allergic asthma. *J Exp Med.* 2010;207(11):2479-91.
298. Leipe J, Grunke M, Dechant C, Reindl C, Kerzendorf U, Schulze-Koops H, et al. Role of Th17 cells in human autoimmune arthritis. *Arthritis Rheum.* 2010;62(10):2876-85.
299. Chabaud M, Durand JM, Buchs N, Fossiez F, Page G, Frappart L, et al. Human interleukin-17: A T cell-derived proinflammatory cytokine produced by the rheumatoid synovium. *Arthritis Rheum.* 1999;42(5):963-70.
300. Kehlen A, Thiele K, Riemann D, Langner J. Expression, modulation and signalling of IL-17 receptor in fibroblast-like synoviocytes of patients with rheumatoid arthritis. *Clin Exp Immunol.* 2002;127(3):539-46.
301. Kokkonen H, Soderstrom I, Rocklov J, Hallmans G, Lejon K, Rantapaa Dahlqvist S. Up-regulation of cytokines and chemokines predates the onset of rheumatoid arthritis. *Arthritis Rheum.* 2010;62(2):383-91.
302. Raza K, Falciani F, Curnow SJ, Ross EJ, Lee CY, Akbar AN, et al. Early rheumatoid arthritis is characterized by a distinct and transient synovial fluid cytokine profile of T cell and stromal cell origin. *Arthritis Res Ther.* 2005;7(4):R784-95.
303. Kirkham BW, Lassere MN, Edmonds JP, Juhasz KM, Bird PA, Lee CS, et al. Synovial membrane cytokine expression is predictive of joint damage progression in rheumatoid arthritis: a two-year prospective study (the DAMAGE study cohort). *Arthritis Rheum.* 2006;54(4):1122-31.

304. Honorati MC, Meliconi R, Pulsatelli L, Cane S, Frizziero L, Facchini A. High in vivo expression of interleukin-17 receptor in synovial endothelial cells and chondrocytes from arthritis patients. *Rheumatology (Oxford)*. 2001;40(5):522-7.
305. Chabaud M, Lubberts E, Joosten L, van Den Berg W, Miossec P. IL-17 derived from juxta-articular bone and synovium contributes to joint degradation in rheumatoid arthritis. *Arthritis Res*. 2001;3(3):168-77.
306. Hirota K, Yoshitomi H, Hashimoto M, Maeda S, Teradaira S, Sugimoto N, et al. Preferential recruitment of CCR6-expressing Th17 cells to inflamed joints via CCL20 in rheumatoid arthritis and its animal model. *J Exp Med*. 2007;204(12):2803-12.
307. Evans HG, Gullick NJ, Kelly S, Pitzalis C, Lord GM, Kirkham BW, et al. In vivo activated monocytes from the site of inflammation in humans specifically promote Th17 responses. *Proc Natl Acad Sci U S A*. 2009;106(15):6232-7.
308. Ferraccioli GF, Tomietto P, De Santis M. Rationale for T cell inhibition by cyclosporin A in major autoimmune diseases. *Ann N Y Acad Sci*. 2005;1051:658-65.
309. Canete JD, Llana J, Collado A, Sanmarti R, Gaya A, Gratacos J, et al. Comparative cytokine gene expression in synovial tissue of early rheumatoid arthritis and seronegative spondyloarthropathies. *Br J Rheumatol*. 1997;36(1):38-42.
310. Olszewski WL, Pazdur J, Kubasiewicz E, Zaleska M, Cooke CJ, Miller NE. Lymph draining from foot joints in rheumatoid arthritis provides insight into local cytokine and chemokine production and transport to lymph nodes. *Arthritis Rheum*. 2001;44(3):541-9.
311. Rasmussen TK, Andersen T, Hvid M, Hetland ML, Horslev-Petersen K, Stengaard-Pedersen K, et al. Increased interleukin 21 (IL-21) and IL-23 are associated with increased disease activity and with radiographic status in patients with early rheumatoid arthritis. *J Rheumatol*. 2010;37(10):2014-20.
312. Thakker P, Leach MW, Kuang W, Benoit SE, Leonard JP, Marusic S. IL-23 is critical in the induction but not in the effector phase of experimental autoimmune encephalomyelitis. *J Immunol*. 2007;178(4):2589-98.
313. Ferraccioli G, Zizzo G. The potential role of Th17 in mediating the transition from acute to chronic autoimmune inflammation: rheumatoid arthritis as a model. *Discov Med*. 2011;11(60):413-24.
314. Sen M, Chamorro M, Reifert J, Corr M, Carson DA. Blockade of Wnt-5A/frizzled 5 signaling inhibits rheumatoid synoviocyte activation. *Arthritis Rheum*. 2001;44(4):772-81.
315. Maurice MM, Lankester AC, Bezemer AC, Geertsma MF, Tak PP, Breedveld FC, et al. Defective TCR-mediated signaling in synovial T cells in rheumatoid arthritis. *J Immunol*. 1997;159(6):2973-8.
316. Isomaki P, Panesar M, Annenkov A, Clark JM, Foxwell BM, Chernajovsky Y, et al. Prolonged exposure of T cells to TNF down-regulates TCR zeta and expression of the TCR/CD3 complex at the cell surface. *J Immunol*. 2001;166(9):5495-507.
317. Zhang Z, Gorman CL, Vermi AC, Monaco C, Foey A, Owen S, et al. TCRzetadim lymphocytes define populations of circulating effector cells that migrate to inflamed tissues. *Blood*. 2007;109(10):4328-35.
318. Zizzo G, De Santis M, Bosello SL, Fedele AL, Peluso G, Gremese E, et al. Synovial fluid-derived T helper 17 cells correlate with inflammatory activity in arthritis, irrespectively of diagnosis. *Clin Immunol*. 2011;138(1):107-16.
319. Fossiez F, Banchereau J, Murray R, Van Kooten C, Garrone P, Lebecque S. Interleukin-17. *Int Rev Immunol*. 1998;16(5-6):541-51.
320. Hwang SY, Kim JY, Kim KW, Park MK, Moon Y, Kim WU, et al. IL-17 induces production of IL-6 and IL-8 in rheumatoid arthritis synovial fibroblasts via NF-kappaB- and PI3-kinase/Akt-dependent pathways. *Arthritis Res Ther*. 2004;6(2):R120-8.

321. Jones CE, Chan K. Interleukin-17 stimulates the expression of interleukin-8, growth-related oncogene-alpha, and granulocyte-colony-stimulating factor by human airway epithelial cells. *Am J Respir Cell Mol Biol.* 2002;26(6):748-53.
322. Zrioual S, Toh ML, Tournadre A, Zhou Y, Cazalis MA, Pachot A, et al. IL-17RA and IL-17RC receptors are essential for IL-17A-induced ELR+ CXC chemokine expression in synoviocytes and are overexpressed in rheumatoid blood. *J Immunol.* 2008;180(1):655-63.
323. Sato K, Suematsu A, Okamoto K, Yamaguchi A, Morishita Y, Kadono Y, et al. Th17 functions as an osteoclastogenic helper T cell subset that links T cell activation and bone destruction. *J Exp Med.* 2006;203(12):2673-82.
324. Kotake S, Udagawa N, Takahashi N, Matsuzaki K, Itoh K, Ishiyama S, et al. IL-17 in synovial fluids from patients with rheumatoid arthritis is a potent stimulator of osteoclastogenesis. *J Clin Invest.* 1999;103(9):1345-52.
325. Pollinger B, Junt T, Metzler B, Walker UA, Tyndall A, Allard C, et al. Th17 cells, not IL-17+ gamma delta T cells, drive arthritic bone destruction in mice and humans. *J Immunol.* 2011;186(4):2602-12.
326. Stamp LK, Cleland LG, James MJ. Upregulation of synoviocyte COX-2 through interactions with T lymphocytes: role of interleukin 17 and tumor necrosis factor-alpha. *J Rheumatol.* 2004;31(7):1246-54.
327. Stamp LK, James MJ, Cleland LG. Interleukin-17: the missing link between T-cell accumulation and effector cell actions in rheumatoid arthritis? *Immunol Cell Biol.* 2004;82(1):1-9.
328. Tat SK, Pelletier JP, Lajeunesse D, Fahmi H, Duval N, Martel-Pelletier J. Differential modulation of RANKL isoforms by human osteoarthritic subchondral bone osteoblasts: influence of osteotropic factors. *Bone.* 2008;43(2):284-91.
329. Nakae S, Nambu A, Sudo K, Iwakura Y. Suppression of immune induction of collagen-induced arthritis in IL-17-deficient mice. *J Immunol.* 2003;171(11):6173-7.
330. Bush KA, Farmer KM, Walker JS, Kirkham BW. Reduction of joint inflammation and bone erosion in rat adjuvant arthritis by treatment with interleukin-17 receptor IgG1 Fc fusion protein. *Arthritis Rheum.* 2002;46(3):802-5.
331. Lubberts E, Koenders MI, Oppers-Walgreen B, van den Bersselaar L, Coenen-de Roo CJ, Joosten LA, et al. Treatment with a neutralizing anti-murine interleukin-17 antibody after the onset of collagen-induced arthritis reduces joint inflammation, cartilage destruction, and bone erosion. *Arthritis Rheum.* 2004;50(2):650-9.
332. Lubberts E, Joosten LA, Oppers B, van den Bersselaar L, Coenen-de Roo CJ, Kolls JK, et al. IL-1-independent role of IL-17 in synovial inflammation and joint destruction during collagen-induced arthritis. *J Immunol.* 2001;167(2):1004-13.
333. Koenders MI, Lubberts E, Oppers-Walgreen B, van den Bersselaar L, Helsen MM, Di Padova FE, et al. Blocking of interleukin-17 during reactivation of experimental arthritis prevents joint inflammation and bone erosion by decreasing RANKL and interleukin-1. *Am J Pathol.* 2005;167(1):141-9.
334. Dong C, Nurieva RI. Regulation of immune and autoimmune responses by ICOS. *J Autoimmun.* 2003;21(3):255-60.
335. Rohn TA, Jennings GT, Hernandez M, Grest P, Beck M, Zou Y, et al. Vaccination against IL-17 suppresses autoimmune arthritis and encephalomyelitis. *Eur J Immunol.* 2006;36(11):2857-67.
336. Koenders MI, Lubberts E, van de Loo FA, Oppers-Walgreen B, van den Bersselaar L, Helsen MM, et al. Interleukin-17 acts independently of TNF-alpha under arthritic conditions. *J Immunol.* 2006;176(10):6262-9.
337. Notley CA, Inglis JJ, Alzabin S, McCann FE, McNamee KE, Williams RO. Blockade of tumor necrosis factor in collagen-induced arthritis reveals a novel immunoregulatory pathway for Th1 and Th17 cells. *J Exp Med.* 2008;205(11):2491-7.

338. Bose F, Raeli L, Garutti C, Frigerio E, Cozzi A, Crimi M, et al. Dual role of anti-TNF therapy: enhancement of TCR-mediated T cell activation in peripheral blood and inhibition of inflammation in target tissues. *Clin Immunol.* 2011;139(2):164-76.
339. Genovese MC, Van den Bosch F, Roberson SA, Bojin S, Biagini IM, Ryan P, et al. LY2439821, a humanized anti-interleukin-17 monoclonal antibody, in the treatment of patients with rheumatoid arthritis: A phase I randomized, double-blind, placebo-controlled, proof-of-concept study. *Arthritis Rheum.* 2010;62(4):929-39.
340. Genovese MC, Durez P, Richards HB, Supronik J, Dokoupilova E, Mazurov V, et al. Efficacy and safety of secukinumab in patients with rheumatoid arthritis: a phase II, dose-finding, double-blind, randomised, placebo controlled study. *Ann Rheum Dis.* 2012.
341. Hueber W, Patel DD, Dryja T, Wright AM, Koroleva I, Bruin G, et al. Effects of AIN457, a fully human antibody to interleukin-17A, on psoriasis, rheumatoid arthritis, and uveitis. *Sci Transl Med.* 2010;2(52):52ra72.
342. Gillies SD, Young D, Lo KM, Foley SF, Reisfeld RA. Expression of genetically engineered immunoconjugates of lymphotoxin and a chimeric anti-ganglioside GD2 antibody. *Hybridoma.* 1991;10(3):347-56.
343. Tao MH, Levy R. Idiotype/granulocyte-macrophage colony-stimulating factor fusion protein as a vaccine for B-cell lymphoma. *Nature.* 1993;362(6422):755-8.
344. Zhao L, Rai SK, Grosmaire LS, Ledbetter JA, Fell HP. Construction, expression, and characterization of anticarcinoma sFv fused to IL-2 or GM-CSF. *J Hematother Stem Cell Res.* 1999;8(4):393-9.
345. Gillies SD, Lan Y, Wesolowski JS, Qian X, Reisfeld RA, Holden S, et al. Antibody-IL-12 fusion proteins are effective in SCID mouse models of prostate and colon carcinoma metastases. *J Immunol.* 1998;160(12):6195-203.
346. Gillies SD, Reilly EB, Lo KM, Reisfeld RA. Antibody-targeted interleukin 2 stimulates T-cell killing of autologous tumor cells. *Proc Natl Acad Sci U S A.* 1992;89(4):1428-32.
347. Becker JC, Pancook JD, Gillies SD, Furukawa K, Reisfeld RA. T cell-mediated eradication of murine metastatic melanoma induced by targeted interleukin 2 therapy. *J Exp Med.* 1996;183(5):2361-6.
348. Trachsel E, Bootz F, Silacci M, Kaspar M, Kosmehl H, Neri D. Antibody-mediated delivery of IL-10 inhibits the progression of established collagen-induced arthritis. *Arthritis Res Ther.* 2007;9(1):R9.
349. Schwager K, Kaspar M, Bootz F, Marcolongo R, Paresce E, Neri D, et al. Preclinical characterization of DEKAVIL (F8-IL10), a novel clinical-stage immunocytokine which inhibits the progression of collagen-induced arthritis. *Arthritis Res Ther.* 2009;11(5):R142.
350. Hughes C, Faurholm B, Dell'Accio F, Manzo A, Seed M, Eltawil N, et al. Human single-chain variable fragment that specifically targets arthritic cartilage. *Arthritis Rheum.* 2010;62(4):1007-16.
351. Taipale J, Saharinen J, Keski-Oja J. Extracellular matrix-associated transforming growth factor-beta: role in cancer cell growth and invasion. *Adv Cancer Res.* 1998;75:87-134.
352. Wakefield LM, Winokur TS, Hollands RS, Christopherson K, Levinson AD, Sporn MB. Recombinant latent transforming growth factor beta 1 has a longer plasma half-life in rats than active transforming growth factor beta 1, and a different tissue distribution. *J Clin Invest.* 1990;86(6):1976-84.
353. Adams G, Vessillier S, Dreja H, Chernajovsky Y. Targeting cytokines to inflammation sites. *Nat Biotechnol.* 2003;21(11):1314-20.
354. Pepinsky RB, LePage DJ, Gill A, Chakraborty A, Vaidyanathan S, Green M, et al. Improved pharmacokinetic properties of a polyethylene glycol-modified form of interferon-beta-1a with preserved in vitro bioactivity. *J Pharmacol Exp Ther.* 2001;297(3):1059-66.
355. Vessillier S, Adams G, Montero-Melendez T, Jones R, Seed M, Perretti M, et al. Molecular engineering of short half-life small peptides (VIP, alphaMSH and gamma(3)MSH) fused to

- latency-associated peptide results in improved anti-inflammatory therapeutics. *Ann Rheum Dis.* 2012;71(1):143-9.
356. DeClerck YA, Perez N, Shimada H, Boone TC, Langley KE, Taylor SM. Inhibition of invasion and metastasis in cells transfected with an inhibitor of metalloproteinases. *Cancer Res.* 1992;52(3):701-8.
 357. Libby P. The interface of atherosclerosis and thrombosis: basic mechanisms. *Vasc Med.* 1998;3(3):225-9.
 358. Anthony DC, Ferguson B, Matyzak MK, Miller KM, Esiri MM, Perry VH. Differential matrix metalloproteinase expression in cases of multiple sclerosis and stroke. *Neuropathol Appl Neurobiol.* 1997;23(5):406-15.
 359. Leppert D, Ford J, Stabler G, Grygar C, Lienert C, Huber S, et al. Matrix metalloproteinase-9 (gelatinase B) is selectively elevated in CSF during relapses and stable phases of multiple sclerosis. *Brain.* 1998;121 (Pt 12):2327-34.
 360. Singer II, Scott S, Kawka DW, Bayne EK, Weidner JR, Williams HR, et al. Aggrecanase and metalloproteinase-specific aggrecan neo-epitopes are induced in the articular cartilage of mice with collagen II-induced arthritis. *Osteoarthritis Cartilage.* 1997;5(6):407-18.
 361. Baugh MD, Perry MJ, Hollander AP, Davies DR, Cross SS, Lobo AJ, et al. Matrix metalloproteinase levels are elevated in inflammatory bowel disease. *Gastroenterology.* 1999;117(4):814-22.
 362. Mease PJ, Wei N, Fudman EJ, Kivitz AJ, Schechtman J, Trapp RG, et al. Safety, tolerability, and clinical outcomes after intraarticular injection of a recombinant adeno-associated vector containing a tumor necrosis factor antagonist gene: results of a phase 1/2 Study. *J Rheumatol.* 2010;37(4):692-703.
 363. Morille M, Passirani C, Vonarbourg A, Clavreul A, Benoit JP. Progress in developing cationic vectors for non-viral systemic gene therapy against cancer. *Biomaterials.* 2008;29(24-25):3477-96.
 364. Zhang G, Gao X, Song YK, Vollmer R, Stolz DB, Gasiorowski JZ, et al. Hydroporation as the mechanism of hydrodynamic delivery. *Gene Ther.* 2004;11(8):675-82.
 365. Hagstrom JE, Hegge J, Zhang G, Noble M, Budker V, Lewis DL, et al. A facile nonviral method for delivering genes and siRNAs to skeletal muscle of mammalian limbs. *Mol Ther.* 2004;10(2):386-98.
 366. Andre F, Mir LM. DNA electrotransfer: its principles and an updated review of its therapeutic applications. *Gene Ther.* 2004;11 Suppl 1:S33-42.
 367. Kim HJ, Greenleaf JF, Kinnick RR, Bronk JT, Bolander ME. Ultrasound-mediated transfection of mammalian cells. *Hum Gene Ther.* 1996;7(11):1339-46.
 368. Endoh M, Koibuchi N, Sato M, Morishita R, Kanzaki T, Murata Y, et al. Fetal gene transfer by intrauterine injection with microbubble-enhanced ultrasound. *Mol Ther.* 2002;5(5 Pt 1):501-8.
 369. Hwang SJ, Davis ME. Cationic polymers for gene delivery: designs for overcoming barriers to systemic administration. *Curr Opin Mol Ther.* 2001;3(2):183-91.
 370. Sokolova V, Epple M. Inorganic nanoparticles as carriers of nucleic acids into cells. *Angew Chem Int Ed Engl.* 2008;47(8):1382-95.
 371. Cai X, Conley S, Naash M. Nanoparticle applications in ocular gene therapy. *Vision Res.* 2008;48(3):319-24.
 372. Davis PB, Cooper MJ. Vectors for airway gene delivery. *AAPS J.* 2007;9(1):E11-7.
 373. Peng XH, Qian X, Mao H, Wang AY, Chen ZG, Nie S, et al. Targeted magnetic iron oxide nanoparticles for tumor imaging and therapy. *Int J Nanomedicine.* 2008;3(3):311-21.
 374. Courtenay JS, Dallman MJ, Dayan AD, Martin A, Mosedale B. Immunisation against heterologous type II collagen induces arthritis in mice. *Nature.* 1980;283(5748):666-8.

375. Holmdahl R, Andersson M, Goldschmidt TJ, Gustafsson K, Jansson L, Mo JA. Type II collagen autoimmunity in animals and provocations leading to arthritis. *Immunol Rev.* 1990;118:193-232.
376. Trentham DE, Townes AS, Kang AH. Autoimmunity to type II collagen an experimental model of arthritis. *J Exp Med.* 1977;146(3):857-68.
377. Wooley PH, Luthra HS, Stuart JM, David CS. Type II collagen-induced arthritis in mice. I. Major histocompatibility complex (I region) linkage and antibody correlates. *J Exp Med.* 1981;154(3):688-700.
378. Stuart JM, Cremer MA, Townes AS, Kang AH. Type II collagen-induced arthritis in rats. Passive transfer with serum and evidence that IgG anticollagen antibodies can cause arthritis. *J Exp Med.* 1982;155(1):1-16.
379. Saijo S, Asano M, Horai R, Yamamoto H, Iwakura Y. Suppression of autoimmune arthritis in interleukin-1-deficient mice in which T cell activation is impaired due to low levels of CD40 ligand and OX40 expression on T cells. *Arthritis Rheum.* 2002;46(2):533-44.
380. Alonzi T, Fattori E, Lazzaro D, Costa P, Probert L, Kollias G, et al. Interleukin 6 is required for the development of collagen-induced arthritis. *J Exp Med.* 1998;187(4):461-8.
381. Mori L, Iselin S, De Libero G, Lesslauer W. Attenuation of collagen-induced arthritis in 55-kDa TNF receptor type 1 (TNFR1)-IgG1-treated and TNFR1-deficient mice. *J Immunol.* 1996;157(7):3178-82.
382. Tada Y, Ho A, Koarada S, Morito F, Ushiyama O, Suzuki N, et al. Collagen-induced arthritis in TNF receptor-1-deficient mice: TNF receptor-2 can modulate arthritis in the absence of TNF receptor-1. *Clin Immunol.* 2001;99(3):325-33.
383. Murphy CA, Langrish CL, Chen Y, Blumenschein W, McClanahan T, Kastelein RA, et al. Divergent pro- and antiinflammatory roles for IL-23 and IL-12 in joint autoimmune inflammation. *J Exp Med.* 2003;198(12):1951-7.
384. Terato K, Harper DS, Griffiths MM, Hasty DL, Ye XJ, Cremer MA, et al. Collagen-induced arthritis in mice: synergistic effect of *E. coli* lipopolysaccharide bypasses epitope specificity in the induction of arthritis with monoclonal antibodies to type II collagen. *Autoimmunity.* 1995;22(3):137-47.
385. Terato K, Hasty KA, Reife RA, Cremer MA, Kang AH, Stuart JM. Induction of arthritis with monoclonal antibodies to collagen. *J Immunol.* 1992;148(7):2103-8.
386. Kagari T, Doi H, Shimozato T. The importance of IL-1 beta and TNF-alpha, and the noninvolvement of IL-6, in the development of monoclonal antibody-induced arthritis. *J Immunol.* 2002;169(3):1459-66.
387. Habu K, Nakayama-Yamada J, Asano M, Saijo S, Itagaki K, Horai R, et al. The human T cell leukemia virus type I-tax gene is responsible for the development of both inflammatory polyarthropathy resembling rheumatoid arthritis and noninflammatory ankylotic arthropathy in transgenic mice. *J Immunol.* 1999;162(5):2956-63.
388. Iwakura Y, Tosu M, Yoshida E, Takiguchi M, Sato K, Kitajima I, et al. Induction of inflammatory arthropathy resembling rheumatoid arthritis in mice transgenic for HTLV-I. *Science.* 1991;253(5023):1026-8.
389. Yamamoto H, Sekiguchi T, Itagaki K, Saijo S, Iwakura Y. Inflammatory polyarthrititis in mice transgenic for human T cell leukemia virus type I. *Arthritis Rheum.* 1993;36(11):1612-20.
390. Iwakura Y, Saijo S, Kioka Y, Nakayama-Yamada J, Itagaki K, Tosu M, et al. Autoimmunity induction by human T cell leukemia virus type 1 in transgenic mice that develop chronic inflammatory arthropathy resembling rheumatoid arthritis in humans. *J Immunol.* 1995;155(3):1588-98.
391. Horai R, Saijo S, Tanioka H, Nakae S, Sudo K, Okahara A, et al. Development of chronic inflammatory arthropathy resembling rheumatoid arthritis in interleukin 1 receptor antagonist-deficient mice. *J Exp Med.* 2000;191(2):313-20.

392. Horai R, Nakajima A, Habiro K, Kotani M, Nakae S, Matsuki T, et al. TNF-alpha is crucial for the development of autoimmune arthritis in IL-1 receptor antagonist-deficient mice. *J Clin Invest*. 2004;114(11):1603-11.
393. Nakae S, Saijo S, Horai R, Sudo K, Mori S, Iwakura Y. IL-17 production from activated T cells is required for the spontaneous development of destructive arthritis in mice deficient in IL-1 receptor antagonist. *Proc Natl Acad Sci U S A*. 2003;100(10):5986-90.
394. Sakaguchi N, Takahashi T, Hata H, Nomura T, Tagami T, Yamazaki S, et al. Altered thymic T-cell selection due to a mutation of the ZAP-70 gene causes autoimmune arthritis in mice. *Nature*. 2003;426(6965):454-60.
395. Yoshitomi H, Sakaguchi N, Kobayashi K, Brown GD, Tagami T, Sakihama T, et al. A role for fungal {beta}-glucans and their receptor Dectin-1 in the induction of autoimmune arthritis in genetically susceptible mice. *J Exp Med*. 2005;201(6):949-60.
396. Hirota K, Hashimoto M, Yoshitomi H, Tanaka S, Nomura T, Yamaguchi T, et al. T cell self-reactivity forms a cytokine milieu for spontaneous development of IL-17+ Th cells that cause autoimmune arthritis. *J Exp Med*. 2007;204(1):41-7.
397. Hata H, Sakaguchi N, Yoshitomi H, Iwakura Y, Sekikawa K, Azuma Y, et al. Distinct contribution of IL-6, TNF-alpha, IL-1, and IL-10 to T cell-mediated spontaneous autoimmune arthritis in mice. *J Clin Invest*. 2004;114(4):582-8.
398. Keffer J, Probert L, Cazlaris H, Georgopoulos S, Kaslaris E, Kioussis D, et al. Transgenic mice expressing human tumour necrosis factor: a predictive genetic model of arthritis. *EMBO J*. 1991;10(13):4025-31.
399. Kontoyiannis D, Pasparakis M, Pizarro TT, Cominelli F, Kollias G. Impaired on/off regulation of TNF biosynthesis in mice lacking TNF AU-rich elements: implications for joint and gut-associated immunopathologies. *Immunity*. 1999;10(3):387-98.
400. Probert L, Plows D, Kontogeorgos G, Kollias G. The type I interleukin-1 receptor acts in series with tumor necrosis factor (TNF) to induce arthritis in TNF-transgenic mice. *Eur J Immunol*. 1995;25(6):1794-7.
401. Kouskoff V, Korganow AS, Duchatelle V, Degott C, Benoist C, Mathis D. Organ-specific disease provoked by systemic autoimmunity. *Cell*. 1996;87(5):811-22.
402. Korganow AS, Ji H, Mangialaio S, Duchatelle V, Pelanda R, Martin T, et al. From systemic T cell self-reactivity to organ-specific autoimmune disease via immunoglobulins. *Immunity*. 1999;10(4):451-61.
403. Matsumoto I, Staub A, Benoist C, Mathis D. Arthritis provoked by linked T and B cell recognition of a glycolytic enzyme. *Science*. 1999;286(5445):1732-5.
404. Ji H, Ohmura K, Mahmood U, Lee DM, Hofhuis FM, Boackle SA, et al. Arthritis critically dependent on innate immune system players. *Immunity*. 2002;16(2):157-68.
405. Nigrovic PA, Binstadt BA, Monach PA, Johnsen A, Gurish M, Iwakura Y, et al. Mast cells contribute to initiation of autoantibody-mediated arthritis via IL-1. *Proc Natl Acad Sci U S A*. 2007;104(7):2325-30.
406. Ji H, Pettit A, Ohmura K, Ortiz-Lopez A, Duchatelle V, Degott C, et al. Critical roles for interleukin 1 and tumor necrosis factor alpha in antibody-induced arthritis. *J Exp Med*. 2002;196(1):77-85.
407. Jacobs JP, Wu HJ, Benoist C, Mathis D. IL-17-producing T cells can augment autoantibody-induced arthritis. *Proceedings of the National Academy of Sciences of the United States of America*. 2009;106(51):21789-94.
408. Geiler T, Kriegsmann J, Keyszer GM, Gay RE, Gay S. A new model for rheumatoid arthritis generated by engraftment of rheumatoid synovial tissue and normal human cartilage into SCID mice. *Arthritis Rheum*. 1994;37(11):1664-71.
409. Pap T, Meinecke I, Muller-Ladner U, Gay S. Are fibroblasts involved in joint destruction? *Ann Rheum Dis*. 2005;64 Suppl 4:iv52-4.

410. Wahid S, Blades MC, De Lord D, Brown I, Blake G, Yanni G, et al. Tumour necrosis factor-alpha (TNF-alpha) enhances lymphocyte migration into rheumatoid synovial tissue transplanted into severe combined immunodeficient (SCID) mice. *Clin Exp Immunol.* 2000;122(1):133-42.
411. Rendt KE, Barry TS, Jones DM, Richter CB, McCachren SS, Haynes BF. Engraftment of human synovium into severe combined immune deficient mice. Migration of human peripheral blood T cells to engrafted human synovium and to mouse lymph nodes. *J Immunol.* 1993;151(12):7324-36.
412. Klimiuk PA, Yang H, Goronzy JJ, Weyand CM. Production of cytokines and metalloproteinases in rheumatoid synovitis is T cell dependent. *Clin Immunol.* 1999;90(1):65-78.
413. Takemura S, Klimiuk PA, Braun A, Goronzy JJ, Weyand CM. T cell activation in rheumatoid synovium is B cell dependent. *J Immunol.* 2001;167(8):4710-8.
414. Nakazawa F, Matsuno H, Yudoh K, Katayama R, Sawai T, Uzuki M, et al. Methotrexate inhibits rheumatoid synovitis by inducing apoptosis. *J Rheumatol.* 2001;28(8):1800-8.
415. Matsuno H, Yudoh K, Katayama R, Nakazawa F, Uzuki M, Sawai T, et al. The role of TNF-alpha in the pathogenesis of inflammation and joint destruction in rheumatoid arthritis (RA): a study using a human RA/SCID mouse chimera. *Rheumatology (Oxford).* 2002;41(3):329-37.
416. Koenders MI, Marijnissen RJ, Joosten LA, Abdollahi-Roodsaz S, Di Padova FE, van de Loo FA, et al. T cell lessons from the rheumatoid arthritis synovium SCID mouse model: CD3-rich synovium lacks response to CTLA-4Ig but is successfully treated by interleukin-17 neutralization. *Arthritis Rheum.* 2012;64(6):1762-70.
417. Sambrook J, Fritsch E, Maniatis T., ed. *Molecular cloning: a laboratory manual: Cold Spring Harbor Laboratory Press; 1989.*
418. Naldini L, Blomer U, Gallay P, Ory D, Mulligan R, Gage FH, et al. In vivo gene delivery and stable transduction of nondividing cells by a lentiviral vector. *Science.* 1996;272(5259):263-7.
419. Wigler M, Pellicer A, Silverstein S, Axel R, Urlaub G, Chasin L. DNA-mediated transfer of the adenine phosphoribosyltransferase locus into mammalian cells. *Proc Natl Acad Sci U S A.* 1979;76(3):1373-6.
420. Rodriguez MS, Thompson J, Hay RT, Dargemont C. Nuclear retention of I κ B protects it from signal-induced degradation and inhibits nuclear factor κ B transcriptional activation. *J Biol Chem.* 1999;274(13):9108-15.
421. Todaro GJ, Green H. Quantitative studies of the growth of mouse embryo cells in culture and their development into established lines. *J Cell Biol.* 1963;17:299-313.
422. Triantaphyllopoulos KA, Williams RO, Tailor H, Chernajovsky Y. Amelioration of collagen-induced arthritis and suppression of interferon-gamma, interleukin-12, and tumor necrosis factor alpha production by interferon-beta gene therapy. *Arthritis Rheum.* 1999;42(1):90-9.
423. Hata K, Andoh A, Shimada M, Fujino S, Bamba S, Araki Y, et al. IL-17 stimulates inflammatory responses via NF- κ B and MAP kinase pathways in human colonic myofibroblasts. *Am J Physiol Gastrointest Liver Physiol.* 2002;282(6):G1035-44.
424. Faour WH, Mancini A, He QW, Di Battista JA. T-cell-derived interleukin-17 regulates the level and stability of cyclooxygenase-2 (COX-2) mRNA through restricted activation of the p38 mitogen-activated protein kinase cascade: role of distal sequences in the 3'-untranslated region of COX-2 mRNA. *J Biol Chem.* 2003;278(29):26897-907.
425. Shimada M, Andoh A, Hata K, Tasaki K, Araki Y, Fujiyama Y, et al. IL-6 secretion by human pancreatic periacinar myofibroblasts in response to inflammatory mediators. *J Immunol.* 2002;168(2):861-8.
426. Teunissen MB, Koomen CW, de Waal Malefyt R, Wierenga EA, Bos JD. Interleukin-17 and interferon-gamma synergize in the enhancement of proinflammatory cytokine production by human keratinocytes. *J Invest Dermatol.* 1998;111(4):645-9.
427. Perretti M, Flower RJ. Modulation of IL-1-induced neutrophil migration by dexamethasone and lipocortin 1. *J Immunol.* 1993;150(3):992-9.

428. Maione F, Paschalidis N, Mascolo N, Dufton N, Perretti M, D'Acquisto F. Interleukin 17 sustains rather than induces inflammation. *Biochem Pharmacol.* 2009;77(5):878-87.
429. Kunkel TA. Rapid and efficient site-specific mutagenesis without phenotypic selection. *Proc Natl Acad Sci U S A.* 1985;82(2):488-92.
430. Derouazi M, Girard P, Van Tilborgh F, Iglesias K, Muller N, Bertschinger M, et al. Serum-free large-scale transient transfection of CHO cells. *Biotechnol Bioeng.* 2004;87(4):537-45.
431. Durocher Y, Perret S, Kamen A. High-level and high-throughput recombinant protein production by transient transfection of suspension-growing human 293-EBNA1 cells. *Nucleic Acids Res.* 2002;30(2):E9.
432. Wilchek M, Miron T. Limitations of N-hydroxysuccinimide esters in affinity chromatography and protein immobilization. *Biochemistry.* 1987;26(8):2155-61.
433. Sica V, Puca GA, Molinari AM, Buonaguro FM, Bresciani F. Effect of chemical perturbation with NaSCN on receptor-estradiol interaction. A new exchange assay at low temperature. *Biochemistry.* 1980;19(1):83-8.
434. Yang Y, Dignam JD, Gentry LE. Role of carbohydrate structures in the binding of beta1-latency-associated peptide to ligands. *Biochemistry.* 1997;36(39):11923-32.
435. Ye P, Garvey PB, Zhang P, Nelson S, Bagby G, Summer WR, et al. Interleukin-17 and lung host defense against *Klebsiella pneumoniae* infection. *Am J Respir Cell Mol Biol.* 2001;25(3):335-40.
436. Hu Y, Ota N, Peng I, Refino CJ, Danilenko DM, Caplazi P, et al. IL-17RC is required for IL-17A- and IL-17F-dependent signaling and the pathogenesis of experimental autoimmune encephalomyelitis. *J Immunol.* 2010;184(8):4307-16.
437. Laan M, Lotvall J, Chung KF, Linden A. IL-17-induced cytokine release in human bronchial epithelial cells in vitro: role of mitogen-activated protein (MAP) kinases. *Br J Pharmacol.* 2001;133(1):200-6.
438. Gaffen SL. Structure and signalling in the IL-17 receptor family. *Nature reviews. Immunology.* 2009;9(8):556-67.
439. Kim KW, Cho ML, Park MK, Yoon CH, Park SH, Lee SH, et al. Increased interleukin-17 production via a phosphoinositide 3-kinase/Akt and nuclear factor kappaB-dependent pathway in patients with rheumatoid arthritis. *Arthritis Res Ther.* 2005;7(1):R139-48.
440. Zhou L, Wang J, Peng S, Duan J, Cai X, Zou M, et al. High-level expression of human interleukin-17 in the yeast *Pichia pastoris*. *Biochem Mol Biol Int.* 1998;46(6):1109-16.
441. Kennedy J, Rossi DL, Zurawski SM, Vega F, Jr., Kastelein RA, Wagner JL, et al. Mouse IL-17: a cytokine preferentially expressed by alpha beta TCR + CD4-CD8-T cells. *J Interferon Cytokine Res.* 1996;16(8):611-7.
442. Fossiez F, Djossou O, Chomarat P, Flores-Romo L, Ait-Yahia S, Maat C, et al. T cell interleukin-17 induces stromal cells to produce proinflammatory and hematopoietic cytokines. *The Journal of experimental medicine.* 1996;183(6):2593-603.
443. Lai T, Wang K, Hou Q, Zhang J, Yuan J, Yuan L, et al. Interleukin 17 induces up-regulation of chemokine and cytokine expression via activation of the nuclear factor kappaB and extracellular signal-regulated kinase 1/2 pathways in gynecologic cancer cell lines. *Int J Gynecol Cancer.* 2011;21(9):1533-9.
444. Kawaguchi M, Kokubu F, Kuga H, Matsukura S, Hoshino H, Ieki K, et al. Modulation of bronchial epithelial cells by IL-17. *J Allergy Clin Immunol.* 2001;108(5):804-9.
445. Kennedy J, Rossi DL, Zurawski SM, Vega F, Jr., Kastelein RA, Wagner JL, et al. Mouse IL-17: a cytokine preferentially expressed by alpha beta TCR + CD4-CD8-T cells. *Journal of interferon & cytokine research : the official journal of the International Society for Interferon and Cytokine Research.* 1996;16(8):611-7.
446. Barin JG, Baldeviano GC, Talor MV, Wu L, Ong S, Quader F, et al. Macrophages participate in IL-17-mediated inflammation. *Eur J Immunol.* 2012;42(3):726-36.

447. Wright JF, Bennett F, Li B, Brooks J, Luxenberg DP, Whitters MJ, et al. The human IL-17F/IL-17A heterodimeric cytokine signals through the IL-17RA/IL-17RC receptor complex. *J Immunol.* 2008;181(4):2799-805.
448. Holmdahl R, Mo J, Nordling C, Larsson P, Jansson L, Goldschmidt T, et al. Collagen induced arthritis: an experimental model for rheumatoid arthritis with involvement of both DTH and immune complex mediated mechanisms. *Clin Exp Rheumatol.* 1989;7 Suppl 3:S51-5.
449. Trentham DE. Collagen arthritis as a relevant model for rheumatoid arthritis. *Arthritis Rheum.* 1982;25(8):911-6.
450. Williams RO, Feldmann M, Maini RN. Anti-tumor necrosis factor ameliorates joint disease in murine collagen-induced arthritis. *Proc Natl Acad Sci U S A.* 1992;89(20):9784-8.
451. Kowanko IC, Gordon TP, Rozenbils MA, Brooks PM, Roberts-Thomson PJ. The subcutaneous air pouch model of synovium and the inflammatory response to heat aggregated gammaglobulin. *Agents Actions.* 1986;18(3-4):421-8.
452. Edwards JC, Sedgwick AD, Willoughby DA. The formation of a structure with the features of synovial lining by subcutaneous injection of air: an in vivo tissue culture system. *J Pathol.* 1981;134(2):147-56.
453. Herweijer H, Wolff JA. Gene therapy progress and prospects: hydrodynamic gene delivery. *Gene Ther.* 2007;14(2):99-107.
454. Maruyama H, Higuchi N, Nishikawa Y, Kameda S, Iino N, Kazama JJ, et al. High-level expression of naked DNA delivered to rat liver via tail vein injection. *J Gene Med.* 2002;4(3):333-41.
455. Zhang G, Budker V, Wolff JA. High levels of foreign gene expression in hepatocytes after tail vein injections of naked plasmid DNA. *Hum Gene Ther.* 1999;10(10):1735-7.
456. Reyes-Sandoval A, Ertl HC. CpG methylation of a plasmid vector results in extended transgene product expression by circumventing induction of immune responses. *Mol Ther.* 2004;9(2):249-61.
457. Yew NS, Cheng SH. Reducing the immunostimulatory activity of CpG-containing plasmid DNA vectors for non-viral gene therapy. *Expert Opin Drug Deliv.* 2004;1(1):115-25.
458. Mosher DF, Doyle MJ, Jaffe EA. Synthesis and secretion of thrombospondin by cultured human endothelial cells. *J Cell Biol.* 1982;93(2):343-8.
459. Hunter NR, Dawes J, MacGregor IR, Pepper DS. Quantitation by radioimmunoassay of thrombospondin synthesised and secreted by human endothelial cells. *Thromb Haemost.* 1984;52(3):288-91.
460. Murphy-Ullrich JE, Poczatek M. Activation of latent TGF-beta by thrombospondin-1: mechanisms and physiology. *Cytokine Growth Factor Rev.* 2000;11(1-2):59-69.
461. van Hamburg JP, Asmawidjaja PS, Davelaar N, Mus AM, Colin EM, Hazes JM, et al. Th17 cells, but not Th1 cells, from patients with early rheumatoid arthritis are potent inducers of matrix metalloproteinases and proinflammatory cytokines upon synovial fibroblast interaction, including autocrine interleukin-17A production. *Arthritis Rheum.* 2011;63(1):73-83.
462. Rosu A, Margaritescu C, Stepan A, Musetescu A, Ene M. IL-17 patterns in synovium, serum and synovial fluid from treatment-naive, early rheumatoid arthritis patients. *Rom J Morphol Embryol.* 2012;53(1):73-80.
463. Leonardi C, Matheson R, Zachariae C, Cameron G, Li L, Edson-Heredia E, et al. Anti-interleukin-17 monoclonal antibody ixekizumab in chronic plaque psoriasis. *N Engl J Med.* 2012;366(13):1190-9.
464. Papp KA, Leonardi C, Menter A, Ortonne JP, Krueger JG, Kricorian G, et al. Brodalumab, an anti-interleukin-17-receptor antibody for psoriasis. *N Engl J Med.* 2012;366(13):1181-9.
465. Mpofo S, Fatima F, Moots RJ. Anti-TNF-alpha therapies: they are all the same (aren't they?). *Rheumatology (Oxford).* 2005;44(3):271-3.
466. Mertens M, Singh JA. Anakinra for rheumatoid arthritis: a systematic review. *J Rheumatol.* 2009;36(6):1118-25.

467. Singh JA, Noorbaloochi S, Singh G. Golimumab for rheumatoid arthritis: a systematic review. *J Rheumatol.* 2010;37(6):1096-104.
468. Smolen J, Landewe RB, Mease P, Brzezicki J, Mason D, Lijitens K, et al. Efficacy and safety of certolizumab pegol plus methotrexate in active rheumatoid arthritis: the RAPID 2 study. A randomised controlled trial. *Ann Rheum Dis.* 2009;68(6):797-804.
469. Zrioual S, Ecochard R, Tournadre A, Lenief V, Cazalis MA, Miossec P. Genome-wide comparison between IL-17A- and IL-17F-induced effects in human rheumatoid arthritis synoviocytes. *J Immunol.* 2009;182(5):3112-20.
470. Hyde SC, Pringle IA, Abdullah S, Lawton AE, Davies LA, Varathalingam A, et al. CpG-free plasmids confer reduced inflammation and sustained pulmonary gene expression. *Nat Biotechnol.* 2008;26(5):549-51.